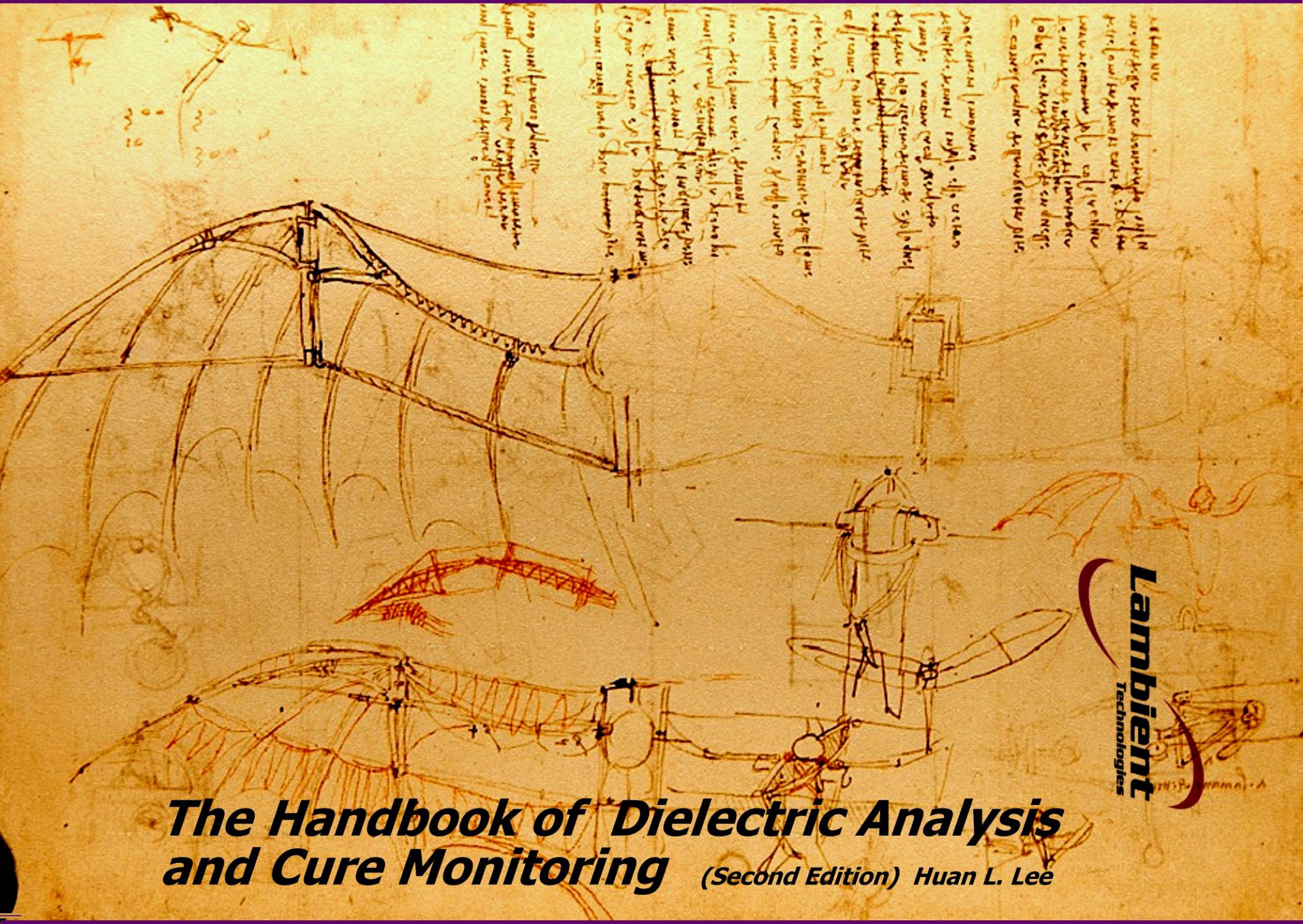

The Handbook of Dielectric Analysis and Cure Monitoring

(Second Edition) Huan L. Lee

Lambient Technologies

Lambient Technologies, LLC.

The Handbook of Dielectric Analysis and Cure Monitoring

(Second Edition)

Huan L. Lee

tech·nol·o·gy

noun **\tek-ˈnä-lə-jē**

1) The use of science in industry, engineering, etc., to invent useful things or to solve problems.

2) A machine, piece of equipment, method, etc., that is created by technology.

plural tech·nol·o·gies

About the second edition

Since the release of the *Handbook of Dielectric Analysis and Cure Monitoring* in 2015, we have seen growing interest in authoritative and practical information about dielectric cure monitoring (DEA) for thermosets and composites. In response, this new edition has been revised, reorganized and enlarged. Case studies of more materials been added to show typical data and highlight techniques for making good measurements with a variety of different sensors, illustrating how DEA can benefit applications in research and development, quality control and manufacturing.

About the cover

A mechanical wing device (ca. 1485) by Leonardo Da Vinci.

Filling many notebooks with thoughts and speculations, artistic studies and sketches of human anatomy, natural phenomena and inventions, Leonardo Da Vinci was a visionary of the Renaissance who anticipated airplanes, helicopters, bicycles, tanks and many other modern devices. He also apparently developed the first man-made plastic.

Da Vinci's Arundel, Forster and Atlantic Codices include recipes for coatings, made from pigments mixed with vegetable or animal glues, that could be applied in layers to the surfaces of objects. The polychromic coating was similar to Bakelite—a phenolic resin—and the monochromic mixtures were possibly tough enough to create cups or vases that would not break if thrown to the floor.

Acknowledgements

Lambient Technologies would like to thank the many people who have been involved in the development of dielectric analysis and cure monitoring over the years. It is impossible to name all those we have worked with but in particular we would like to acknowledge Stephen Senturia, David Day, Norman Sheppard, Michael Coln and David Shepard for contributions too numerous to mention and too important to forget.

About Lambient Technologies

Lambient Technologies, LLC develops instruments, sensors and software for monitoring the properties of curing thermosets. Lambient Technologies was founded by members of the team that developed products for Micromet Instruments, which commercialized dielectric cure monitoring technology developed at the Massachusetts Institute of Technology.

Address : Lambient Technologies
649 Massachusetts Avenue
Cambridge, MA 02139
USA

Telephone: (857) 242-3963
e-mail : info@lambient.com

URL : https://lambient.com

Table of Contents

Section III—Cure Index and Degree of Cure

Section IV—Dielectric Measurements In-Depth

Section V—From the Archives

Terms and Definitions

e = 2.71828	Base of natural logarithm
i = √-1	Square root of -1
π = 3.14159	Pi
ε_0 = 8.854 x 10^{-14} F/cm	Permittivity of free space
k = 8.61733 x 10^{-5} eV/K	Boltzmann's constant
q = 1.602 x 10^{-19} C	Magnitude of electronic charge
f	Frequency (cycles/s or Hz)
$\omega = 2\pi f$	Angular frequency (radians/s)
q	Charge (coulomb)
t	Time (s)
σ	Conductivity (ohm^{-1} – cm^{-1})
$\rho = 1/\sigma$	Resistivity, or ion viscosity (ohm-cm)
ε	Permittivity (F/cm)
$\varepsilon^* = \varepsilon_0 (\varepsilon' - i\varepsilon'')$	Permittivity as a complex quantity (F/cm)
$\kappa = \varepsilon' - i\varepsilon''$	Relative permittivity* or dielectric constant (unitless)
$\varepsilon' = \mathrm{Re}(\varepsilon^*/\varepsilon_0)$	Relative permittivity* or dielectric constant (unitless)
$\varepsilon'' = \mathrm{Im}(\varepsilon^*/\varepsilon_0) = \sigma/\omega\varepsilon_0$	Loss factor or loss index (unitless)
$D = \tan\delta = \varepsilon''/\varepsilon'$	Dissipation factor or loss tangent (unitless)
$\delta = \tan^{-1}(\varepsilon''/\varepsilon')$	Delta (unitless)
$\delta \sim \varepsilon''/\varepsilon'$	Delta for small $\varepsilon''/\varepsilon'$ (unitless)
A/D	Ratio of electrode area to distance between parallel plate electrodes (cm)
V	Voltage (volt)
$I = q/t$	Current (amp)
$C = q/V$	Capacitance (farad)
$G = I/V$	Conductance (ohm^{-1})
$R = V/I = 1/G$	Resistance (ohm)
$C = \varepsilon_0 \varepsilon' A/D$	Capacitance (farad)
$G = \sigma A/D$	Conductance (siemens or ohm^{-1})
$R = \rho/(A/D)$	Resistance (ohm)
$Y = G + i\omega C$	Admittance (siemens or ohm^{-1})
$Z = 1/Y = 1/(G + i\omega C)$	Impedance (ohm)

* There is inconsistency in use of the term *relative permittivity*. In some literature it is the complex quantity $\varepsilon/\varepsilon_0 = (\varepsilon' - i\varepsilon'')/\varepsilon_0$ and in others it is the real part of permittivity $\mathrm{Re}(\varepsilon/\varepsilon_0) = \varepsilon'$.

α	Degree of cure (unitless, between 0 and 1)
α_{max}	Maximum degree of cure at cure temperature
M_w	Molecular weight (gm/mole)
M_{w0}	Molecular weight at α = 0 (uncured)
$M_{w\infty}$	Molecular weight at α = 1 (fully cured)
T_{Cure}	Cure or process temperature (K or °C)
T_g	Glass transition temperature (K or °C)

ε' (free space)	= 1.0	Relative permittivity of free space
ε' (air)	= 1.0	Relative permittivity of air
ε' (teflon)	~ 2.2	Relative permittivity of teflon
ε' (mineral oil)	~ 2.2	Relative permittivity of mineral oil
ε' (polyimide)	~ 3.6	Relative permittivity of polyimide
ε' (alumina)	~ 9.8	Relative permittivity of alumina

DiBenedetto T_g model:

$$\frac{(T_g - T_{g0})}{(T_{g\infty} - T_{g0})} = \frac{\lambda\,\alpha}{(1 - (1 - \lambda)\,\alpha)}$$

Where: T_g = Glass transition temperature (K or °C)
T_{g0} = Glass transition temperature at α = 0 (uncured)
T_{gmax} = Maximum glass transition at T_{Cure}
$T_{g\infty}$ = Glass transition temperature at α = 1 (fully cured)
λ = Adjustable parameter

Debye relaxation for relative permittivity and loss factor:

$$\varepsilon' = \varepsilon'_u + \frac{\varepsilon'_r - \varepsilon'_u}{1 + (\omega\tau)^2} \quad , \quad \varepsilon'' = \sigma/\omega\varepsilon_0 + (\varepsilon'_r - \varepsilon'_u)\frac{\omega\tau}{1 + (\omega\tau)^2}$$

Where: ε'_u = Unrelaxed (high frequency) relative permittivity
ε'_r = Relaxed (low frequency) relative permittivity
ω = $2\pi f$ (radians/s)
τ = Dipole relaxation time (s)

Havriliak-Negami relaxation for relative permittivity and loss factor:

$$\varepsilon' = \varepsilon'_u + (\varepsilon'_r - \varepsilon'_u)\,(1 + 2(\omega\tau)^{\alpha}\cos(\pi\alpha/2) + (\omega\tau)^{2\alpha})^{-\beta/2}\cos(\beta\theta)$$

$$\varepsilon'' = (\varepsilon'_r - \varepsilon'_u)\,(1 + 2(\omega\tau)^{\alpha}\cos(\pi\alpha/2) + (\omega\tau)^{2\alpha})^{-\beta/2}\sin(\beta\theta)$$

Where: $\theta = \tan^{-1}[(\omega\tau)^{\alpha}\sin(\pi\alpha/2) / (1 + (\omega\tau)^{\alpha}\cos(\pi\alpha/2))]$
α = Empirical "broadness" parameter
β = Empirical "asymmetry" parameter
ε'_u = Unrelaxed (high frequency) relative permittivity
ε'_r = Relaxed (low frequency) relative permittivity
$\omega = 2\pi f$ (radians/s)
τ = Dipole relaxation time (s)

Apparent relative permittivity and loss factor due to electrode polarization:

$$\varepsilon'_x = \varepsilon'\,(D / 2t_b)\,\frac{(\varepsilon''/\varepsilon')^2 + (D / 2t_b)}{(\varepsilon''/\varepsilon')^2 + (D / 2t_b)^2)}$$ Apparent relative permittivity

$$\varepsilon''_x = \varepsilon''\,(D / 2t_b)\,\frac{(D / 2t_b) - 1}{(\varepsilon''/\varepsilon')^2 + (D / 2t_b)^2)}$$ Apparent loss factor

Where: t_b = boundary layer thickness
D = distance between electrodes or plate separation
ε'_x = uncorrected permittivity
ε''_x = uncorrected loss factor
ε' = actual permittivity
ε'' = actual loss factor

Introduction

Thermoset and composite materials, with their formability, high strength and low weight, have revolutionized the design of structures such as automobile bodies, aerospace components and wind turbine blades. While irreplaceable for these high-performance applications, thermosets also find use in a range of industries: adhesive; sheet molding compound (SMC); bulk molding compound (BMC); epoxy molding compound (EMC); glass, Kevlar and carbon fiber prepreg; automotive, aerospace, electronics, consumer goods and many others.

Manufacturers, however, are often hindered by limited understanding of how these materials cure and harden. As a result the integrity of the end product often can't be determined until after the process has ended—too late to make necessary improvements. For mission-critical applications such as the heat shield of a spacecraft, the wing of an airplane, or a wind turbine blade failure is not an option.

Many researchers are studying the chemistry of cure as well as improving manufacturing methods. Laboratory tests, including differential scanning calorimetry (DSC), dynamic mechanical analysis (DMA) and dielectric analysis (DEA) yield valuable information. Only DEA provides critical insights into thermoset processing in real time and across the fields of research and development; quality control/quality assurance; and manufacturing.

The intent of this handbook is to provide the background for making dielectric measurements as well as practical information for using and understanding dielectric cure monitoring. We present data from actual cures and discuss how to interpret them, with the goal of assisting all who use these advanced materials.

The following chapters cover dielectric measurements and cure monitoring. While the development of these subjects proceeds from basic concepts to practical results then theory, each chapter is relatively self-contained and users can read them alone or in any order. Those interested in seeing data from cure monitoring of specific thermosets and composites may wish to start with the case studies of those materials.

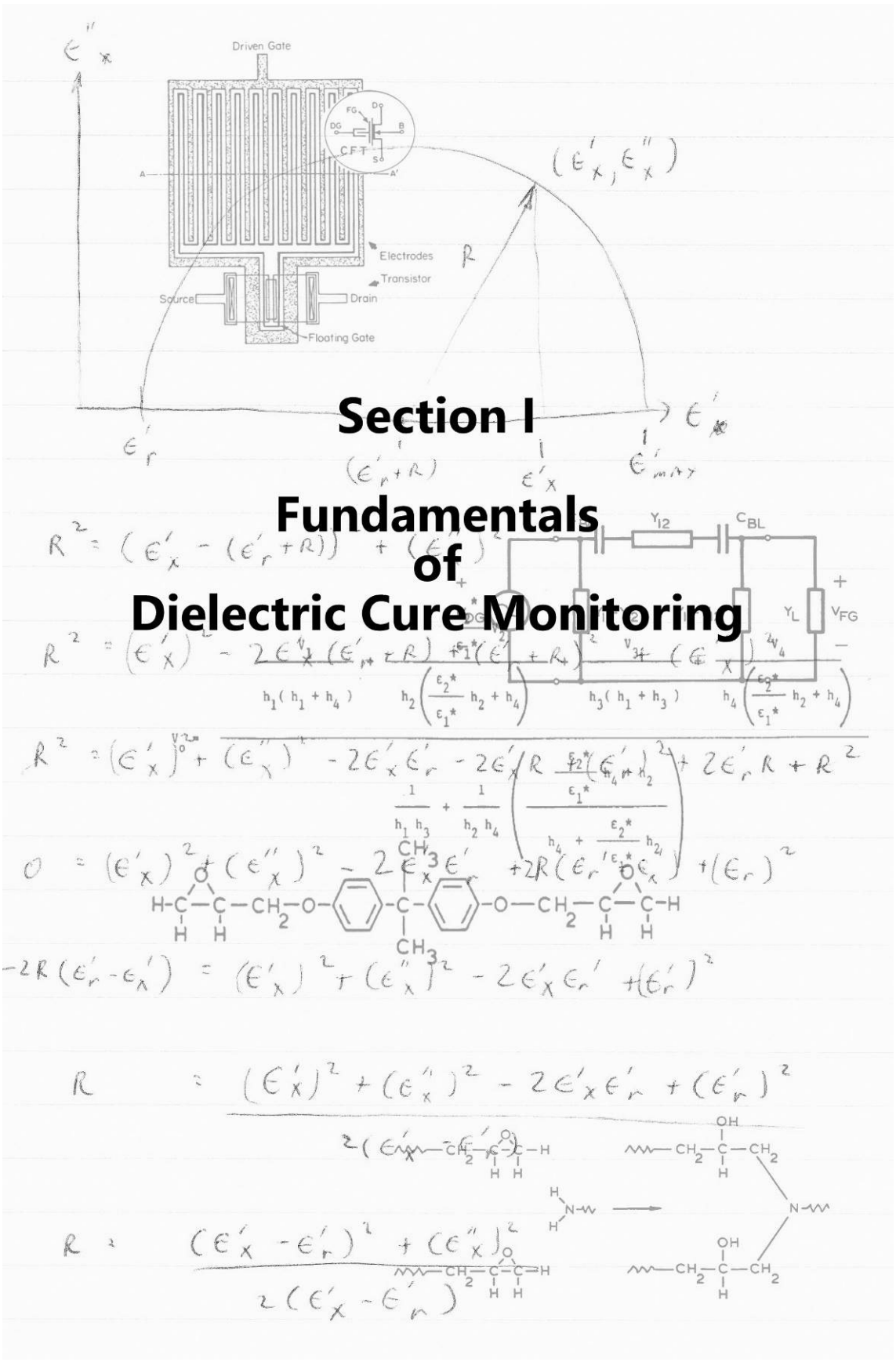

Section I
Fundamentals of Dielectric Cure Monitoring

Chapter 1—Frequently Asked Questions

Q1. What is Dielectric Analysis (also known as DEA) or dielectric cure monitoring?

- Dielectric Analysis (DEA) or dielectric cure monitoring is a thermal analysis technique for determining cure state
    - DEA tracks the cure state of a material by measuring the electrical properties of permittivity and resistivity
    - Permittivity (ε) is related to energy storage in a material
    - Resistivity (ρ) is related to energy loss in a material
    - Frequency independent resistivity, or DC resistivity, (ρ_{DC}) is also called ion viscosity
    - Ion viscosity tracks cure state throughout cure
    - The change in log(*ion viscosity*) is often proportional to the change in mechanical viscosity for significant portions of cure before gelation—see Figure 1-1
    - The change in log(*ion viscosity*) is often proportional to the change in modulus after gelation

Q2. What are the benefits of dielectric cure monitoring?

- Dielectric cure monitoring provides insight into cure state
    - DEA can determine the effects of chemistry and formulation
    - DEA can determine the effects of time, temperature and other process parameters
    - DEA provides information about material viscosity, rigidity, glass transition temperature and degree of cure
- Dielectric cure monitoring saves time, effort and expense
    - Electrical measurements are simple
        - Instruments and software are easy to set up and use
    - Sample preparation is simple
        - Sensors are rugged and can be used in presses, molds or ovens
        - Samples can be applied to sensors in any form

  - Materials can be tested with production process configurations
  - Materials can be tested under production process conditions
- The same measurement can be used in R&D, QA/QC and manufacturing
  - Data from Research and Development are the same as data from Quality Assurance/Quality Control and manufacturing

Q3. What materials can dielectric cure monitoring study?

- Thermosets
- Epoxies
- Acrylics
- Silicones
- Polyesters/polyurethanes/polystyrenes/polyimides/polyamides
- Composites and laminates
- Bulk Molding Compounds (BMC)/Sheet Molding Compounds (SMC)/Epoxy Molding Compounds (EMC)
- Paints, coatings and adhesives
- Oils

Q4. What applications can use dielectric cure monitoring?

- Formulation, reaction rate, cure and process development/monitoring
- Water and solvent diffusion
- UV curing
  - Dental and optical adhesives
  - Photoresist
  - 3-D printing
  - Coatings
- Nondestructive materials testing
- Rheology
- Research & Development
- Quality Assurance/Quality Control
- Manufacturing

Q5. What processing environments can use dielectric cure monitoring?

- Ovens
- Presses and molds
- Autoclaves
- Pultruders and extruders
- Batch reaction vessels
- Injection molding

Q6. What types of companies use dielectric cure monitoring?

- Raw resin/materials manufacturers
    - Suppliers of monomers, resins and catalysts
    - Suppliers of adhesives, paints and coatings
- Suppliers of pre-impregnated (prepreg) composites
    - Carbon fiber or glass fiber/Kevlar prepreg
    - Bulk Molding Compound (BMC) / Sheet Molding Compound (SMC) / Carbon-Fiber Sheet Molding Compound (CF-SMC)
    - Epoxy-fiber/Polyester-fiber/Polystyrene-fiber thread, sheet or laminates
    - Epoxy Molding Compound (EMC)
- Manufacturers of composite end products
    - Aircraft / spacecraft
    - Automobile
    - Wind turbine blades
    - Electronic packaging
    - Consumer products
- Government agencies with R&D—Army, Navy, NASA, etc.

Q7. What are thermosets?

- Thermosets are materials that solidify ("cure") with an irreversible reaction
    - Monomers link into a network and form a polymer
    - Catalysts often facilitate the curing reaction

- The reaction rate increases as temperature increases
- Thermosets cannot melt and be reformed
- Ion viscosity is a measure of viscosity, modulus/rigidity the state of cure and network formation

Q8. What are thermoplastics?

- Thermoplastics are materials that melt and can be reformed multiple times
  - Thermoplastics do not cure and ion viscosity is a measure of viscosity and modulus/rigidity

Q9. What does dielectric cure monitoring data look like?

- Ion viscosity, which is frequency independent electrical resistivity, follows cure state and Figure 1-1 shows typical behavior for a thermoset when processed with a ramp and hold in temperature

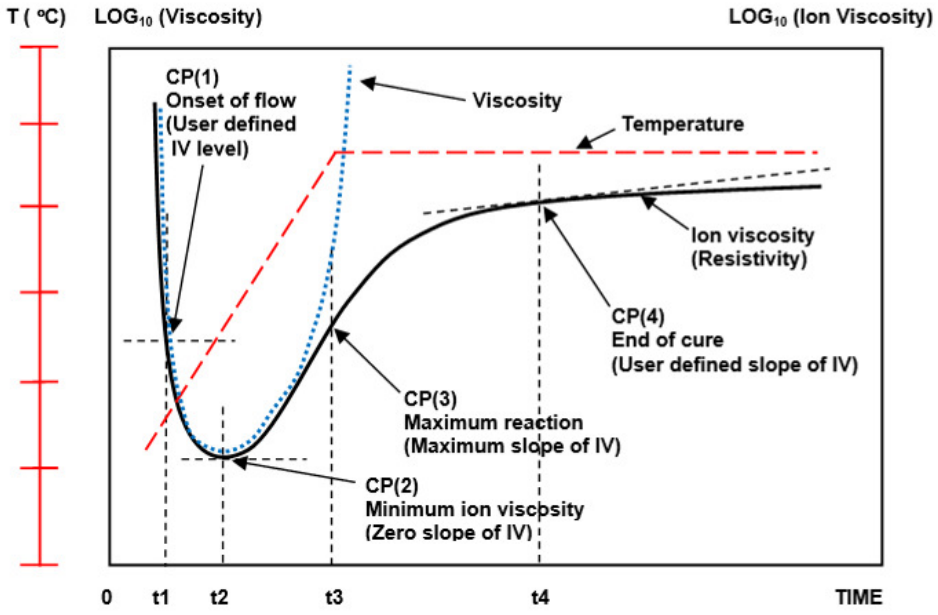

Figure 1-1
Comparison of ion viscosity (frequency independent resistivity) and mechanical viscosity during cure

- Four Critical Points characterize the dielectric cure curve:
    - CP(1)—A user defined level of ion viscosity, which can identify the onset of material flow.
    - CP(2)—Ion viscosity minimum, which typically also corresponds to the mechanical viscosity minimum. This Critical Point indicates the time accelerating polymerization begins to dominate the behavior of the system.
    - CP(3)—Inflection point or maximum slope, which identifies when the reaction rate has reached a maximum. CP(3) *does not indicate gelation* but can be *associated* with gelation.
    - CP(4)—A user defined slope that can define the end of cure. The decreasing slope corresponds to the decreasing reaction rate. Note that dielectric cure monitoring continues to reveal changes in the evolving material past the point when measurement of mechanical viscosity is not possible.

Q10. How does the user prepare samples for dielectric cure monitoring?

Dielectric cure monitoring requires only a small sample, weighing no more than a few grams in most cases, and a simple setup. The user places the sample on a sensor, applies heat and/or pressure then starts the data acquisition software.

Q11. How does sample preparation for dielectric cure monitoring compare to other types of cure tests?

In one common test for gelation, a technician stirs quantity of resin on a hot plate at a set temperature. The time when the material stiffens enough to draw a string or clump to the stirring stick is considered the gel time. This method, while simple, is very subjective and suffers from considerable variation with different technicians.

The spiral flow test forces uncured material through a heated spiral mold. The material cures as it flows, becoming more viscous and eventually stopping at some point. The length at which the material has stopped flowing is a measure of gel or cure time. At best this method crudely indicates the time to gelation or cure, but requires considerable apparatus, is labor intensive and gives no information at all about the reaction during the process.

A Barcol test presses a cone indentor or other hard object into a material. The amount of indentation is a measure of hardness, which in turn is an indirect measure of the composite's or thermoset's degree of cure.

The acetone extraction test dissolves plasticizers or other chemical agents from the material. The amount of these agents in solution is a measure of degree of cure, or conversely the degree not cured.

Q12. How do end-users use dielectric cure monitoring to manage quality control during manufacturing of thermoset materials?

Because sample preparation for dielectric cure monitoring is simple, the cost of testing decreases, allowing companies to be more vigilant about product quality. Some sheet molding compound (SMC) or bulk molding compound (BMC) manufacturers test their materials very frequently—sometimes daily—to confirm and document curing behavior. When their fresh product is processed at a given temperature, they want to know the cure time is what they expect, or else they want to see problems immediately.

Q13. How does dielectric cure monitoring assist in the quality assurance of products?

Consistent quality of a thermoset product results in a consistent cure profile. Aged material, deviant processing conditions or different formulations can change the cure curve, so monitoring Critical Points is a way to quickly and easily identify problems.

Q14. How is dielectric cure monitoring used in manufacturing and for what applications?

In the development of raw resins and thermosets, dielectric cure monitoring allows a researcher to see how the material cures, how fast it cures in response to different formulations, how the reaction responds to the additions of catalysts or additives, and how the reaction rate changes at different temperatures.

For manufacturers of SMC/BMC and prepregs, dielectric cure monitoring is largely used to check consistency of the product, to assure *their* customers that these products will cure as expected.

In aerospace applications, different sections of single, large composite parts can cure at different rates because of varying thicknesses and thermal conditions. Several current aerospace projects around the world use dielectric cure monitoring to control the manufacture of large components. Dielectric cure monitoring provides information for adjusting the process temperature, therefore ensuring that a large part cures uniformly.

Q15. What future applications can use dielectric cure monitoring

The growing field of commercial space ventures has many opportunities for dielectric cure monitoring. Spacecraft components such as fuselages and heat shields use composites because of their unique combination of high strength and low weight. Even more than for aircraft, the safety requirements for spacecraft are paramount and dielectric cure monitoring can document that a life and mission critical component was manufactured to specification.

Other growing applications:

- Wind turbines
- Construction materials

Q16. How does dielectric cure monitoring work?

Dielectric cure monitoring works by measuring the conductivity of a curing material. Under the influence of the electric field of across a dielectric sensor, ions flow through the resin under test. As the material cures, more and more of the molecules within it bond to each other, increasing mechanical viscosity and at the same time restricting the flow of these ions, which in turn decreases conductivity, or conversely increases resistivity (the inverse of conductivity).

It is more common to consider the frequency independent (DC) resistivity when discussing cure monitoring. During the early part of cure, frequency independent resistivity tracks viscosity. This correspondence has given rise to the term *ion viscosity*, which is simply another name for frequency independent resistivity.

Even after the resin has become rigid and viscosity is immeasurable, ion viscosity continues to increase and dielectric measurements can still observe the advancing cure.

Q17. How does dielectric cure monitoring measure material properties?

The dielectric properties of conductivity (σ), and permittivity (ε), arise from ionic current and dipole rotation in the material. For polymers, mobile ions are typically due to impurities and additives, while dipoles result from the separation of charge in the monomers making up the material. When analyzing dielectric properties, it is possible to separate the influence of ions from dipoles, as shown in Figure 1-2, to consider their individual effects.

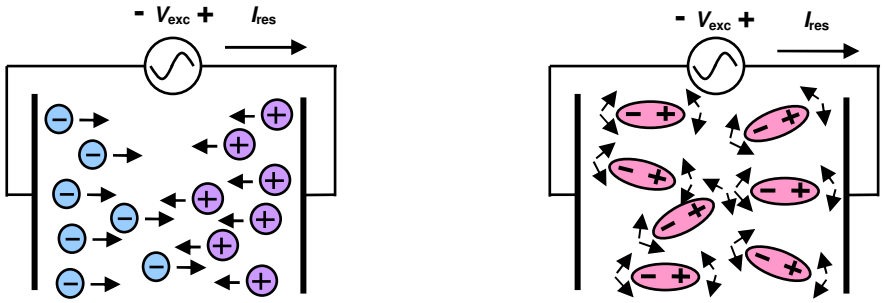

Figure 1-2
Mobile ions and dipole rotation in a material

The flow of ions under the influence of an electric field is responsible for conductive current, and therefore for conductivity (σ) and its inverse, resistivity (ρ). Consequently, the effect of mobile ions can be modeled as a conductance, as shown in Figure 1-3. This conductance may be frequency dependent, and changes as the bulk material changes. The mobility of ions highly depends on the nature of the medium—ions flow more easily through a material with low viscosity and with greater difficulty as the viscosity increases.

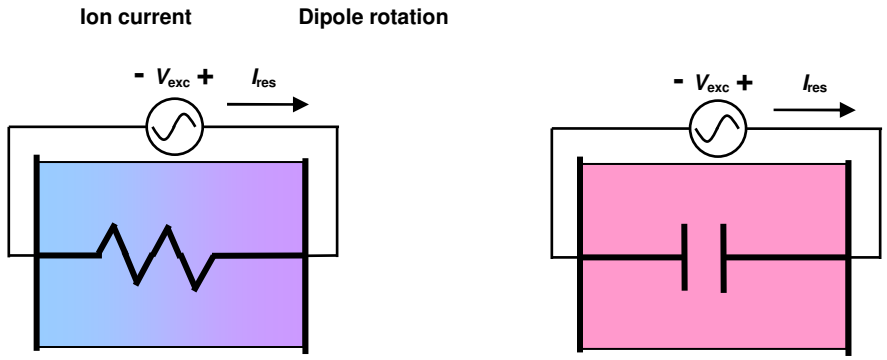

Figure 1-3
Electrical circuit equivalent to mobile ions and dipole rotation

For dielectric cure monitoring, it is convenient to observe *ion viscosity*, which is simply the frequency independent, or DC, resistivity (ρ_{DC})—i.e. the

inverse of frequency independent conductivity. As the physical viscosity of a curing polymer increases, the ion viscosity presented to ion current also increases. This relationship is the principle behind the usefulness of dielectric cure monitoring and makes possible the observation of cure state.

Q18. How are parallel plate sensors different from interdigitated sensors?

Researchers studying dielectric properties often use parallel plate electrodes, for which plate separation sometimes cannot be accurately controlled. The distance between the plates may change upon the application of pressure, or as the material between them expands or contracts. For such situations tan δ is used to characterize dielectric properties because $\varepsilon''/\varepsilon'$ does not vary with plate spacing. However, tan δ alone cannot provide information about either permittivity or loss factor, and therefore has limited usefulness—especially because permittivity and loss factor are themselves complicated functions of several factors.

Interdigitated electrodes on a substrate can be used instead of parallel plate electrodes, as shown in Figure 1-4. The planar structure of interdigitated electrodes has a geometry that does not change with pressure or expansion or contraction of the material under test, and therefore can accurately measure both permittivity and loss factor.

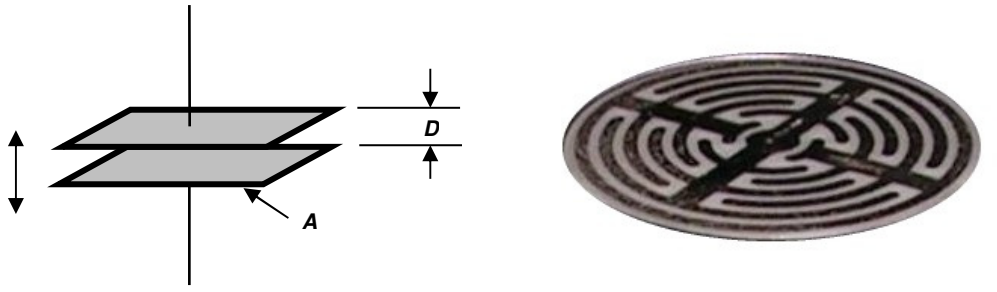

Figure 1-4
Parallel plate and interdigitated electrode geometries

Chapter 2—Applications of Dielectric Cure Monitoring

Understanding composite and thermoset cure

When working on a new composite or a new formulation of a thermoset, the cure process is essentially unknown. What happens when the material is heated? When is the best time to apply pressure to squeeze out voids? How fast does the material react at different temperatures? Dielectric cure monitoring, also known as *dielectric analysis* (DEA), complements more conventional thermal analysis techniques of differential scanning calorimetry (DSC) and dynamic mechanical analysis (DMA) to bridge the gap between laboratory and manufacturing environments.

Characteristics of thermoset cure

Dielectric cure monitoring measures a polymer's resistivity (ρ) and permittivity (ε'), which are dielectric properties. In general resistivity provides the most useful information about cure state. More specifically, before gelation the change in *frequency independent resistivity* (ρ_{DC}), due to the flow of mobile ions, is often proportional to the change in mechanical viscosity. To emphasize this relationship, the term *ion viscosity* (*IV*) was coined as a synonym for frequency independent resistivity.

A thermoset cures when monomers react to form polymer chains then a crosslinked network. The reaction is usually exothermic—generating heat—and may additionally be driven by the heat of a press or oven. A plot of log(ion viscosity) is a simple way to characterize the progress of cure and Figure 2-1 shows the behavior of a typical thermoset with one ramp and hold step in temperature.

At first as temperature increases, the material softens or melts and mechanical viscosity decreases. Mobile ions also experience less resistance to movement and ion viscosity decreases. At this point the reaction is still slow.

As the material becomes hotter, the cure rate increases. At some time the accelerating reaction begins to dominate; mechanical viscosity reaches a minimum then the material becomes more viscous. Electrically, the increase in ion viscosity due to polymerization overcomes the decrease in ion viscosity due to higher temperature. Ion viscosity also reaches a minimum then increases due to chain extension, which presents a greater and greater impediment to the flow of ions.

The gel point is the beginning of infinite network formation or crosslinking. At gelation mechanical viscosity rapidly increases until it becomes infinite. Although viscosity becomes immeasurable at the gel point, the change in ion viscosity continues to provide useful information and after gelation is often proportional to the change in modulus. As a result, DEA can follow material state throughout cure.

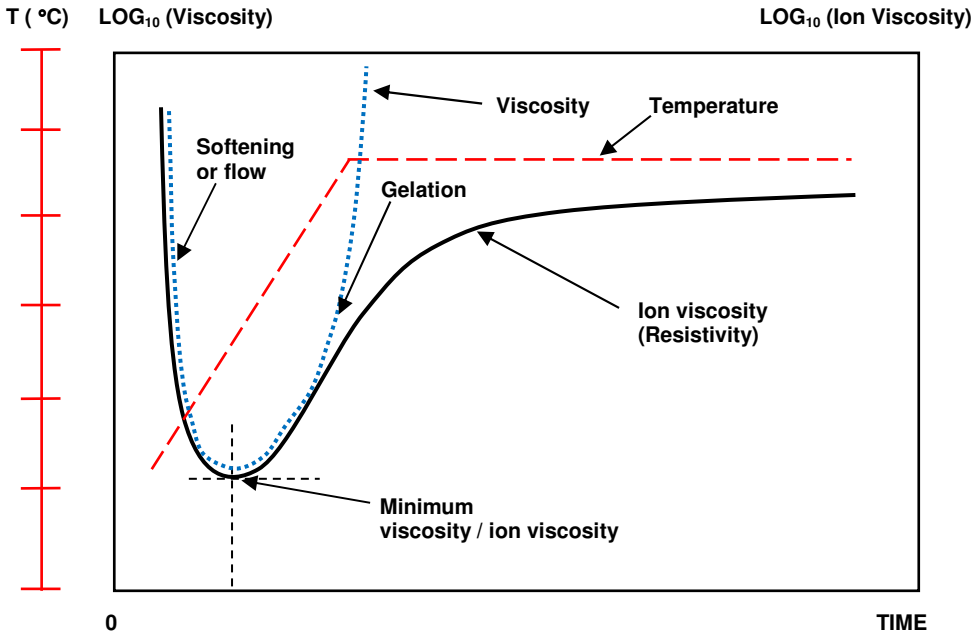

Figure 2-1
Typical ion viscosity behavior of thermoset cure during thermal ramp and hold

As cure progresses, ion viscosity increases continuously until the concentration of unreacted monomers diminishes and the reaction rate decreases. Consequently, the slope of ion viscosity also decreases and eventually reaches a value of zero when cure has stopped completely.

Differential scanning calorimetry

Differential scanning calorimetry, one method for studying polymers, measures glass transition temperature T_g, which changes with cure state. For a particular epoxy, Figure 2-2 shows T_g measured with DSC and compared with results from dielectric cure monitoring.

Each DSC data point requires curing the material to a chosen time, quenching the sample to stop cure and then performing the DSC analysis. This test must be repeated at multiple points during processing to obtain enough

data to see the cure curve—a very tedious and repetitive task. In contrast, the cure curve from dielectric cure monitoring was obtained from a *single* test.

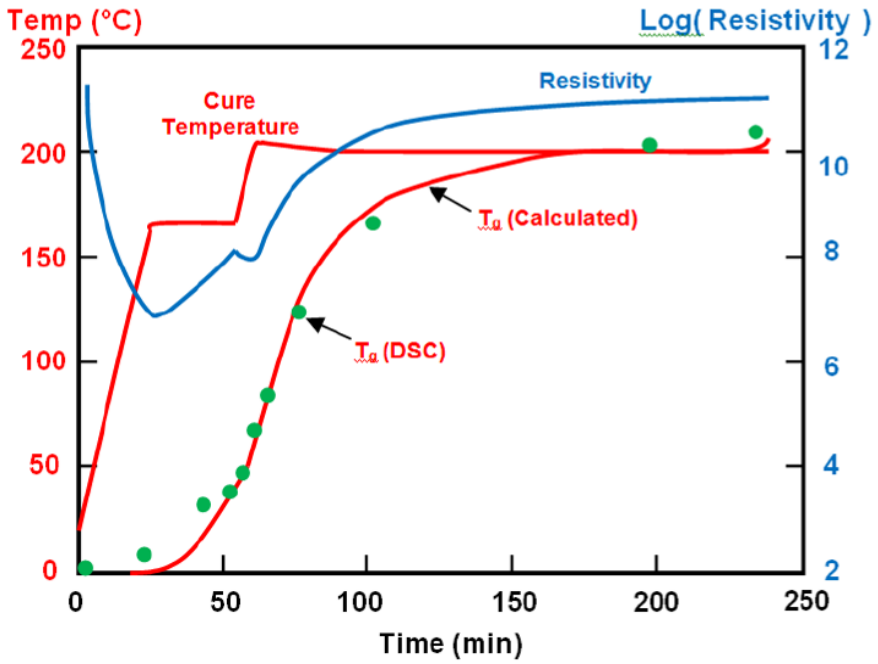

Figure 2-2
Data comparing DEA and DSC tests[1]

Glass transition temperatures from dielectric measurements come from a calculation that yields *Cure Index*, and in this case happen to overlay DSC data very well. Furthermore, the frequency independent resistivity—ion viscosity—provides information about viscosity and modulus, which DSC cannot do. Ion viscosity shows the time of minimum viscosity, the time of maximum reaction rate and the end of cure. All this information is available quickly and in real time, in contrast to the delay between process and test for DSC.

Even if DEA and DSC data do not superimpose as neatly as in Figure 2-2, a direct correspondence still exists between DEA and DSC measurements. One can use dielectric cure monitoring to very quickly evaluate the progress of cure under given conditions, change those conditions, observe the result and change conditions again as often as necessary. Sample preparation for DEA is very simple—apply material to a sensor and heat it. After using DEA for rapid iterations to reach a final formulation or process, *then* DSC can verify thermal-physical properties, saving time, effort and expense.

Dynamic mechanical analysis

Dynamic Mechanical Analysis is a second common technique for studying thermoset cure. Depending on the operating mode, DMA can measure certain moduli for either the early part of cure or the later part of cure. DMA is a direct measure of mechanical properties such as viscosity or modulus, but a single mode usually does not work for the entire cure. Furthermore, some DMA methods require careful sample preparation for consistent results.

Dielectric cure monitoring can supplement DMA because ion viscosity is often directly proportional to the change in viscosity before gelation and to the change in modulus after gelation. Note that DMA can detect gelation but DEA cannot. Gelation is a mechanical phenomenon due to the onset of crosslinking. Although a rapid increase in ion viscosity coincides with the increase in viscosity that accompanies crosslinking, no distinct electrical event occurs at this time.

With proper frequency selection, DEA can measure electrical properties that directly relate to mechanical properties during the entire cure. In fact, the overlap between DEA and DMA data is generally recognized, and at least two major manufacturers of thermal analysis instruments offer combined DMA-DEA test cells. Simultaneous DMA-DEA tests extend the portion of cure during which mechanical properties can be measured or inferred.

Again, dielectric cure monitoring may be used to easily evaluate preliminary formulations or processes, allowing rapid iterations to achieve a desired result. At the end of development, DMA can then verify mechanical properties.

DEA in the process development cycle

DEA, DSC and DMA each measures different material properties. DEA does not replace either DSC or DMA, but instead compliments them. In R&D or process development, DEA has the advantage of very simple sample preparation and the ability to make measurements during the entire cure in real time. Dielectric cure monitoring can accelerate R&D by deferring the need to make laborious DSC or DMA tests until near end of development.

Dielectric analysis or cure monitoring requires a sensor that is in good contact with the material under test. If the sensor is reusable, it is typically embedded in a platen or mold, which has the advantage of reducing long-term costs over many thousands of tests. If the sensor is disposable, the material is placed on the sensor and after the test everything is either stored for purposes of documentation or thrown away. After connecting the sensor to dielectric

measurement instrumentation, software controls the measurement process—acquiring, storing and processing the data. If necessary, the material is compressed for good contact with the sensor and then heated to initiate cure.

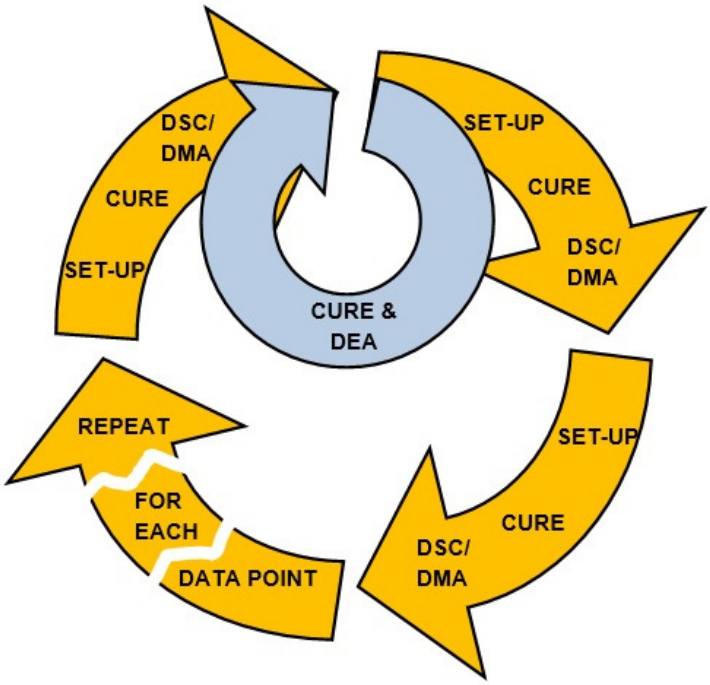

Figure 2-3
Dielectric Analysis (DEA) enables rapid feedback in the process development cycle

DEA has the advantage of allowing material tests in a wide variety of conditions, both in the laboratory, the QA/QC bench or the manufacturing floor. No other method has this versatility. Dielectric cure monitoring may be performed in an oven, on a hot plate, in a press or mold, in an autoclave or in an actual part being developed or manufactured. When embedded in a part or a large mass of material, the dielectric sensor can directly measure the effect of an exotherm on the rate of cure.

In contrast, DMA is confined to a laboratory. If the sample is liquid, it must be tested in a special cell or impregnated in a matrix of some kind. If the sample is solid, it must be prepared with a specific geometric configuration. DSC is similarly limited to a laboratory, and the sample confined to a tiny DSC pan.

DEA in manufacturing

During the manufacture of composites, parts are typically cured using a fixed recipe for temperature and time. This process can be compared to baking a cake at 175 °C for 30 minutes—at the end of that time the cake might or might not be done. The baker must stick a toothpick into the cake to test it. If the cake is not done then it must stay in the oven and be tested again later. If testing the cake is not possible, the only choice is to bake it longer, maybe for 60 minutes—but then it might burn.

DEA is currently is most often used to confirm that parts are made consistently. For example, the nominal cure of an automobile body panel made of sheet molding compound (SMC) might look like Figure 2-4. By comparing characteristic features of the curve, known as *Critical Points*, the cure of every panel can be judged against this nominal curve. Results for each panel can be recorded for statistical quality control (SQC). Deviations beyond defined limits indicate that something in the curing process has drifted and information from the cure is available to correct the problem. Thus, part quality is assured.

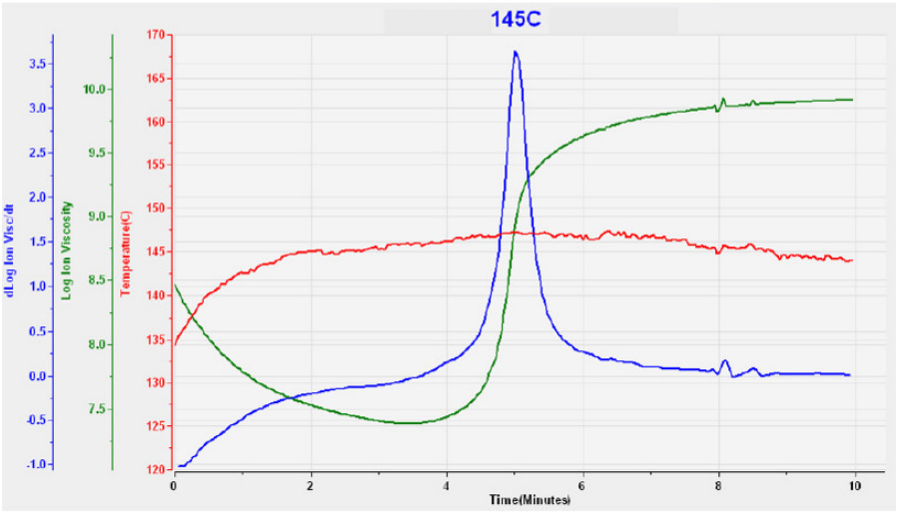

Figure 2-4
Typical sheet molding compound (SMC) cure

For highly critical parts such as composite aircraft or spacecraft components, every step in manufacturing is documented, both to record that the part is made according to specification and for analysis in the event of failure. Many manufacturers measure temperature of the part as a very indirect and inaccurate way to infer the progress of cure. DEA, however, measures ion viscosity, which is a sensitive probe of cure state. So dielectric cure monitoring is valuable for documentation because no other technique can observe cure state in manufacturing and in real-time.

Closed loop process control

Related to productivity is the possibility of closed loop process control. The cure profile of a thermoset or composite varies with temperature and the time to end of cure decreases with increasing temperature—expected behavior for a thermally driven reaction.

One study of closed loop process control used the hardware of Figure 2-5 at a company that manufactures commercial SMC products.

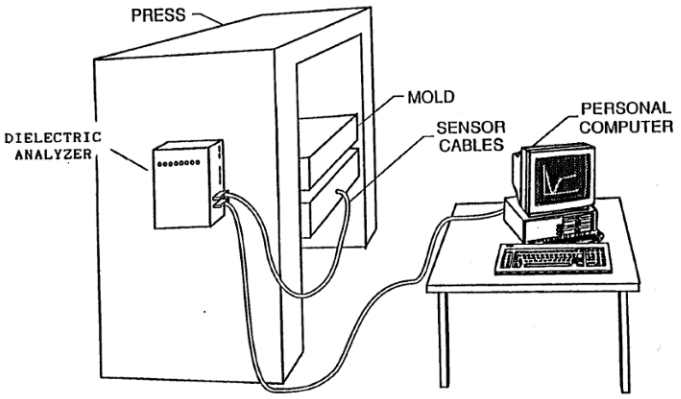

Figure 2-5
Closed-loop process control with dielectric cure monitoring[2]

Manufacturers of molded thermosets use timers to determine when products are cured and may be removed from a press. This standard practice must allow for normal variation in process temperature and other factors that affect cure. To be conservative, demold time is chosen to guarantee that all parts are good, with the result that some parts may be cured longer than necessary. Over many thousands of parts, the use of timers wastes considerable time, effort and productivity.

In this study a reusable dielectric sensor was embedded in the lower mold of a 2000-ton press. The sensor was coated with mold release before each charge of SMC was loaded. Then the press was closed. Upon detecting end of cure, the dielectric cure monitor automatically issued a signal to open the press.

Figure 2-6 shows the distribution of cure time during production of about 1000 parts. A fixed timer setting would have been 60 seconds to ensure 100% good parts. In comparison, closed loop control with dielectric cure monitoring reduced average press cycle time to 50 seconds.[2] This 10 second reduction would have saved $70,000/year/press in labor costs alone.

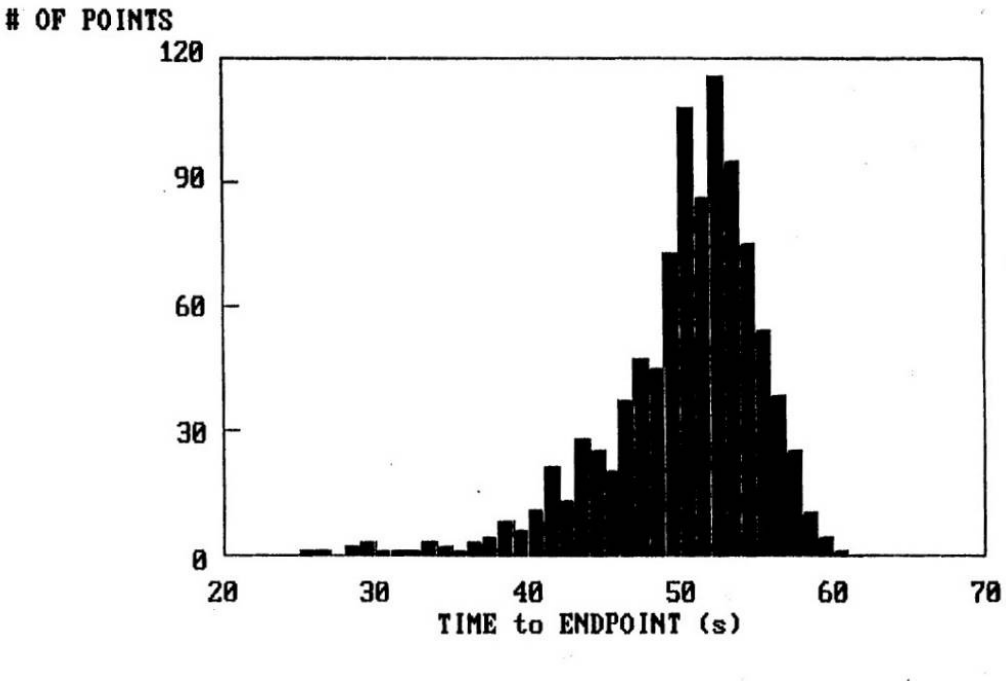

Figure 2-6
Distribution of SMC cure time for 1000 parts[2]

A convergence of cure monitoring technologies

For large composite structures, such as a wind turbine blade, bridge beam or an aircraft fuselage, DEA-based closed-loop control is on the verge of becoming a reality. Two critical technologies of a large scale, closed-loop control heating system have existed for decades: dielectric cure monitoring, commercialized in the 1980s, and the demonstration of closed-loop molding control with dielectric cure monitoring in 1992.[2]

Most recently, Spirit AeroSystems of Wichita, Kansas developed the third critical technology: an intelligent, multi-zone heated tool that replaces an autoclave.[3] This tool allows complete control of the curing process with real-time monitoring and feedback, adjusting cure time for individual segments of a part—depending on its geometry and thermal requirements—and reducing cycle times, cutting production costs and decreasing energy use. Although the Spirit AeroSystems tool uses temperature for control information, it is only a small step to incorporate dielectric measurements for feedback about material state.

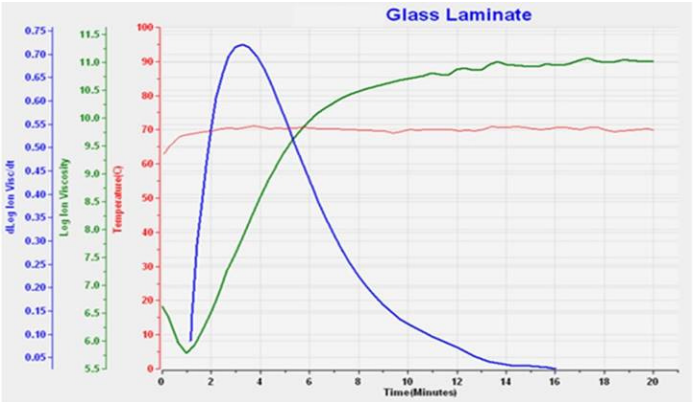

a. Dielectric cure monitoring (ca. 1980)

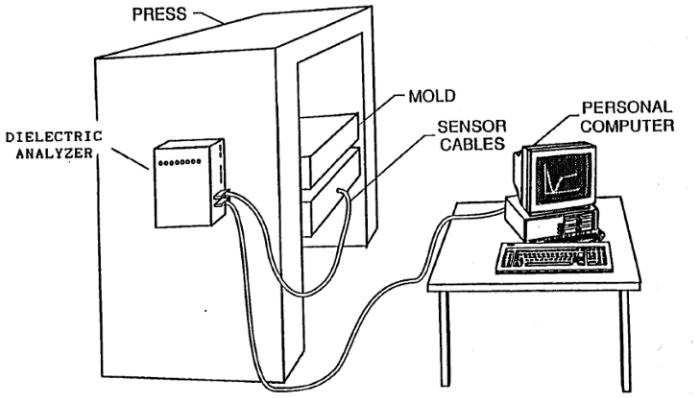

b. DEA closed loop feedback control (1992)[2]

c. Intelligent control of multi-zone heating (2018)[3]

Figure 2-7
Technologies for closed-loop control in the production of large structures

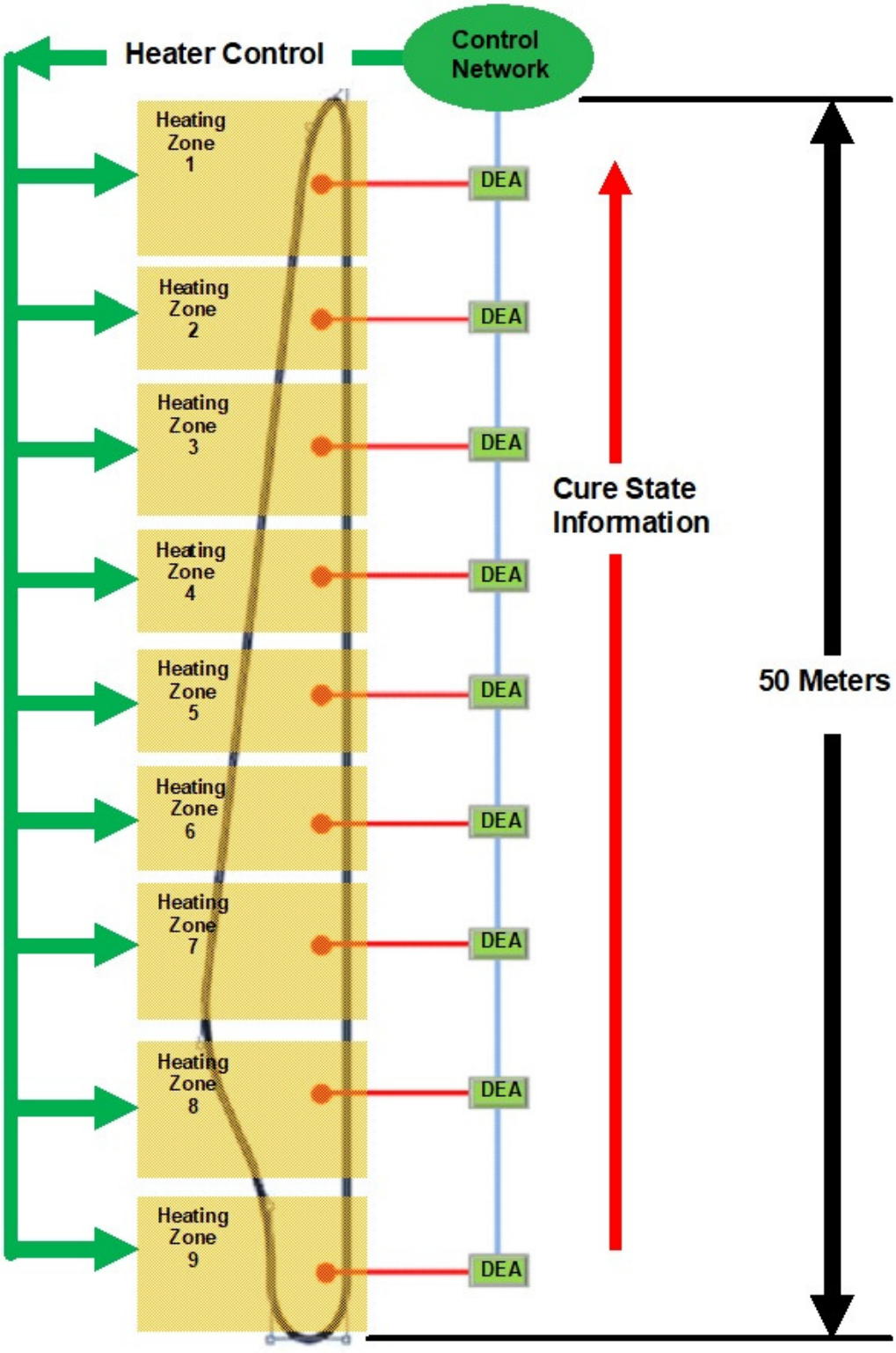

Figure 2-8

Distributed DEA for closed loop process control
(Wind turbine blade manufacture)

The convergence of these technologies comes at a time when the development of larger and larger wind turbine blades is crucial to the rapidly growing renewable energy sector. These blades, often more than 50 meters long, are fabricated in a mold. The thickness of the blade, the exotherm and the thermal environment vary along its length. Consequently, widely spaced locations cure at different rates. Manufacturers must use trial and error to determine the optimum demold time. Removing a blade too soon can damage it because of insufficient stiffness, and removing a blade later than necessary reduces throughput.

Dielectric sensors installed in the mold at strategic locations—every five meters along its length, for example—can determine when cure along the entire part has reached a desired point. Only at that time would the wind turbine blade be removed from its mold.

With the use of independent heaters and distributed DEA instruments, as in Figure 2-8, like the Spirit AeroSystems tool, dielectric measurements would allow a closed-loop control system to adjust heating so the entire structure cures at a uniform rate for optimum throughput. As a benefit, if a factory ships even as little as one more blade a week, or reduces scrap by one blade a week, profitability increases.

Dielectric cure monitoring is a simple electrical measurement that requires minimal sample preparation or skill to perform. In addition, the same sensors and measurement techniques may be used in research, quality control and manufacturing applications. Dielectric analysis correlates with measurements from more conventional laboratory tests, such as differential scanning calorimetry or dynamic mechanical analysis. As a result, DEA can act as the "go between" that brings information from the research lab to the manufacturing floor, and from the manufacturing floor to the manager responsible for product quality.

References

1. Day, D.R., *Dielectric Properties of Polymeric Materials*, Micromet Instruments, (1988). (Figure has been redrawn for clarity)

2. Day, D.R. and Lee, H.L., "Analysis and Control of SMC Part to Part Variations," Session 13-C of *Proceedings of the 17th Annual Conference, Composites Institute, the Society of the Plastics Industry, Inc., Feb 3-6, 1992.*

3. Spirit AeroSystems, "Spirit AeroSystems Develops New Composites Manufacturing Technology," Press release, Dec 14, 2017. https://www.spiritaero.com/release/136953/spirit-aerosystems-develops-new-composites-manufacturing-technology

Chapter 3—Basics of Thermoset Cure

Stages of thermoset cure

Thermosets are an important class of materials used for adhesives, coatings and composites. They include epoxies, (poly)urethanes, acrylics, phenolics, vinyl esters, silicones and many other compounds. Uncured thermosets, or *A-stage* materials, are composed of small molecules called monomers, as shown in Figure 3-1.

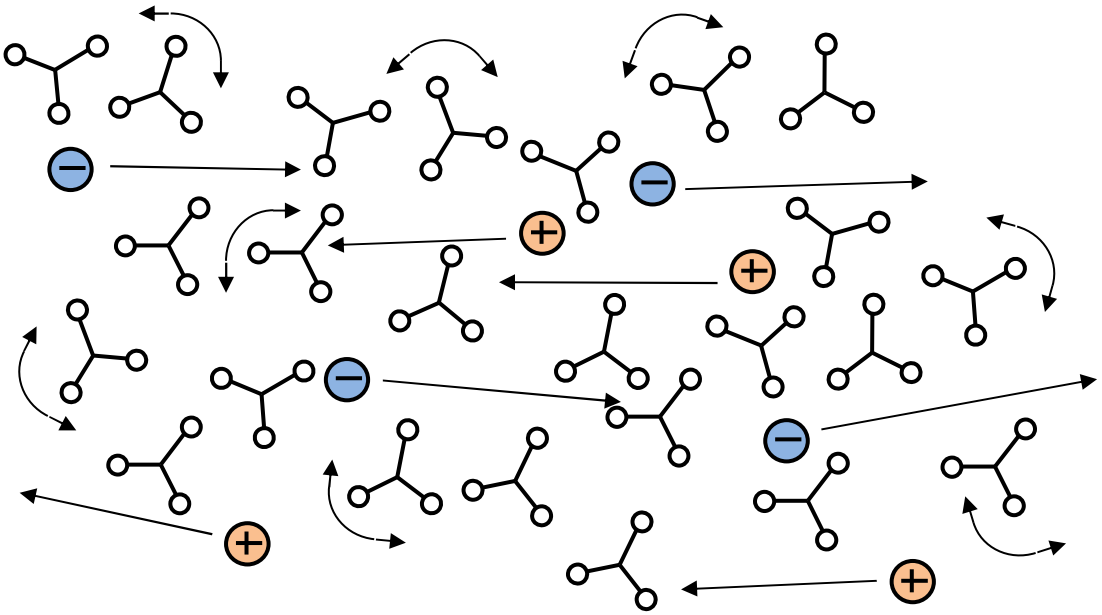

Figure 3-1
A-Stage thermoset (uncured)

Characteristics of A-Stage thermoset

Physical

- Fluidity measured by viscosity
- Viscosity low
- Glass transition temperature T_g low
- Mean free path long
- Diffusion coefficient large
- Free ion mobility high
- Dipole rotation large

Chemical

- Monomers unreacted
- Molecular weight low
- Degree of cure α low
- No network formation

Electrical

- Conductivity at maximum (resistivity at minimum)
- Dielectric constant at maximum

With the application of a catalyst, hardener, or energy such as heat or light, these monomers react and bond to one another to form longer and longer chains called polymers. Once curing begins, but while still fluid, the thermoset is a *B-Stage* material, represented in Figure 3-2. During this period the number of molecules decreases while their molecular weight increases. The thermoset's viscosity also increases, as does its resistance to the flow of mobile ions in an electric field. Dipoles in the polymer can rotate in response to an oscillating electric field, and this ability to rotate also decreases as cure advances.

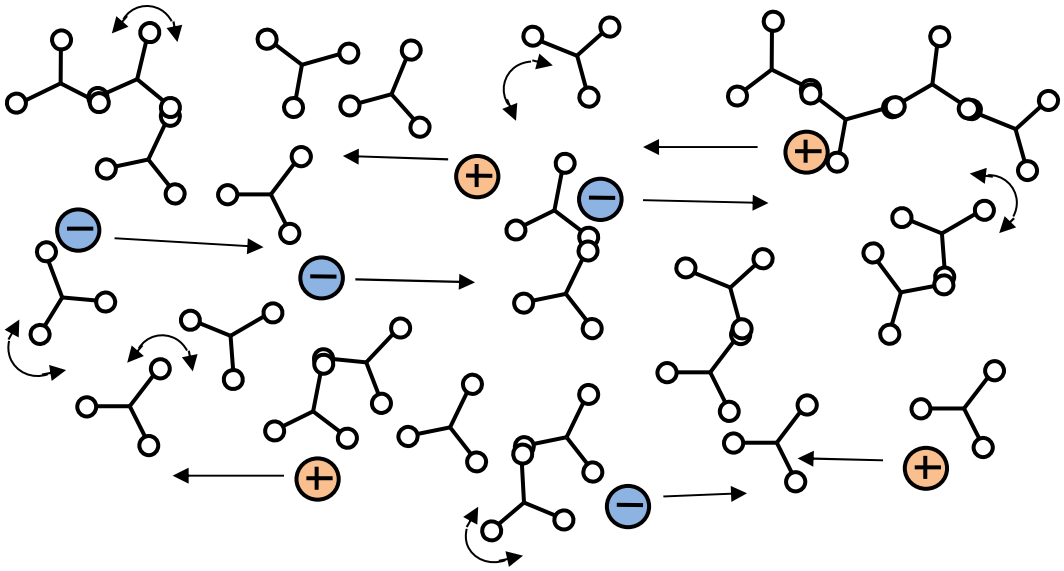

Figure 3-2
B-Stage thermoset (partial curing, before gel point)

Characteristics of B-Stage thermoset

Physical

- Fluidity measured by viscosity
- Viscosity increasing
- Glass transition temperature T_g increasing
- Mean free path shortening
- Diffusion coefficient decreasing
- Free ion mobility decreasing
- Dipole rotation decreasing

Chemical

- Monomers reacting and molecular chains lengthening
- Molecular weight increasing
- Degree of cure α increasing
- Little network formation

Electrical

- Conductivity decreasing (resistivity increasing)
- Dielectric constant decreasing

Through the process of crosslinking, which is the formation of bonds that link one polymer chain to another, an extended branching network appears as shown in Figure 3-3. Crosslinks restrict the movement of polymer chains and the thermoset's viscosity increases rapidly.

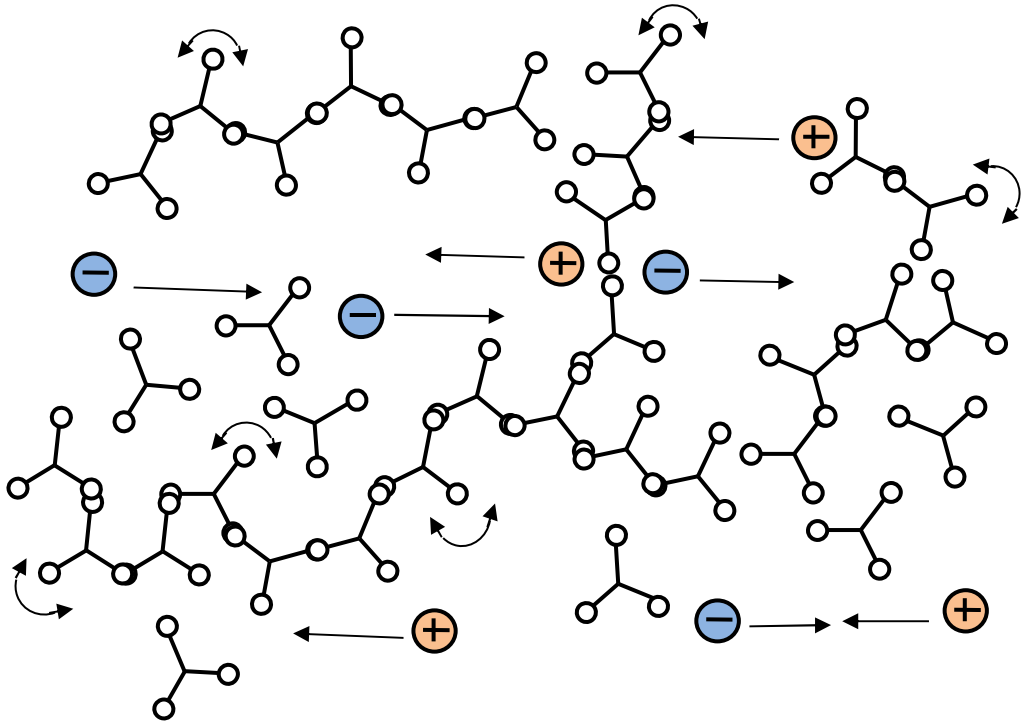

Figure 3-3
Gel point (start of infinite network)

Characteristics of thermoset at gel point

Physical

- Viscosity increasing rapidly to infinity
- Rigidity measured by modulus
- Modulus low
- Glass temperature T_g increasing
- Mean free path shortening
- Diffusion coefficient decreasing
- Free ion mobility decreasing
- Dipole rotation decreasing

Chemical

- Monomers reacting, molecular chains lengthening and branching
- Molecular weight increasing
- Degree of cure α increasing
- Beginning of infinite network formation

Electrical

- Conductivity decreasing (resistivity increasing)
- Dielectric constant decreasing
- No sudden change in dielectric properties

At some point the network essentially becomes a single molecule of infinite molecular weight, and the beginning of infinite network formation is called *gelation* or the *gel* point—the material changes from a viscous liquid that can flow to a gel or rubber that cannot.

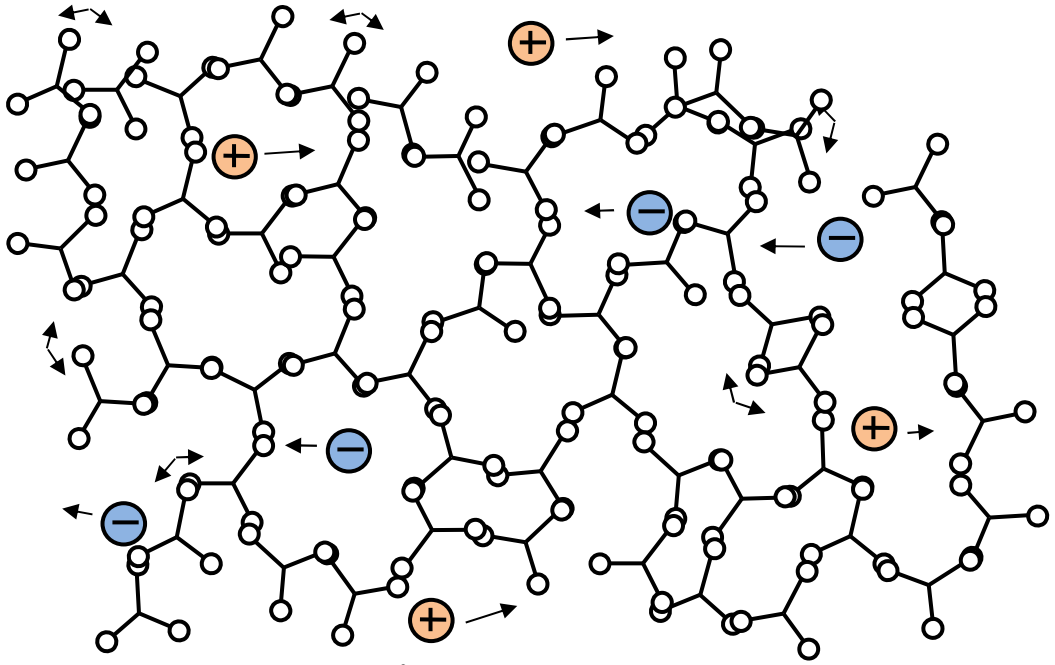

Figure 3-4
C-Stage resin (end of cure)

Characteristics of C-Stage thermoset

Physical

- Rigidity measured by modulus
- Modulus increasing to maximum for cure temperature
- Glass transition temperature T_g reaching maximum for cure temperature
- Mean free path shortening
- Diffusion coefficient decreasing
- Free ion mobility decreasing
- Dipole rotation decreasing

Chemical

- Reaction approaching end of cure
- Molecular chains lengthening and branching
- Molecular weight approaching infinity
- Degree of cure α approaching maximum for cure temperature
- Infinite network approaching maximum

Electrical

- Conductivity reaching minimum (resistivity reaching maximum)
- Dielectric constant reaching minimum

Note that gelation is a mechanical condition that does not cause a corresponding change in electrical properties. After gelation the thermoset hardens into a solid. Upon full cure the thermoset is a *C-Stage* material as shown in Figure 3-4.

At constant temperature, as a thermoset cures from A-Stage to B-Stage to C-Stage, both free ion mobility and the amount of dipole rotation decrease continuously. Ion mobility and dipole rotation vary with temperature as well as cure state, however, and their behavior is more complex if these factors change at the same time.

The electrical quantities of resistivity and permittivity depend on free ion mobility and dipole rotation, respectively. As a result, these dielectric properties correlate with viscosity before gelation, and with rigidity or modulus after gelation.

Degree of cure and glass transition temperature

The degree of cure α is a measure of the amount of reaction for the thermoset. Each bond releases a fixed amount of heat, and the degree of cure is defined as:

(eq. 3-1) $$\alpha = \Delta H \,/\, \Delta H_R$$

Where:

ΔH = Total heat released
ΔH_R = Heat of reaction

The degree of cure also correlates with *crosslink density*; α therefore is useful for indicating physical state.

A material undergoes a glass transition when it changes from a glassy and relatively brittle solid to one that is rubbery and relatively soft. Above the glass transition temperature T_g (actually a range of temperature) a polymer is rubbery because sufficient thermal energy is available to increase the flexibility of crosslinks. Below T_g the polymer vitrifies and is rigid. Like degree of cure, glass transition temperature increases with crosslink density, increases as cure

progresses and is a measure of cure state. The DiBenedetto model, below, is often used to relate degree of cure to glass transition temperature.

(eq. 3-2)
$$\frac{(T_g - T_{g0})}{(T_{g\infty} - T_{g0})} = \frac{\lambda\,\alpha}{(1 - (1 - \lambda)\,\alpha)}$$

Where:

T_g = Glass transition temperature (K or °C)
T_{g0} = Glass transition temperature at α = 0 (uncured)
$T_{g\infty}$ = Glass transition temperature at α = 1 (fully cured)
λ = Adjustable parameter

The relationships among degree of cure, glass transition temperature and electrical properties of the thermoset are the basis for dielectric cure monitoring, which uses electrical measurements to measure cure.

Chapter 4—Basics of Dielectric Measurements

ASTM standard for measuring dielectric properties

The ASTM standard E 2039-04 **Standard Test Methods for Determining and Reporting Dynamic Dielectric Properties** describes general configurations of sensors, circuits and instruments. Although withdrawn in 2009 without replacement, this standard still provides useful background and guidance for making dielectric measurements.

Section 4.1 of E 2039-04, cited below, recognizes that the dielectric properties of material between two electrodes are determined by measuring the current passing through the material along with the voltage driving that current between the electrodes.

> **4. Summary of Practice**
>
> 4.1 An oscillatory electric potential (voltage) is applied to a test specimen by means of an electrode of known geometry. An electric current is measured at a sensing electrode separated from the transmitting electrode by the specimen under test. From the amplitude and phase shift of the measured current relative to the applied voltage and from known geometrical constants, such as electrode spacing and electrode arrangement, desired dielectric properties of the specimen under test may be obtained. Such properties include conductivity, dielectric constant, dielectric dissipation factor, dielectric loss angle, dipole relaxation time, dissipation factor, relative permittivity, loss factor, and tangent delta. The desired dielectric properties may be obtained as a function of frequency, temperature, or time by varying and measuring these independent parameters during the course of the experiment.
>
> NOTE 1—The particular method for measurement of amplitude and phase shift depends upon the operating principle of the instrument used.

(From ASTM 2039-04, withdrawn without replacement in 2009)

Electrical model of Material Under Test (MUT)

Dielectric instrumentation measures the conductance *G* (or resistance *R*) and capacitance *C* between a pair of electrodes at a given frequency. The Material Under Test (MUT) between these electrodes can be modeled as a conductance in parallel with a capacitance, as shown in Figure 4-1.

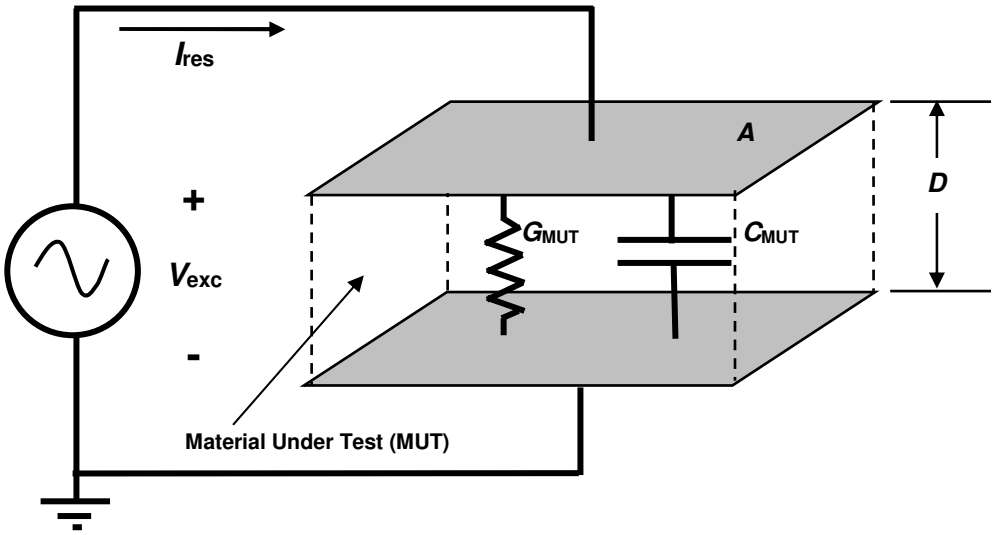

Figure 4-1
Electrical model of dielectric Material Under Test

An AC excitation voltage V_{exc}, applied between a pair of parallel plate electrodes, drives response current I_{res} through the MUT. The amplitude of this current and the phase relationship between V_{exc} and I_{res} provide the information to calculate admittance Y, as shown in Figure 4-2.

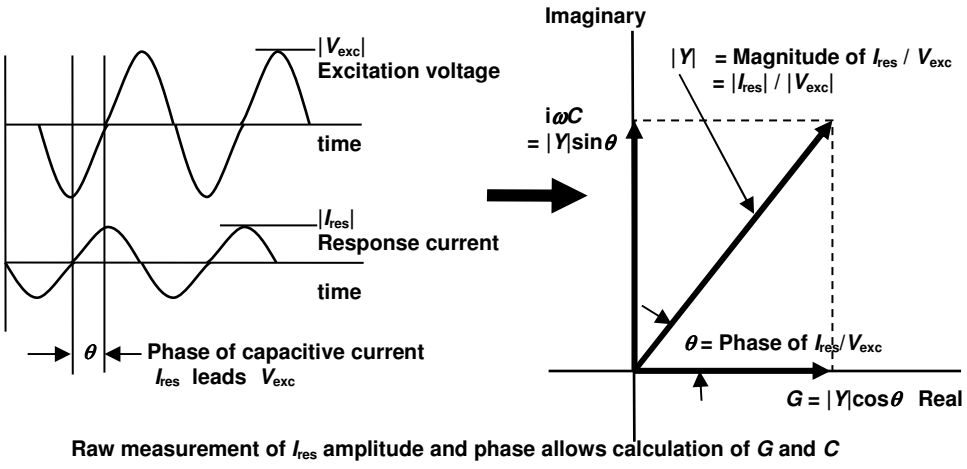

Figure 4-2
Signal relationships for the admittance of Material Under Test

Admittance *Y*, and therefore conductance *G* and capacitance *C*, of the MUT are defined by equation 4-1:

(eq. 4-1) $$Y_{MUT} = G_{MUT} + i\omega C_{MUT} = I_{res} / V_{exc}$$

Where:

I_{res}	= AC current through MUT	(a complex number, amps)
V_{exc}	= AC voltage across MUT	(a complex number, volts)
C_{MUT}	= Capacitance of MUT	(a real number, Farads)
G_{MUT}	= Conductance of MUT	(a real number, ohms^{-1})
f	= Excitation frequency	(Hz)
ω	= $2\pi f$	(angular frequency, radians/sec)

The material properties of relative conductivity σ', and relative permittivity ε'**,** can be calculated from equations 4-2 and 4-3, as shown in Figure 4-3.

(eq. 4-2) $$\sigma' = G / (\varepsilon_o A/D)$$ (relative conductivity)

(eq. 4-3) $$\varepsilon' = C / (\varepsilon_o A/D)$$ (relative permittivity)

Where:

ε_0 = 8.85 x 10^{-14} F/cm

A = Electrode area (cm^2)

D = Distance between electrodes (cm)

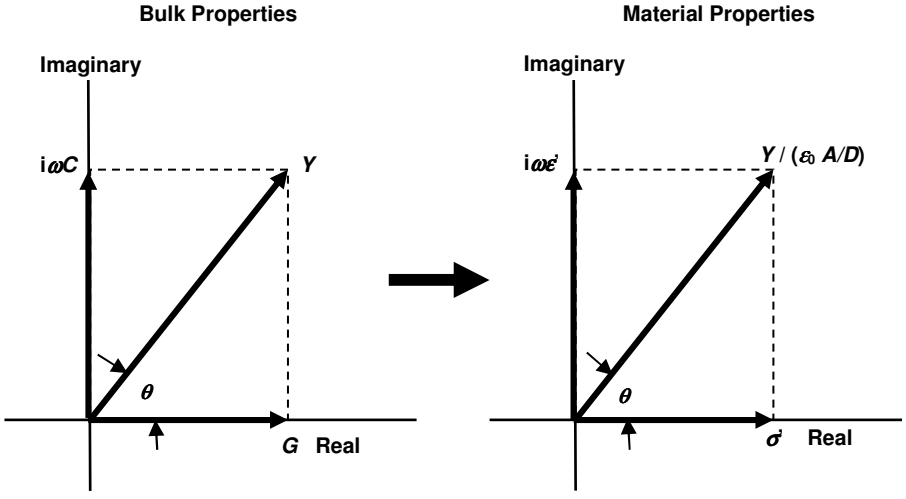

Figure 4-3
Converting bulk properties to material properties

It is preferable to obtain relative permittivity ε'_r and relative conductivity σ' (or conductivity σ) because they are fundamental material properties, which do not depend on the quantity of material being measured.

Chapter 5—Linear vs. Logarithmic Scales: Seeing All the Information

Conductance change during cure

During thermoset cure the conductance G_{MUT} between the electrodes of a sensor changes by several orders of magnitude. Before processing starts, conductance is normally low because the material is either solid or at a temperature too low for significant polymerization. Typically the thermoset is cured by heating to an elevated temperature. As the material becomes warm and softens, the conductance increases. The rate of reaction increases with temperature, also, and at some point its influence dominates and the material becomes more viscous—conductance reaches a maximum at this time then decreases as the material becomes rubbery then rigid. By the end of cure the conductance may have decreased by a factor of 100 or more from its peak value.

Data plotted on linear scales

Figure 5-1 shows how conductance varied during cures of several samples from the same batch of sheet molding compound (SMC). The data are plotted against a linear scale and reveal considerable sample to sample variation, with a 140% difference between the maximum and minimum values of peak conductance. At first glance the lack of consistency casts doubt about the usefulness of dielectric cure monitoring; however, to avoid misinterpretation, it is necessary to understand the factors that determine conductance.

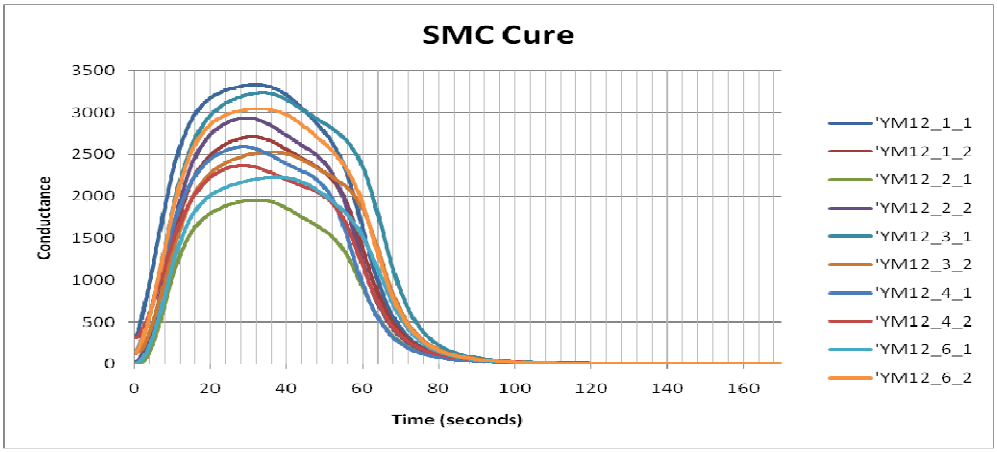

Figure 5-1
SMC conductance during cure, on a linear scale

Figure 5-2 shows a model of the conductance and capacitance of a material under test (MUT) between parallel plate electrodes. Note that only conductance is relevant in this section.

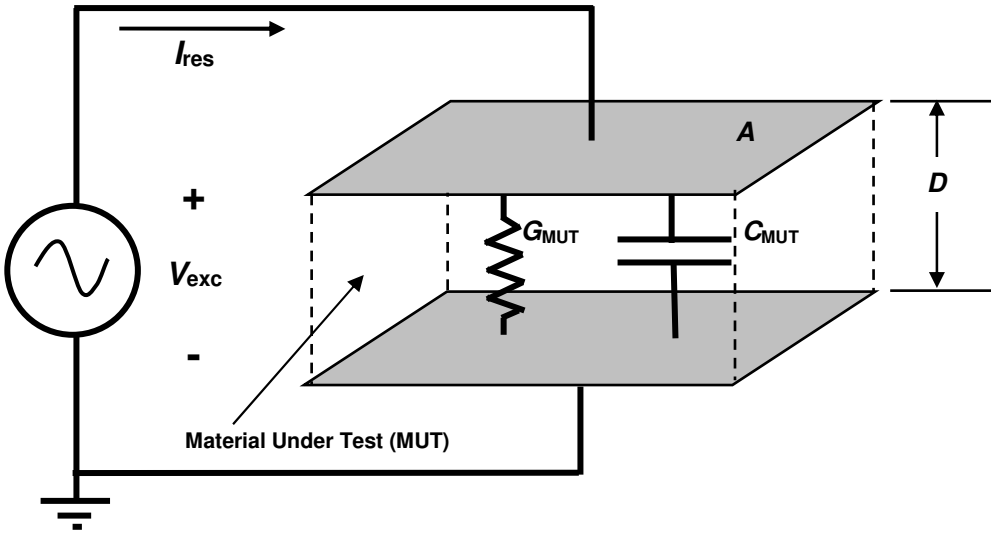

Figure 5-2
Electrical model of dielectric Material Under Test

Conductance and conductivity

Conductance is a bulk property that depends on the amount of Material Under Test, the geometry of the electrodes and the *conductivity* of the material between them. Like density, conductivity is a property that is independent of the quantity of material and how it is measured. During cure this conductivity changes with time, and the measured bulk conductance as a function of time, $G_{MUT}(t)$, is given by equation 5-1.

(eq. 5-1) $$G_{MUT}(t) = \sigma(t)\ (A/D) \qquad (ohm^{-1})$$

Where: $\sigma(t)$ = time varying conductivity (ohm^{-1}-cm^{-1})
A/D = ratio of electrode area to electrode separation (cm)

Several factors determine the time varying conductivity, which is given by equation 5-2.

(eq. 5-2) $\sigma(t) = n\ q\ \mu(t)$ $(ohm^{-1}\text{-}cm^{-1})$

Where: n = free ion concentration (cm^{-3})
q = magnitude of electronic charge (coulombs)
$\mu(t)$ = free ion mobility (cm^2 / (V-s))

Assuming the free ion concentration and the charge of the free ions do not change during cure, then only the change in free ion mobility, $\mu(t)$, affects conductivity and ultimately conductance. In a thermoset, perhaps the most significant factor determining mobility is the polymerization of monomers. As molecular chain length or crosslink density increase, the growing network impedes the flow of ions and reduces their mobility.

Combining equations 5-1 and 5-2 produces the following expression:

(5-3) $G_{MUT}(t) = [n\ (A/D)\ q]\ \mu(t)$

In reality, the value of $[n\ (A/D)\ q]$ may change from sample to sample and test to test. The free ion concentration, n, increases with conductive additives and decreases with non-conductive filler. The geometry (A/D) of the electrodes may differ from sensor to sensor because of variations in fabrication or set up. The free ion charge normally does not change but is included with the terms in brackets for simplicity. Equation 5-3 may then be reduced to:

(5-4) $G_{MUT}(t) = [B]\ \mu(t)$

Here $B = n\ (A/D)\ q$, the variable terms unrelated to curing. Expressed logarithmically, equation 5-4 becomes:

(5-5) $\log_{10}(G_{MUT}(t)) = \log_{10}(B) + \log_{10}(\mu(t))$

From equation 5-5, plotting the measured conductance on a logarithmic scale captures the entire range of $G_{MUT}(t)$ caused by the mobility, which can change by several orders of magnitude during cure.

Plotting on a logarithmic scale also produces an offset, which is $\log_{10}(B)$, caused by the terms unrelated to curing. If the free ion concentration and the electrode geometry are constant for a particular sample and test, then *the result is a constant offset from the baseline behavior* of $\log_{10}(\mu(t))$.

Effect of mixing and fillers

For a single batch of liquid resin, good mixing can produce a homogeneous free ion concentration, and the measured conductance can be uniform from sample to sample. In contrast, a material like SMC has a high content of non-conductive chopped glass fibers mixed with polyester, vinyl ester or epoxy resin. This composite is semi-solid, is difficult to mix well, and as a result different samples may have different ratios of fiber to resin. The measured conductance of SMC is therefore likely to vary among samples from a single batch, as illustrated in Figure 5-3.

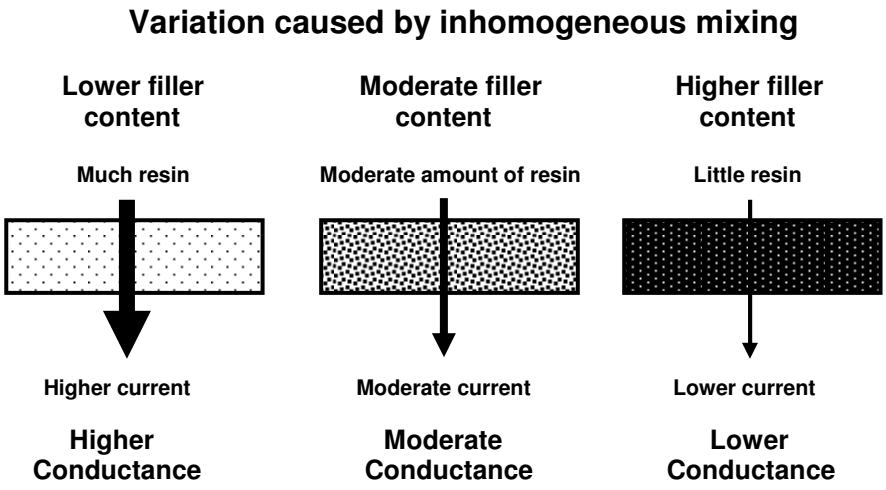

Figure 5-3
Addition of non-conductive filler reduces amount of conductive resin

Data plotted on logarithmic scales

When the data of Figure 5-1 are plotted on the logarithmic scale, the curves are largely parallel to one another and differ by an offset in conductance. This offset is typically caused by sample-to-sample variation in filler content, which does not affect the cure rate.

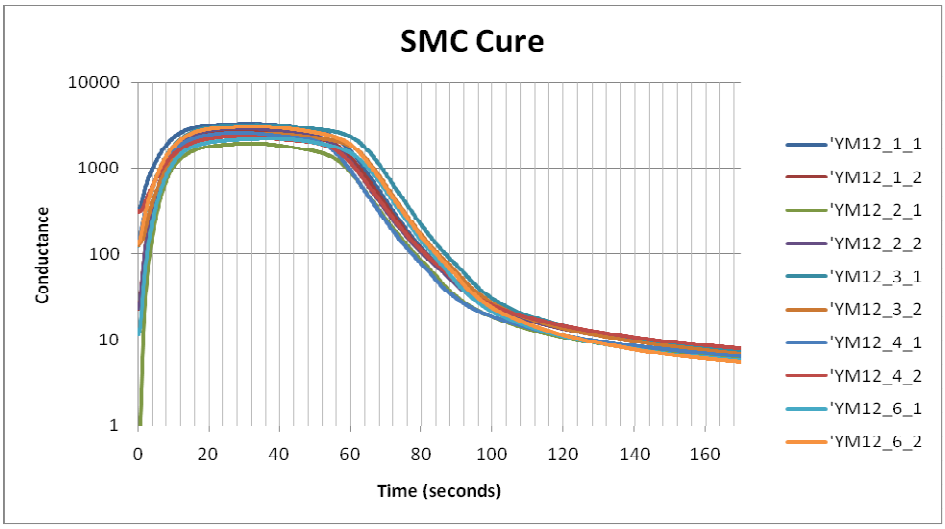

Figure 5-4
SMC conductance during cure, on a logarithmic scale

Plotting conductance on a logarithmic scale has significant advantages compared to a linear scale:

- The entire range of conductance is visible
- Only factors that affect cure determine the shape of the curve
- Factors that do not affect cure, such as variations in filler content or sensor geometry, determine offsets of the curve but not its shape

Consequently, using a logarithmic scale is the optimum method for seeing all information available from dielectric cure monitoring. Conductance, however, is not typically used to study thermoset cure. Resistance is the reciprocal of conductance and measuring the material property of frequency independent resistivity—ion viscosity—is more conventional.

By representing the SMC cure of Figure 5-4 as resistance, Figure 5-5 shows resistive behavior is simply the inverse of conductive behavior. At the beginning of processing, resistance is normally high because the material is either solid or at a temperature too low for significant polymerization. As temperature increases, the material softens and resistance decreases. The rate of reaction increases with temperature and at some point its influence dominates and the material becomes more viscous—resistance reaches a minimum at this time then increases as the material becomes rubbery then rigid. By the end of cure the resistance may have increased by several orders of magnitude from its minimum value.

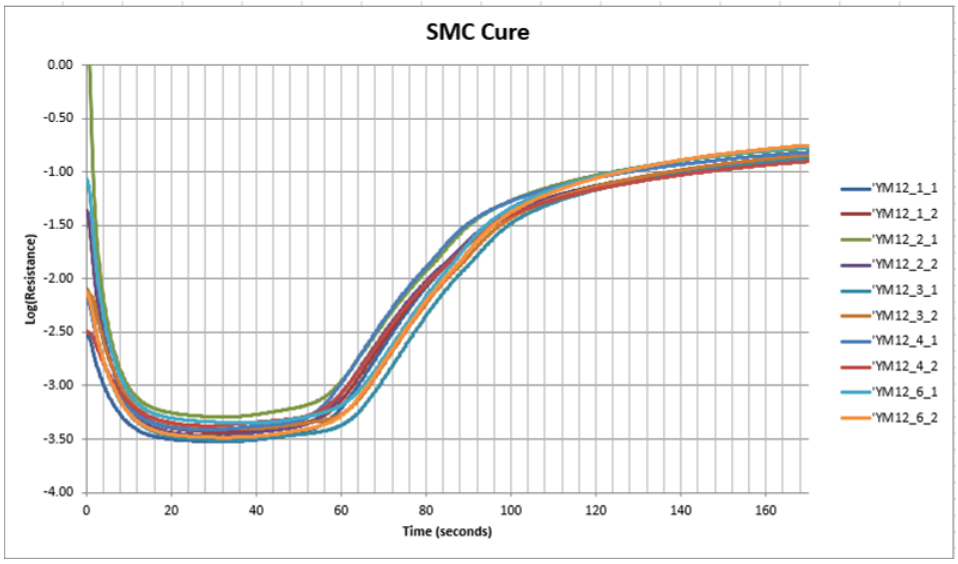

Figure 5-5
SMC resistance during cure, on a logarithmic scale

As with conductance, resistance plotted on a logarithmic scale reveals the progress of cure in the shape of the curve. Factors unrelated to cure, such as differences in background ion concentration or sensor geometry, cause offsets in the curve.

The two most common sensor configurations are the parallel plate and the planar interdigitated electrode, both depicted in Figure 5-6.

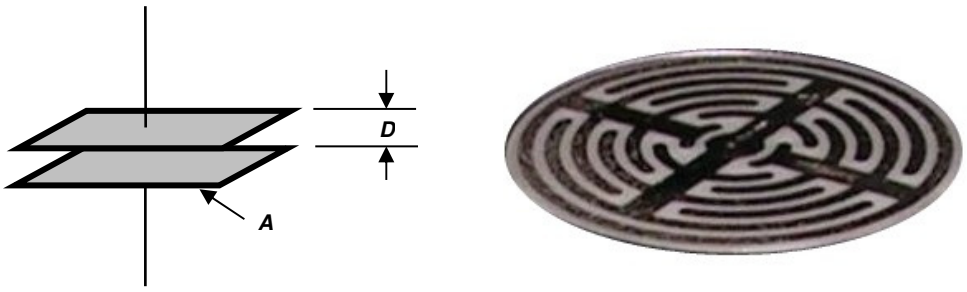

Parallel plates—
***R* = *ρ* / (*A*/*D*)**

Interdigitated electrodes—
***R* = *ρ* / (*A*/*D*)**

Figure 5-6
Parallel plate and interdigitated electrode geometries

The bulk property of resistance (*R*) is related to the material property of resistivity (*ρ*) by a scaling factor or cell constant. For the parallel plate

configuration of Figure 5-2 this scaling factor is the ratio of plate area *A* to plate distance *D*, or *A/D*. For planar interdigitated electrodes, this scaling factor is still called the *A/D* ratio even though area and distance are not as apparent.

As with conductivity, resistivity changes with time during cure, and the measured bulk resistance as a function of time, $R_{MUT}(t)$, is given by equation 5-6.

(eq. 5-6) $$R_{MUT}(t) = \rho(t) / (A/D) \quad \text{(ohm)}$$

Where: $\rho(t)$ = time varying resistivity (ohm-cm)
A/D = ratio of electrode area to electrode separation (cm)

The goal of dielectric cure monitoring is to reduce measurement of this resistance to the material property of resistivity, to produce data that are independent of sensor geometry.

Chapter 6–Sensors, A/D Ratio and Base Capacitance

Sensors and A/D ratios

Measurements of dielectric properties often involve the use of simple parallel plate electrodes. However, their separation can change with pressure, or expansion and contraction of the material between them. The ratio of electrode area *A* and the distance *D* between them—the *A*/*D* ratio—therefore may not be well known. As the cell constant or scaling factor between conductance and conductivity, or capacitance and permittivity, uncertainty in *A*/*D* causes inaccuracies in determining dielectric material properties.

A common alternative is the interdigitated electrode like the one shown in Figure 6-1. A rigid substrate supports the electrodes and resulting the planar structure does not change with pressure, or expansion and contraction of the Material Under Test.

The *A*/*D* ratio of parallel plate electrodes may be generalized for application to interdigitated electrodes. In this case, *A* is not simply the area of the electrodes and *D* is not simply the distance between them. For interdigitated electrodes, the *A*/*D* ratio also accounts for fringing electric fields and as a result can also act as the scaling factor between conductance and conductivity, and capacitance and permittivity.

Two-dimensional numerical simulations and experimental results have validated this generalization across a wide range of conductivity. The benefit of using interdigitated electrodes is an *A*/*D* ratio that is not affected by pressure, or expansion and contraction.

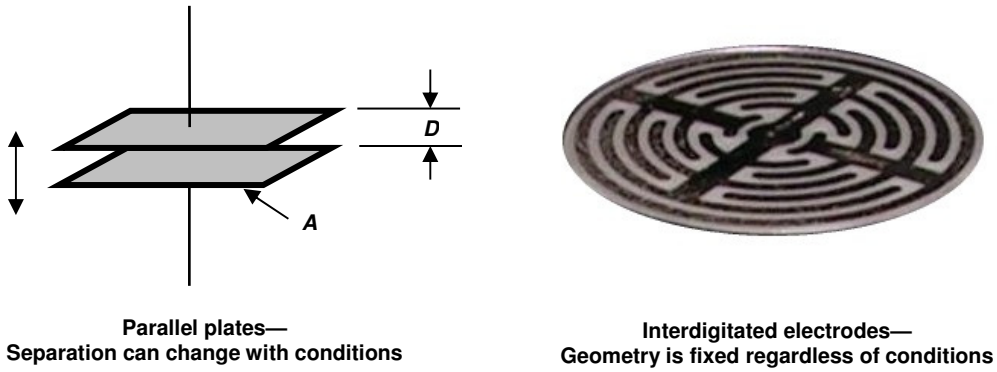

Figure 6-1
Comparison of parallel plate and interdigitated electrodes

Base capacitance

The substrate supporting interdigitated electrodes introduces an additional component into the system being measured. The cross-section of Figure 6-2 shows capacitance C_{tot} has a contribution C_{MUT} from the Material Under Test (MUT) above electrodes. However, there is also a contribution C_{base} from the substrate beneath the electrodes. This second component is called the *base capacitance*.

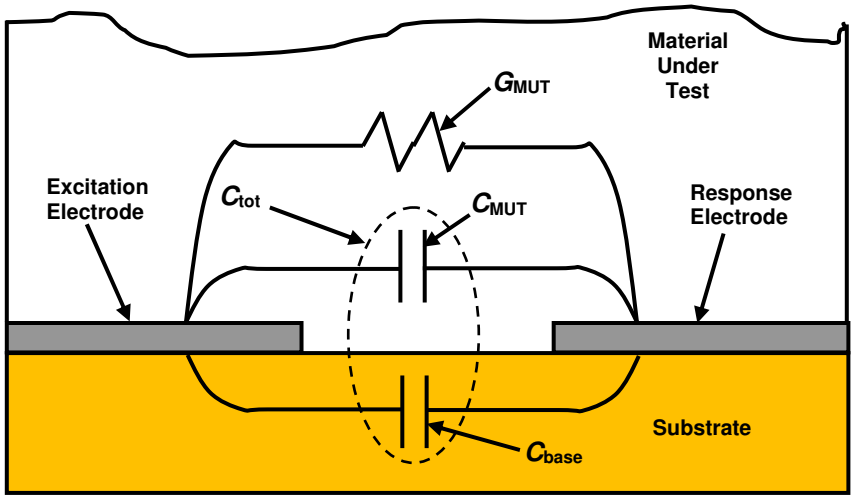

Figure 6-2
Cross section of interdigitated electrode structure

The total capacitance between the interdigitated electrodes is:

(eq. 6-1) $$C_{tot} = C_{MUT} + C_{base}$$

Therefore the capacitance of the MUT is:

(eq. 6-2) $$C_{MUT} = C_{tot} - C_{base} = \varepsilon_o \, \varepsilon'_{MUT} \, A/D$$

Where:

ε_0 = 8.85 x 10^{-14} F/cm
ε'_{MUT} = Relative permittivity of Material Under Test
A = Electrode area (cm^2)
D = Distance between electrodes (cm)

Finally, the conductivity (σ), ion viscosity (IV) and relative permittivity (ε'_{MUT}) of the MUT are:

(eq. 6-3) $$\sigma_{MUT} = G_{MUT} / (A/D)$$

(eq. 6-4) $$IV = \rho_{MUT} = (A/D) / G_{MUT}$$

(eq. 6-5) $$\varepsilon'_{MUT} = C_{MUT} / [\varepsilon_o (A/D)] = (C_{tot} - C_{base}) / [\varepsilon_o (A/D)]$$

Comparison of measurements with different sensors

If electrode geometry is properly factored into dielectric measurements, a material property like resistivity (ρ) will have the same value regardless of the sensor. For example, the Ceramicomb-1"[1] and Mini-Varicon[2] sensors of Figure 6-3, have very different constructions and electrode configurations. Specifications of these two sensors are listed in Table 6-1.

a. **b.**

Figure 6-3
Ceramicomb-1" sensor (a.) and Mini-Varicon sensor (b.)

Table 6-1
Comparison of Ceramicomb-1" and Mini-Varicon sensors

Sensor	Ceramicomb-1"	Mini-Varicon
Electrode Width	0.020"	0.004"
Electrode Spacing	0.020"	0.004"
Substrate	Alumina (ε_r = 9.8)	Polyimide (ε_r = 3.6)
A/D	10 cm	80 cm
Base Capacitance	≈25 pF	≈25 pF

The Ceramicomb-1" has an A/D ratio 1/8th that of the Mini-Varicon, and correspondingly has 1/8th the sensitivity. To compare results from different sensors, a Ceramicomb-1" measured dielectric properties during cure on the surface of a graphite-epoxy prepreg and a Mini-Varicon measured dielectric properties between two layers of the same prepreg, as shown in Figure 6-4.

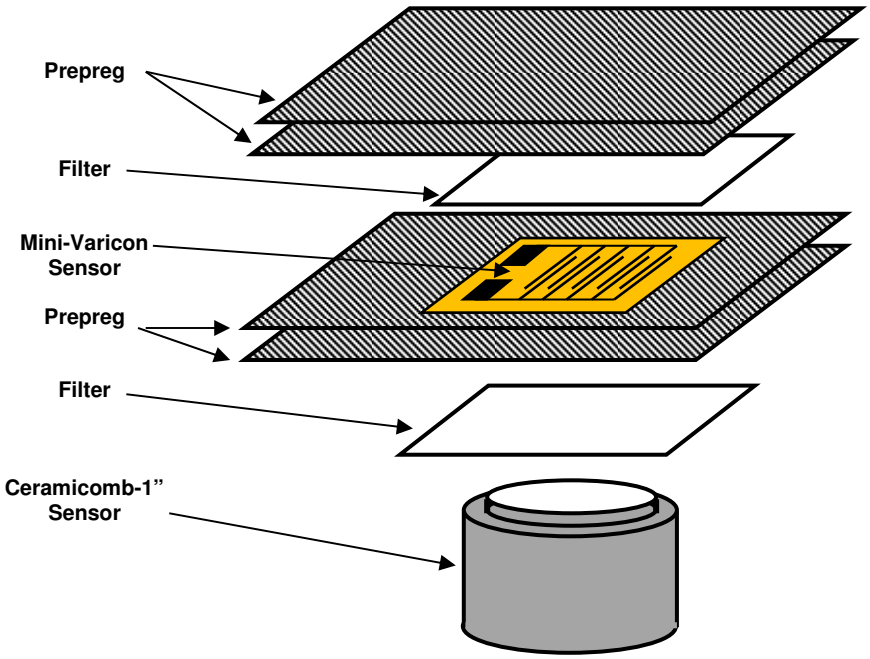

Figure 6-4
Lay-up of Ceramicomb-1" and Mini-Varicon sensors

Figure 6-5 shows the log(*ion viscosity*) and slope of log(*ion viscosity*) obtained with a frequency of 100 Hz from the two sensors during a single experiment. For brevity, log*(ion viscosity)* will be called log*(IV)* and the slope of log*(ion viscosity)* will simply be called *slope*.

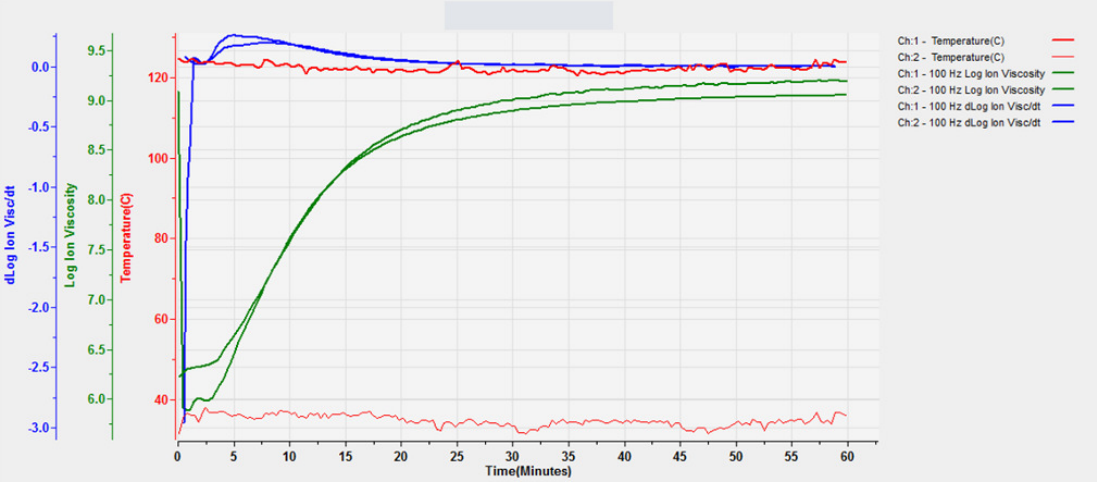

Figure 6-5
Cure of prepreg, two sensors simultaneously
(Ceramicomb-1" sensor on surface, Mini-Varicon sensor between plies)

Both the log*(IV)* and *slope* curves overlap very well, demonstrating measurement of a material property independent of the amount of sample or the geometry of the sensor. After 10 minutes the curves for *slope* overlap almost completely, indicating that cure rates at the end are essentially identical on the surface and within the laminate. For clarity, only the log(*IV*) curves are displayed in Figure 6-6 and only the *slope* curves are displayed in Figure 6-7.

Figures 6-6 and 6-7 illustrate that with the correct *A/D* ratio, different sensors provide the same cure data and are interchangeable for measuring ion viscosity. Note that equation 6-4 indicates *only A/D ratio is used to calculate ion viscosity* from the conductance between electrodes, G_{MUT}. Equation 6-5, however, shows that the base capacitance must be subtracted from the capacitance between electrodes, C_{tot}, to obtain the capacitance of the Material Under Test, C_{MUT}.

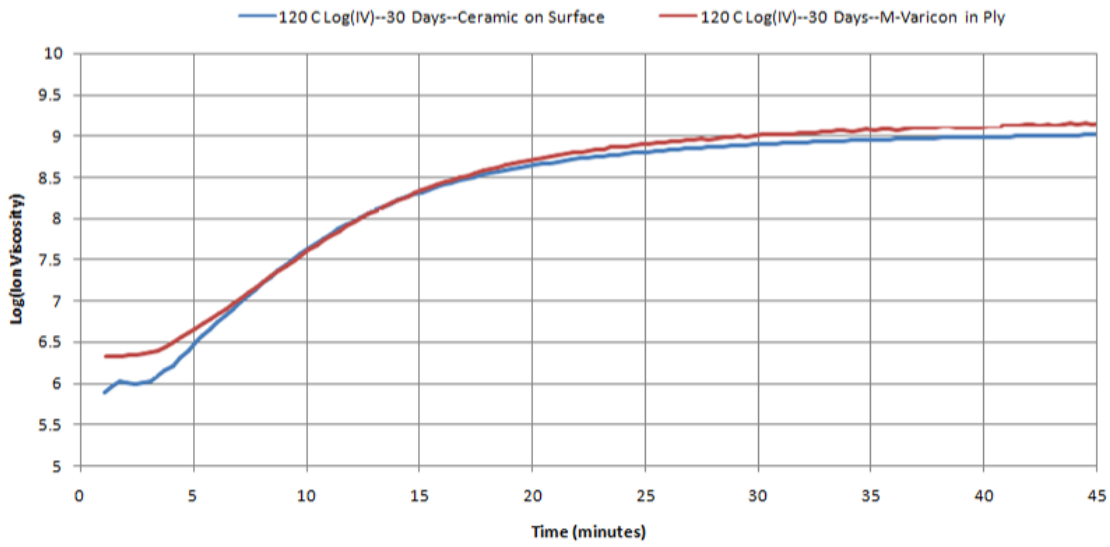

Figure 6-6
Log(*IV*) for Ceramicomb-1" and Mini-Varicon sensors

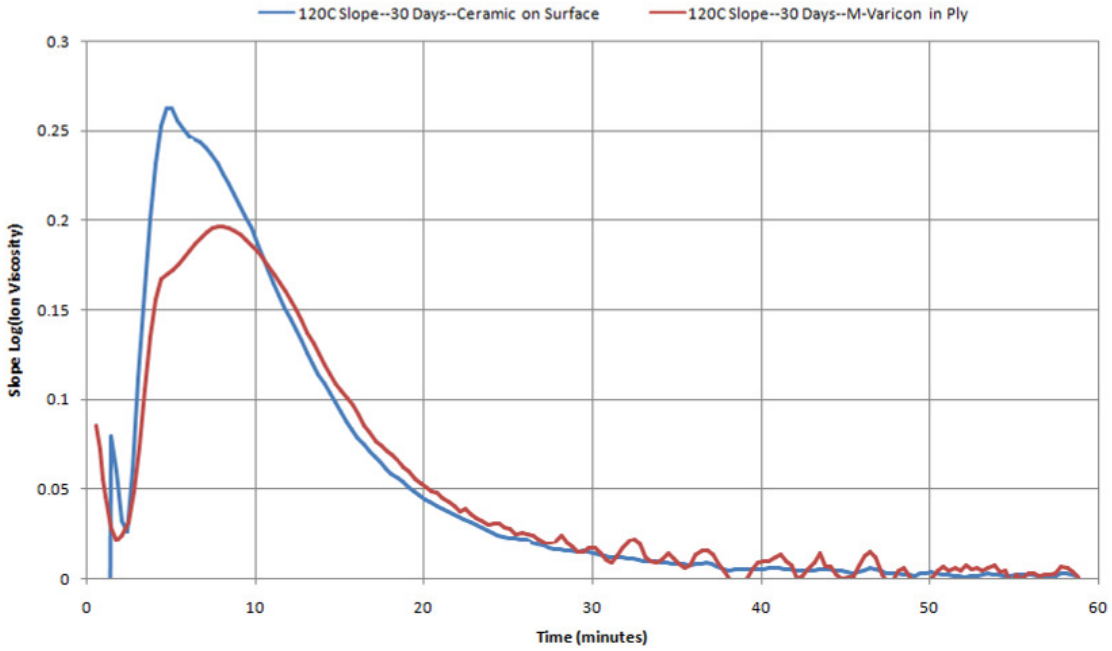

Figure 6-7
***Slope* for Ceramicomb-1" and Mini-Varicon sensors**

References

1. Ceramicomb-1" sensor, manufactured by Lambient Technologies, Cambridge, MA USA. https://lambient.com

2. Mini-Varicon sensor, manufactured by Lambient Technologies, Cambridge, MA USA

Chapter 7–Viscosity, Ion Viscosity and Critical Points

Conductivity and resistivity in materials

Dielectric cure monitoring measures the bulk conductance and capacitance of a Material Under Test (MUT), which are used to calculate the material properties of conductivity and permittivity.

Conductivity (σ) has both frequency independent (σ_{DC}) and frequency dependent (σ_{AC}) components. In an oscillating electric field, σ_{DC} arises from the flow of mobile ions while σ_{AC} arises from the rotation of stationary dipoles. These two responses act like electrical elements in parallel and add together to produce the total conductivity:

(Eq. 7-1) $\sigma = \sigma_{DC} + \sigma_{AC}$ $(ohm^{-1} - cm^{-1})$

Resistivity (ρ) is the inverse of conductivity as shown below:

(Eq. 7-2) $\rho = 1 / \sigma$ (ohm-cm)

Like conductivity, resistivity has both frequency independent (ρ_{DC}) and frequency dependent (ρ_{AC}) components.

Of particular interest for cure monitoring is the frequency independent resistivity, $\rho_{DC,}$ because of its relationship to mechanical viscosity. Before gelation, the amount of polymerization affects both mechanical viscosity and the movement of ions, and therefore influences ρ_{DC}.

For convenience, unless otherwise indicated, this chapter will use the term *frequency independent resistivity* to refer to ρ_{DC}. Similarly, the term *viscosity* will refer to *mechanical viscosity*.

Viscosity and resistivity

Viscosity is a measure of how easily the molecules of a fluid move past one other in response to shear forces, and in the case of polymeric materials is determined by the motion of polymer chain segments. In contrast, resistivity is a measure of the mobility of free ions through a medium under the influence of an electric field. Frequency independent resistivity (ρ_{DC}) is given by equation 7-3.

(eq. 7-3) $\rho_{DC} = 1 / (q \mu n)$ (ohm-cm)

Where: q = magnitude of electronic charge (coulombs)
μ = free ion mobility (cm^2 / (V-s))
n = free ion concentration (cm^{-3})

Mobility determines the rate of ionic diffusion through a medium, and is given by the Einstein relationship of equation 7-4:

(eq. 7-4) $\mu = q D / (k T)$ (cm^2 / (V-s))

Where: D = diffusion coefficient (cm^2 / s)
k = Boltzmann's constant (eV / K)
T = temperature in degrees Kelvin (K)

If mobile ions are modeled as spherical particles, then in the limit of low Reynold's numbers, the diffusion coefficient, D, is given by the Stokes-Einstein relation of equation 7-5:

(eq. 7-5) $D = k T / (6\pi \eta r)$ (cm^2 / s)

Where: η = mechanical viscosity (g / (cm-s))
r = radius of sphere (cm)

Combining equations 7-3, 7-4 and 7-5 yields the following relationship between frequency independent resistivity and viscosity:

(eq. 7-6) $\rho_{DC} = (6\pi \eta r) / (q^2 n)$ (ohm-cm)

$\therefore \quad \rho_{DC} \propto \eta$

Consequently, frequency independent resistivity is proportional to viscosity. To emphasize this relationship, the term *ion viscosity* (*IV*) was coined as a synonym for frequency independent resistivity and is defined as:

(Eq. 7-7) $IV = \rho_{DC} = 1 / \sigma_{DC}$ (ohm-cm)

Often differing by only a scaling factor, the change in ion viscosity and the change in mechanical viscosity are related to the cure state of thermosets and composites. The electrical measurement of ion viscosity requires no mechanical components, yet provides information about a mechanical property.

Empirical results show the proportionality of equation 7-6 is valid in many cases, although for poorly understood reasons some systems obey a power law:

(eq. 7-8) $\rho_{DC} \propto \eta^n$ where n = 1, 2, 3 . . . (ohm-cm)

Simultaneous measurements of viscosity and ion viscosity

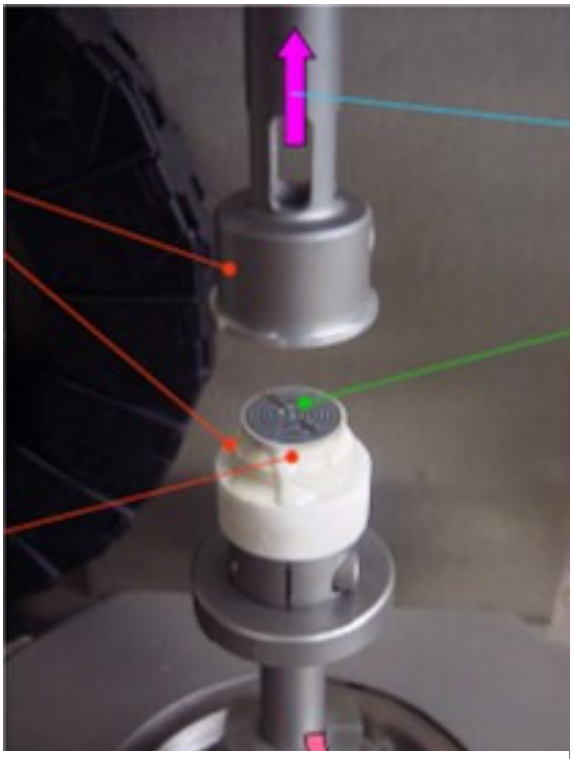

Figure 7-1
Simultaneous DMA-DEA apparatus

Simultaneous measurements of viscosity and ion viscosity are possible with combined dynamic mechanical analysis (DMA) and dielectric cure monitoring (DEA) equipment, such as in Figure 7-1. Results of DMA-DEA testing with this particular apparatus are plotted in Figure 7-2, showing the correlation between viscosity and ion viscosity for this particular epoxy.

A similar simultaneous test used a rheometer to monitor viscosity during the cure of another epoxy. Viscosity was measured with a Rheological Dynamic Spectrometer and ion viscosity was measured with a Micromet Instruments Eumetric III Microdielectrometer. The two curves in Figure 7-3 show strong correlation from the beginning of cure up to gelation at about 135 minutes. After the gel point, viscosity increases rapidly and becomes immeasurable. Ion viscosity, however, continues to provide information and after gelation is often proportional to the change in modulus. As a result, DEA can follow material state through the entire cure.

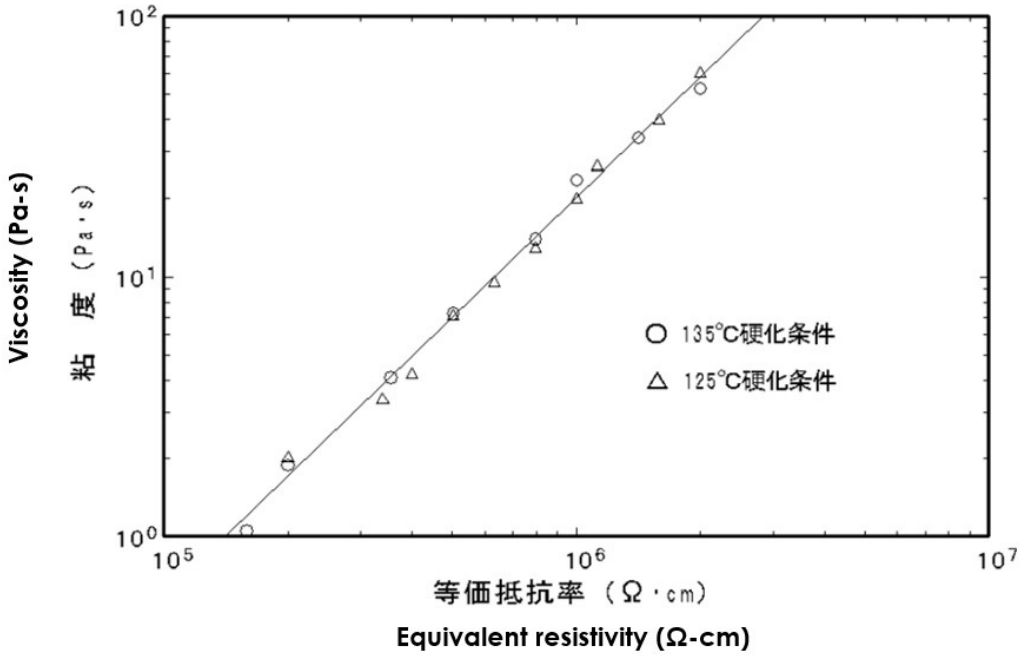

Figure 7-2[1]
Viscosity and resistivity (ion viscosity) for simultaneous DMA-DEA measurement during cure of an epoxy

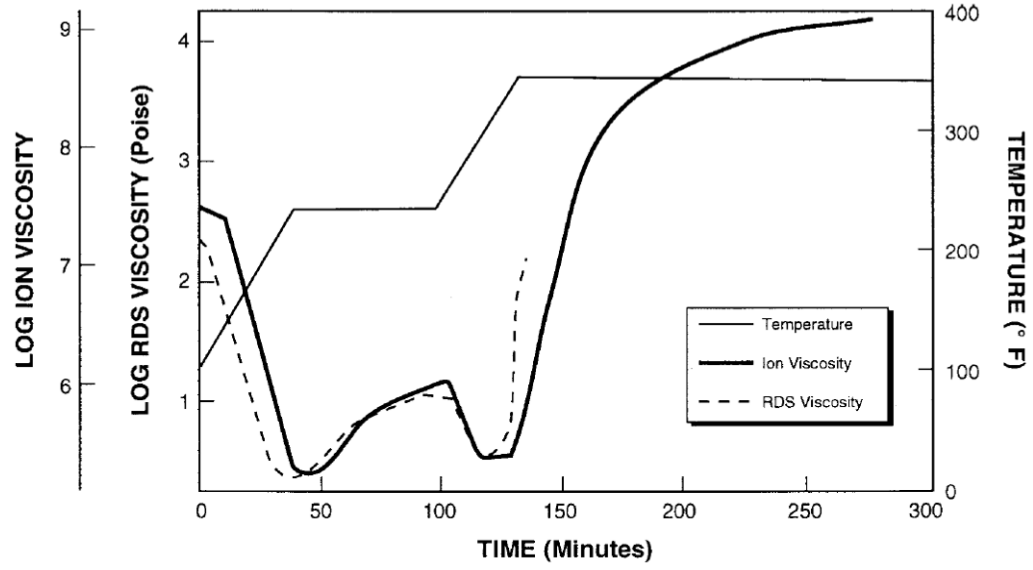

Figure 7-3[2]
Viscosity and ion viscosity during cure of an epoxy

Critical Points during thermoset cure

A thermoset cures when monomers react to form polymer chains then a network. The reaction is usually exothermic—generating heat—and may additionally be driven by the heat of a press or oven. A plot of log(*ion viscosity*) is a simple way to characterize the progress of cure and Figure 7-4 shows the behavior of a typical thermoset with one ramp and hold step in temperature.

At first as temperature increases, the material softens or melts and mechanical viscosity decreases. Mobile ions also experience less resistance to movement and ion viscosity decreases. At this point the reaction is still slow.

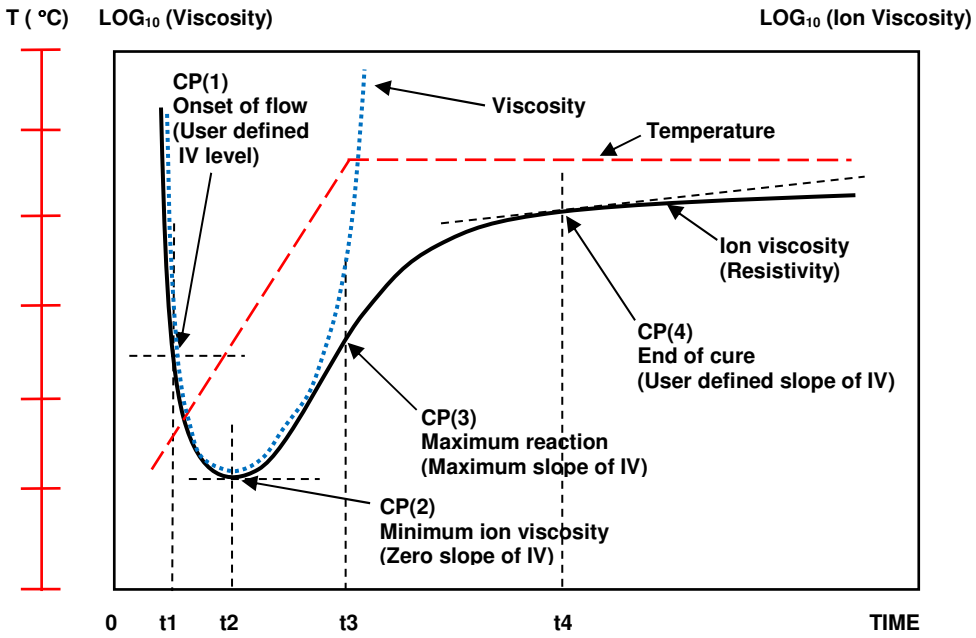

Figure 7-4
Typical ion viscosity behavior of thermoset cure during thermal ramp and hold

As the material becomes hotter, the cure rate increases. At some time the accelerating reaction begins to dominate; mechanical viscosity reaches a minimum then the material becomes more viscous. Electrically, the increase in ion viscosity due to polymerization overcomes the decrease in ion viscosity due to higher temperature. Ion viscosity also reaches a minimum then increases due to chain extension, which presents a greater and greater impediment to the flow of ions.

After the minimum point, ion viscosity increases continuously until the concentration of unreacted monomers diminishes and the reaction rate

decreases. Consequently, the slope of ion viscosity also decreases and eventually reaches a value of zero when cure has stopped completely.

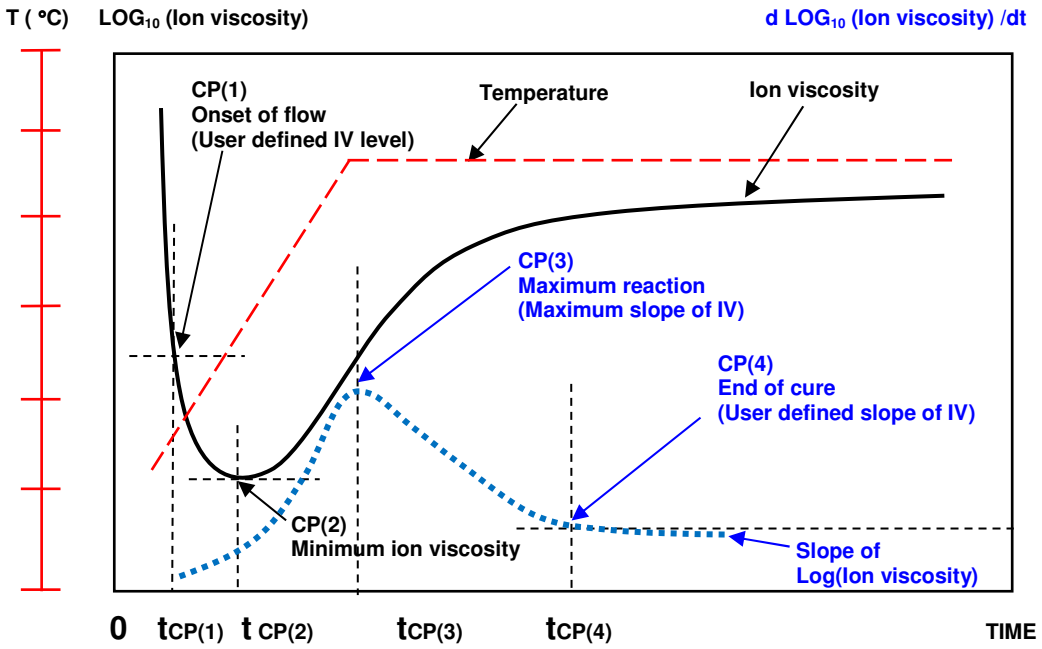

Figure 7-5
Ion viscosity curve and slope of ion viscosity of thermoset cure during thermal ramp and hold

As shown in Figure 7-5, four Critical Points characterize the dielectric cure curve:

- CP(1)—A user defined level of *log(IV)* to identify the onset of material flow.
- CP(2)—Minimum ion viscosity, which closely corresponds to minimum mechanical viscosity, indicating when polymerization and increasing viscosity begin to dominate the material's behavior.
- CP(3)—Maximum *slope*, which identifies the time of maximum reaction rate. The height of CP(3) is a relative measure of the reaction rate and CP(3) is often used as a signpost associated with gelation.
- CP(4)—A user defined *slope* that can define the end of cure. The decreasing *slope* corresponds to the decreasing reaction rate.

Figures 7-4 and 7-5 illustrate the typical behavior of curing thermosets when temperature gradually ramps to a hold value. The response is slightly different when the material under test is essentially isothermal, as shown in Figure 7-6.

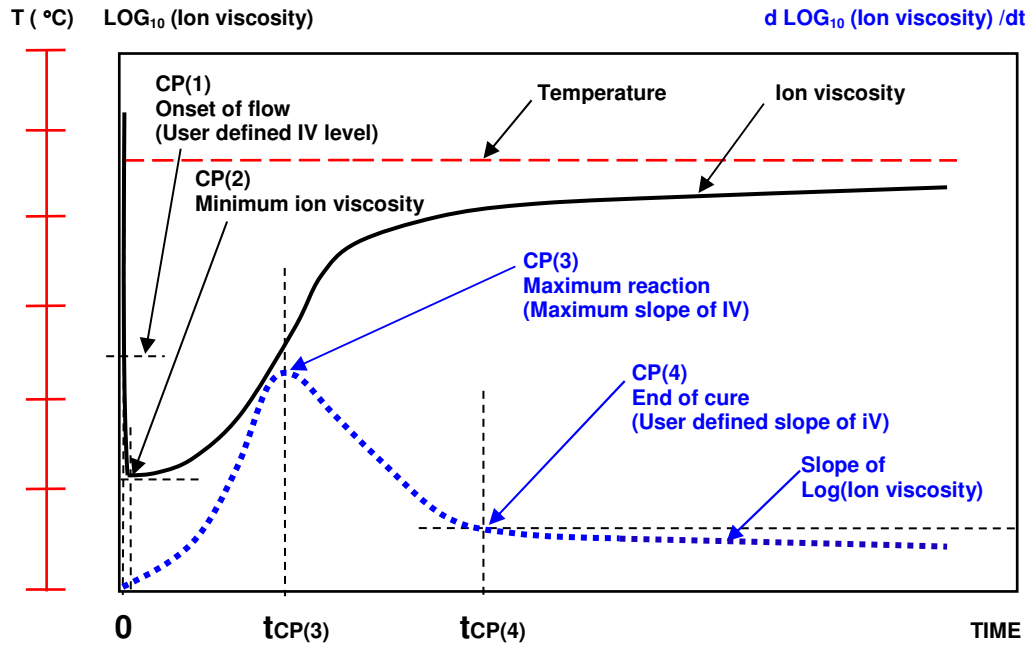

Figure 7-6
Ion viscosity curve and slope of ion viscosity of thermoset cure during isothermal processing

In this case CP(1) either is meaningless or occurs immediately after the application of heat, when material flows and contacts the sensor. Minimum ion viscosity also occurs at t = 0 or shortly afterwards because cure begins immediately. For isothermal cures, CP(3) and CP(4) are conceptually the same as for ramp and hold conditions.

Correlation of ion viscosity with other properties

In addition to mechanical viscosity, other properties also depend on the degree of polymerization or crosslinking and it is useful to investigate their relationship to ion viscosity. Figures 7-7, 7-8 and 7-9 show published data correlating viscosity, glass transition temperature and sound speed with ion viscosity or its reciprocal, conductivity. Each of these cases demonstrates how electrical measurements can probe material or cure state.

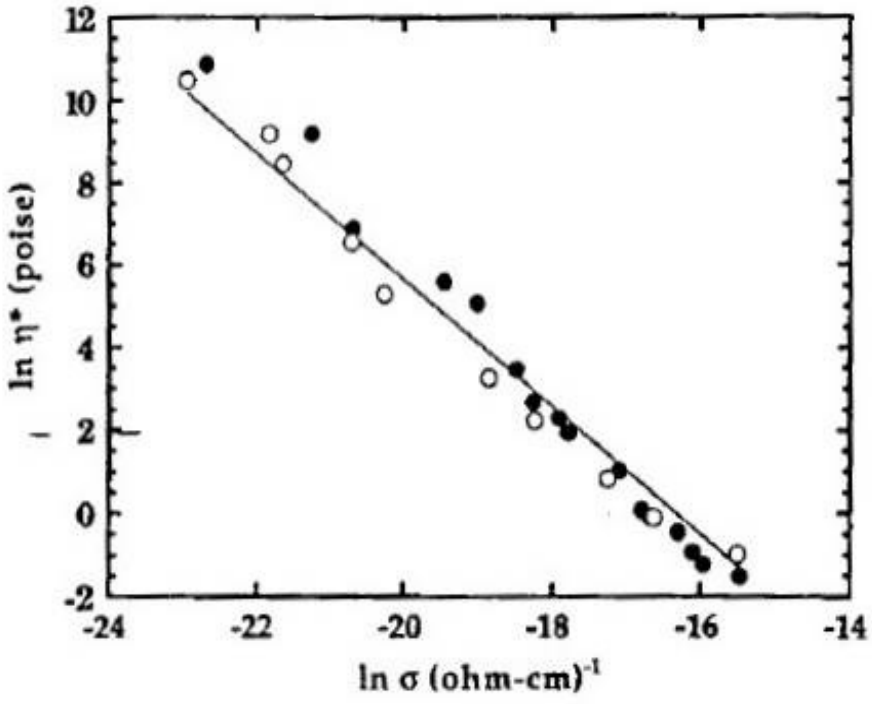

Figure 7-7[3]
Viscosity vs. conductivity (ion viscosity = 1/conductivity) for an epoxy

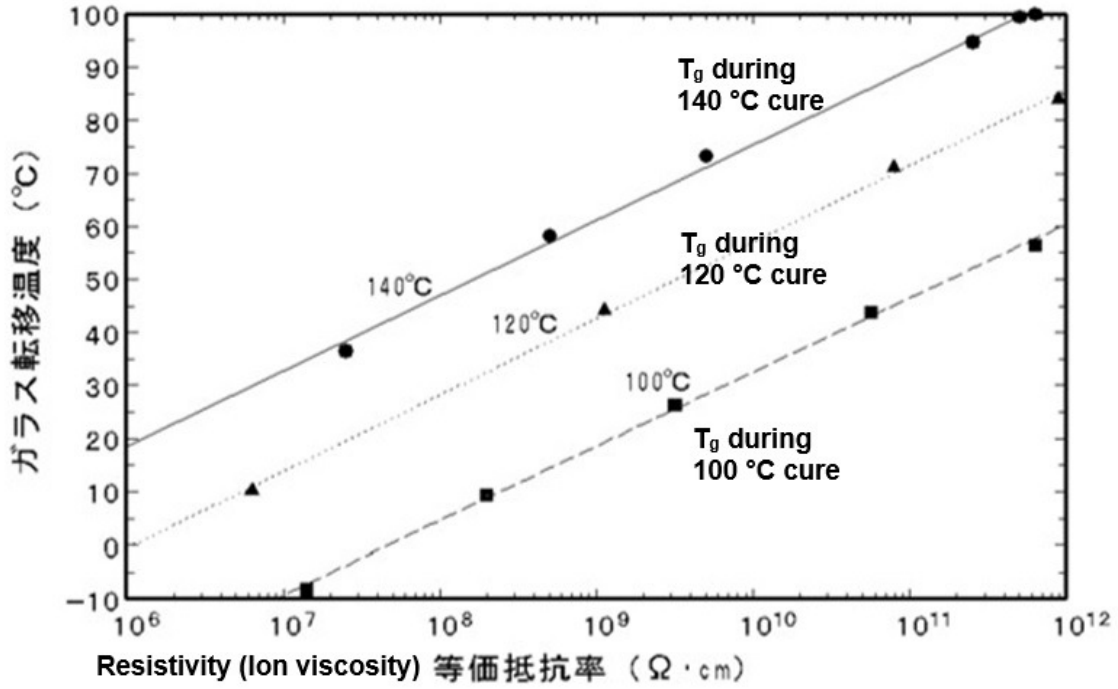

Figure 7-8[1]
Glass transition temperature vs. resistivity (ion viscosity) for an epoxy

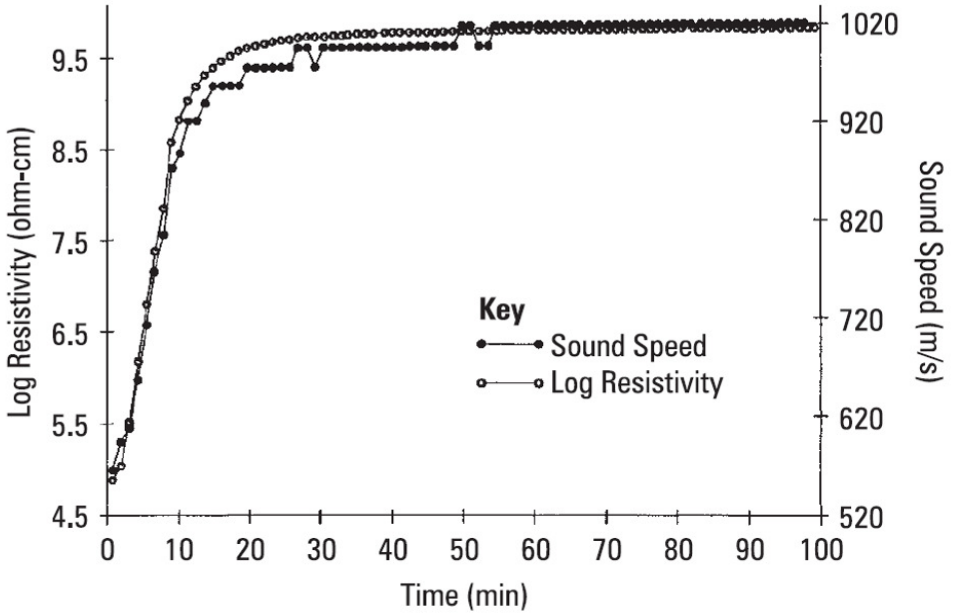

Figure 7-9[4]
Resistivity (ion viscosity) vs. sound speed
for a curing epoxy-fiberglass prepreg

Every material is different and users should always confirm correlations of ion viscosity with other properties. Nevertheless, dielectric cure monitoring (DEA) joins other thermal analysis techniques like differential scanning calorimetry (DSC) and dynamic mechanical analysis (DMA) as a valuable tool for studying curing thermosets and composites.

References

1. S. Makishima, T. Nakano, M. Koyama, Y Inoue,"Dielectric Property of Curing Epoxy Resin and Application for Casting Process," IEEE Electrical Electronics Insulation Conference, Sept. 18-21, 1995

2. Shepard, D., "Cure Monitoring of Thermosetting Resins Utilizing Dielectric Sensors," Holometrix-Micromet, Cambridge, MA USA

3. J. Simpson and S. Bidstrup, "Rheological and Dielectric Changes During Isothermal Epoxy-Amine Cure," J. of Polymer Science Part B: Polymer Physics, vol. 33, issue 1, pp 55-62 (1.1995)

4. D. Shepard and K. Smith, "Ultrasonic Cure Monitoring of Advanced Composites," Sensor Review, vol. 19 Issue: 3, pp. 187-194 (1999)

Chapter 8–Ion Viscosity and Loss Factor

Permittivity and loss factor

Dielectric permittivity ε^* is a quantity with real and imaginary parts:

(Eq. 8-1) $$\varepsilon^* = \varepsilon_0 (\varepsilon' + i\,\varepsilon'') = \varepsilon_0 [\varepsilon' + i\,\sigma / (\varepsilon_0\,\omega)]$$

Where: $\varepsilon_0 = 8.854 \times 10^{-14}$ F/cm (permittivity of free space)
$\omega = 2\pi \bullet f$ (angular frequency)
f = oscillation frequency (Hz)

Conductivity (σ) is the sum of frequency independent (σ_{DC}) and frequency dependent (σ_{AC}) components, as expressed below:

(Eq. 8-2) $$\sigma = \sigma_{DC} + \sigma_{AC}$$

The real part of relative permittivity or relative dielectric constant (ε') also has frequency independent and frequency dependent components, but they will not be treated in this chapter.

In an oscillating electric field, σ_{DC} arises from the flow of mobile ions while σ_{AC} arises from the rotation of stationary dipoles. The dimensionless term *loss factor* (ε'') is a measure of the dissipation, or loss, of electromagnetic energy as heat and is given by:

(Eq. 8-3) $$\varepsilon'' = \sigma / (\omega\,\varepsilon_0) = (\sigma_{DC} + \sigma_{AC}) / (\omega\,\varepsilon_0)$$

During the early part of cure, when a thermoset is most conductive, σ_{DC} tends to dominate the dielectric response across a broad range of frequencies. At sufficiently low frequencies σ_{DC} may also be the significant component through the entire cure. When σ_{DC} dominates cure behavior, σ_{AC} is insignificant and loss factor may be approximated as:

(Eq. 8-4) $$\varepsilon'' \approx \sigma_{DC} / (\omega\,\varepsilon_0)$$

In this case, loss factor is inversely proportional to frequency. For example, if the excitation frequency (ω) *decreases* by a factor of 10, loss factor *increases* by the same factor of 10—this relationship identifies when σ_{DC} dominates the dielectric response and can indicate cure state.

During the latter part of cure, frequency *dependent* conductivity due to dipoles may dominate the dielectric response, especially at higher frequencies. It is important to identify these times and frequencies to avoid misinterpreting data when studying cure.

Cure monitoring with multiple frequencies

Figure 8-1 shows dielectric data at multiple frequencies during the cure of "five-minute epoxy." A plot of loss factor can reveal when frequency independent conductivity σ_{DC} dominates the dielectric response. In the early part of this cure, loss factors for 10 Hz, 100 Hz, 1 kHz, and 10 kHz all are inversely proportional to frequency.

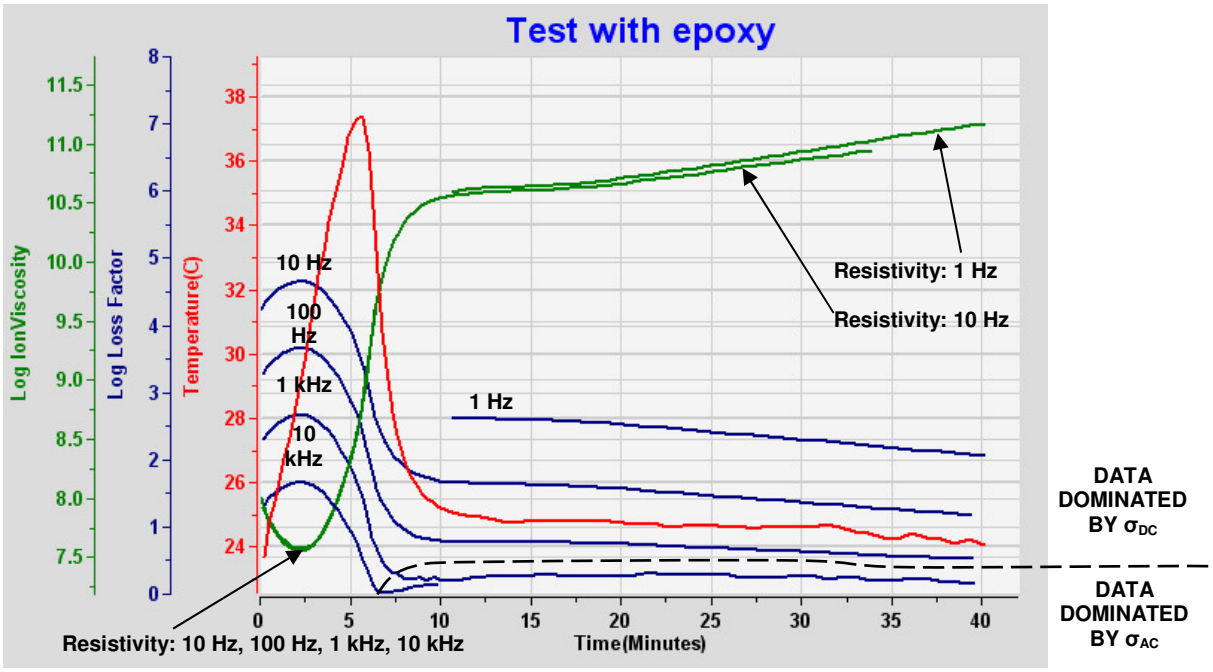

Figure 8-1
Multiple frequency data from cure of five-minute epoxy

In the latter part, however, only loss factors for 1 Hz, 10 Hz and 100 Hz are inversely proportional to frequency.

Resistivity ρ is the inverse of conductivity, as expressed in equation 8-5:

(Eq. 8-5) $$\rho = 1 / (\sigma_{DC} + \sigma_{AC}) = 1/(\omega \varepsilon_0 \varepsilon'')$$

When frequency independent conductivity σ_{DC} dominates the data, resistivity is also largely frequency independent. Frequency independent resistivity ρ_{DC} is

called *ion viscosity*, and is characterized by the overlap of curves at multiple frequencies, as shown in Figure 8-1.

During thermoset cure, the change in ion viscosity is typically proportional to the change in mechanical viscosity until they diverge around the time of gelation (See Figure 7-4). Even after mechanical viscosity becomes immeasurable, however, crosslinking continues and the growing polymer network still presents greater and greater resistance to the flow of ions. Consequently, frequency independent resistivity ρ_{DC}—ion viscosity—can be used for determining cure state through the entire cure.

Chapter 9–Ion Viscosity and Temperature

Temperature dependence of ion viscosity

For the measurement of mechanical viscosity and cure state, ion viscosity (*IV*) provides valuable information from a simple electrical measurement. Ion viscosity depends on the mobility of free ions under the influence of an electric field but also varies with temperature. Therefore, correct interpretation of ion viscosity requires knowledge of temperature at the time of measurement.

At a constant cure state ion viscosity decreases as temperature rises because mobility increases with temperature. Ion viscosity is another term for frequency independent resistivity, ρ_{DC}, and is given by equation 9-1.

(eq. 9-1) $$IV = \rho_{DC} = 1 / (q\ \mu\ n)$$

Where: q = magnitude of electronic charge (coulombs)
μ = free ion mobility (cm^2 / (V-s))
n = free ion concentration (cm^{-3})

Free ion mobility determines the rate of ionic diffusion through a medium, and is given by the Einstein relationship of equation 9-2:

(eq. 9-2) $$\mu = q\ D / (k\ T) \qquad (cm^2 / (V\text{-}s))$$

Where: D = diffusion coefficient (cm^2 / s)
k = Boltzmann's constant (eV / K)
T = temperature in degrees Kelvin (K)

The diffusion coefficient itself is exponentially temperature dependent:

(eq. 9-3) $$D = D_0\ e^{-Q/kT} \qquad (cm^2 / s)$$

Where: D_0 = Maximum value of diffusion coefficient (cm^2 / s)
Q = Activation energy (eV)

The maximum value of diffusion coefficient D_0 is constant with temperature, but decreases as cure progresses because greater degrees of polymerization or crosslinking reduce the mean free path of a mobile ion. Combining equations 9-1, 9-2 and 9-3 results in the following expression for ion viscosity (frequency independent resistivity):

(eq. 9-4) $$IV = \rho_{DC} = (k / (q^2 n D_0)) T e^{Q/kT}$$

The logarithm of ion viscosity then becomes:

(eq. 9-5) $$\log_{10}(IV) = \log_{10}(k / (q^2 n D_0)) + \log_{10}(T) + (Q / (kT \ln(10)))$$

which may be expressed as:

(eq. 9-6) $$\log_{10}(IV) = A + \log_{10}(T) + B (1 / T)$$

Where: $A = \log_{10}[k / (q^2 n D_0)]$
$B = Q / (k \ln(10))$

At a given cure state, D_0 is constant and coefficients A and B are also both constants. The $1 / T$ term of equation 9-6 dominates the response because it varies more with temperature than $\log_{10}(T)$. As a result, for a fixed cure state, ion viscosity decreases as temperature increases.

Figure 9-1 shows how ion viscosity changes with temperature for an epoxy resin with catalyst. Figure 9-2 shows how ion viscosity changes for a thermoplastic polyimide.[1] Overlaid on the data are results from equation 9-6, where coefficients A and B are determined for best fit. The good correspondence between equation 9-6 and the data validates this model of the ion viscosity temperature response. As the cure state advances, D_0 decreases, causing the offset between calculated lines for 0% and 100% cure.

As seen in Figures 9-1 and 9-2, the activation energy Q, which largely determines the slope of each calculated line, may vary with degree of cure.

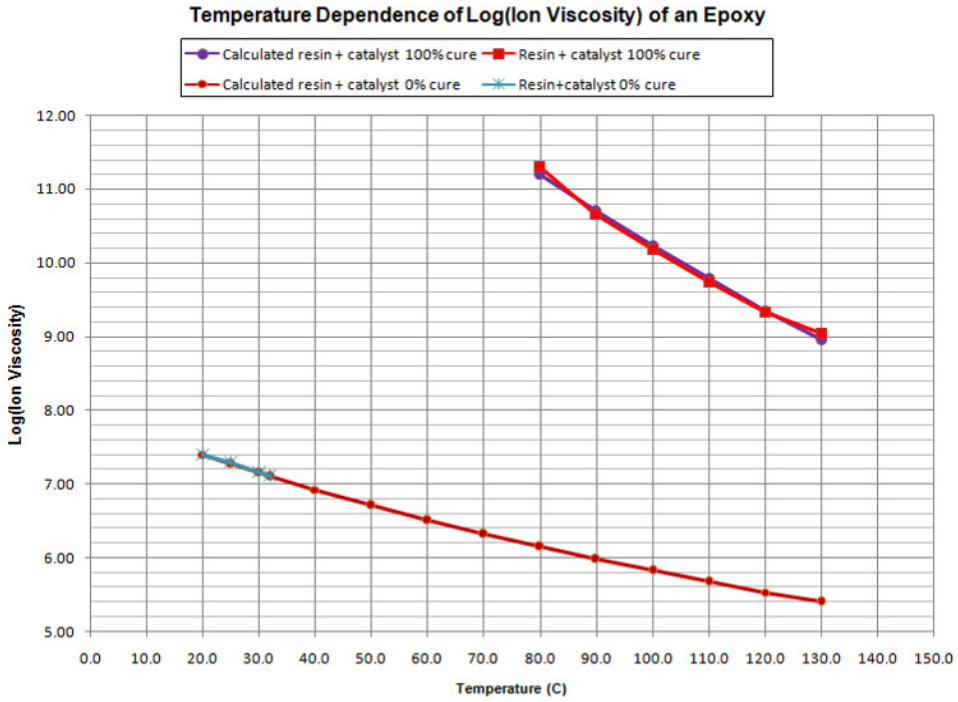

Figure 9-1
Variation in log(*IV*) with temperature for an epoxy resin

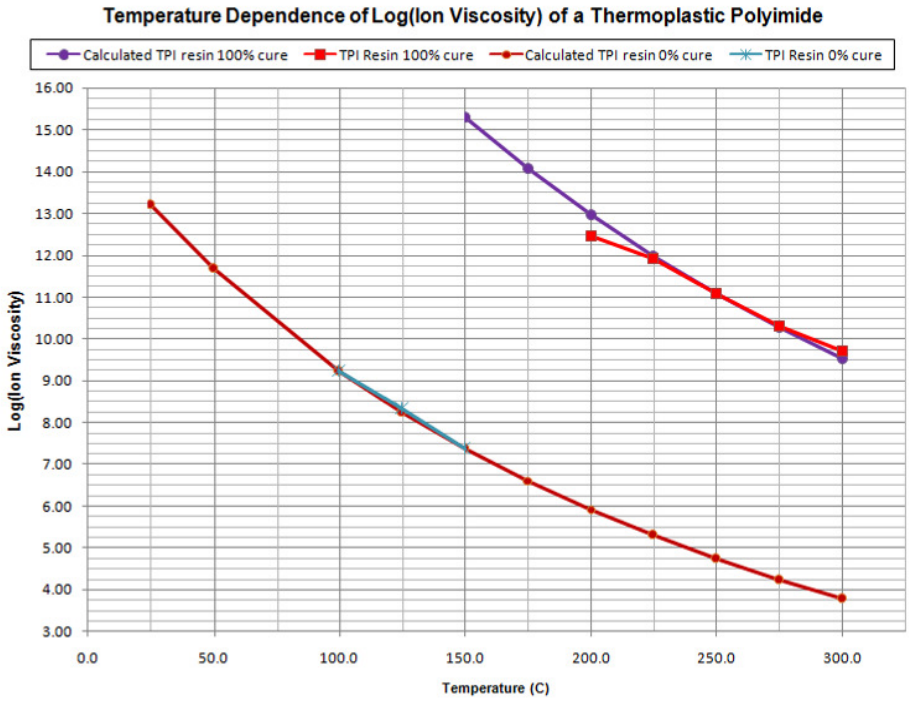

Figure 9-2
Variation in log(*IV*) with temperature for a thermoplastic polyimide[1]

Prepreg processing

A common temperature schedule for vacuum bag curing of prepregs begins with an initial ramp-and-hold step, called the *B-Stage*. During the B-Stage, volatiles and reaction by-products are free to escape as the resin heats and softens. After the B-Stage a second ramp-and-hold heats the prepreg to a higher temperature for final curing. Pressure is applied during this second step to compress together the laminates of prepreg and consolidate the part. At this time any residual volatiles are unable to escape.

Figure 9-3 shows dielectric and viscosity data from the cure of an epoxy resin with two ramp-and-hold steps. Here the first minimum in ion viscosity (*IV*) occurs at 50 minutes. At this time the increase in *IV* due to the accelerating reaction dominates the decrease in *IV* caused by the temperature rise.

After the second temperature ramp begins, *IV* again decreases as temperature increases. In this case the second decrease in mechanical viscosity may cause resin to flow excessively under the application of pressure, causing undesirable loss of resin and producing dry fibers and voids in the laminate. Eventually the thermally driven cure dominates once more and ion viscosity rises again.

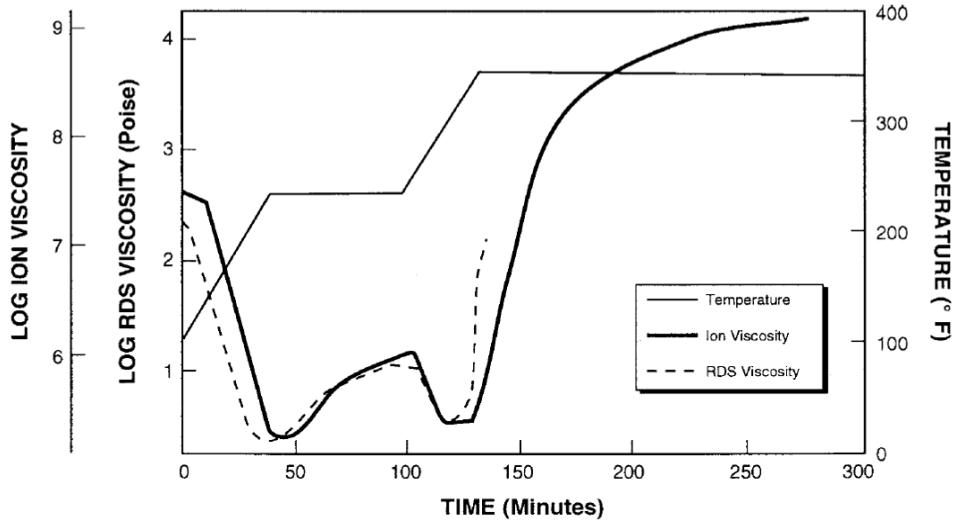

Figure 9-3
Ion viscosity for an epoxy resin cure with two ramp-and-hold steps[2]

Dielectric cure monitoring is uniquely able to observe thermoset cure in real time, and can provide valuable information for process development and control. Because ion viscosity depends on both temperature and cure state, it is important to measure and account for temperature to achieve an accurate understanding of material state.

References

1. Proprietary thermoplastic polyimide adhesive, derived from FM901 polyamic-acid polymer solution, provided by Fraivillig Technologies Company, Boston, MA USA. http://www.fraivillig.com

2. Shepard, D., "Cure Monitoring of Thermosetting Resins Utilizing Dielectric Sensors," Holometrix-Micromet, Cambridge, MA USA

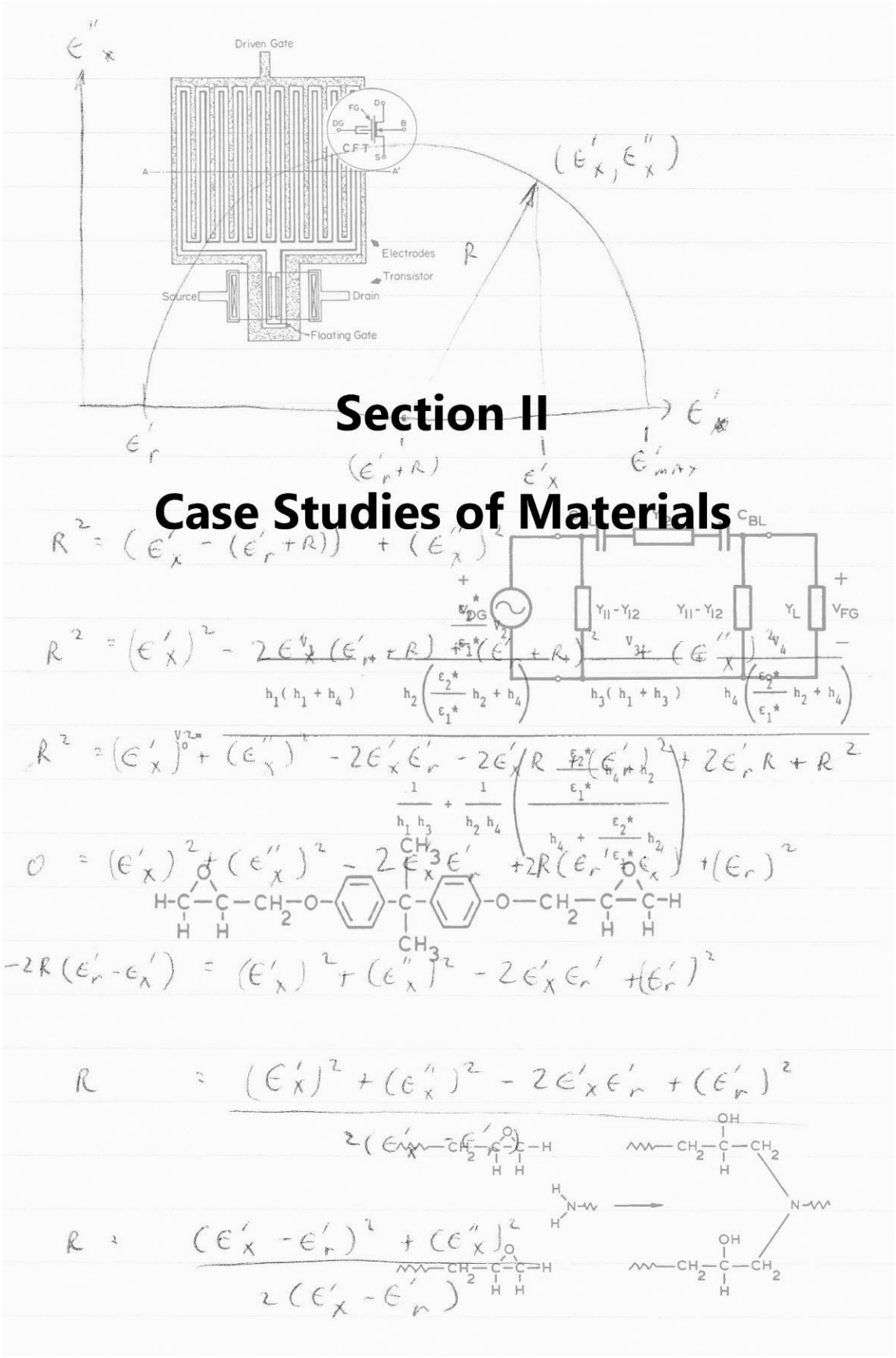
Driven Gate
Electrodes
Transistor
Source
Drain
Floating Gate
Section II
Case Studies of Materials

Chapter 10—Review of Ion Viscosity During Cure

Definitions for dielectric cure monitoring

Dielectric cure monitoring, also known as *dielectric analysis* (DEA), measures a thermoset's resistivity and permittivity, which are the material's dielectric properties. Resistivity (ρ) has both a frequency independent component (ρ_{DC}) from the flow of ions and frequency dependent component (ρ_{AC}) from the rotation of dipoles. The degree of polymerization or crosslinking, which are measures of cure state, affect both mechanical viscosity and the movement of ions, and therefore influence ρ_{DC}. As a result, the term *ion viscosity* (*IV*) has become a synonym for frequency independent resistivity.

Ion viscosity (*IV*) is defined as:

(eq. 10-1) $IV = \rho_{DC}$ (ohm-cm)

Although often called DC resistivity, frequency independent resistivity actually extends across a range of frequencies that includes DC (0 Hz). This distinction is important because frequency independent resistivity correlates with cure state and is a useful material probe. By taking advantage of optimal frequencies, AC measurements—unlike DC methods—can deal with distortion of data caused by electrode polarization and can work through release films and vacuum bags.

Although the strict definition of ion viscosity is frequency independent resistivity, for convenience ion viscosity may also be used to describe resistivity in general. *Note, however, that cure state and mechanical viscosity relate best to frequency independent resistivity, ρ_{DC}, which is true ion viscosity.*

These case studies present and discuss data for *log(ion viscosity)* and *slope of log(ion viscosity)*. Plots show characteristic features such as minimum ion viscosity, maximum slope of log(ion viscosity) and the time to a chosen end of cure. For brevity, log(*ion viscosity*) will be called *log(IV)* and slope of log(*ion viscosity*) will simply be called *slope*.

Selecting an optimum frequency for measuring ion viscosity

Figure 10-1 shows resistivity (ρ) across a range of frequencies for a cure of five-minute epoxy.

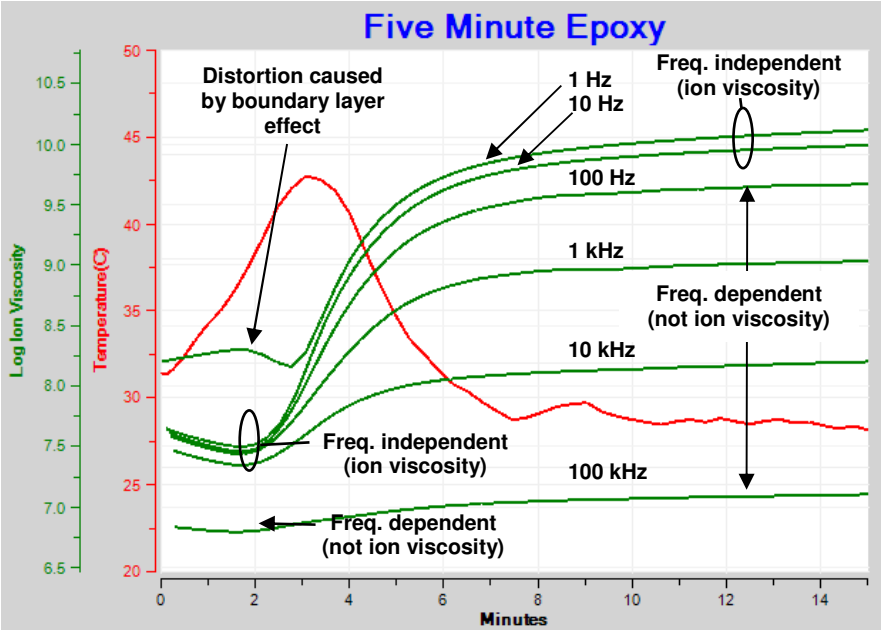

Figure 10-1
Resistivity of curing epoxy (plotted against log(ion viscosity) axis)

Resistivity has both frequency independent (ρ_{DC}) and frequency dependent (ρ_{AC}) terms. Frequency independent resistivity, from mobile ions, dominates where curves overlap, although sometimes the overlap may not be perfect because of a slightly non-ideal response.

The resistivity curves of Figure 10-1 reveal both frequency independent and frequency dependent components. When this total resistivity is unknowingly represented as ion viscosity, misleading interpretations of cure state may result. Which curve or part of a curve is ion viscosity and follows viscosity? Or Modulus? Therefore it is necessary to correctly identify ion viscosity.

Figure 10-2 shows the family of resistivity curves after using an algorithm to present only data dominated by mobile ions. This plot now shows the progression of frequency independent resistivity, properly called *ion viscosity*, which indicates cure state of the material.

To determine the time of maximum reaction rate or the time to end of cure, we must calculate the slope of log(*IV*). Unfortunately, the ion viscosity segments of Figure 10-2 do not overlap perfectly and would yield a series of discontinuous curves for slope. If possible, slope should be calculated from a

single frequency, such as from the 10 Hz data shown in Figure 10-3. This simplification is possible because ion viscosity—frequency independent resistivity—from a properly chosen *optimum* frequency is often is very similar to the composite from multiple frequencies.

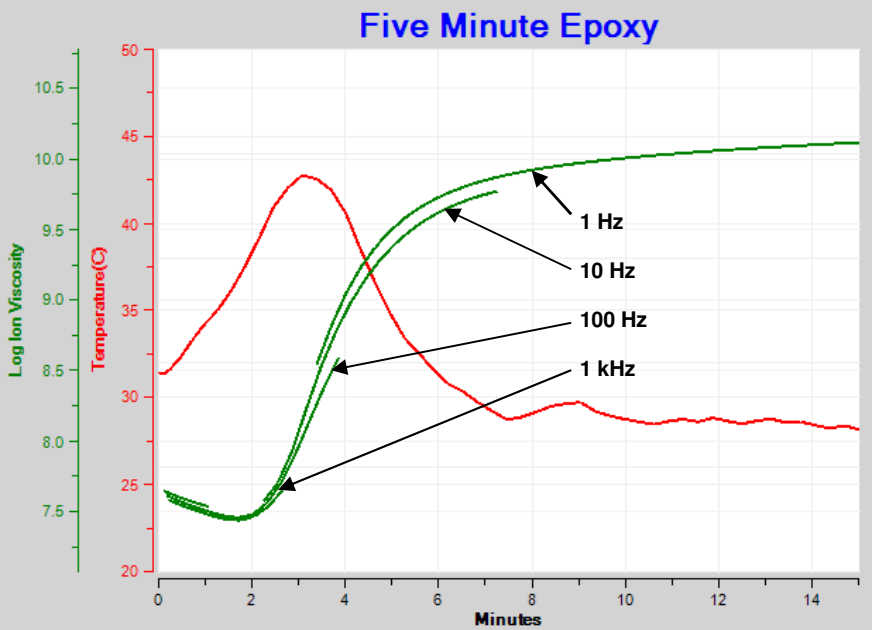

Figure 10-2
Ion viscosity—frequency independent resistivity only

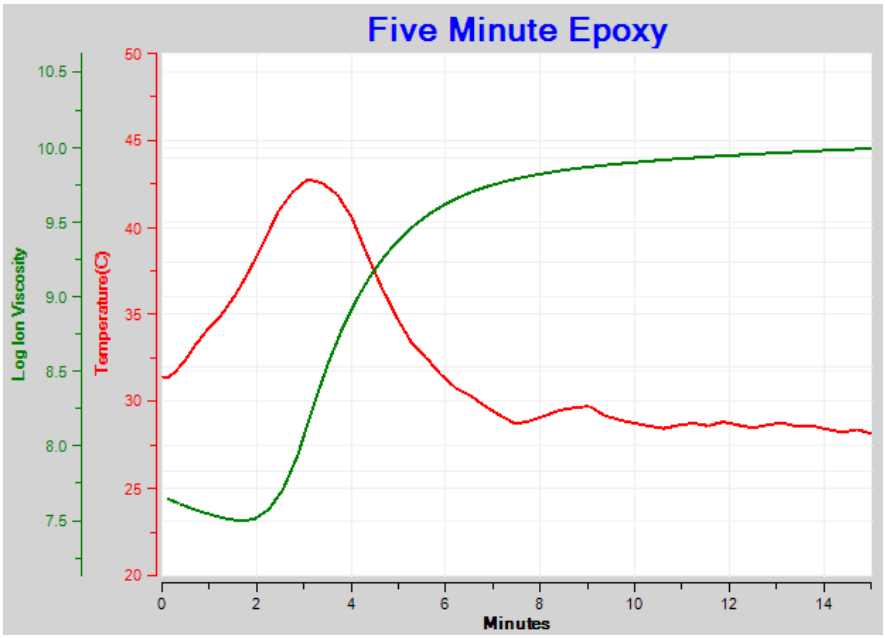

Figure 10-3
Ion viscosity for optimum 10 Hz frequency

Figure 10-4 shows log(*IV*) from 10 Hz data as well as the resulting curve for slope.

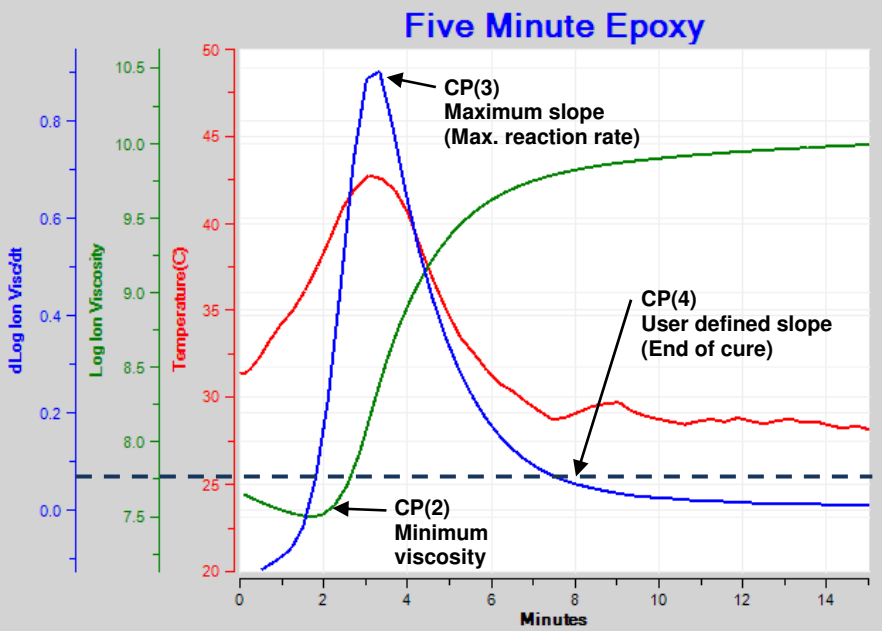

Figure 10-4
Ion viscosity and slope for optimum 10 Hz frequency

The optimum frequency for measuring ion viscosity depends on the material and its conductivity. Selecting this optimum frequency often requires a balance or tradeoff between the portions of cure to measure and the acceptable deviations from an ideal response. Following are a few points to consider:

- An optimum frequency for an entire cure tends to be in the range between 0.1 Hz and 1 kHz for most materials.
- Materials with higher conductivities require a higher frequency to measure ion viscosity (frequency independent resistivity) without distortion caused by the boundary layer effect (see Figure 10-1 and Chapter 19—Electrode Polarization with AC and DC Cure Monitoring)
- Materials with lower conductivities require a lower frequency to measure ion viscosity (frequency independent resistivity)

Characteristics of thermoset cure

In many cases the change of log*(IV)* is proportional to the change of mechanical viscosity before gelation and proportional to the change of modulus after gelation. A plot of ion viscosity is a simple way to characterize the progress

of cure. In simplified form, Figures 10-5 and 10-6 show the behavior of a typical thermoset with one temperature ramp step and one temperature hold step.

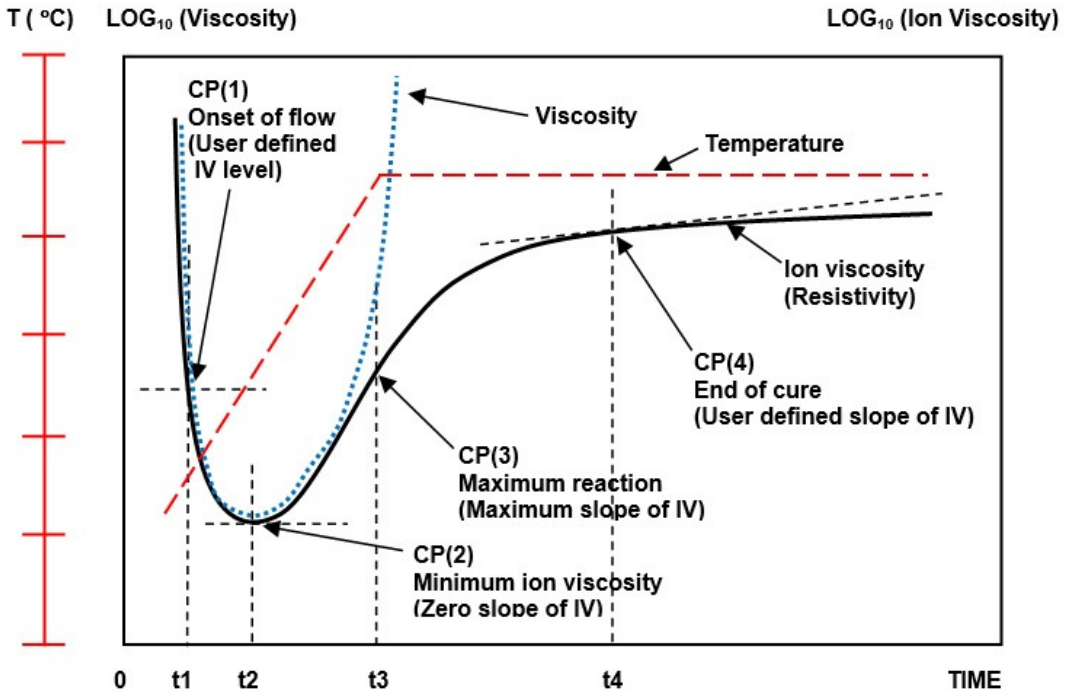

Figure 10-5
Typical behavior of ion viscosity and mechanical viscosity during thermal ramp and hold

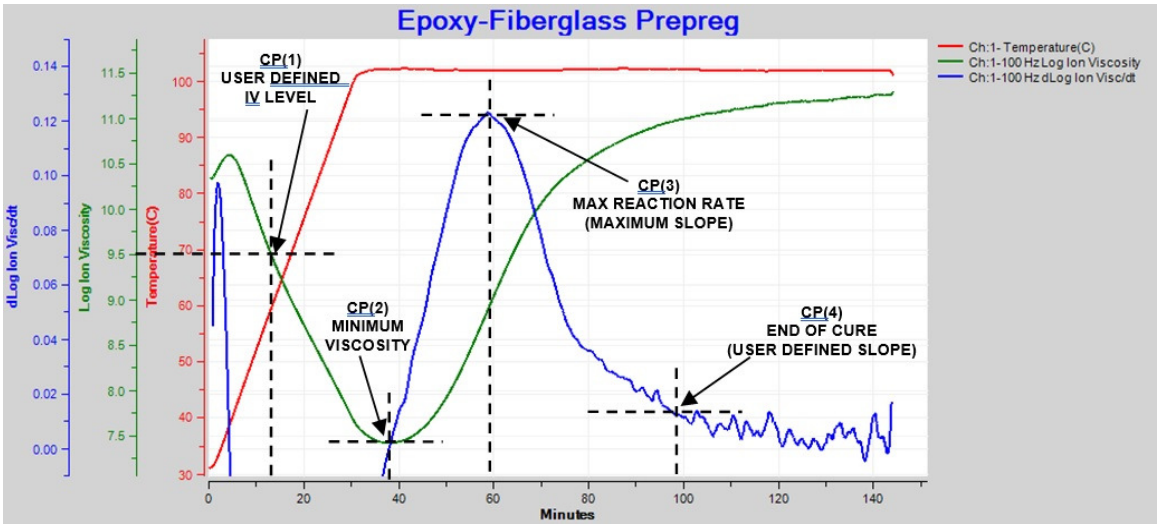

Figure 10-6
Ion viscosity and slope during thermal ramp and hold

Four Critical Points characterize the dielectric cure curve:

- CP(1)—A user defined level of *log(IV)* that is typically used to identify the onset of material flow at the beginning of cure.
- CP(2)—Ion viscosity minimum, which also corresponds to the physical viscosity minimum. This Critical Point indicates the time when polymerization and the resulting increasing viscosity begin to dominate the decreasing viscosity due to heating.
- CP(3)—Inflection point, which identifies the time when the curing reaction begins to slow. CP(3) is often used as a signpost that can be associated with gelation. The height of CP(3) is a relative measure of the reaction rate.
- CP(4)—A user defined *slope* that can identify the end of cure. The decreasing *slope* corresponds to the decreasing reaction rate. Note that dielectric cure monitoring continues to reveal changes in the evolving material past the point when measurement of mechanical viscosity is not possible.

Figures 10-5 and 10-6 illustrate the usual behavior of curing thermosets when temperature gradually ramps to a hold stage. The response is slightly different when the processing is essentially isothermal, as shown in Figure 10-7.

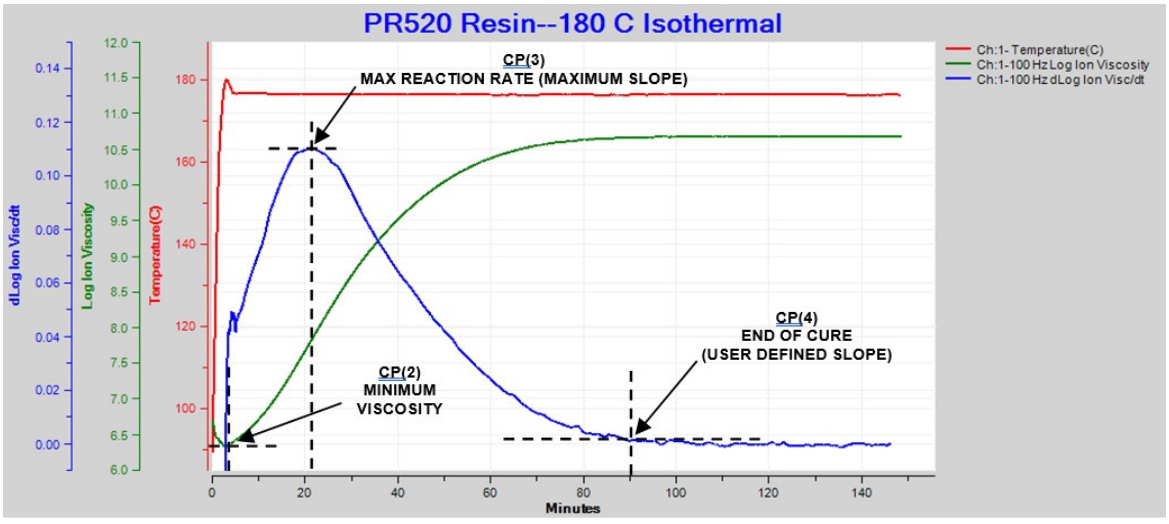

Figure 10-7
Ion viscosity and slope of thermoset cure during isothermal processing

In this case CP(1) either is meaningless or occurs at t = 0, immediately after the application of heat, when material flows to make contact with the sensor. Minimum ion viscosity also occurs at t = 0 or shortly afterwards because cure begins immediately.

For isothermal cures, CP(3) and CP(4) are conceptually the same as for ramp and hold conditions.

Chapter 11—Equipment for Dielectric Cure Monitoring

Dielectric cure monitors

Dielectric cure monitors measure the dielectric properties of thermoset or composite. The use of a range of frequencies selectively reveals the response of ion motion and dipole rotation, allowing the study of material state through the entire cure.

Dielectric/conductivity sensors

Dielectric cure monitors measure the resistance (*R*) and capacitance (*C*) of material between a pair of electrodes, which can be modeled as a resistance in parallel with a capacitance, as shown in Figure 11-1.

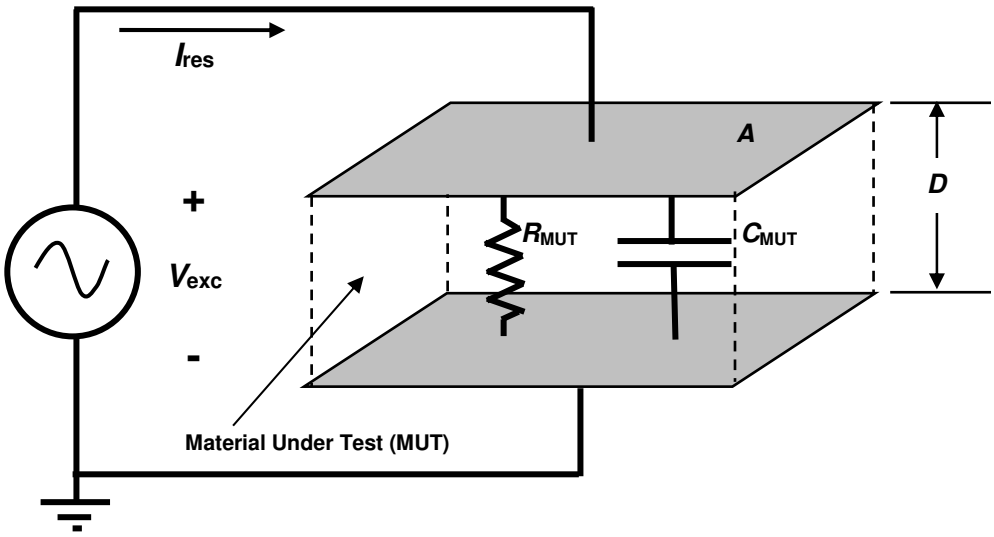

Figure 11-1
Dielectric model of a Material Under Test

Simple parallel plate electrodes, shown in Figure 11-2, are often used for this purpose. The ratio of electrode area *A* and the distance *D* between them—the *A*/*D* ratio—is a figure of merit. A larger *A*/*D* ratio corresponds to greater sensor sensitivity. The *A*/*D* ratio is also the scaling factor for calculating resistivity (ρ) from resistance, and permittivity (ε') from capacitance. Unfortunately, distance *D* can change with pressure, or with expansion and contraction of the material, causing inaccurate results.

An alternative is the interdigitated electrode, also shown in Figure 11-2. A rigid substrate supports the electrodes and resulting the planar structure does not change with pressure, or expansion and contraction of the material under test (MUT). While the parallel plate sensor makes a bulk measurement, an interdigitated sensor makes a surface measurement.

As a rule of thumb, interdigitated electrodes with the same width and separation measure to a depth approximately equal to the electrode width. The parameter of *A*/*D* ratio also applies to interdigitated electrodes as a figure of merit and is the scaling factor for calculating resistivity and permittivity.

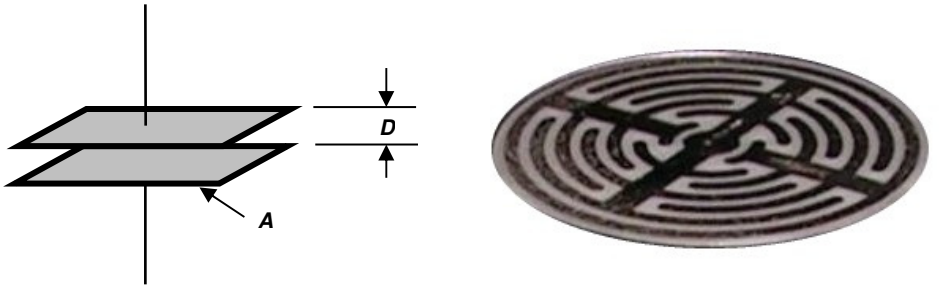

Parallel plates—
ρ = R • (*A*/*D*)

Interdigitated electrodes—
ρ = R • (*A*/*D*)

Figure 11-2
Comparison of parallel plate and interdigitated electrodes

Figure 11-3 shows a Varicon[1] disposable dielectric/conductivity sensor with interdigitated electrodes 100 microns wide. Constructed as a Kapton® flex circuit, this sensor is thin enough to be inserted between the plys of a laminate and may be discarded after use. The narrow electrodes, too small to be visible in the photograph, result in a large A/D = 160, with correspondingly great sensitivity. The trade-off is the measurement of dielectric properties only within 100 microns of the surface.

Figure 11-4 shows a Ceramicomb-1″[2] reusable dielectric/conductivity sensor embedded in a platen for a small press. This sensor is constructed with interdigitated electrodes embedded in ceramic and has *A*/*D* = 10. When mounted as shown, it is possible to place a sample in the press, then heat and compress it and simultaneously make dielectric measurements to monitor cure. Afterwards the sample can be removed from the sensor and the process can be repeated.

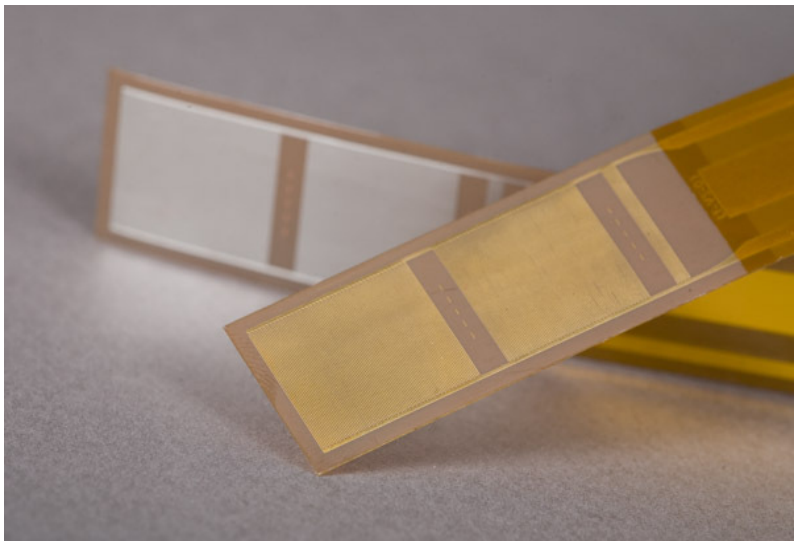

Figure 11-3
Disposable Varicon[1] dielectric/conductivity sensor on polyimide flex circuit

Reusable sensors are convenient for applications such as Quality Assurance/Quality Control (QA/QC), which involve repetitive testing. Note the wider electrodes, visible in Figure 11-4. This sensor is able to measure more deeply into the material, with the trade-off of decreased sensitivity because of the smaller *A*/*D* ratio.

Figure 11-4
Reusable Ceramicomb-1"[2] dielectric/conductivity sensor embedded in press platen

AC vs. DC measurements

Interestingly, it is often *not* useful to measure frequency independent resistivity (ρ_{DC}) using DC signals. A phenomenon called *electrode polarization* can create a blocking layer across sensor electrodes during early cure, when material is most conductive. This blocking layer acts like a capacitor and prevents the passage of DC current. In the presence of electrode polarization, dielectric data from very low excitation frequencies are distorted, as shown in Figures 11-5 and 11-6 for the cure of a "five-minute" epoxy.

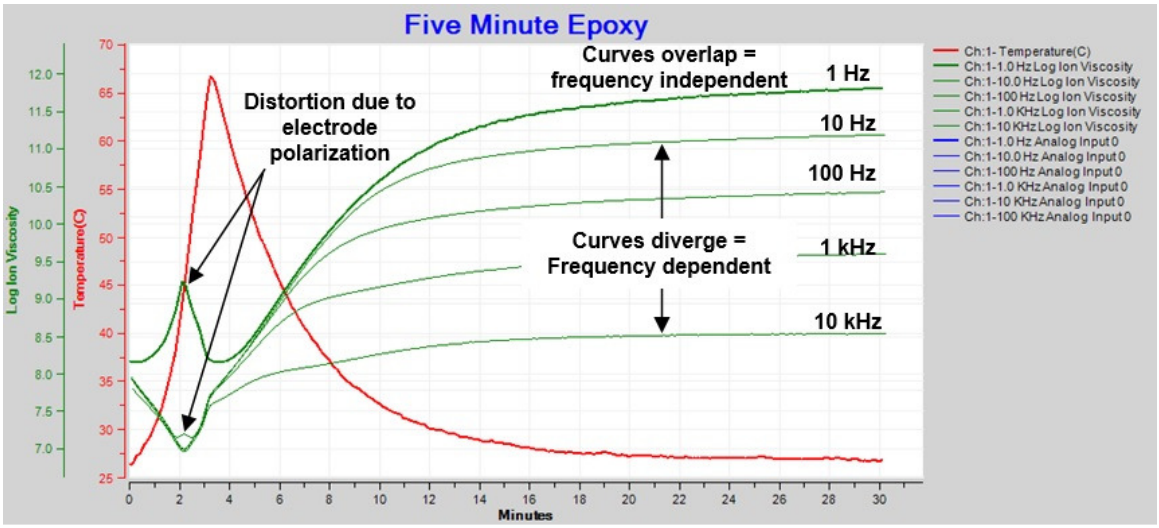

Figure 11-5
Distortion in ion viscosity from electrode polarization

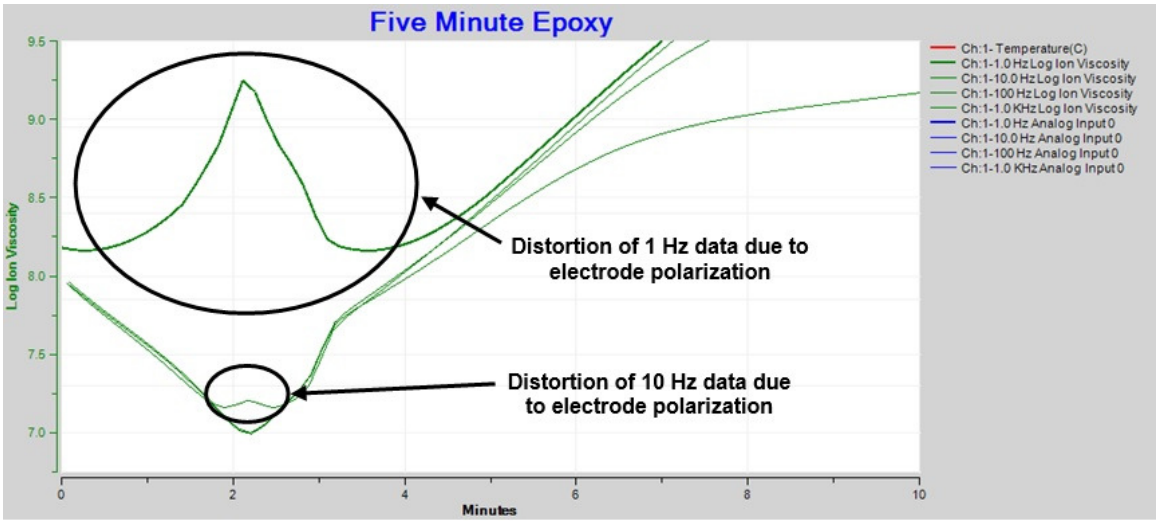

Figure 11-6
Distortion in ion viscosity from electrode polarization (detail)

Figures 11-5 and 11-6 show plots of resistivity against an axis labeled *ion viscosity*. For convenience, these data may collectively be called ion viscosity. At the beginning of cure, measurements at the higher excitation frequencies—1 kHz to 10 kHz—show no distortion and correctly identify the ion viscosity minimum.

Electrode polarization causes a small amount of distortion in the 10 Hz data, visible in the expanded plot of Figure 11-6. This distortion changes the expected single minimum in resistivity/ion viscosity to a peak with *two* local minima.

Data from 1 Hz measurements display much greater distortion because the boundary layer effect increases with decreasing frequency. This distortion becomes worse at lower frequencies, and with DC signals a conductive material can even appear *non-conductive*.

Besides avoiding distorted data from blocking layers, AC signals can also make measurements through a release film, which is a very thin layer of plastic used to prevent material from adhering to a mold or platen.

AC signals have significant advantages over DC signals. For dielectric cure monitoring, the optimum range of frequencies depends on the material and application. Extremely low frequency data require long acquisition times and are subject to distortion from electrode polarization. For most thermosets 0.1 Hz to 10 Hz is a reasonable lower limit. High frequency data tends to be dominated by dipolar rotation, which masks ion viscosity at the end of cure as shown in Figure 11-5. For most thermosets 10 kHz to 100 kHz is a good upper frequency limit for measurements of ion viscosity.

LCR meters and four-wire connections

Many researchers make their own dielectric cure monitors with LCR (Inductance-Capacitance-Resistance) meters, which measure resistance and capacitance across a range of frequencies. Typical LCR meters use a four-wire, or Kelvin, connection to eliminate the effect of cable resistances, as shown in Figure 11-7.

Bulkier and more complex than a two-wire connection, a four-wire connection is useful when the resistance under test is small (less than 10 Ω) and comparable to lead wire resistances. However, the resistances encountered with a typical sensor during thermoset cure are on the order of 10,000 Ω or more. As a result, for dielectric cure monitoring a simpler two-wire connection may replace the cumbersome four-wire connection without loss of accuracy.

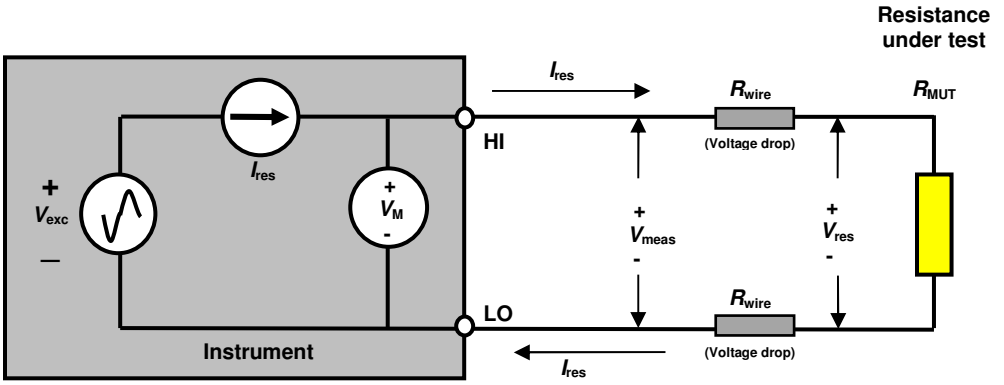

V_{meas} = Voltage measured by instrument
V_{res} = Voltage across resistor R_{MUT}
I_{res} = Current through resistor R_{MUT}

Measured resistance = $V_{meas}/I_{res} = R_{MUT} + 2(R_{wire})$

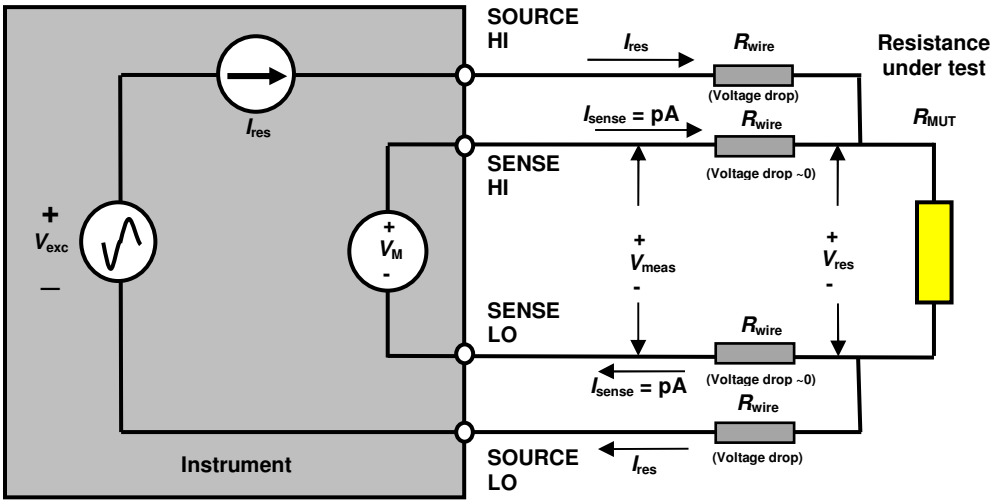

V_{meas} = Voltage measured by instrument
V_{res} = Voltage across resistor R_{MUT}
I_{res} = Current through resistor R_{MUT}

Sense current negligible so $V_{meas} = V_{res}$

Measured resistance = $V_{meas}/I_{res} = V_{res}/I_{res} = R_{MUT}$

Figure 11-7
Two-wire and four-wire (Kelvin) connection for resistance measurements

Temperature measurements

Temperature measurement, usually with a thermocouple, is an essential function for dielectric cure monitoring because ion viscosity depends on both cure state and temperature. At a given cure state, ion viscosity decreases as temperature increases and increases as temperature decreases. Knowing temperature provides additional insight into the nature of the cure and can avoid misinterpretation of data. Figure 11-8 shows the isothermal cure of an epoxy, in which the minimum ion viscosity occurs at time $t = 0$ and ion viscosity increases monotonically during cure.

In contrast, Figure 11-9 shows the cure of a "five-minute" epoxy, which produces an exotherm. Here temperature initially increases as curing begins, liberating heat and resulting in a decrease in ion viscosity. Eventually the reaction dominates, ion viscosity goes through a minimum then increases. Notice also how the peak exotherm occurs at the same time as the maximum slope of ion viscosity—identifying the point of maximum reaction rate. Temperature data is valuable to understanding how a material cures, and is necessary when developing a process or formulation.

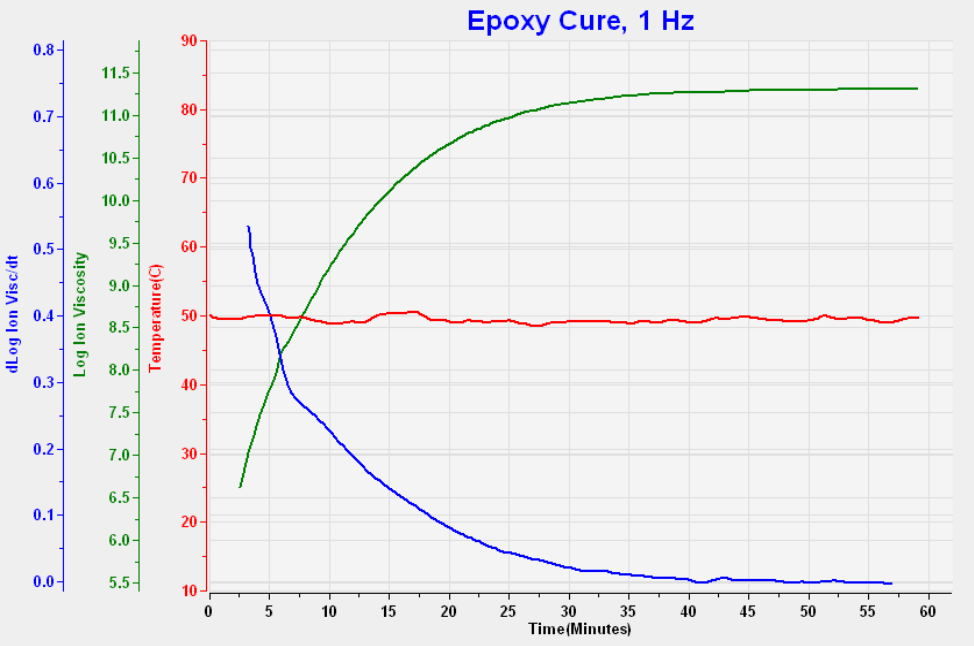

Figure 11-8
Isothermal epoxy cure at 50 °C

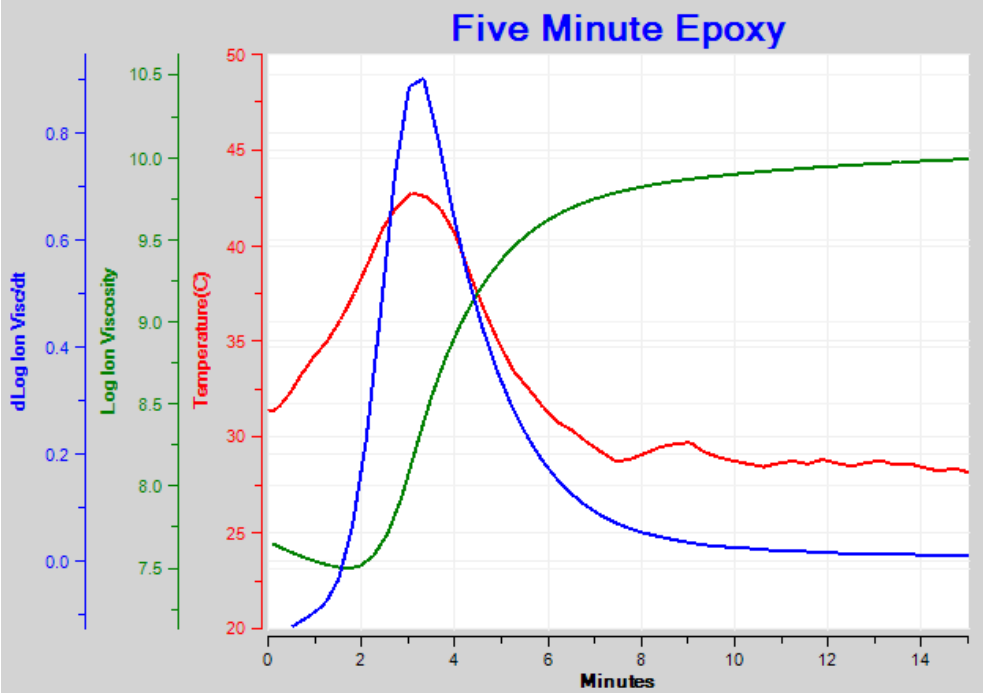

Figure 11-9
Five-minute epoxy cure with exotherm

A dielectric cure monitoring system

Figure 11-10 shows the essential elements of a dielectric cure monitoring system. Making contact with the thermoset under test, dielectric/conductivity sensors have two general configurations, parallel plate or interdigitated electrodes. The selection of a sensor depends on the desired type of measurement, either surface or bulk, and the desired sensitivity as indicated by the *A*/*D* ratio.

Sensors connect to an instrument. The most versatile instruments use AC signals for measurement. A wide range of excitation frequencies allow selection of an optimal frequency for observing ion viscosity, and multiple frequencies enable studies of the dipolar response. Temperature measurement is important for understanding cure, especially under non-isothermal conditions.

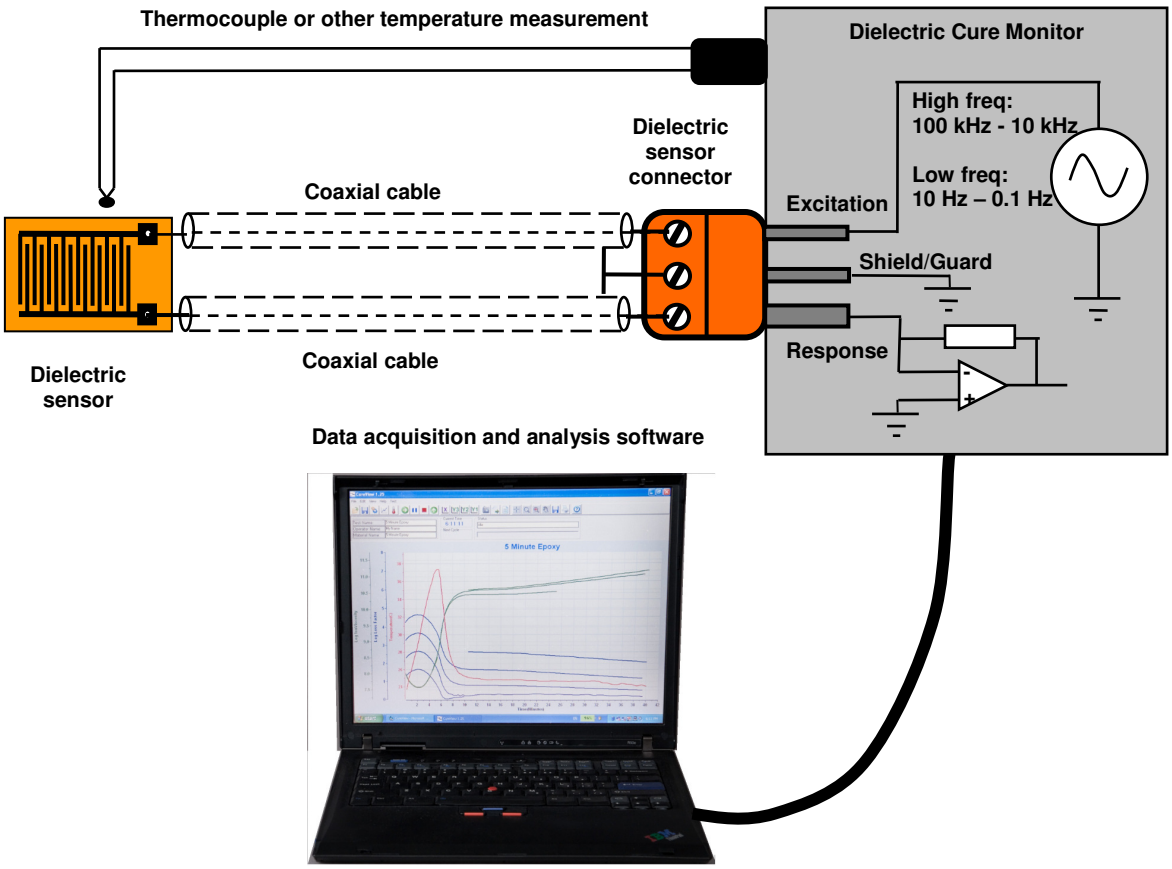

Figure 11-10
Essential elements of a dielectric cure monitoring system

Finally, software controls the instrument, usually through a computer connected to the dielectric cure monitor. Cure state cannot be determined from a single point measurement, but must be extracted from the change of ion viscosity and the shape of the curve over time. So software, which makes repetitive measurements, and stores and analyzes data, is crucial to the performance of the system.

References:

1. Varicon sensor, manufactured by Lambient Technologies, Cambridge, MA USA. https://lambient.com

2. Ceramicomb-1" sensor, manufactured by Lambient Technologies, Cambridge, MA USA

Chapter 12—Guidelines for Successful Dielectric Measurements

Making good measurements

Following are some guidelines for successful dielectric cure monitoring. Although the method of DEA is simple, care and good practice are very helpful for making good measurements.

Preparing the sensor and sample

- Do remove oils or other contaminants by cleaning sensors with acetone, alcohol or other solvent
    - Remove adsorbed solvents, which might interfere with test measurements in air, by heating sensors above 60 °C for a short time
- Do prevent material from adhering to ceramic or reusable sensors by applying silicone or non-conductive mold release, as shown in Figure 12-1

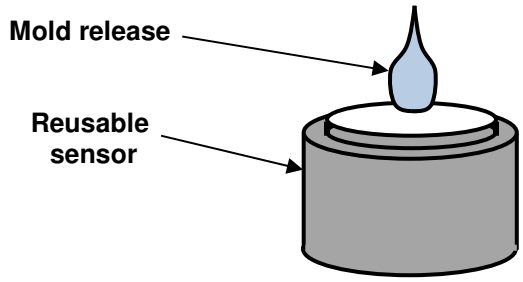

Figure 12-1
Apply mold release to reusable sensors

- Do prevent short circuits by avoiding contact between sensor bond pads and electrically conductive surfaces
    - Wrap bond pads with Kapton® or polyimide tape, as shown in Figure 12-2
- Do run sensor leads parallel to each other to reduce capacitance between leads
    - Don't use twisted leads, which increase cable or base capacitance

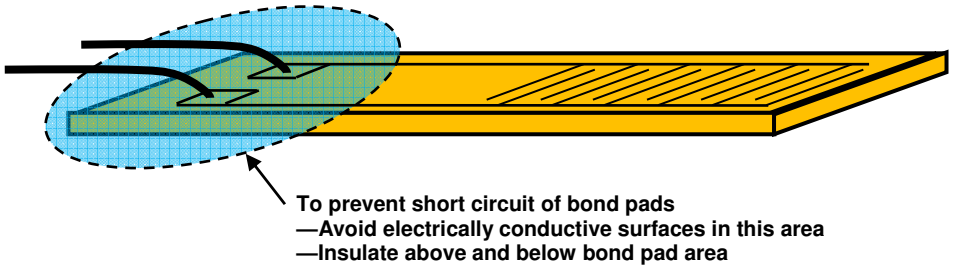

Figure 12-2
Insulating bond pad area

- Do place sample over entire electrode area, as shown in Figure 12-3

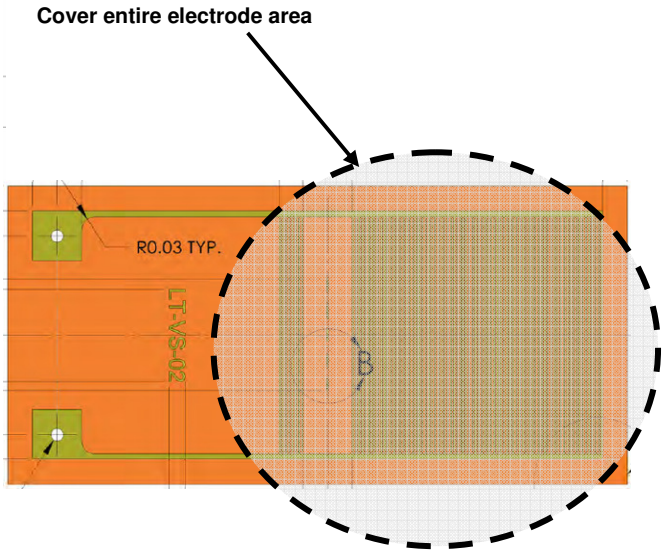

Figure 12-3
Sample application area on sensor

- Do use samples thicker than the separation between interdigitated electrodes
    - When the sample is thinner than the electrode separation, the sensor will also detect air or material on the top side of the sample
- Do stack at least two or three layers of prepreg on top of a sensor to ensure enough resin for good measurements
- Do use a filter between the sensor and materials containing graphite or conductive fibers, as shown in Figure 12-4
    - Fiberglass felt or laboratory filter paper are good filter materials

- Do use aluminum foil or release film above and below the lay-up, as shown in Figure 12-4, to prevent the sample from adhering to platen or mold surfaces
- Do apply pressure to solid samples, or solid samples that melt during processing, for good contact with the sensor

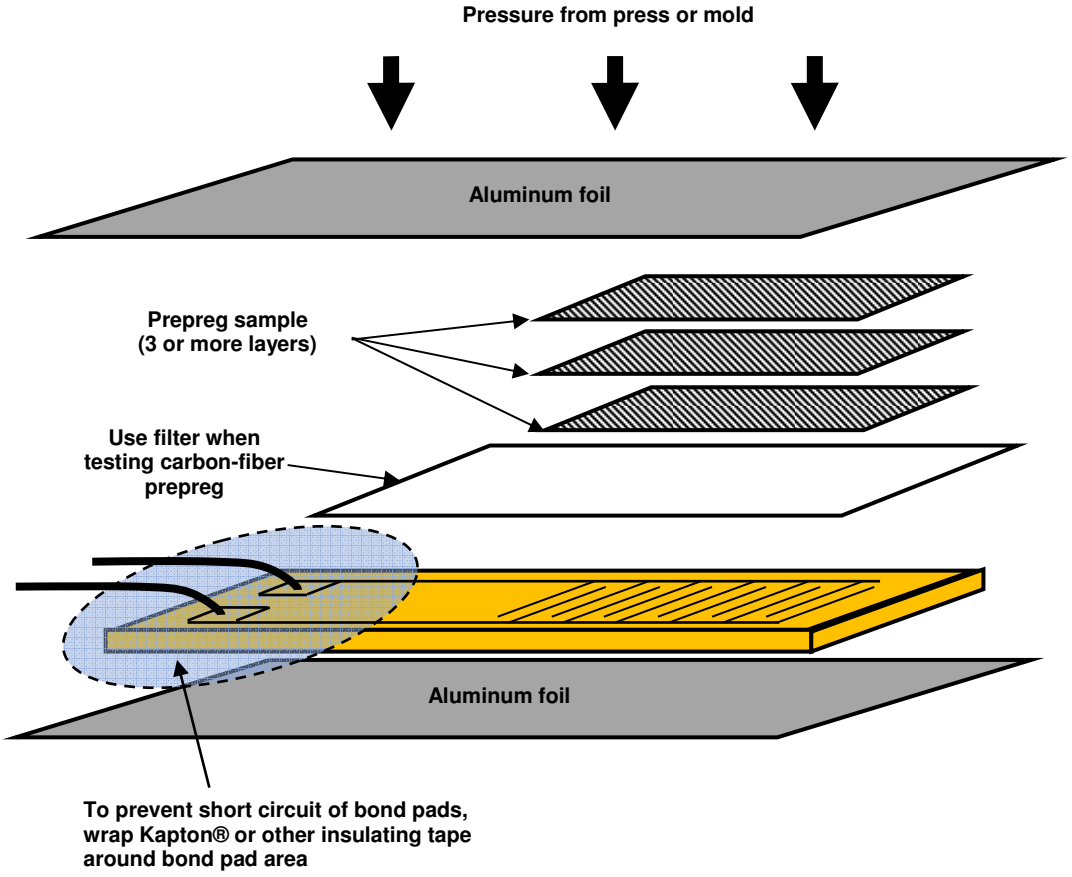

Figure 12-4
Suggested lay-up for prepregs

Reducing noise in leads, extension cables and sensors

- Don't use long, unshielded leads, which act like antennas and can pick up interference
  - Signal levels at the end of cure are low and measurements are more susceptible to noise at this time
  - Use coaxial cable with guarded or grounded shields for long leads
- Don't place the sensor on or near large ungrounded metal surfaces

- Ungrounded metal acts like an antenna that can pick up noise, which the sensor detects
- Ground metal surfaces around the sensor

- Don't place power cords near the sensor
  - AC mains voltages are around 100 – 240 VAC but sensor signals may be in the range of only 10 mV

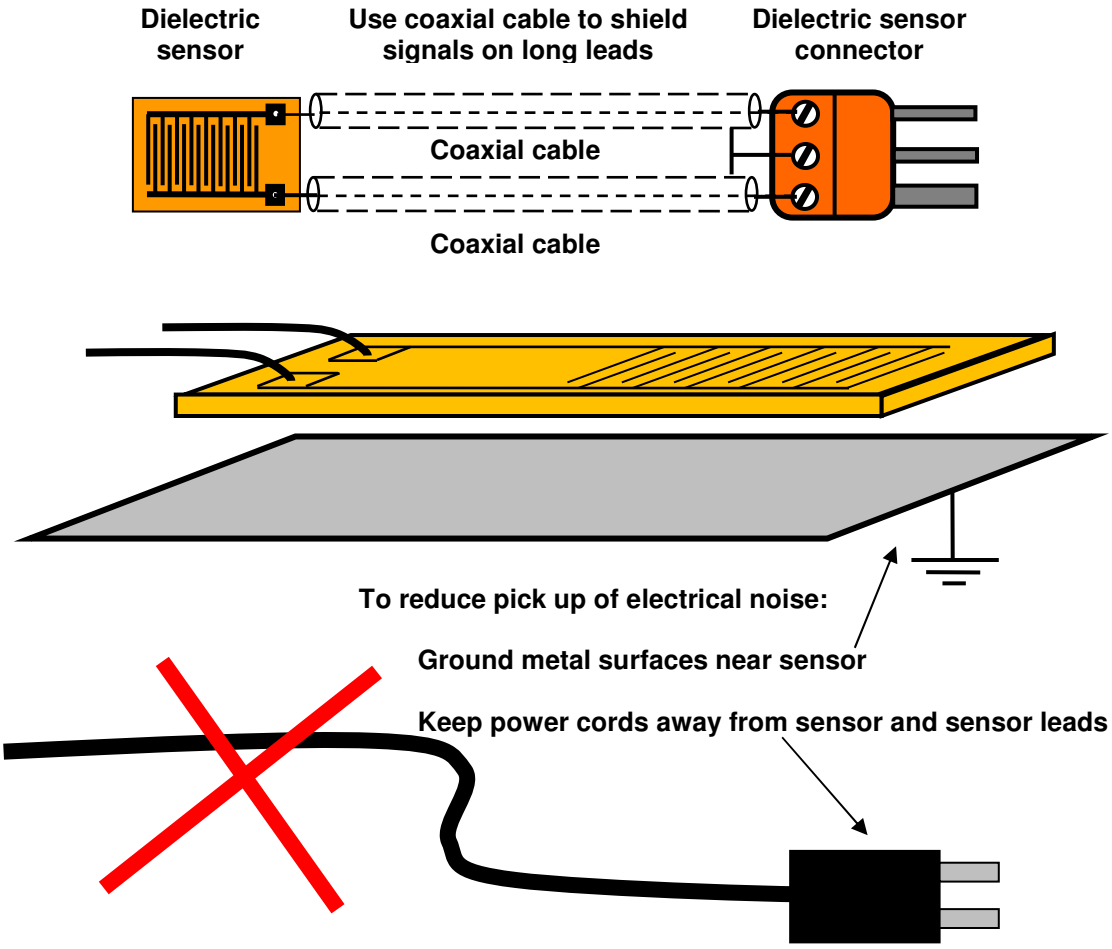

Figure 12-5
Ways to reduce noise in dielectric sensors

If an instrument measures a response voltage from the dielectric sensor, then a guarded cable is usually more suitable. Figure 12-6 shows a typical configuration for guarded cables. Note that the shields around the leads connect

to a x1 amplifier that outputs the guard signal. This guard signal drives the shields with a reproduction of the response, reducing capacitive interaction between the sensitive response line and the outside world.

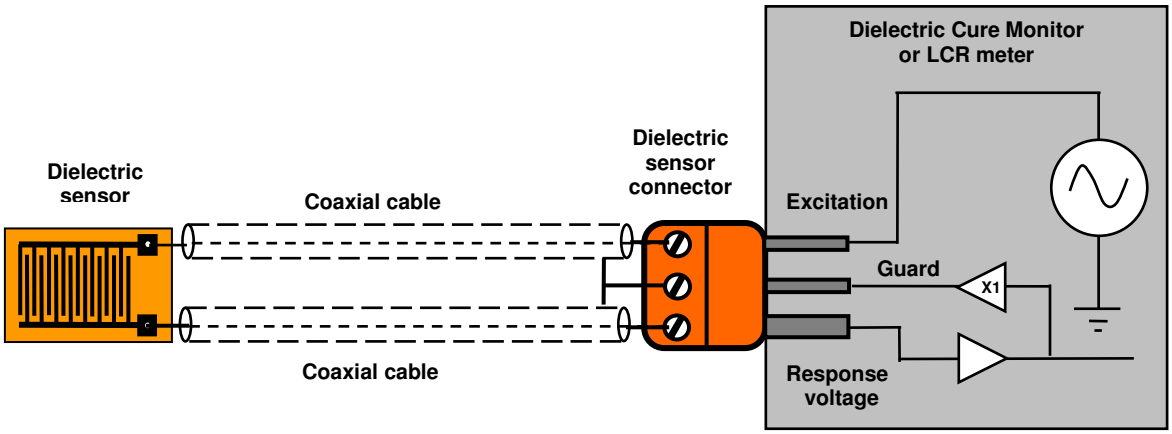

Figure 12-6
Connecting a dielectric sensor using coaxial cable with guarded shields

If an instrument measures a response current from the dielectric sensor, then this current typically goes into a virtual ground. In this case a grounded shield is more suitable, as shown in Figure 12-7.

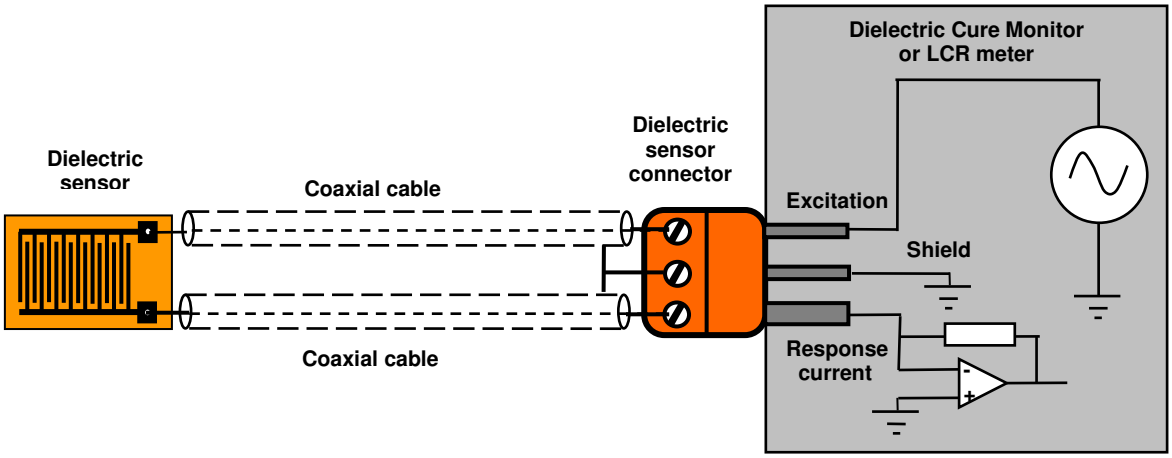

Figure 12-7
Connecting a dielectric sensor using coaxial cable with grounded shields

Interpreting dielectric data

- Do look at loss factor, as in Figure 12-8, when studying the dipole response

- Total loss factor is the sum of loss from the flow of mobile ions and the loss from dipole rotation
- Using loss factor makes it easier to see and separate the mobile ion response from the dipole response
- Loss factor is inversely proportional to frequency when mobile ions dominate response

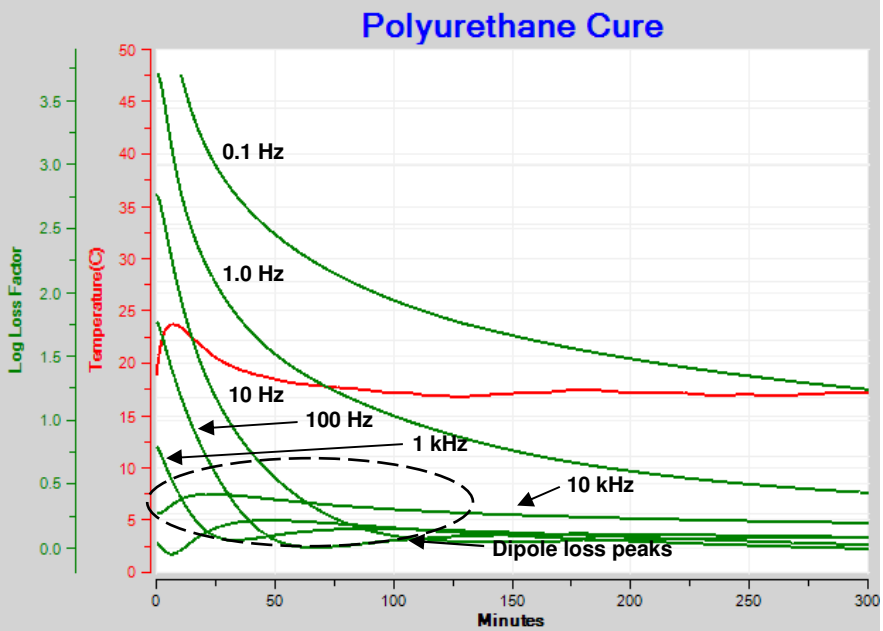

Figure 12-8
Loss factor of curing polyurethane

- Do look at resistivity from multiple frequencies, as in Figure 12-9, to determine ion viscosity
  - Change of ion viscosity indicates cure state
    - Often proportional to change of viscosity before gelation
    - Often proportional to change of modulus after gelation
  - Ion viscosity is frequency independent resistivity due to mobile ions
  - Ion viscosity dominates where curves from different frequencies closely or completely overlap
  - Dipole response dominates where curves from different frequencies do not overlap

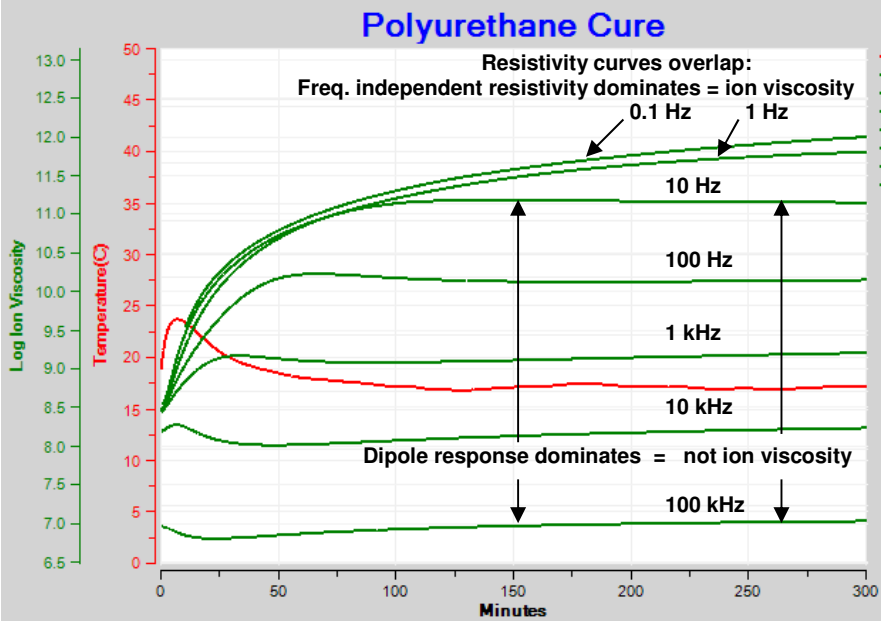

Figure 12-9
Resistivity of curing polyurethane (plotted against ion viscosity axis)

- Do use a single, optimum frequency—if possible—for ion viscosity response for entire cure, as shown in Figure 12-10
    - A single frequency allows calculation of slope for the entire cure

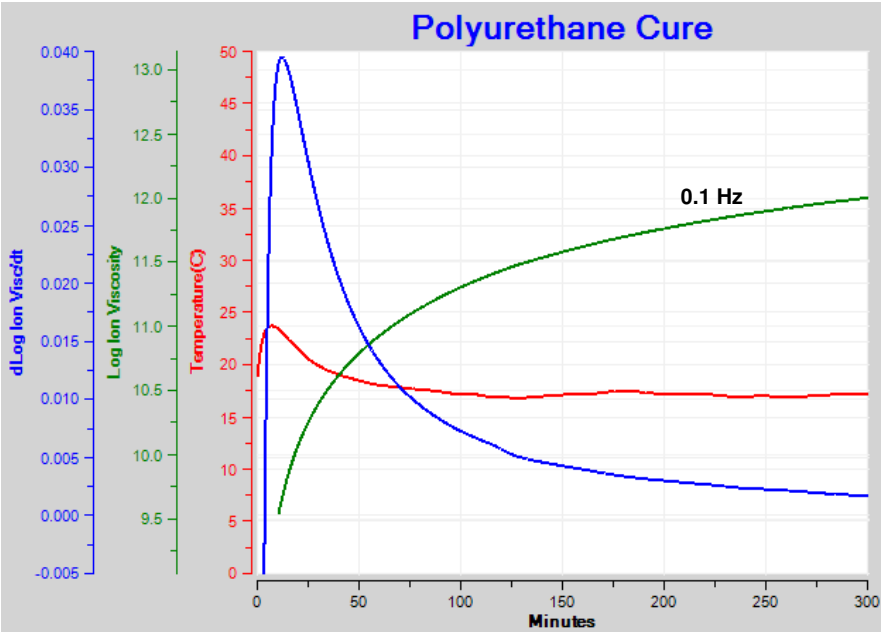

Figure 12-10
Ion viscosity and slope for curing polyurethane

- Do use lower frequencies for better ion viscosity response at end of cure
- Do use higher frequencies for better ion viscosity response at beginning of cure

With proper sample preparation, lay-up, shielding of leads and attention to the electrical environment it is possible to make good, reproducible dielectric measurements for monitoring the cure of thermosets and composites.

Chapter 13—Cure Monitoring of Sheet Molding Compound (SMC)

Cure of sheet molding compound

The curing behavior of Sheet Molding Compound (SMC) was observed using the LT-451 Dielectric Cure Monitor.[1] Bulk Molding Compound (BMC) is the generally the same material as SMC but in bulk form, so the overall behavior applies to BMC as well. The data from dielectric cure monitoring clearly show:

- Critical Points identify characteristic features of the cure such as minimum ion viscosity, maximum slope of log(ion viscosity) and the time to a chosen end of cure.
- Cure time decreases as cure temperature increases, as expected for a reaction that is thermally driven.

Procedure

Samples of SMC were placed on Mini-Varicon[2] sensors, shown in Figure 13-1, with the lay-up of Figure 13-2. The samples were cured in a laboratory press at 135 °C, 145 °C and 155 °C. Previous tests had identified 10 Hz as an optimum excitation frequency for cure monitoring.

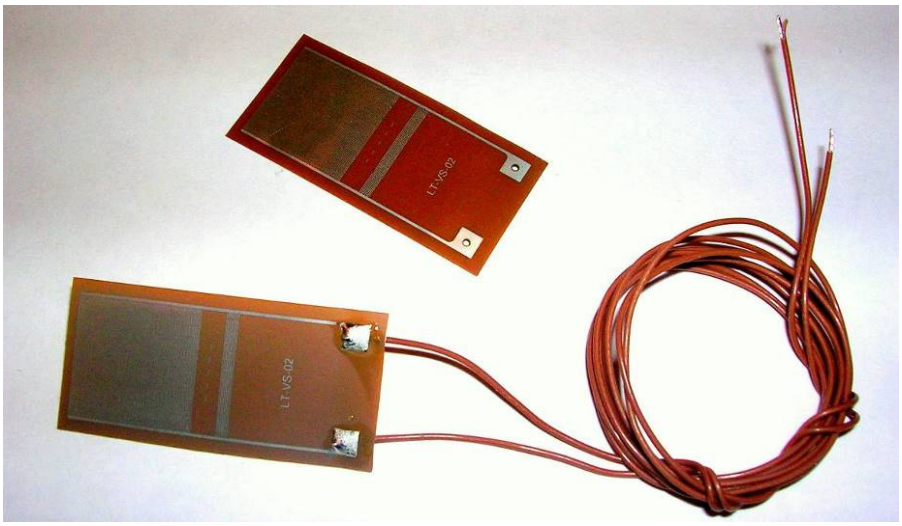

Figure 13-1
Mini-Varicon disposable sensor

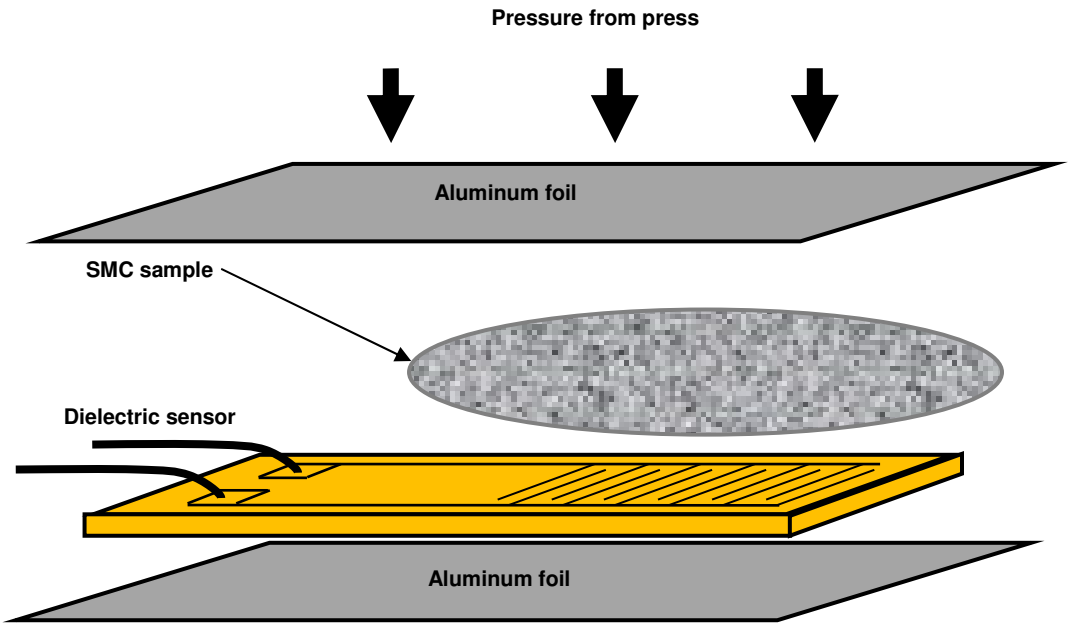

Figure 13-2
Lay-up of SMC for cure monitoring

An LT-451 Dielectric Cure Monitor measured the dielectric properties of each sample at 10 Hz and was triggered to start data acquisition when the press closed. CureView[3] software acquired and stored the data, and performed post-analysis and presentation of the results.

Results

Figures 13-3, 13-4 and 13-5 show data from the tests of SMC at 135 °C, 145 °C and 155 °C, respectively, and demonstrate how SMC cures more quickly at higher process temperatures. The time of minimum ion viscosity, which indicates the start of accelerating cure, occurs sooner at higher temperatures. Furthermore, once cure dominates, ion viscosity rises more steeply at higher temperatures until the curve flattens as it approaches the end of cure.

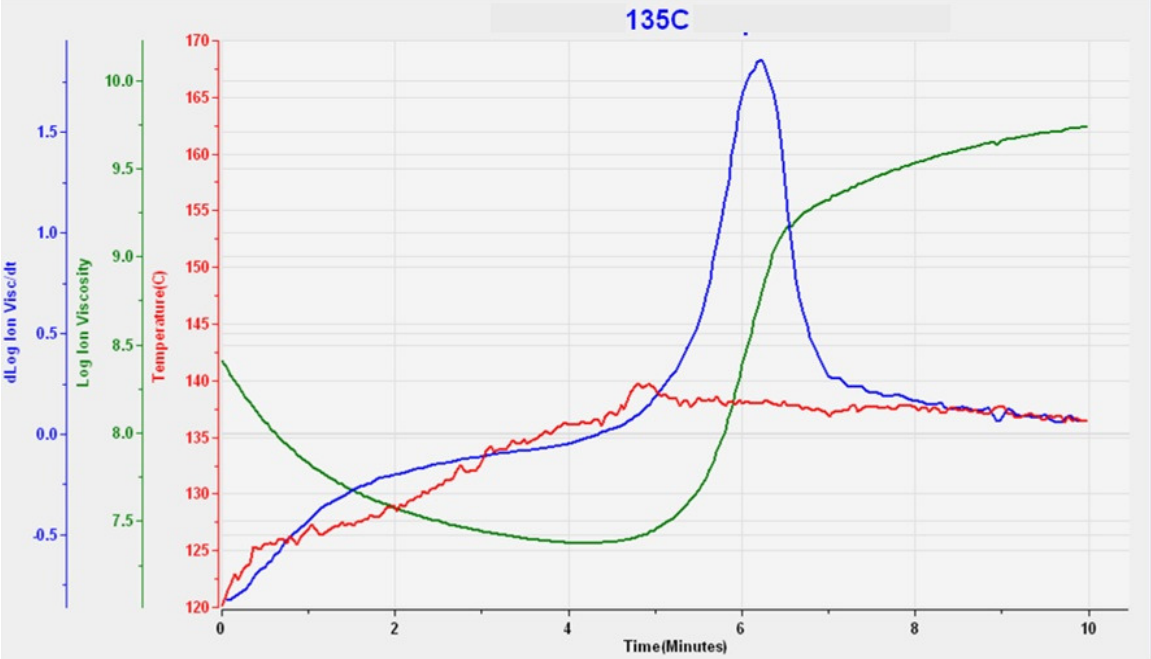

Figure 13-3
135 °C SMC cure data at 10 Hz

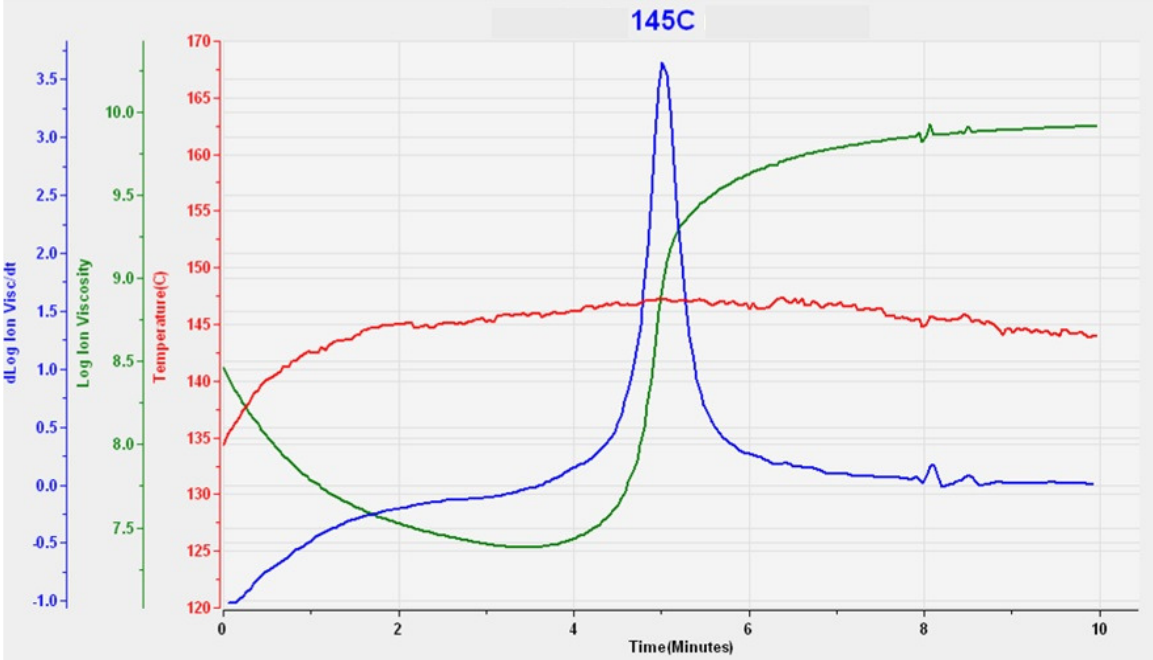

Figure 13-4
145 °C SMC cure data at 10 Hz

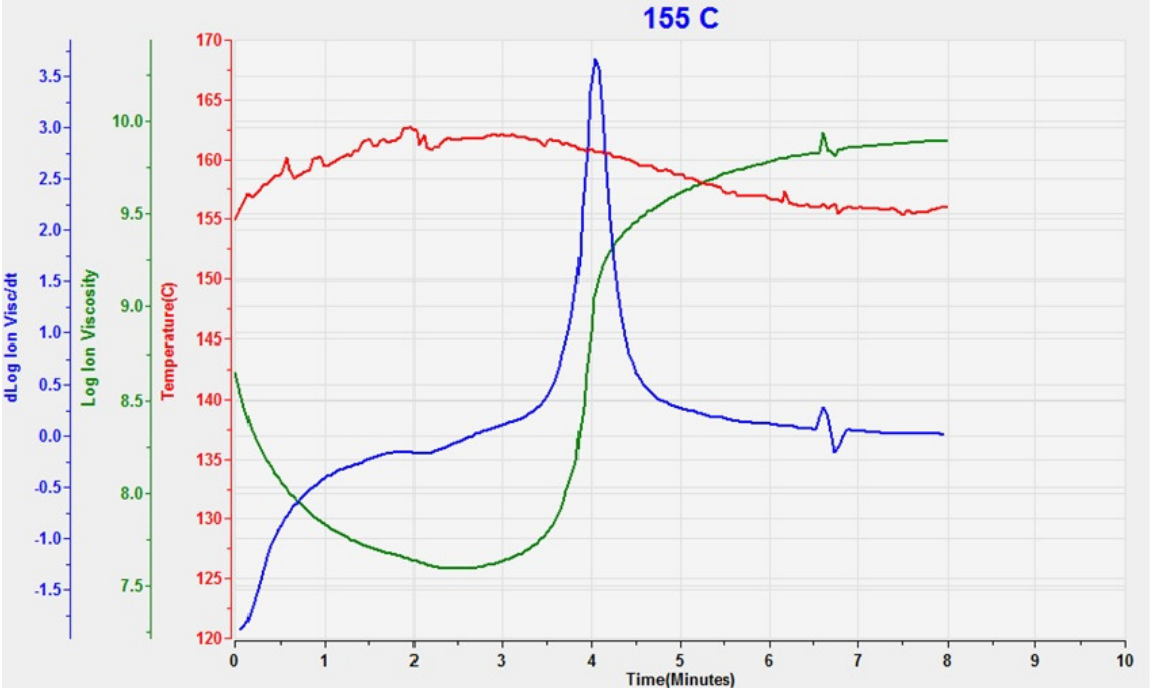

Figure 13-5
155 °C SMC cure data at 10 Hz

The Critical Points that characterize each cure are shown in Table 13-1. *Note that the slope of 0.25 to define CP(4), the end of cure, was chosen arbitrarily*. In actuality a user must determine the slope to indicate end of cure based on the needs of the application.

Table 13-1
Critical Points from SMC cure monitoring

Cure Temp. (°C)	CP(1) Crit. Visc.		CP(2) Min. Visc.		CP(3) Max Slope		CP(4) Crit. Slope	
	Value	Time	Value	Time	Value	Time	Value	Time
135	8.0	0.65 min (39 s)	7.38	4.17 min (250 s)	1.86	6.23 min (374 s)	0.25	7.21 min (433 s)
145	8.0	0.60 min (36 s)	7.39	3.42 min (205 s)	3.65	5.01 min (301 s)	0.25	6.13 min (368 s)
155	8.0	0.65 min (39 s)	7.60	2.48 min (149 s)	3.67	4.03 min (242 s)	0.25	5.14 min (308 s)

As plotted in Figure 13-6, the times to reach each Critical Point are shorter for cures at higher temperatures, which is expected for thermally driven reactions.

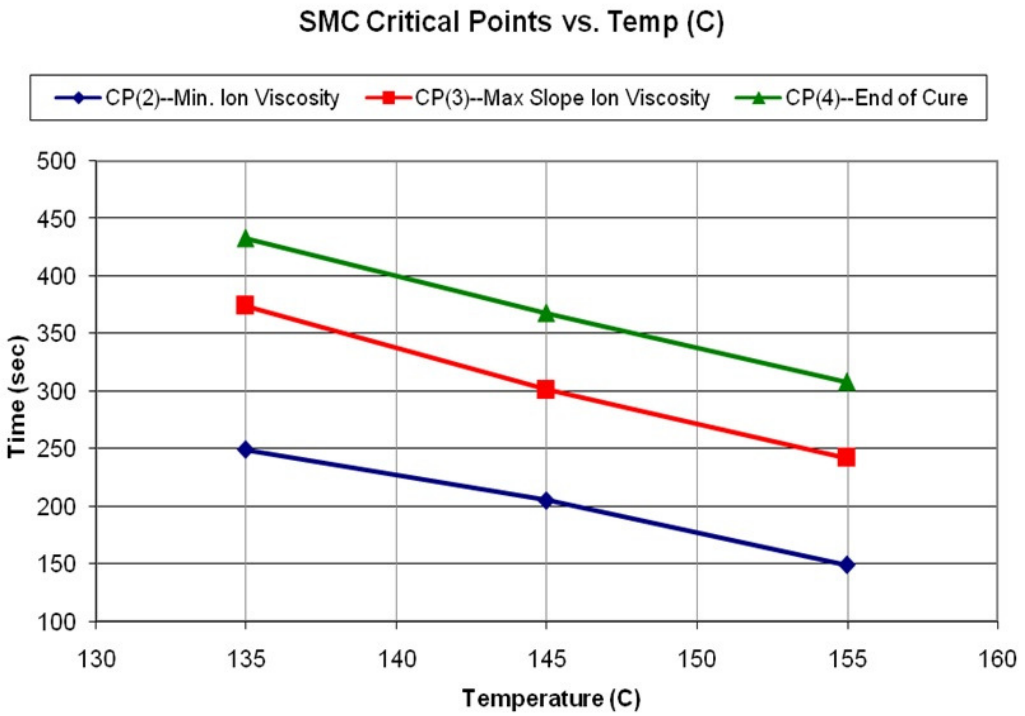

Figure 13-6
Critical Point time vs. cure temperature for SMC

The time to Critical Point 1—CP(1)—is not plotted in Figure 13-5. CP(1) determines when the ion viscosity of the SMC has decreased to the user selected value of 8.0, which was chosen to indicate the onset of flow. The time to flow is a measure of heating time and not of curing, consequently CP(1) has been omitted for clarity.

Within the 20 °C range of the plot of Figure 13-6, the time to reach CP(2)—the ion viscosity minimum—decreases by approximately 50 seconds for each 10 °C increase in processing temperature. The times to reach CP(3) and CP(4) vary by a similar amount with temperature.

References

1. LT-451 Dielectric Cure Monitor, manufactured by Lambient Technologies, Cambridge, MA, USA. https://lambient.com

2. Mini-Varicon sensor, manufactured by Lambient Technologies, Cambridge, MA USA

3. CureView software, manufactured by Lambient Technologies, Cambridge, MA USA

Chapter 14—Cure Monitoring of Bulk Molding Compound (BMC)

Cure of bulk molding compound

The curing behavior of Bulk Molding Compound (BMC) was observed using the LTF-631 High Speed Dielectric Cure Monitor.[1] Bulk Molding Compound is generally the same material as Sheet Molding Compound (SMC) but in bulk form, so the overall results apply to SMC as well. The data from dielectric cure monitoring (DEA) clearly show:

- Critical Points identify characteristic features of the cure such as minimum ion viscosity, maximum slope of log(ion viscosity) and the time to a chosen end of cure.
- Cure time decreases and reaction rate increases as cure temperature increases, as expected for a reaction that is thermally driven.

Procedure

Samples of BMC were placed on disposable Mini-Varicon[2] sensors, shown in Figure 14-1, then compressed and cured in an LTP-250 MicroPress,[3] which applied pressure and heat for separate runs at 130 °C, 140 °C, 150 °C, 160 °C and 170 °C. Previous tests had identified 100 Hz as an optimum excitation frequency for cure monitoring.

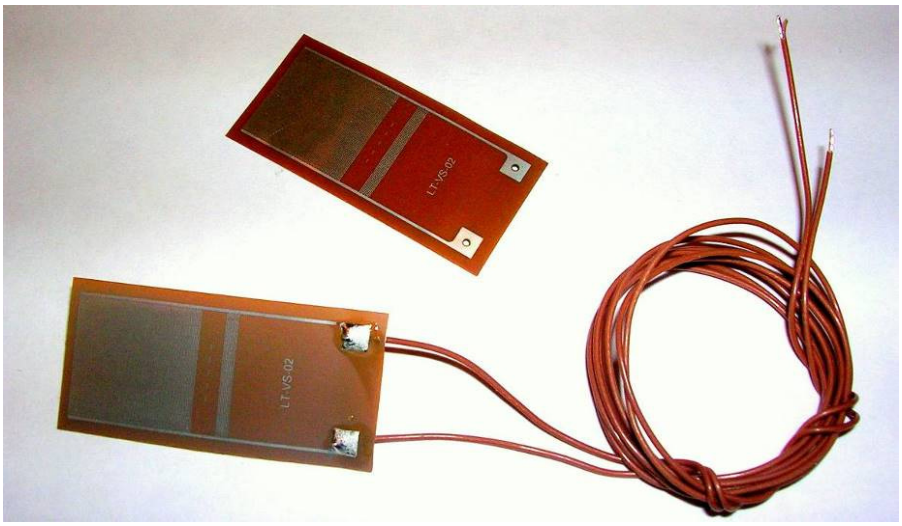

Figure 14-1
Mini-Varicon disposable sensor

The cure time for these samples is less than two minutes so an LTF-631 High Speed Dielectric Cure Monitor measured the dielectric properties of each sample. The measurement interval was 100 ms/data point and a trigger on the LTP-250 initiated data acquisition at a consistent point in the compression cycle. CureView[4] software acquired and stored the data, and later performed Critical Point analysis and presentation of the results.

Results

Figures 14-2, 3, 4, 5 and 6 show data from the cures of BMC at 130 °C, 140 °C, 150 °C, 160 °C and 170 °C, respectively. The ability of dielectric cure monitoring to observe the effect of temperature on cure is apparent in this sequence of plots.

As expected for a thermally activated reaction, the *log(IV)* curves rise and flatten more quickly with increasing temperature. The ion viscosity minimum—CP(2)—and the peak slope—CP(3)—also occur sooner at higher temperatures. Furthermore, the peak value of CP(3), which is related to the maximum reaction rate, increases with temperature. After acquiring these data, CureView was able to extract the Critical Points that characterize each cure and allow direct comparison of their behavior across the temperature range.

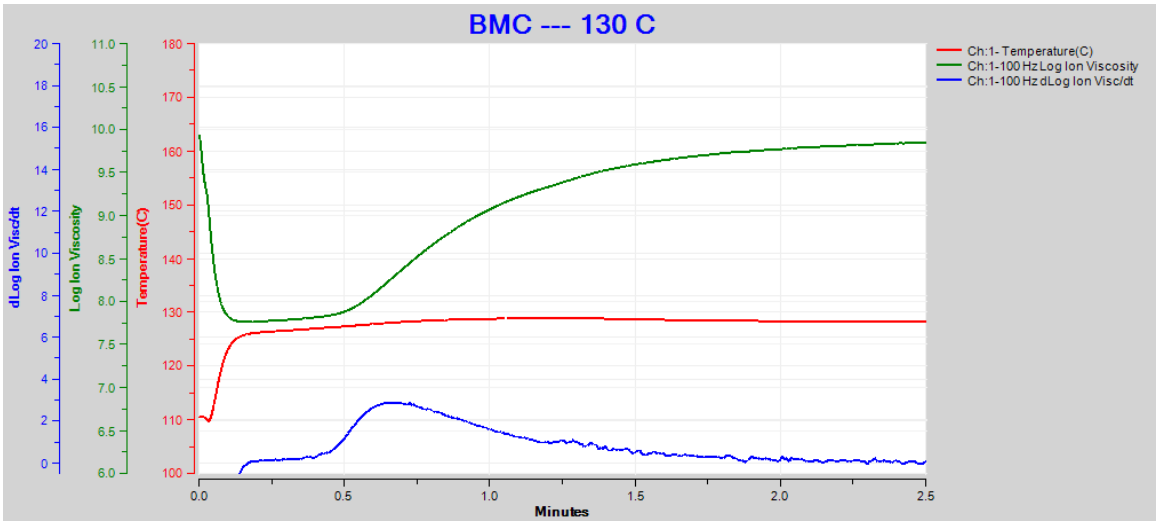

Figure 14-2
130 °C BMC cure data at 100 Hz

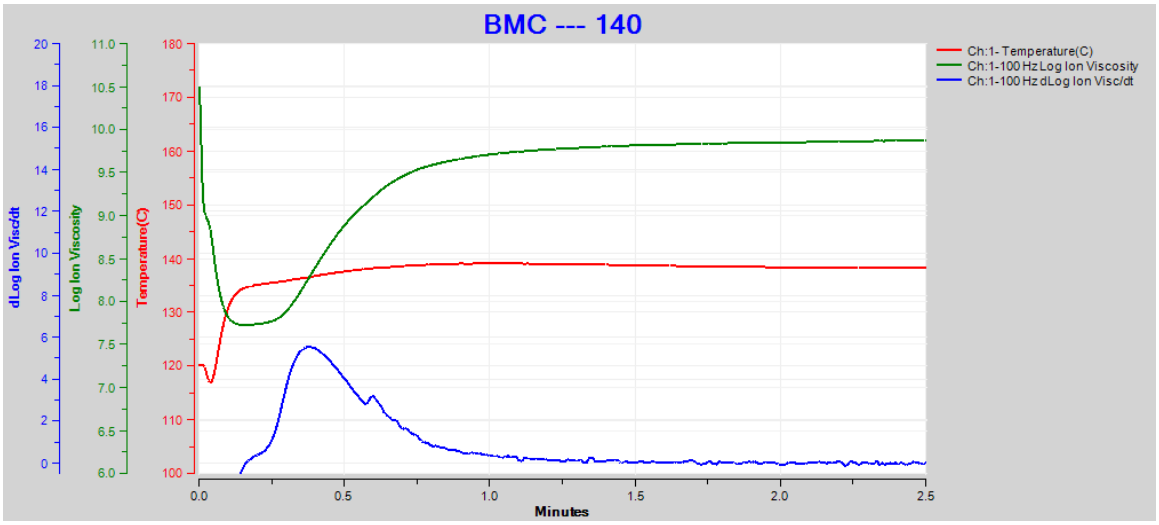

Figure 14-3
140 °C BMC cure data at 100 Hz

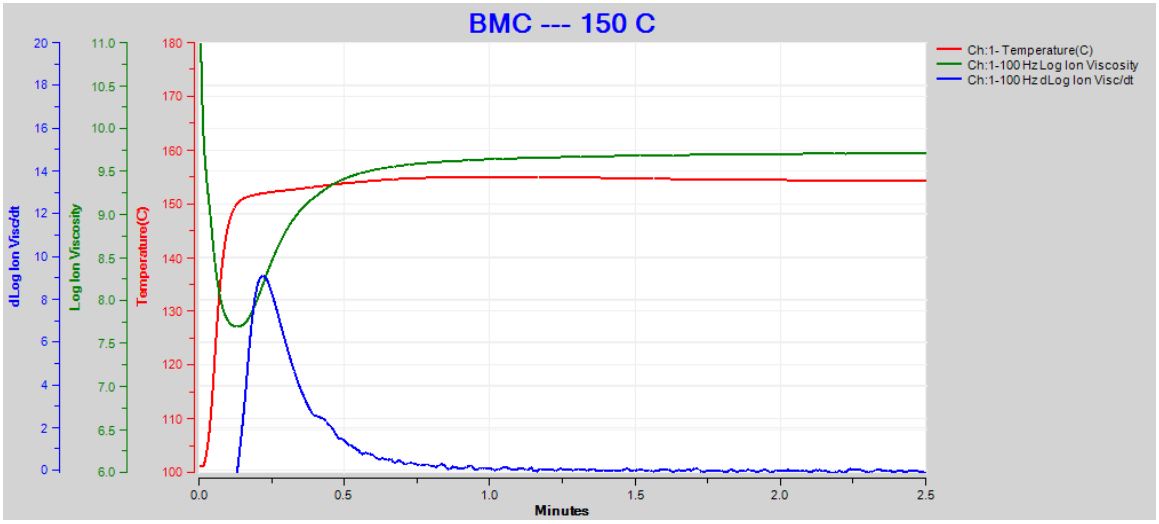

Figure 14-4
150 °C BMC cure data at 100 Hz

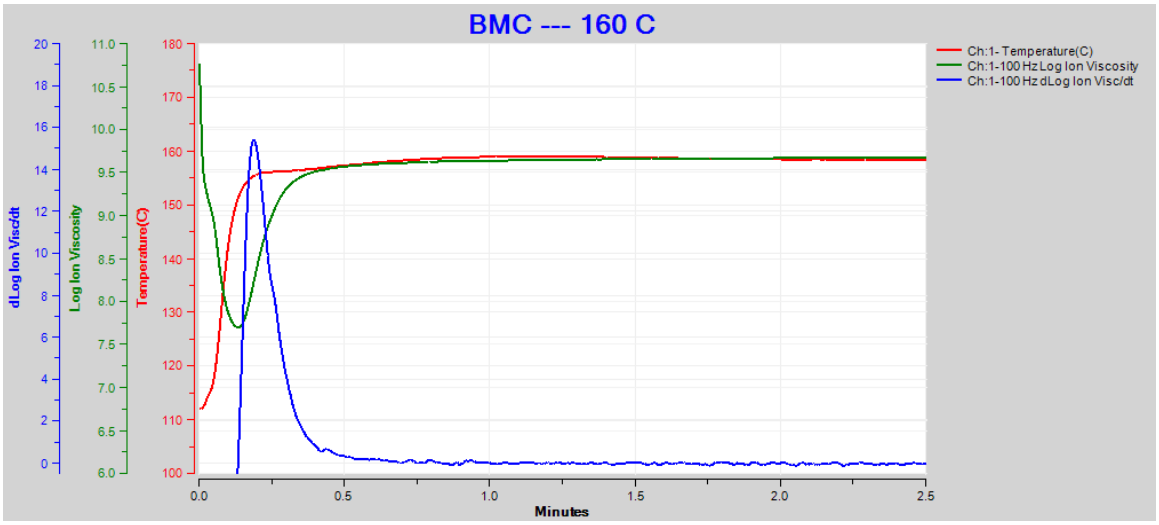

Figure 14-5
160 °C BMC cure data at 100 Hz

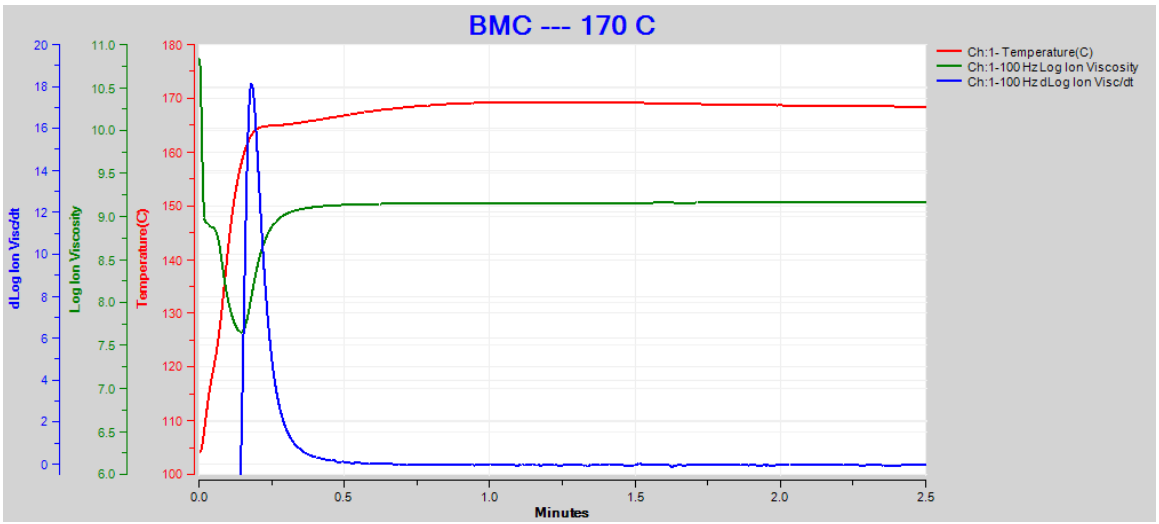

Figure 14-6
170 °C BMC cure data at 100 Hz

Figure 14-7 overlays the *log(IV)* and *slope* curves for 140 °C, 150 °C and 160 °C. For clarity, the data for 130 °C and 170 °C are omitted. This comparison shows the sensitivity of dielectric cure monitoring to changes in cure due to differences in process temperature.

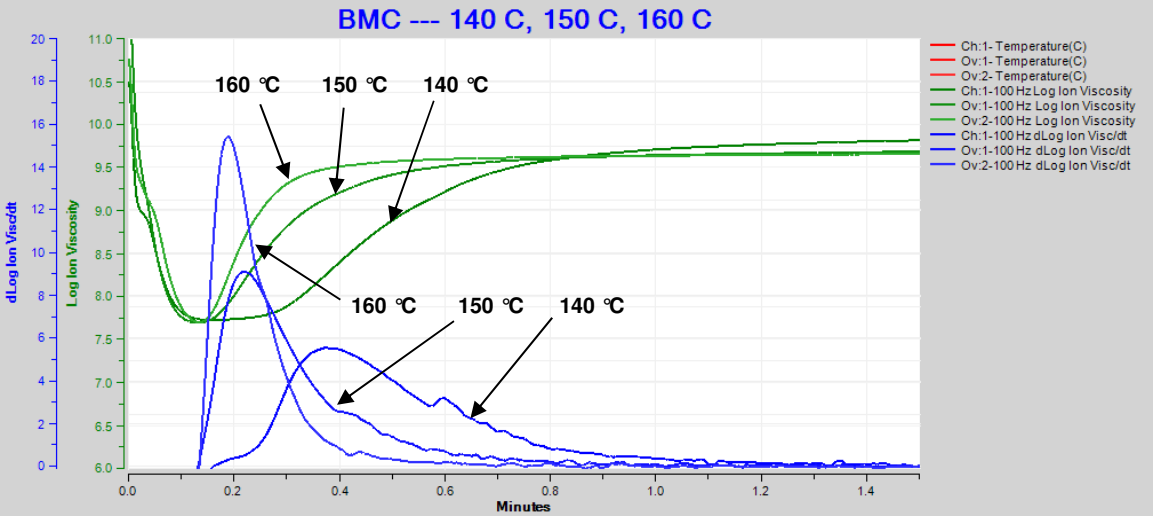

Figure 14-7
Overlay of 140 °C, 150 °C and 160 °C BMC cure data at 100 Hz

As expected, the maximum value of *slope* increases with process temperature, showing the relationship between reaction rate and temperature. Critical Points that characterize each cure are shown in Table 14-1, with the following notes:

- The time to CP(1) indicates onset of flow and is not a measure of cure, so CP(1) data are not shown
- The slope of 0.1 to define CP(4) was chosen arbitrarily; in fact, a user must determine a suitable slope based on the needs of the application to indicate end of cure.

Table 14-1
Critical Points from BMC cure monitoring

Cure Temp. (℃)	CP(1) Crit. Visc.		CP(2) Min. Visc.		CP(3) Max Slope		CP(4) End of Cure	
	Value	Time	Value	Time	Value	Time	Value	Time
130	---	---	7.77	0.164 m (9.8 s)	2.93	0.681 m (40.9 s)	0.10	2.138 m (128.3 s)
140	---	---	7.74	0.157 m (9.4 s)	5.58	0.373 m (22.4 s)	0.10	1.321 m (79.3 s)
150	---	---	7.72	0.153 m (9.2 s)	9.36	0.249 m (14.9 s)	0.10	0.908 m (54.5 s)
160	---	---	7.71	0.135 m (8.1 s)	15.42	0.189 m (11.3 s)	0.10	0.681 m (40.9 s)
170	---	---	7.66	0.144 m (8.6 s)	18.14	0.180 m (10.8 s)	0.10	0.517 m (31.0 s)

As plotted in Figure 14-8, the times to reach each Critical Point decrease for cures at higher temperatures, which is expected for thermally driven reactions.

The time to Critical Point 2—CP(2)—is the point when the BMC has the lowest mechanical viscosity. This information is often useful for identifying the optimum time to apply compression to squeeze out voids, consolidate the layers of a laminate or fill a mold.

The time to Critical Point 3—CP(3)—indicates the moment of fastest reaction. Before CP(3) the reaction is accelerating as temperature increases from the exotherm and external heating. After CP(3) the reaction slows as the network grows and monomers are depleted. *Although CP(3) is not the gel point, CP(3) is often used as a signpost associated with the gel point.*

The time to Critical Point 4—CP(4)—is the time to a user defined slope indicating end of cure. True end of cure occurs when the reaction stops and the material is no longer changing; at this time the slope is zero. The reaction may continue at a very low level for considerable time, so for practical purposes a small, non-zero slope is usually selected, with a value depending on the needs of the application.

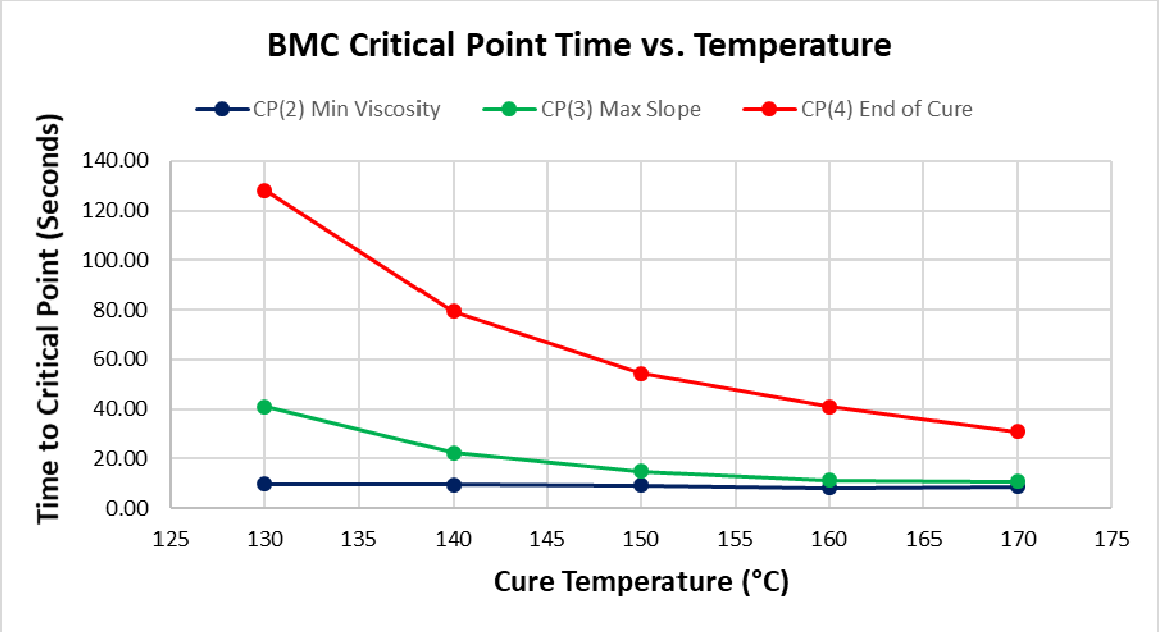

Figure 14-8
Critical Point time vs. cure temperature for BMC

Figure 14-9 shows how the maximum value of *slope*, which is a relative measure of reaction rate, increases with temperature. Again, this relationship is expected for a thermally driven reaction.

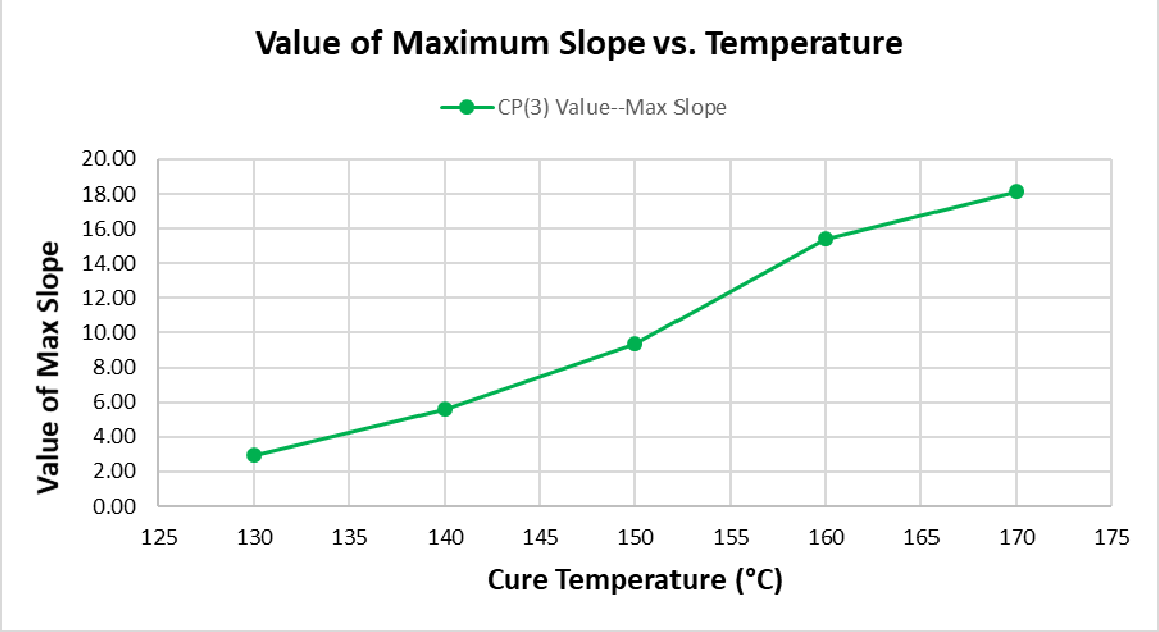

Figure 14-9
Value of maximum slope vs. cure temperature for BMC

References

1. LTF-631 High Speed Dielectric Cure Monitor, manufactured by Lambient Technologies, Cambridge, MA, USA. https://lambient.com

2. Mini-Varicon sensor, manufactured by Lambient Technologies, Cambridge, MA USA

3. LTP-250 MicroPress, manufactured by Lambient Technologies, Cambridge, MA USA

4. CureView software, manufactured by Lambient Technologies, Cambridge, MA USA

Chapter 15—Cure Monitoring of Epoxy Molding Compound (EMC)

Epoxy molding compound for electronic packaging

The curing behavior of epoxy molding compound (EMC) was observed using the LTF-631 High Speed Dielectric Cure Monitor.[1] Data from dielectric cure monitoring (DEA) clearly show:

- Critical Points identify characteristic features of the cure such as minimum ion viscosity, maximum slope of log(ion viscosity) and the time to a chosen end of cure.
- Cure time decreases and reaction rate increases as cure temperature increases, as expected for a reaction that is thermally driven.
- Dielectric cure monitoring of EMC samples show very high repeatability.

Normally available in either B-staged powders or pellets, as shown in Figure 15-1, for transfer molding, EMC is essential for electronics packaging and is used to encapsulate billions of integrated circuits each year.

Figure 15-1
Granular (left) and pelletized (right) epoxy molding compound[2]

Spiral flow test

The viscosity and curing behavior of EMC vary with the hundreds of available formulations and the high-speed, high-volume requirements of manufacturing demand consistent, reliable material performance. Presented

schematically in Figure 15-2, the spiral flow test is one of the principal methods for evaluating EMC. This test uses a mold with an Archimedean spiral channel and EMC is injected into it with a specified charge mass, mold temperature and transfer plunger speed.

As material flows through the channel, it cures, undergoes gelation and finally solidifies enough to stop flow. The length of the cured portion, shown in Figure 15-3, is a measure of the combined characteristics of fusion under pressure, melt viscosity and gelation rate under the test conditions.

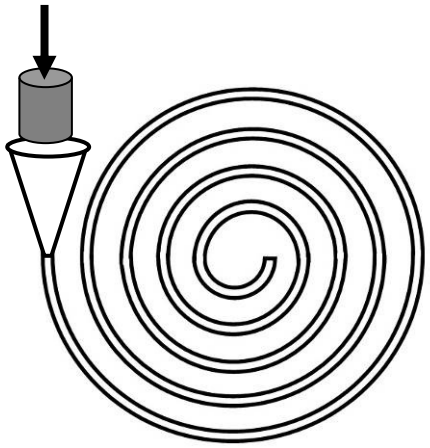

Figure 15-2
Spiral flow test of epoxy molding compound with initial charge

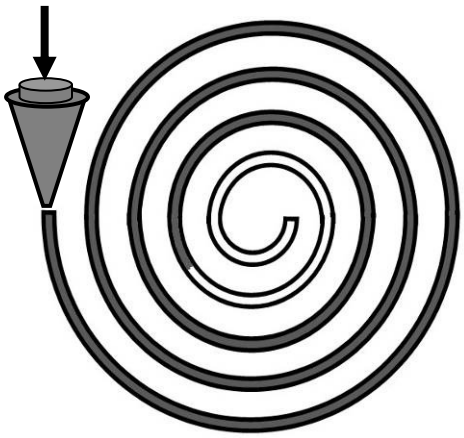

Figure 15-3
Spiral flow test after solidification and flow has stopped

Integrated circuits are manufactured with steps similar to those of Figure 15-4, in which EMC is heated until it melts then is injected into a mold with cavities for each integrated circuit. With a process temperature usually between

160 °C and 180 °C, the EMC must flow with low viscosity to avoid damaging delicate wire bonds and must fill the mold before gelation.

To maximize productivity, parts are removed from the mold when the EMC has reached about 40% epoxy conversion and is rigid enough to retain its form. Then they are baked in ovens at about 175 °C for an additional three or four hours until full cure.

Although the spiral flow test roughly emulates this process up to the gel point, it gives little insight into how the material cures. Nevertheless, if a manufacturer has established that consistent, specific results of the spiral flow test correspond to well molded products, then any change in test results is a warning that the EMC is not behaving as required.

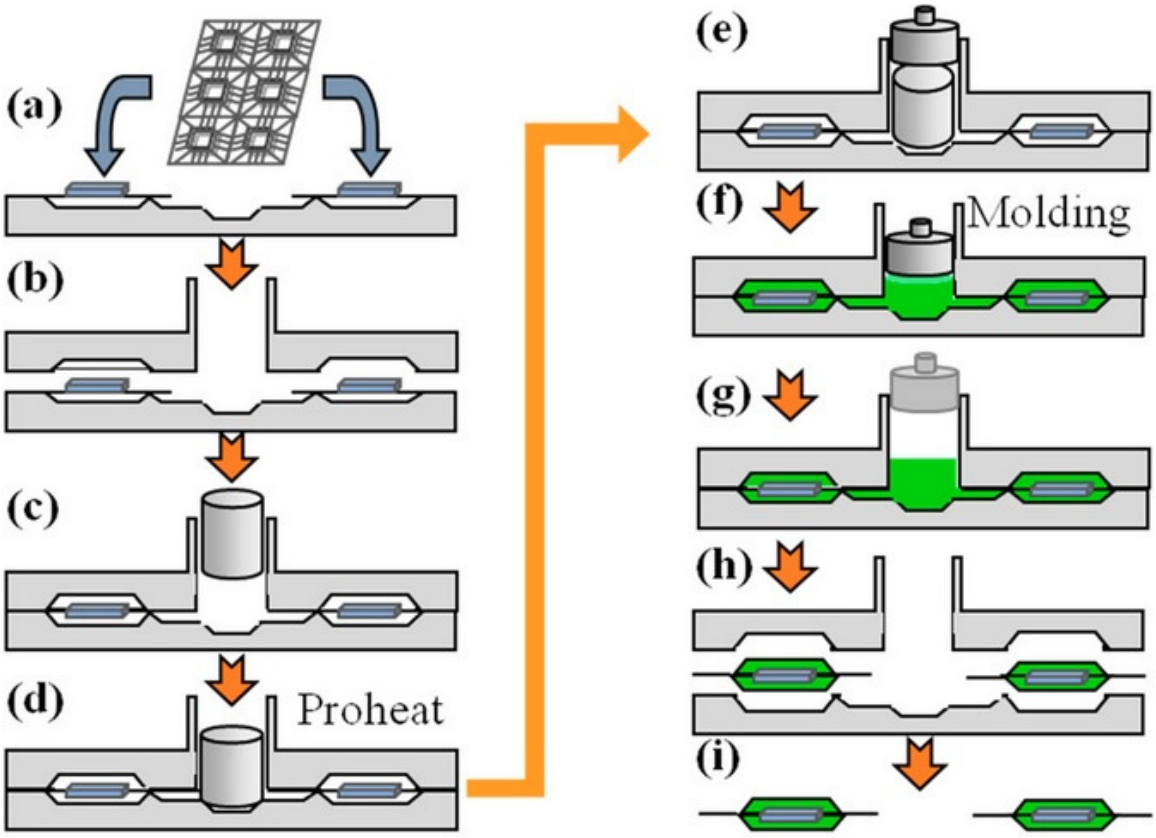

Figure 15-4
Steps in the EMC transfer molding process for electronic packaging[3]

Dielectric cure monitoring (DEA) can provide valuable additional information for quality control and manufacturing. The viscosity of EMC and the result of the spiral flow test depend on how the resin interacts with the filler, which often consists of spherical silica particles. The cure of EMC, however,

depends only on the resin, which is commonly epoxy cresol novolac with phenolic curing agents.

Procedure

Samples of EMC were placed on a reusable 1" Single-Electrode Sensor,[4] shown in Figure 15-5, then compressed and cured in an LTP-250 MicroPress[5], which applied pressure and heat for separate runs at 150 °C, 160 °C, 170 °C and 180 °C. Previous tests had identified 10 Hz as an optimum excitation frequency for cure monitoring.

The cure time for these samples can be less than three minutes so an LTF-631 High Speed Dielectric Cure Monitor[1] measured the dielectric properties of each sample. The measurement interval was 100 ms/data point and a trigger on the LTP-250 initiated data acquisition at a consistent point in the compression cycle. CureView software acquired and stored the data, and later performed Critical Point analysis and presentation of the results.

Figure 15-5
Single-Electrode reusable sensor

Results

Figures 15-6, 7, 8, 9 show data from the cures of EMC at 150 °C, 160 °C, 170 °C and 180 °C, respectively. For each cure *log(IV)* and *slope* follow the typical behavior of a thermoset during isothermal cure. The ability of dielectric measurements to observe the effect of temperature on cure is apparent in this sequence of plots.

As expected for a thermally activated reaction, the *log(IV)* curves rise and flatten more quickly with increasing temperature. The ion viscosity minimum—

CP(2)—and the peak slope—CP(3)—also occur sooner at higher temperatures. Furthermore, the peak value of CP(3), which is related to the maximum reaction rate, increases with temperature. After acquiring these data, CureView was able to extract the Critical Points that characterize each cure and allow direct comparison of their behavior across the temperature range.

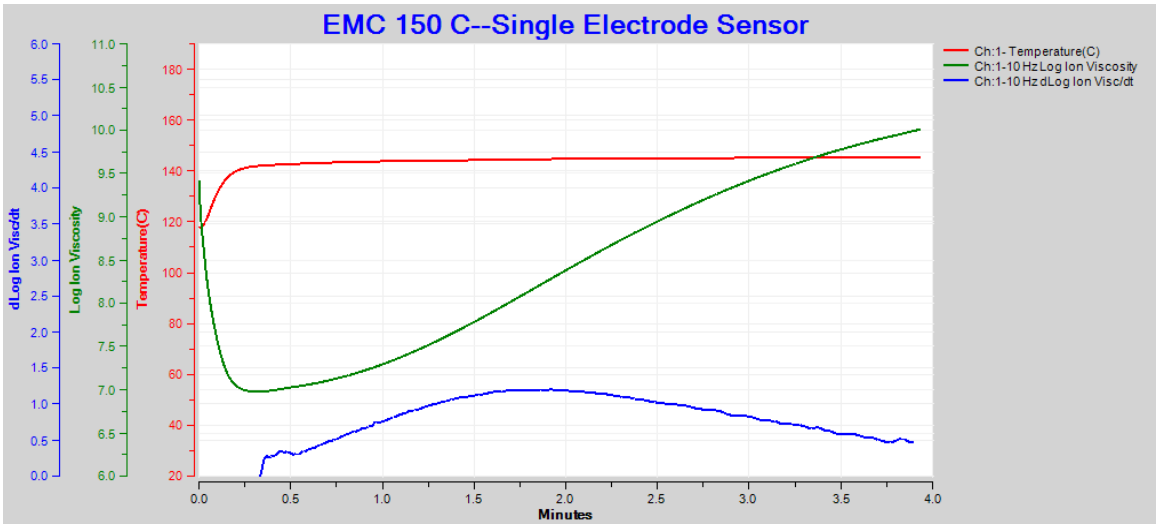

Figure 15-6
150 °C EMC cure data at 10 Hz

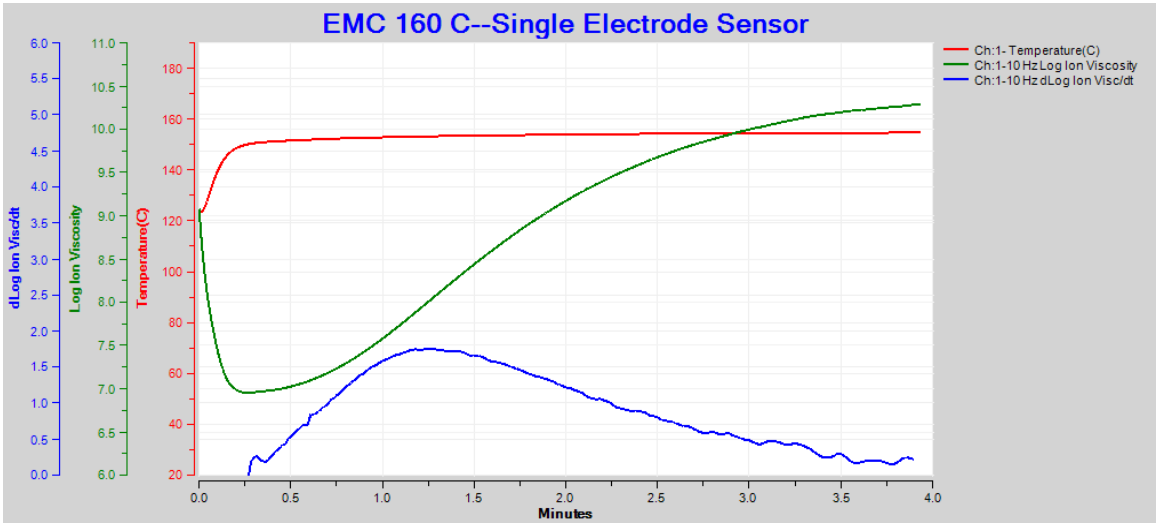

Figure 15-7
160 °C EMC cure data at 10 Hz

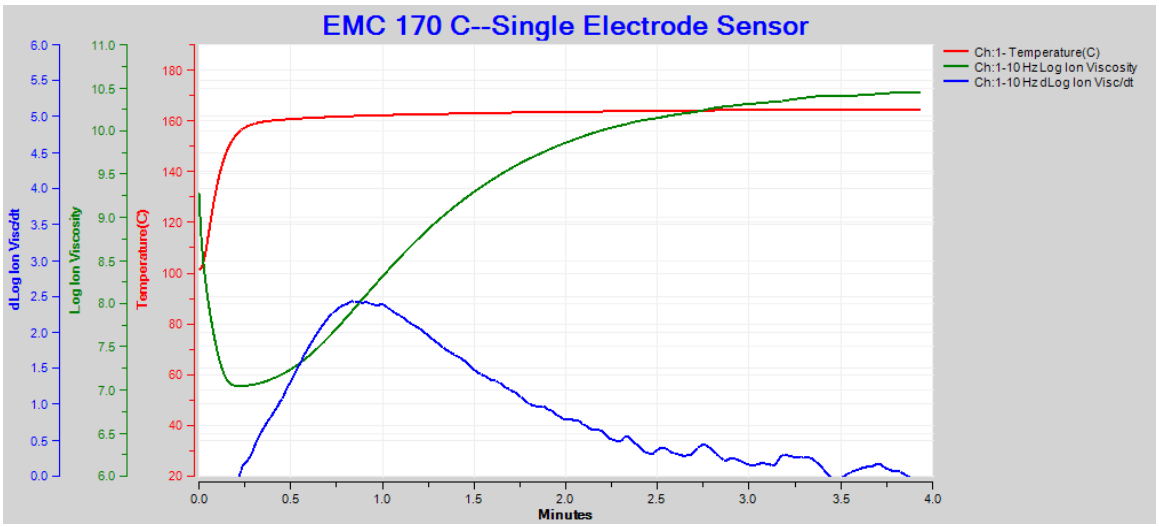

Figure 15-8
170 °C EMC cure data at 10 Hz

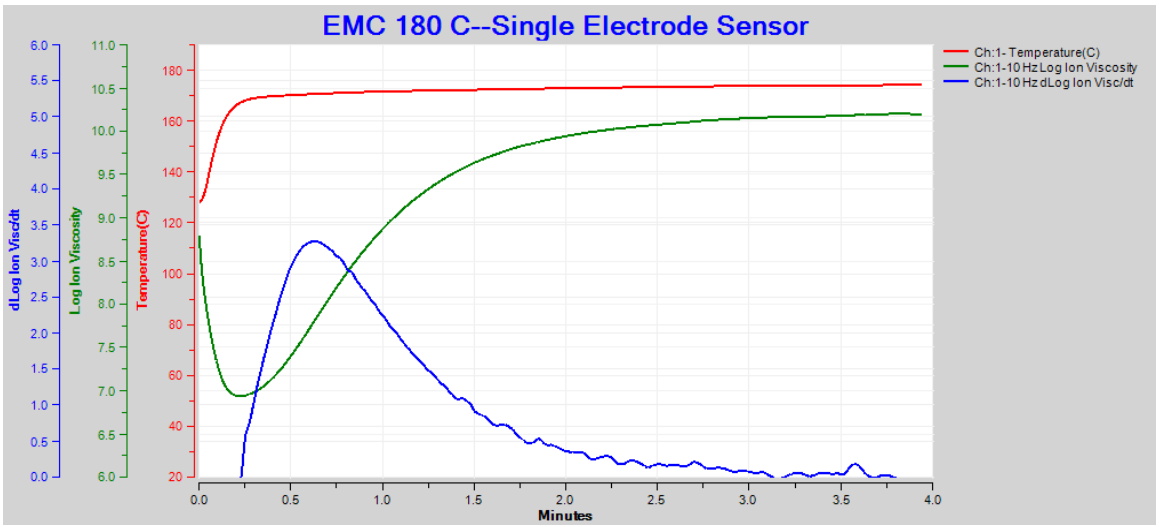

Figure 15-9
180 °C EMC cure data at 10 Hz

Figure 15-10 overlays the *log(IV)* and *slope* curves for these four cures. This comparison shows the sensitivity of dielectric cure monitoring to changes in cure due to temperature differences.

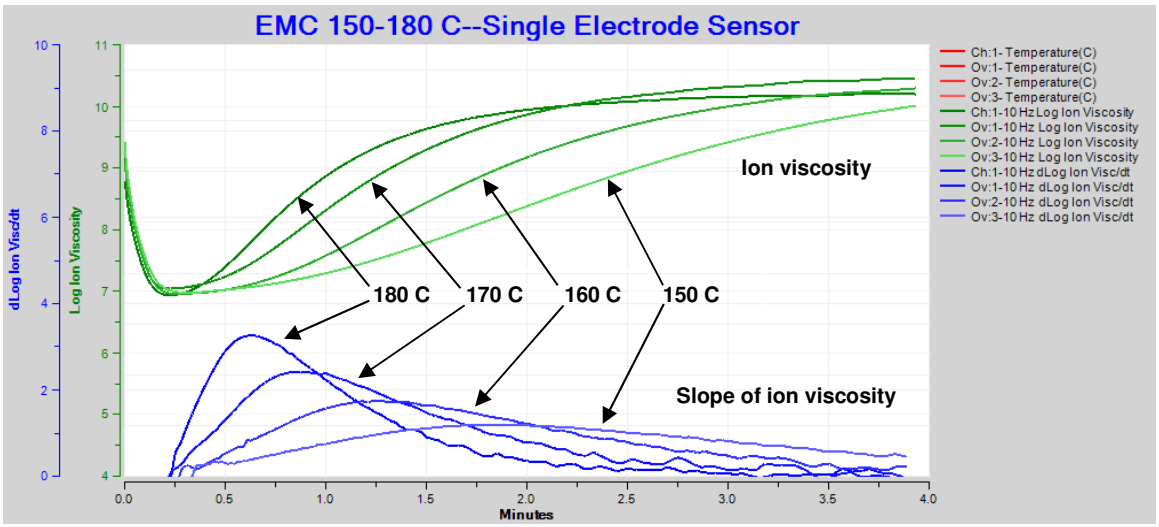

Figure 15-10
EMC *ion viscosity* (green) and *slope* (blue) at 10 Hz, cures at 150 °C, 160 °C, 170 °C and 180 °C

As expected, the maximum value of *slope* increases with process temperature and shows the relationship between reaction rate and temperature. Critical Points that characterize each cure are shown in Table 15-1, with the following notes:

- The time to CP(1) indicates onset of flow and is not a measure of cure, so CP(1) data are not shown
- The slope of 0.5 to define CP(4) was chosen arbitrarily; in fact, a user must determine a suitable slope based on the needs of the application to indicate end of cure.

Table 15-1
Critical Points from EMC cure monitoring

Cure Temp. (°C)	CP(1) Crit. Visc.		CP(2) Min. Visc.		CP(3) Max Slope		CP(4) End of Cure	
	Value	Time	Value	Time	Value	Time	Value	Time
150	---	---	6.99	0.334 m (20.0 s)	1.21	1.92 m (114.9 s)	0.50	3.728 m (223.7 s)
160	---	---	6.96	0.270 m (16.3 s)	1.76	1.26 m (75.9 s)	0.50	2.997 m (179.8 s)
170	---	---	7.06	0.218 m (13.1 s)	2.44	0.833 m (50.0 s)	0.50	2.282 m (136.9 s)
180	---	---	6.95	0.228 m (13.7 s)	3.28	0.636 m (38.2 s)	0.50	1.779 m (106.7 s)

The time to Critical Point 2—CP(2)—is the point when the EMC has the lowest mechanical viscosity. This information is often useful for identifying the optimum time to apply compression to squeeze out voids, consolidate the layers of a laminate or fill a mold.

The time to Critical Point 3—CP(3)—indicates the moment of fastest reaction. Before CP(3) the reaction is accelerating as temperature increases from the exotherm and external heating. After CP(3) the reaction slows as the network grows and monomers are depleted. **Although CP(3) is not the gel point, CP(3) is often used as a signpost *associated* with the gel point.**

The time to Critical Point 4—CP(4)—is the time to a user defined slope indicating end of cure. True end of cure occurs when the reaction stops and the material is no longer changing; at this time the slope is zero. The reaction may continue at a very low level for considerable time, so for practical purposes a small, non-zero slope is usually selected, with a value depending on the needs of the application.

The times to reach CP(2) depend largely on how quickly the EMC heats and do not significantly reflect the rate of cure, so it is not surprising to see fairly constant times at different process temperatures. As seen in Figure 15-11, the times to reach CP(3) and CP(4) decrease as temperature increases, which is expected for thermally driven reactions.

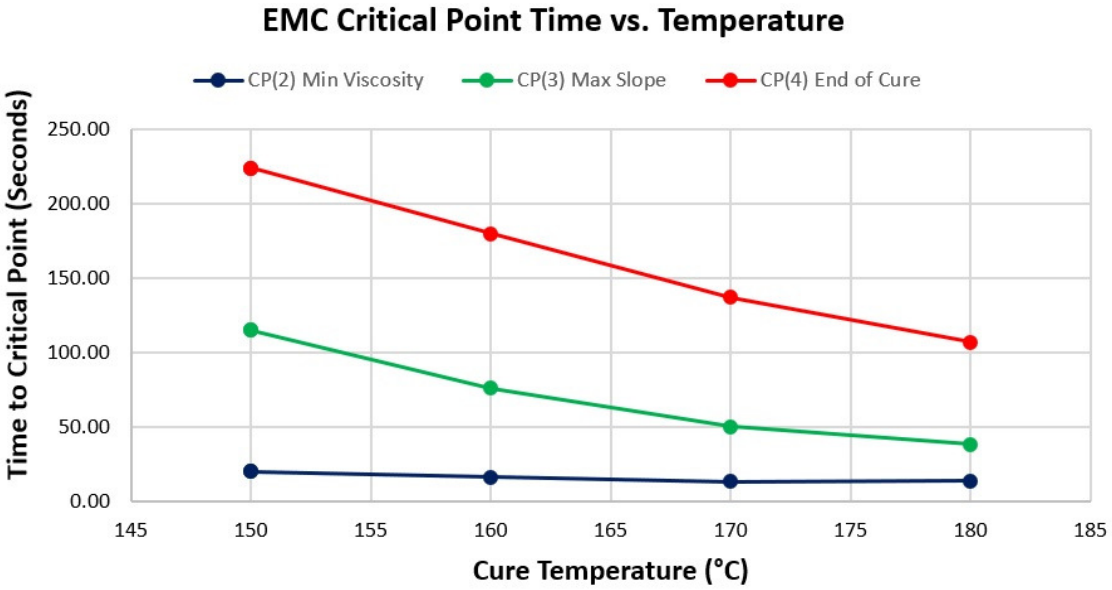

Figure 15-11
Critical Point time vs. cure temperature for BMC

Figure 15-12 shows how the maximum value of *slope* increases with temperature. Again, this relationship is expected because the height of CP(3) is a relative measure of the maximum reaction rate.

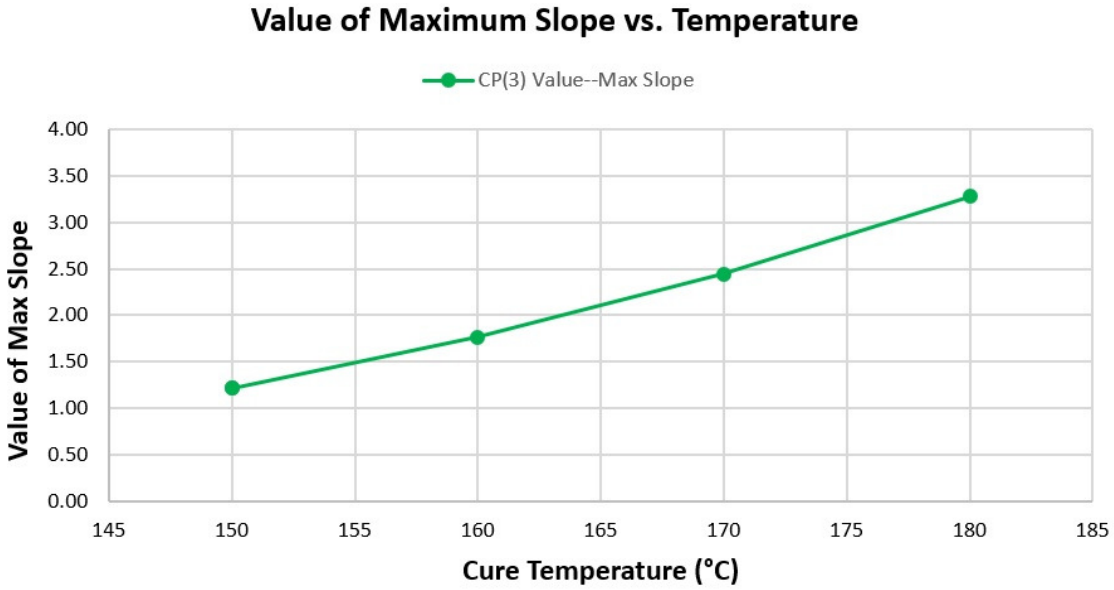

Figure 15-12
Value of maximum slope vs. cure temperature for EMC

Quality control of epoxy molding compound

The spiral flow test provides limited insight into a material because a single number—the length of the solidified EMC—can only partly characterize the combined behavior of cure and viscosity. In the high-speed, high-volume manufacture of integrated circuits, consistency is an encapsulant's most important quality. Dielectric cure monitoring can supplement the spiral flow test by providing information about the entire cure, allowing the documentation of consistency in far greater detail.

Figure 15-13 shows data from four consecutive tests of EMC at 170 °C. In this case the ion viscosity curves are virtually indistinguishable from one another, verifying high repeatability. When dielectric cure monitoring is used for quality control of outgoing material, formulators of EMC can assure customers their product has been fully tested for consistency.

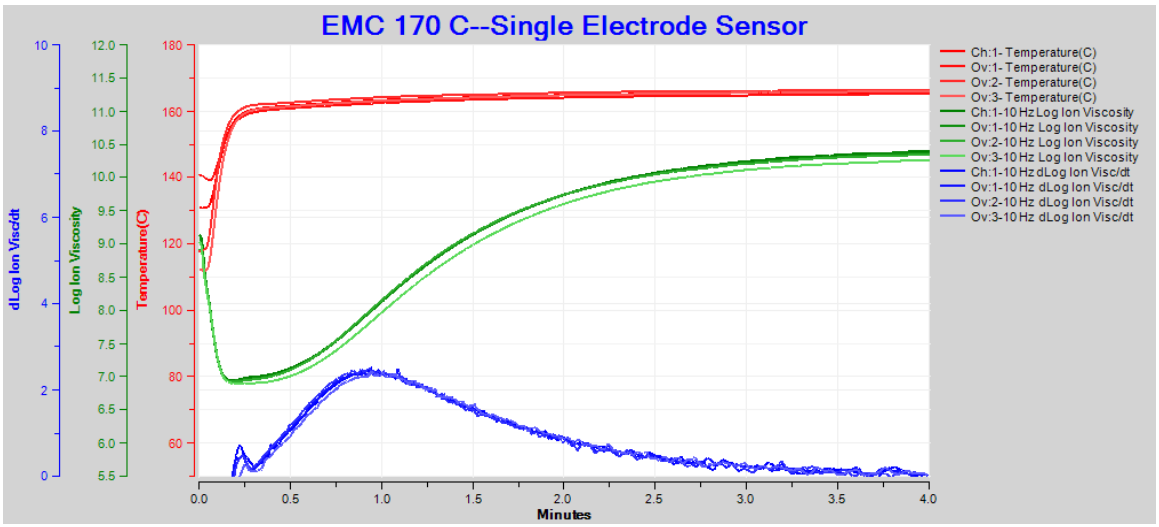

Figure 15-13
Repeatability of EMC cure at 170 °C (four consecutive tests)

Some electronics manufacturers have installed dielectric sensors in both the input and output ports of a mold, illustrated schematically in Figure 15-14.

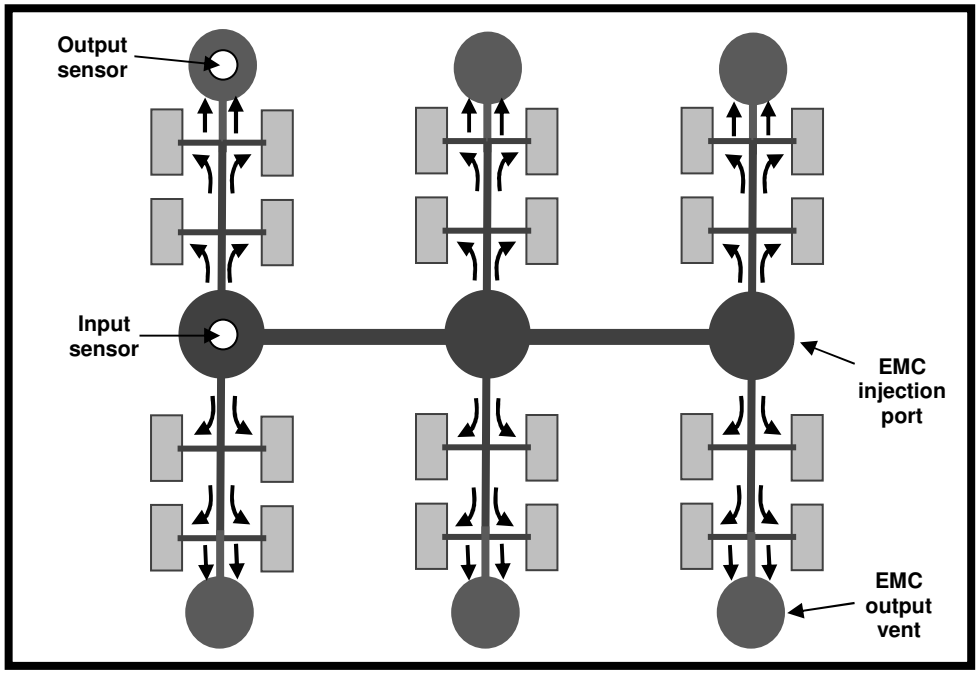

Figure 15-14
Mold with sensors for EMC cure monitoring

By continuously monitoring the ion viscosity of EMC at both the injection port and output vent, it is possible to understand the behavior of the material between these two points and determine:

- Flow time from input to output
- Variation of minimum viscosity at the mold cavities
- Cure rate at mold cavities
- Cure state at time of demold

These additional parameters provide important information for keeping the packaging process in control. Changes beyond specified limits warn the manufacturing engineer of potential problems with the epoxy molding compound.

References

1. LTF-631 High Speed Dielectric Cure Monitor, manufactured by Lambient Technologies, Cambridge, MA USA. https://lambient.com

2. Epoxy molding compound picture credit: Shyama Construction & Waterproofing Co., Kolkata, West Bengal, India

3. Huang, Wan-Chiech; Hsu, Chao-Ming and Yang, Cheng-Fu, "Recycling and Refurbishing of Epoxy Packaging Mold Ports and Plungers," *Inventions* **2016**, *1*(2), 11; https://doi.org/10.3390/inventions1020011, June 6, 2016

4. 1" Single-Electrode sensor, manufactured by Lambient Technologies, Cambridge, MA USA

5. LTP-250 MicroPress, manufactured by Lambient Technologies, Cambridge, MA USA

Chapter 16– Cure Monitoring and Aging of Carbon-Fiber Sheet Molding Compound (CF-SMC)

Aging of carbon-fiber sheet molding compound

Dielectric cure monitoring was used to study aging of carbon-fiber sheet molding compound (CF-SMC). The CF-SMC was wrapped in plastic and stored in a refrigerator for the duration of the study, and samples were cured periodically at 150 °C. Under the storage conditions, the CF-SMC log(*ion viscosity*) at end of cure remained at a consistent high level for at approximately 50 days, indicating high degree of cure and a shelf life at least this long.

Material aged more than 80 days showed a significant reduction in the final log(*ion viscosity*) due to loss of styrene, which lowered the maximum achievable degree of cure. Consequently, dielectric measurements can identify a fundamental difference between CF-SMC that is good and CF-SMC that has aged beyond its useful lifetime.

Procedure

Disposable Mini-Varicon[1] sensors were used for all tests. A piece of laboratory grade filter paper covered the sensor and three layers of CF-SMC were stacked on the filter paper. The filter paper prevented conductive carbon fibers from short circuiting the electrodes, while allowing resin to reach the sensor. A sheet of aluminum foil was placed on top of the sample to prevent material from adhering to the platen that would heat it. The resulting lay-up is shown in Figure 16-1. A thermocouple placed next to the sensor measured CF-SMC temperature during the test. The sample was cured in an LTP-250 MicroPress,[2] which applied pressure and heat at 150 °C.

The cure time for these samples can be less than one minute so an LTF-631 High Speed Dielectric Cure Monitor[3] was used to measure the dielectric properties of each sample. Previous tests had identified 100 Hz as an optimum excitation frequency for cure monitoring. The measurement interval was 100 ms/data point and a trigger on the LTP-250 initiated data acquisition at a consistent time in the compression cycle. CureView[4] software acquired and stored the data, and later performed Critical Point analysis and presentation of the results.

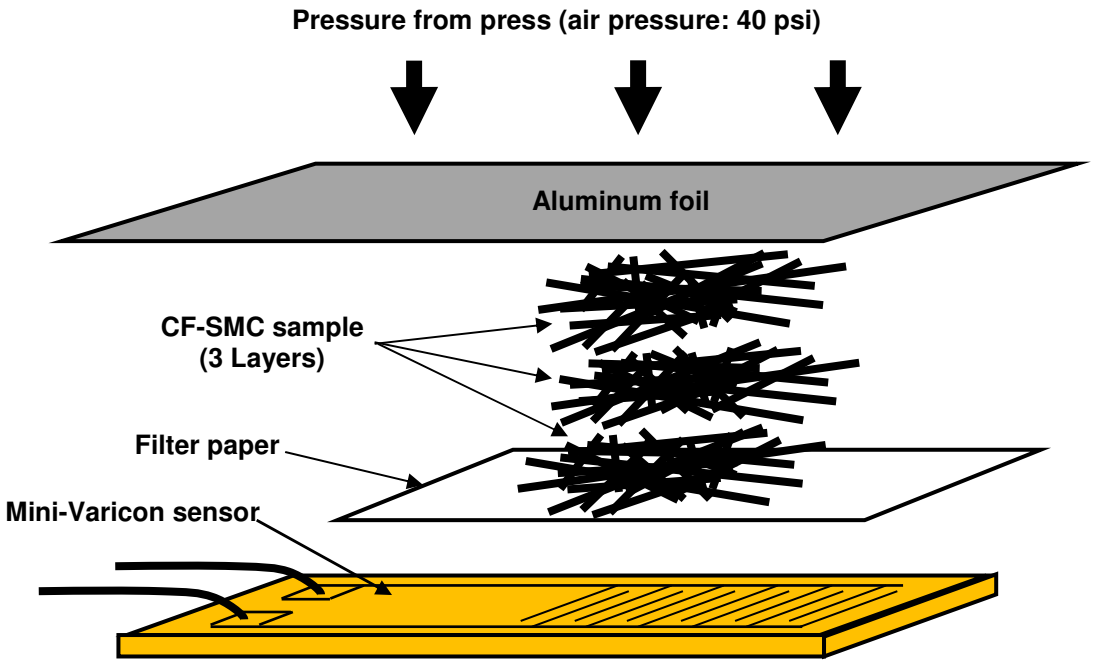

Figure 16-1
Lay-up of CF-SMC for tests

Results

Figure 16-2 shows repeatability of log(*IV*) at end of cure after the first day of storage.

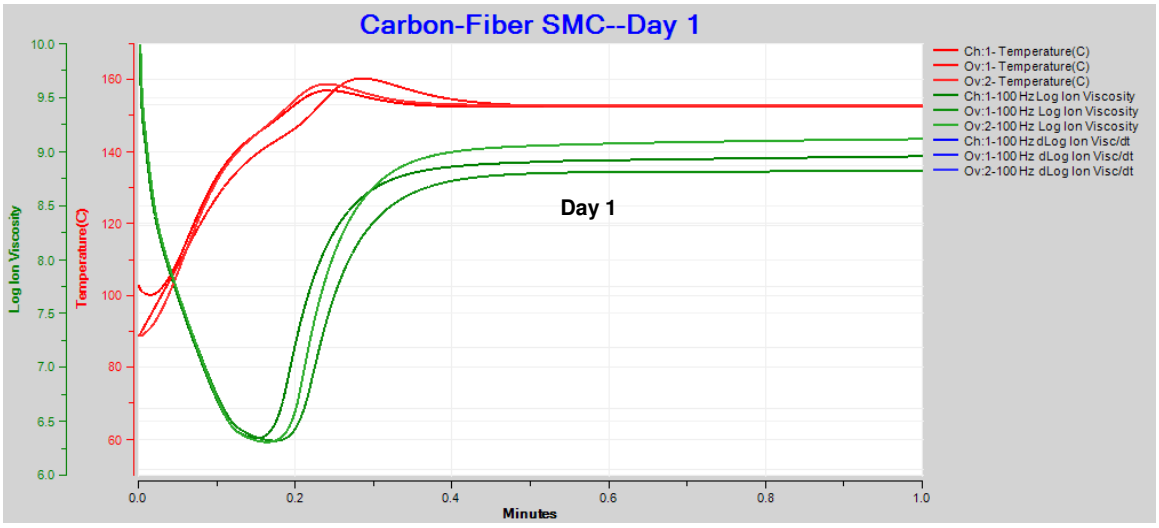

Figure 16-2
Repeatability of CF-SMC cure, day 1

Variation in the amount of sample causes different flow rates as the CF-SMC spreads under pressure. In turn, different flow rates cause different heating rates, visible in the temperature data, and affects the curing rates for individual tests. Regardless of the rate of early cure, all samples reach approximately the same log(*IV*) of 9.0 at the end of cure.

Figure 16-3 shows good consistency of log(*IV*) at end of cure over a period of 50 days. During this period log(*IV*) at end of cure remains about 9.0 for all tests.

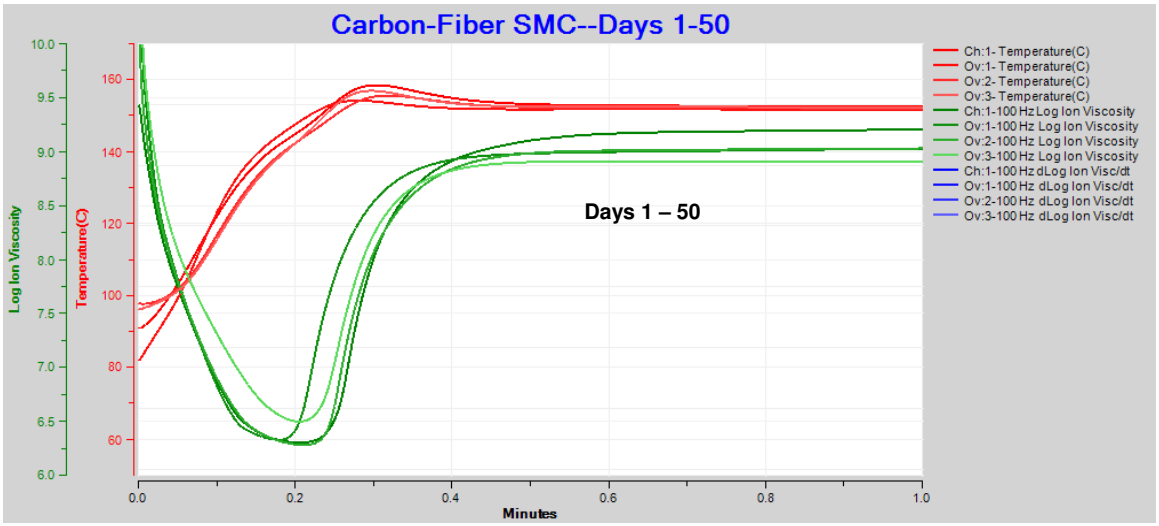

Figure 16-3
CF-SMC cure, days 1-50

Figure 16-4 shows the cure curves over 100 days. After 80 days final log(*IV*) falls significantly to approximately 8.2, compared to the first 50 days when final log(*IV*) is 9.0. Lower values of log(*IV*) at end of cure correspond to lower degrees of cure, so after 80 days the loss of styrene is great enough to prevent complete cure. This result indicates the refrigerated CF-SMC degrades and becomes unusable sometime between day 50 and day 80.

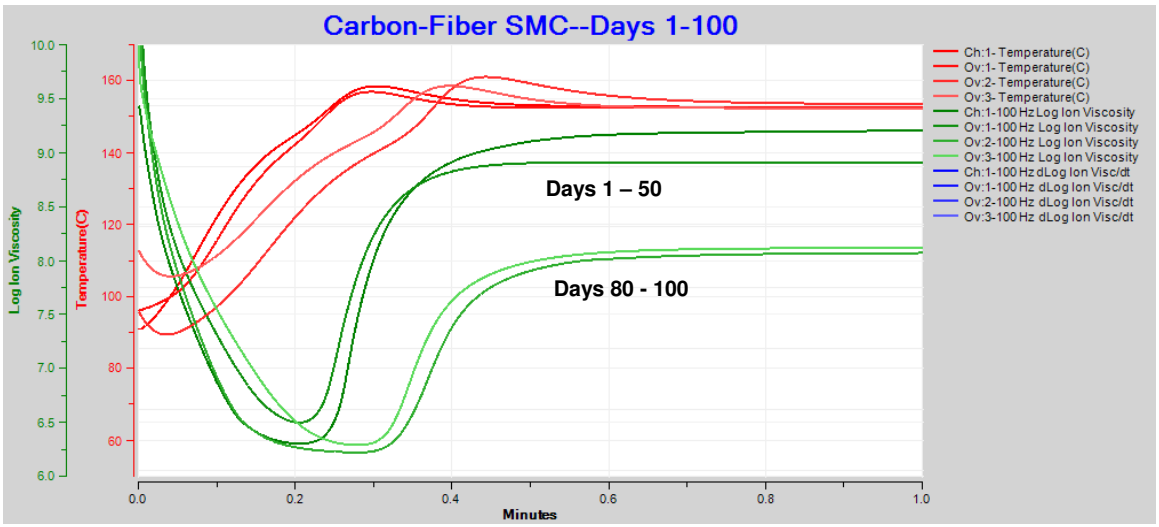

Figure 16-4
CF-SMC cure, days 1-100

Figure 16-5 shows good repeatability of log(*IV*) at end of cure after 80 days. The four curves shown represent tests between days 80 and 100.

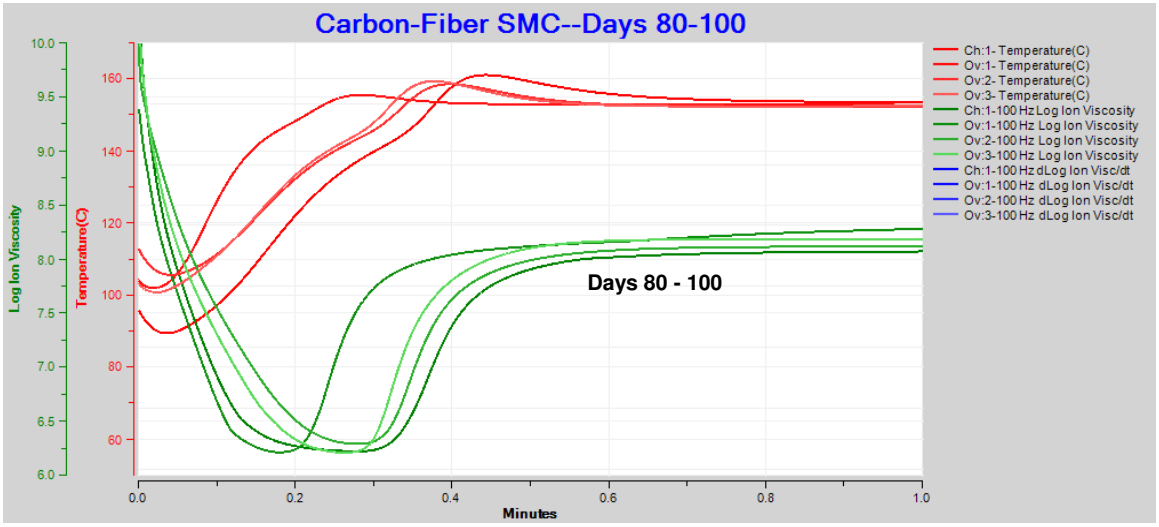

Figure 16-5
Repeatability of CF-SMC cure, days 80-100

Table 16-1 shows the results of all tests for aging of the CF-SMC. There is a clear correlation among the age of the material, the qualitative physical properties (pliability, tackiness and odor) and log(*IV*) at end of cure.

Table 16-1
Results of tests

Day	Final log(IV)	Average	Notes (Qualitative)
1	9.0	9.1	Fresh, very pliable, very tacky, strong styrene odor
1	9.1		
7	9.0	9.1	Very pliable, very tacky, strong styrene odor
7	9.1		
14	9.2	9.3	Very pliable, very tacky, strong styrene odor
14	9.4		
21	9.1	9.1	Very pliable, very tacky, strong styrene odor
21	9.1		
28	9.0	9.1	Pliable, tacky, noticeable styrene odor
28	9.1		
35	9.0	9.1	Pliable, tacky, noticeable styrene odor
35	9.2		
42	8.7	8.9	Pliable, tacky, noticeable styrene odor
42	9.0		
49	9.2	9.0	Pliable, tacky, noticeable styrene odor
49	8.8		
56	8.9	8.9	Pliable, less tacky, noticeable styrene odor
56	8.9		
80	8.1	8.2	Less pliable, slightly tacky, faint styrene odor
80	8.3		
100	8.1	8.2	Less pliable, minimally tacky, very faint styrene odor
100	8.2		

Figure 16-6 plots the data of Table 1 for all tests of the CF-SMC versus storage time.

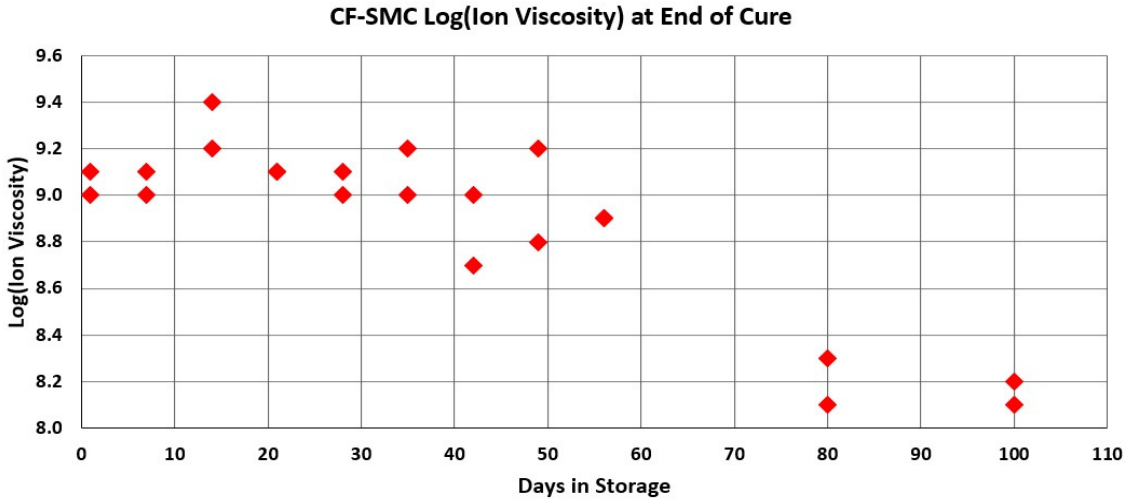

Figure 16-6
Plot of log(*IV*) at end of cure vs. refrigerated storage time

The data fall into two distinct clusters, which may be interpreted as:

- "Good" CF-SMC indicated by final log(IV) of approximately 9.0
- "Bad" CF-SMC indicated by final log(IV) of approximately 8.2

The boundary between "Good" and "Bad" CF-SMC is in the period between 50 and 80 days.

Dielectric cure monitoring is a simple and easy method of identifying carbon-fiber sheet holding compound that has aged beyond its useful shelf-life. By periodically testing CF-SMC during storage, a manufacturer can check the quality of their stock and ensure the use of only good CF-SMC for the molding of products.

References

1. Mini-Varicon sensor, manufactured by Lambient Technologies, Cambridge, MA USA. https://lambient.com

2. LTF-631 High Speed Dielectric Cure Monitor, manufactured by Lambient Technologies, Cambridge, MA USA

3. LTP-250 MicroPress, manufactured by Lambient Technologies, Cambridge, MA USA

4. CureView software, manufactured by Lambient Technologies, Cambridge, MA USA

Chapter 17– Cure Monitoring of Carbon Fiber Reinforced Prepreg (CFRP)

Behavior of carbon fiber reinforced prepreg during cure

Samples from of carbon fiber reinforced prepreg (CFRP) were tested for repeatability and the effect of temperature on cure rate. The data from dielectric cure monitoring clearly show:

- Critical Points identify characteristic features of the cure such as minimum ion viscosity, maximum slope of log(ion viscosity) and the time to a chosen end of cure.
- Cure time decreases as cure temperature increases, as expected for a thermally driven reaction.

Procedure

Samples of CFRP were tested with a Ceramicomb-1"[1] sensor, which was embedded in a press platen as shown in Figure 17-1.

Figure 17-1
Ceramicomb-1" reusable sensor embedded in press platen

Laboratory grade filter paper was placed on the sensor to prevent passage of carbon fibers while allowing resin to flow to the electrodes. Two layers of CFRP approximately 1" x 1" were placed on the filter paper. Aluminum foil was placed on the CFRP to prevent the sample from adhering to the upper press platen. During each test a press applied heat and pressure to the lay-up of Figure 17-2.

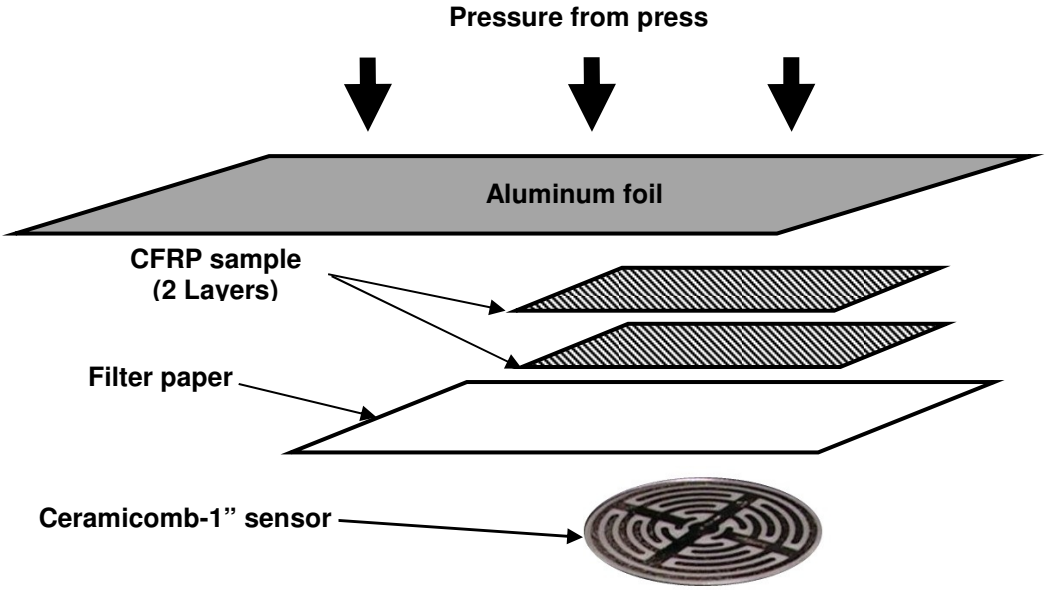

Figure 17-2
Lay-up of carbon-fiber prepreg for tests

An LT-451 Dielectric Cure Monitor[2] measured dielectric properties at 100 Hz and 1.0 kHz excitation frequencies. Previous tests indicated that 100 Hz was an optimum frequency, but 1 kHz was also used to investigate differences when measuring with another frequency. CureView[3] software acquired and stored the data, and performed post-analysis and presentation. Critical Points were determined only for data at the optimal, 100 Hz frequency.

Repeatability of measurements

Figure 17-3 shows the results from an isothermal test of fresh CFRP cured at 120 °C. Minimum log(*IV*)—Critical Point 2 (CP(2))—occurs at the beginning of the test, which is typical for isothermal processing. Minimum mechanical viscosity would occur at about the same time as CP(2), when the increase in viscosity due to curing dominates the decrease in viscosity due to rising temperature.

Maximum slope—Critical Point 3 (CP(3))—occurs at approximately 15 minutes, indicating the time of maximum reaction rate. After this point the reaction slows and the cure is ending. Although some users identify CP(3) with gelation, gelation is actually a mechanical event that has no dielectric equivalent. However, even though CP(3) is not gelation, it may be used as a signpost *associated* with gelation.

By the end of the test the sample is still slowly curing, as indicated by the non-zero slope of log(*IV*). Over time slope would continue to decrease, approaching zero asymptotically until end of cure when the reaction finally stops, the dielectric properties no longer change and the slope reaches zero. In reality, a user would choose a very small, non-zero slope to define end of cure—Critical Point 4 (CP(4))—based on the needs of the application.

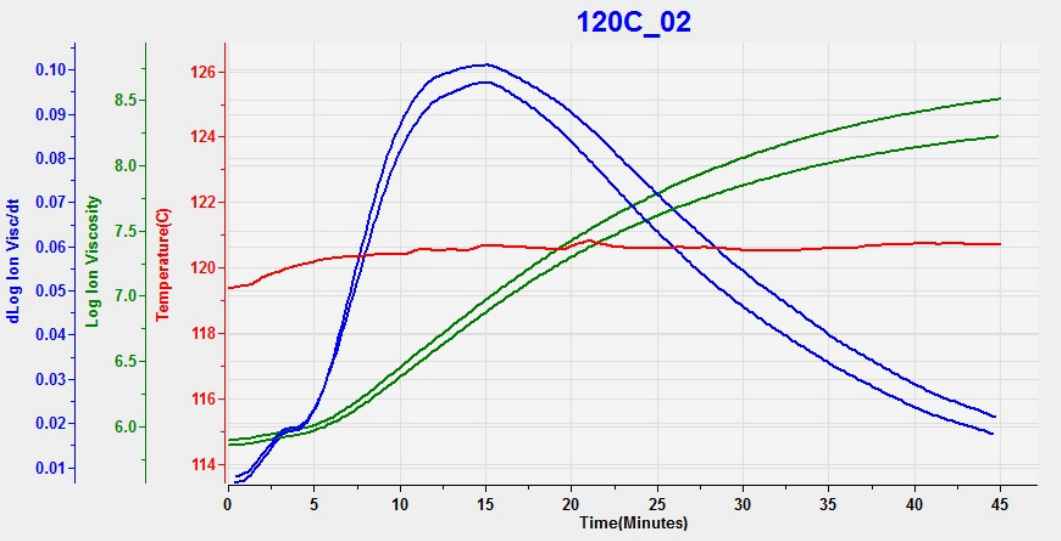

Figure 17-3
CFRP cure at 120 °C, 100 Hz and 1 kHz data

Figures 17-4 and 17-5 are plots of log(*IV*) and slope from six tests with 100 Hz excitation. The curves are superimposed to show typical reproducibility and range of variation. Toward the end of cure, differences in the level of log(*IV*) and resulting slope are likely caused by variability in the amount of resin that passes through the filter.

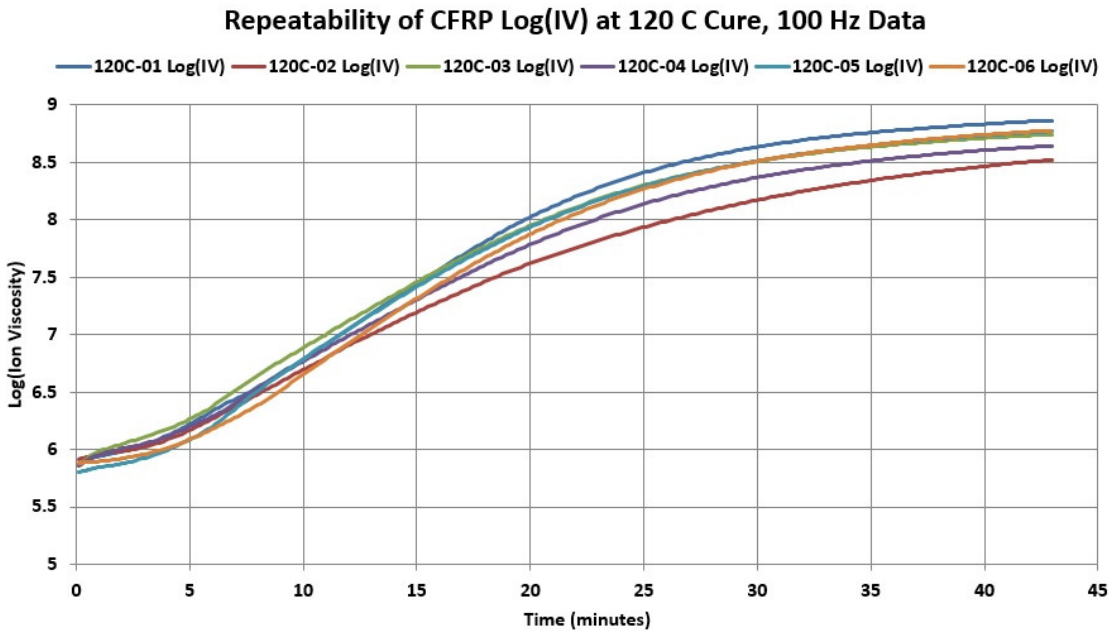

Figure 17-4
Log(*IV*) from cures at 120 °C of six samples of CFRP, 100 Hz data

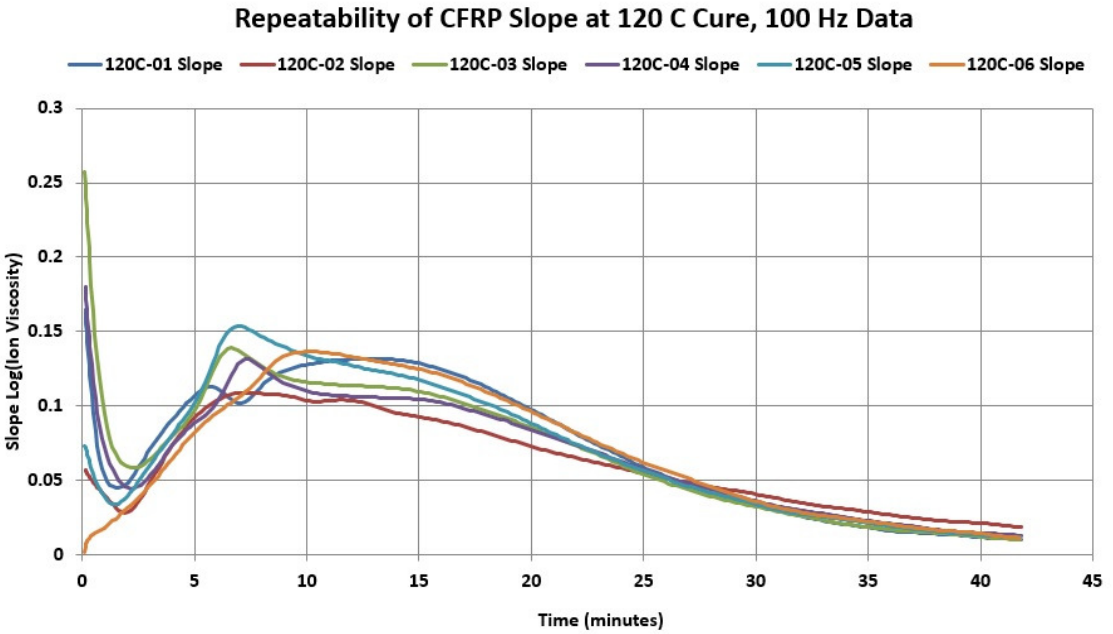

Figure 17-5
Slope from cures at 120 °C of six samples of CFRP, 100 Hz data

Effect of process temperature on cure rate

Figures 17-6 through 17-9 show results from samples of the same fresh CFRP tested at 120 °C, 135 °C, 150 °C and 165 °C.

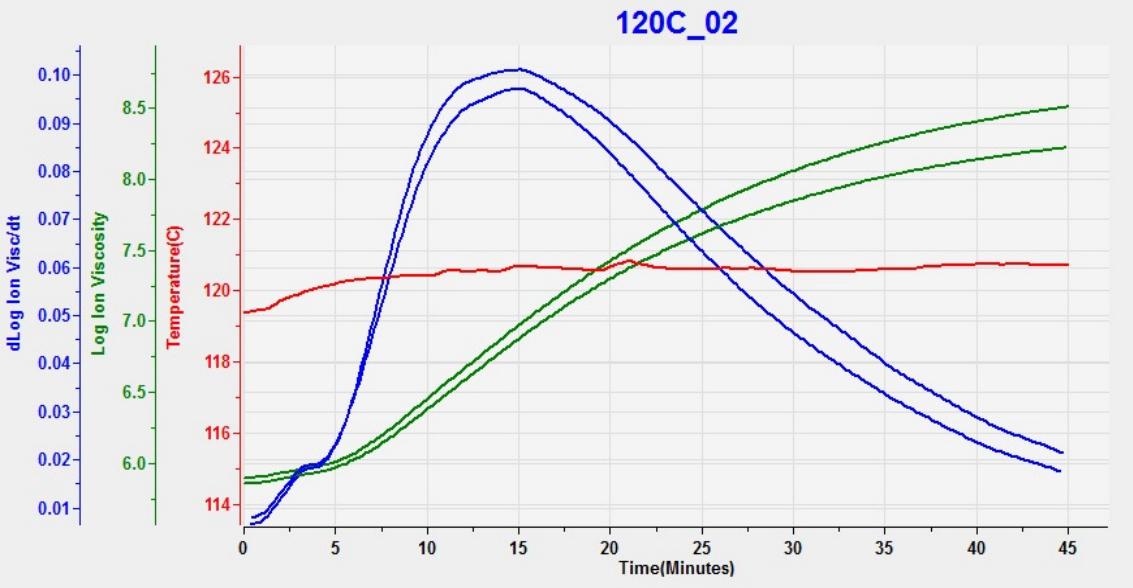

Figure 17-6
CFRP cure at 120 °C, 100 Hz and 1 kHz data

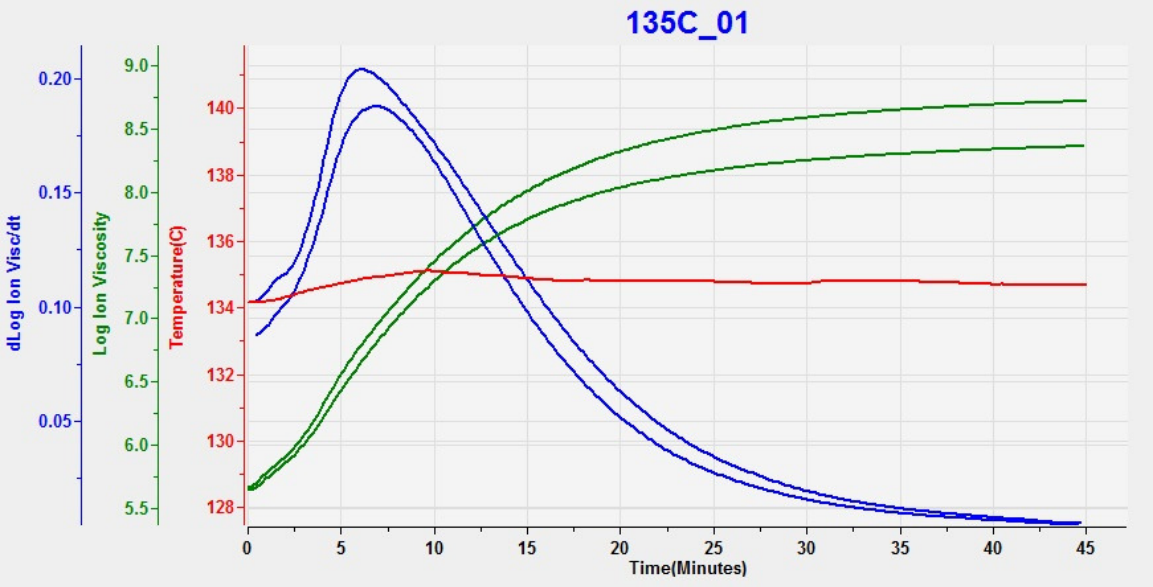

Figure 17-7
CFRP cure at 135 °C, 100 Hz and 1 kHz data

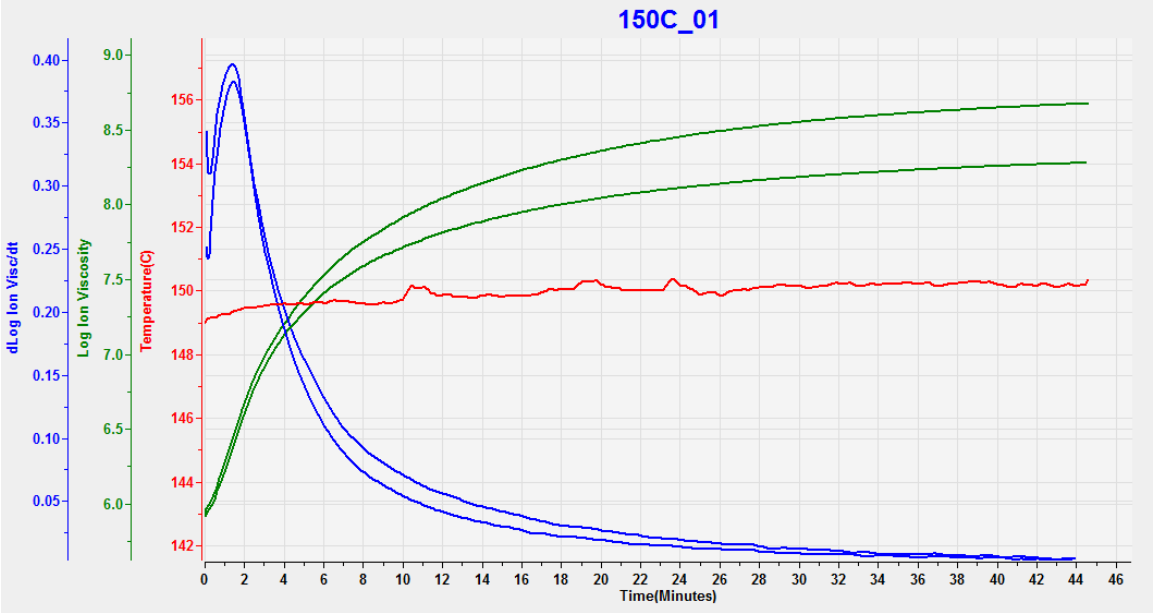

Figure 17-8
CFRP cure at 150 °C, 100 Hz and 1 kHz data

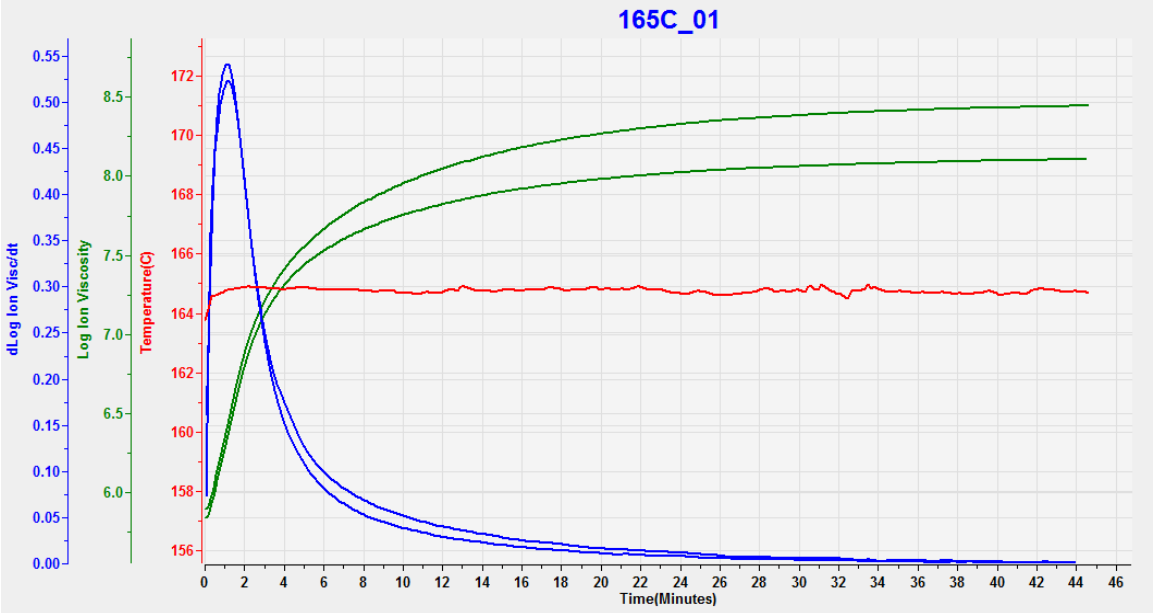

Figure 17-9
CFRP cure at 165 °C, 100 Hz and 1 kHz data

Figure 17-10 overlays 100 Hz log(*IV*) data for the cures at 120 °C, 135 °C, 150 °C and 165 °C. Figure 17-11 overlays slope data for these cures. As expected,

higher processing temperatures result in faster cures but the determination of Critical Points is necessary to quantify this relationship.

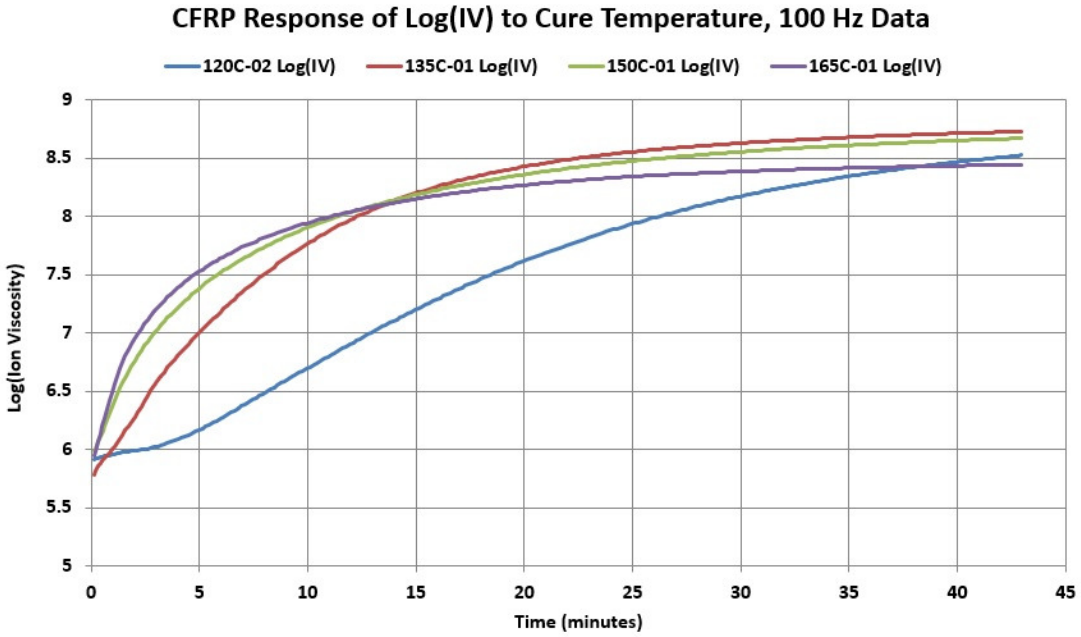

Figure 17-10
Dependence of log(*IV*) with isothermal cure temperature

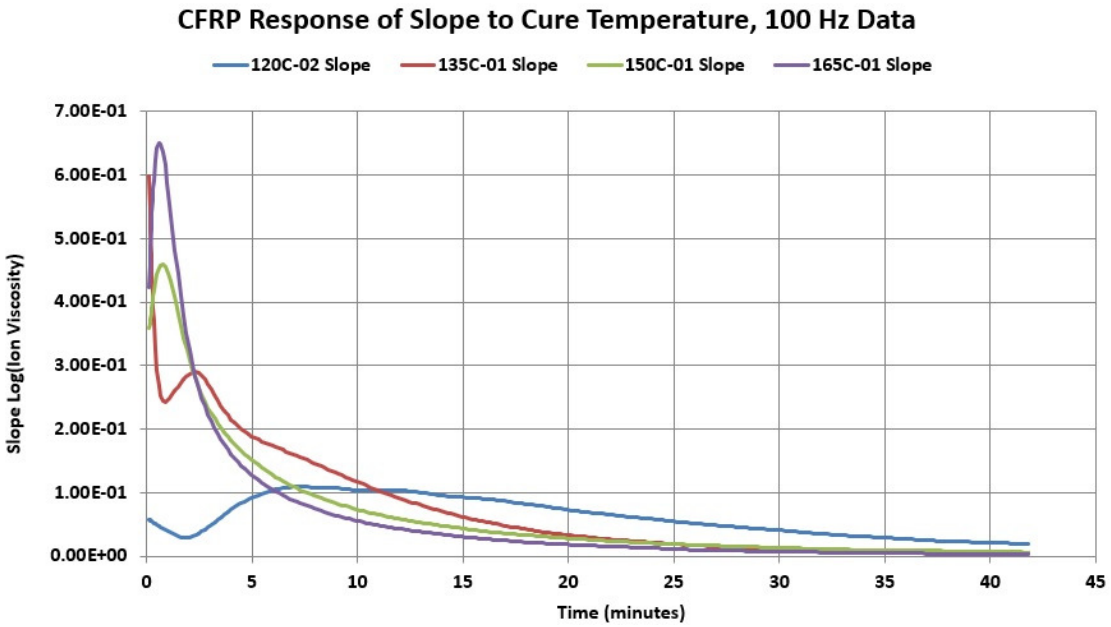

Figure 17-11
Dependence of slope with isothermal cure temperature

Critical Points that characterize each cure are shown in Table 17-1, with the following notes:

- The time to CP(1) indicates onset of flow and is not a measure of cure, so it is not shown
- The time to CP(2), minimum ion viscosity, occurs at or very near time t = 0 for an isothermal cure, does not reflect cure in this case and is not shown
- The slope of 0.05 to define CP(4) was chosen arbitrarily for analytical purposes

Table 17-1
Effect of temperature on Critical Points

Cure Temp. (°C)	CP(1) Crit. Visc.		CP(2) Min. Visc.		CP(3) Max Slope		CP(4) Crit. Slope	
	Value	Time (min)	Value	Time (min)	Value	Time (min)	Value	Time (min)
120	---	---	---	---	8.96E-02	7.282	5.00E-02	26.453
135	---	---	---	---	2.90E-01	2.314	5.00E-02	16.603
150	---	---	---	---	4.58E-01	0.782	5.00E-02	13.612
165	---	---		---	6.50E-01	0.576	5.00E-02	11.970

Figure 17-12 plots the time to CP(3) and CP(4), and shows how they decease with increasing cure temperature. The time to CP(3), which is the time to the point of maximum reaction rate, decreases exponential as temperature increases. The time to CP(3) at 165 °C deviates from the straight trend line at lower temperatures, possibly because of limited accuracy in identifying CP(3) for times less than one minute.

Figure 17-13 shows the level of CP(3)—the level of maximum slope—which indicates maximum reaction rate. Like the time to CP(3), the level of CP(3) shows an exponential relationship with temperature except at the lowest cure temperature of 120 °C.

Figure 17-14 plots the level of CP(3) vs. the time to reach CP(3), showing a rough log-log relationship between the two.

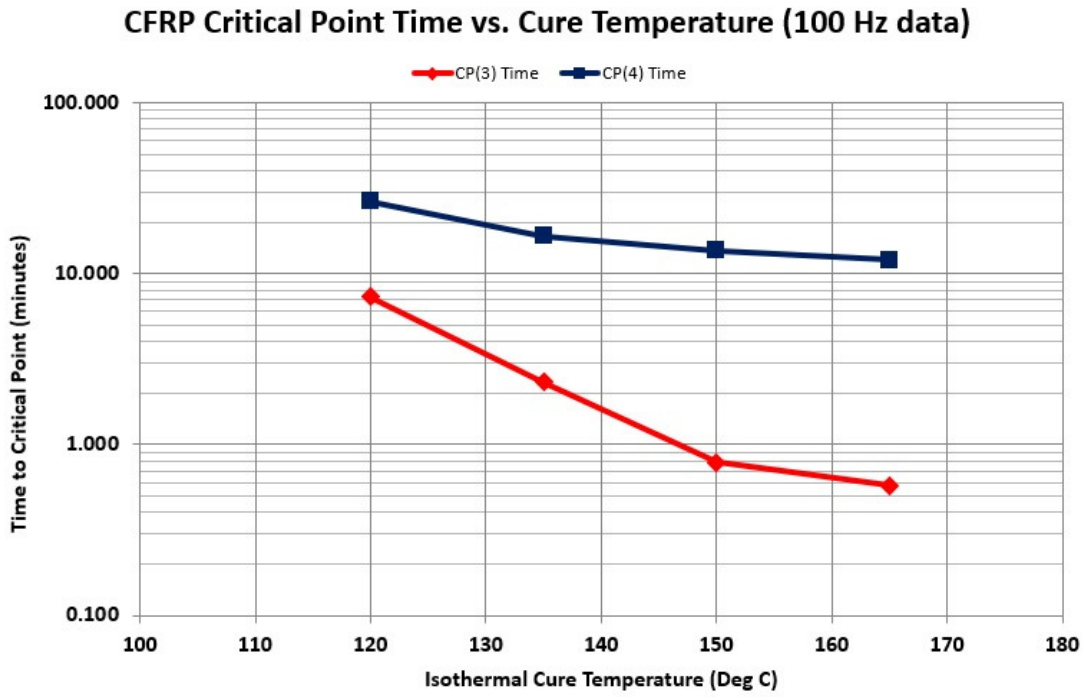

Figure 17-12
Time to Critical Points 3 and 4 vs. cure temperature

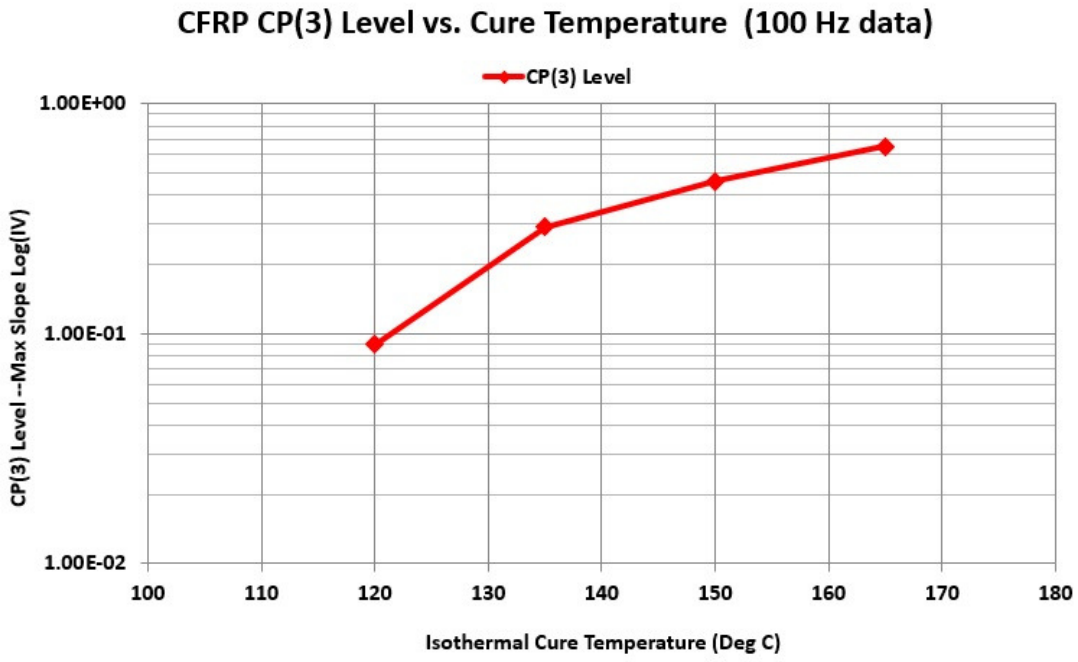

Figure 17-13
CP(3) level vs. cure temperature

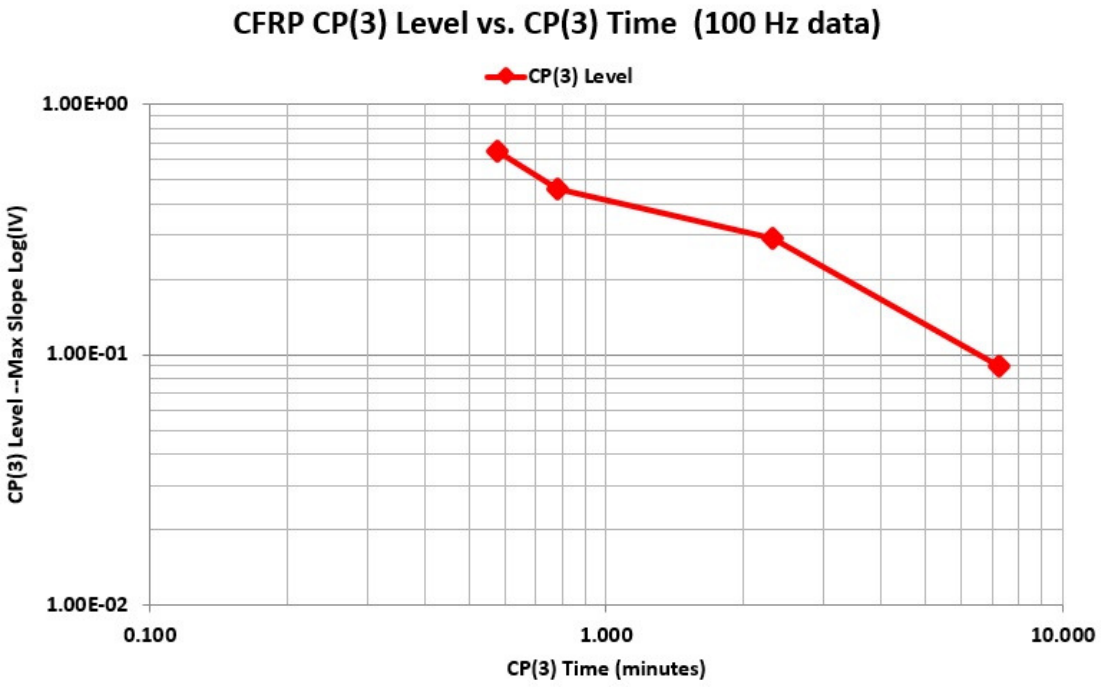

Figure 17-14
CP(3) level vs. CP(3) time

Dielectric measurements allow observation of the cure of thermosets in real time, and the extraction of Critical Points quantify the characteristics of the reaction. The data for CFRP cure show results are repeatable and consistent, with some variation probably caused by differences in the amount of resin that passes through the filter to reach the sensor. Dielectric cure monitoring over temperatures from 120 °C to 165 °C clearly reveal the direct correlation between temperature and cure rate.

References

1. Ceramicomb-1" sensor, manufactured by Lambient Technologies, Cambridge, MA USA. https://lambient.com

2. LT-451 Dielectric Cure Monitor, manufactured by Lambient Technologies, Cambridge, MA USA

3. CureView software, manufactured by Lambient Technologies, Cambridge, MA USA

Chapter 18—Real-Time Monitoring of Ultraviolet Cure

Quad-Cure™ 1933 ultraviolet curing bonder

Quad-Cure™ 1933[1] is a urethane acrylate glass-metal bonder that may be cured with UV, visible, LED light and heat. Under UV irradiation, this resin reacts rapidly and exhibits dynamic behavior that would be difficult or impossible to see with differential scanning calorimetry (DSC), the conventional method of studying cure state. In contrast, dielectric cure monitoring (DEA) has the unique ability to measure cure in real-time, which is valuable for studying materials that polymerize in seconds like Quad-Cure™ 1933.

Procedure

The SunSpot 2 UV/Visible Light Curing System[2] was the UV source for this study. The output from its arc lamp is wide-band and intensity at the end of the light guide is typically >18,000 mW/cm^2 in UVA (320-390 nm), adjustable from 25% to 100%.

As natural consequence of the optics, light intensity varied radially across the projected spot and approximately uniform illumination was only possible with a small area. Consequently, resin was applied on half of a Quatro-Varicon[3] dielectric sensor, resulting in a sample approximately 7 mm x 10 mm in area. The set-up is shown in Figure 18-1.

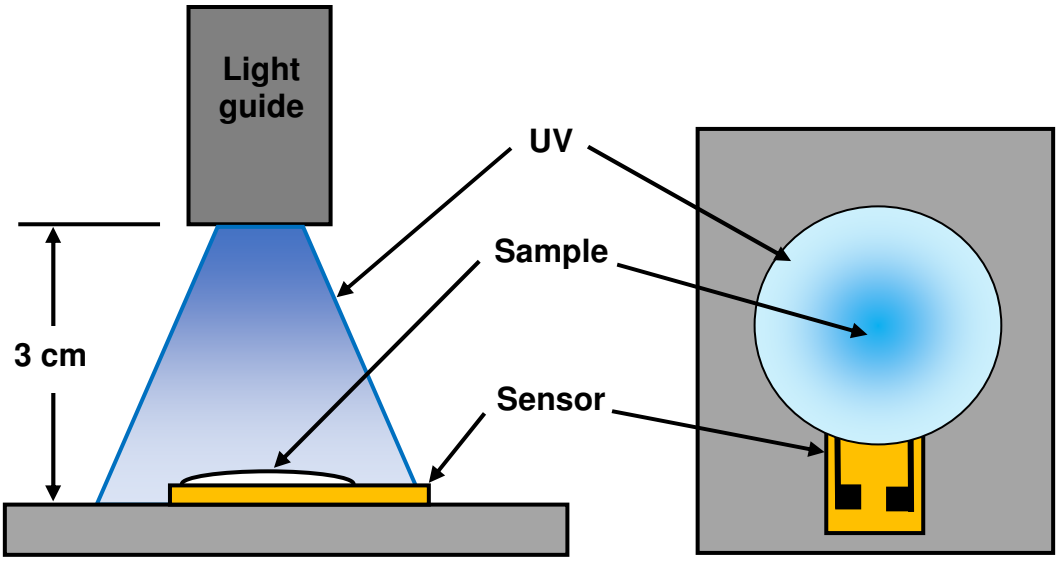

Figure 18-1
Test setup for UV cure

The SunSpot 2 uses both a dichroic filter and mirror to nearly eliminate IR transmission through the light guide. Absorption of high intensity radiation in the remaining visible/UVA/UVB/UVC wavelengths nevertheless produces considerable heating, which can damage a sample.

Before the tests, a thermocouple measured temperature at the center of the light spot for a 20 second exposure at 60% intensity. Peak temperature as shown in Figure 18-2 was just over 150 °C. The manufacturer recommends a maximum temperature of 120 °C for Quad-Cure™ 1933 to avoid thermal damage.

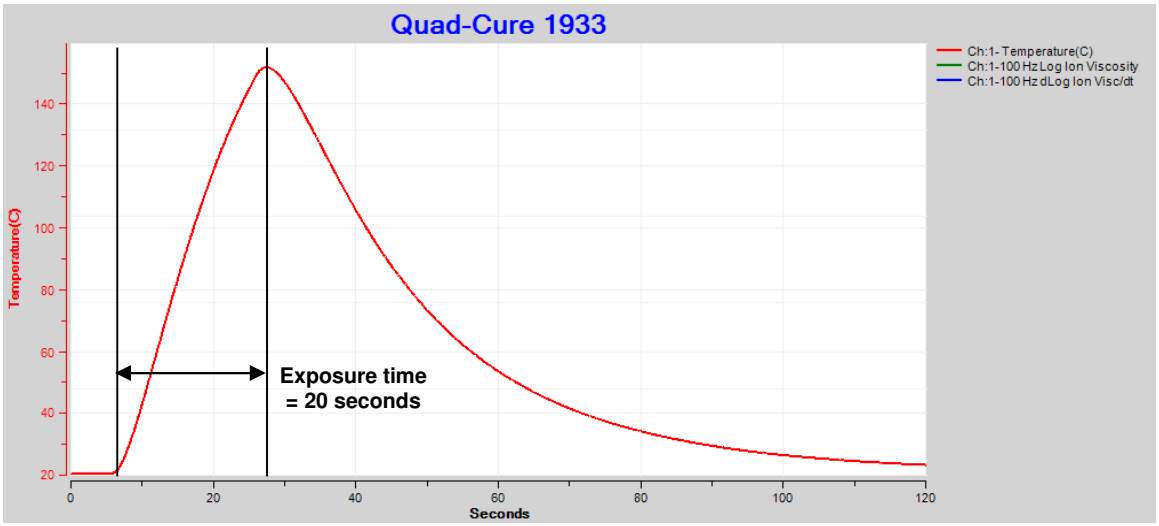

Figure 18-2
Thermocouple temperature, exposure time = 20 seconds, intensity = 60%

An LT-631 High-Speed Dielectric Cure Monitor[4] measured ion viscosity at a rate of 50 ms/data point. The first test used UV irradiation at 60% intensity for 20 seconds to observe the effects of severe over-exposure.

Results

Figure 18-3 shows ion viscosity data with five distinct events:

1. Initial decrease in ion viscosity due to temperature increase
2. UV cure
3. Cure plateau
4. Post-exposure heat cure
5. End of cure

Cure reaches a plateau between ~17 and 27 seconds, possibly from an equilibrium between UV polymerization and UV breakdown of bonds. The slight decrease in ion viscosity during this time is caused by increased conductivity from the continually rising temperature shown in Figure 18-2.

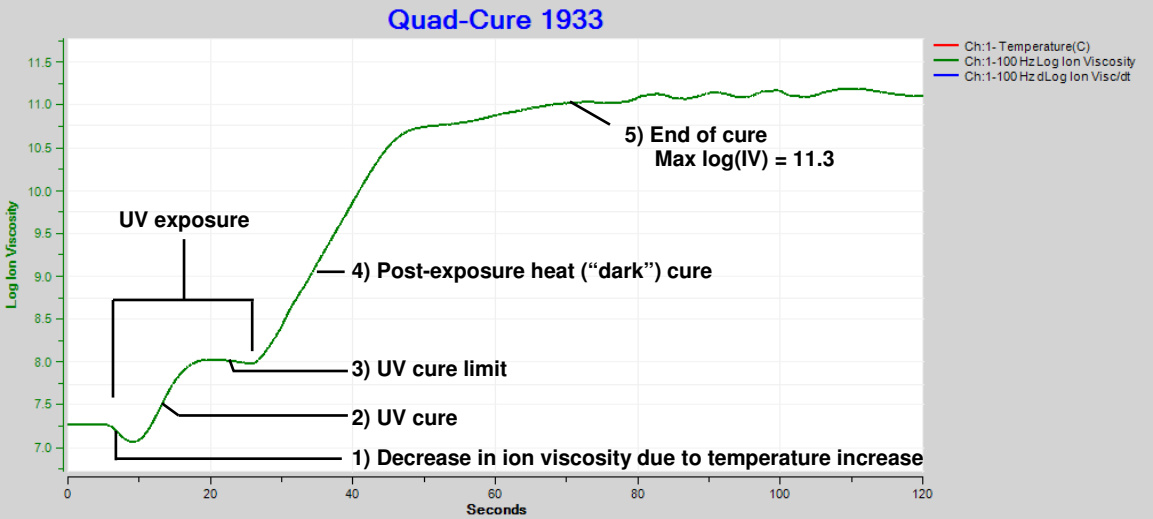

Figure 18-3
Ion viscosity of Quad-Cure™ 1933, exposure intensity = 60%, time = 20 sec.

Figure 18-4 shows a) correct exposure, b) slight over-exposure and c) significant over-exposure. As a result of over-exposure, excessive UV energy causes yellowing of the material and excessive heat creates bubbles and brittleness. The sample of this first test is significantly over-exposed and looks like Figure 18-4.c.

After UV exposure ends, the activated photoinitiators persist and accelerate polymerization driven by heat. This post-exposure, or "dark," cure continues for nearly 70 seconds.

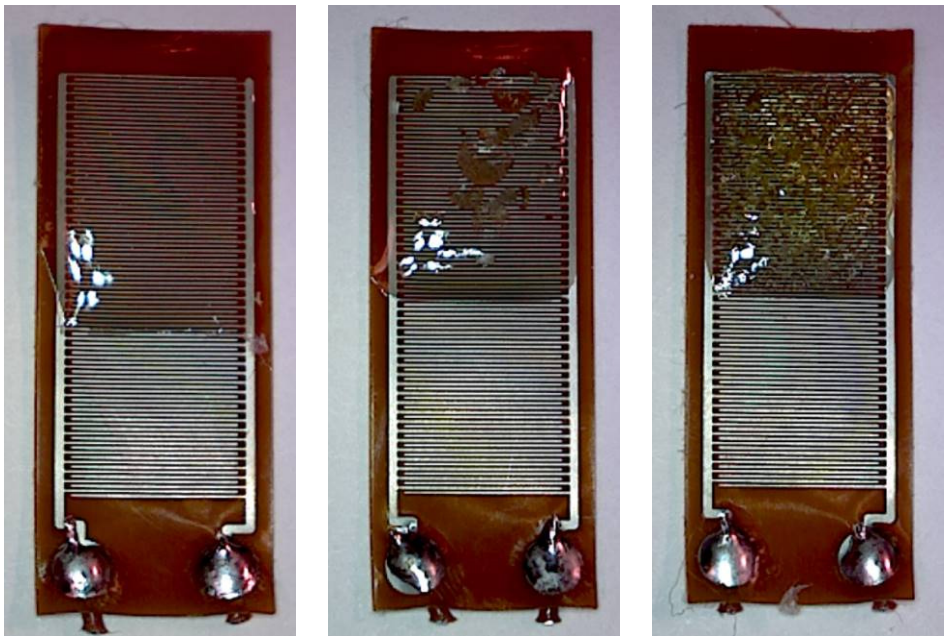

a. **b.** **c.**

Figure 18-4
Correctly exposed (a), slightly (b) and significantly (c) over-exposed samples

Thermal damage is undesirable and the irradiation time should be shortened to reduce overall heating of the sample. Figure 18-5 compares cure with 10 and 20 second exposures. Even though 10 second irradiation eliminates the plateau, the sample still exhibits bubbling from excessive heat, like Figure 18 3.c.

Final ion viscosity after 10 seconds of UV illumination is significantly less than after 20 seconds. A direct relationship exists between degree of cure and ion viscosity; consequently, the shorter exposure, which produces fewer activated photoinitiators, results in less cure and a lower maximum ion viscosity.

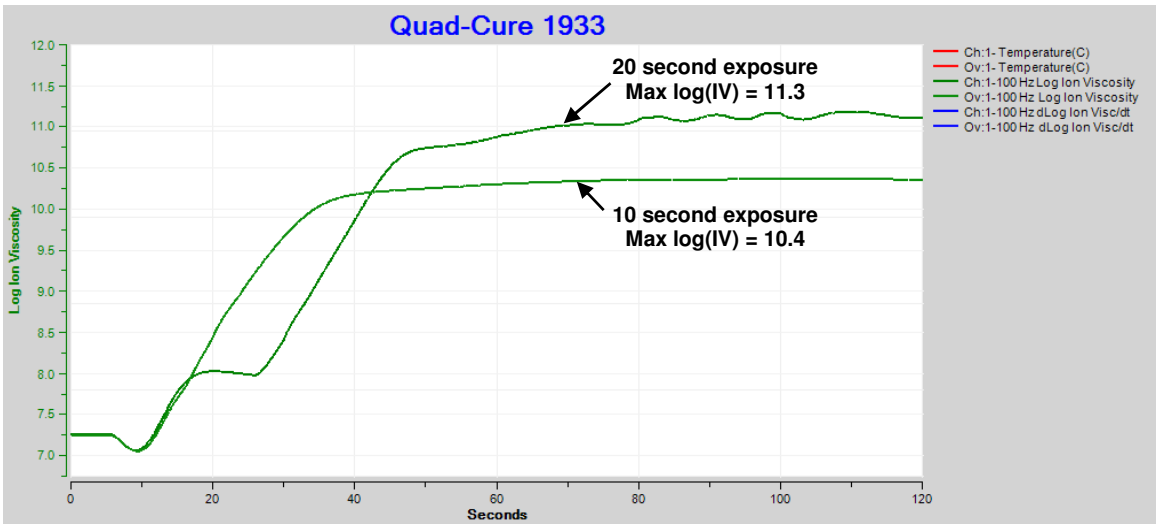

Figure 18-5
Ion viscosity of Quad-Cure 1933, exposure intensity = 60%, comparison of exposure time = 10 sec. and 20 sec.

Figure 18-6 shows how higher exposure energy results in higher ion viscosity at the end of cure, which in turn indicates a greater degree of cure. Note that a single exposure was used for each test and that exposure energy is the product of intensity and exposure time. Although not apparent from the ion viscosity data, the exposure at the highest energy also damaged the sample from excessive heat.

The results may be summarized as follows:

- Values of log(*IV*) < ~9 are associated with surface tackiness and indicate under-cure
- Values of log(*IV*) between ~9.0 and ~9.6 correspond to optimum cure, which produces a "sleek" surface without damage
- Values of log(*IV*) > ~10 accompany brittleness and thermal damage from the excessive exposure to high intensity light

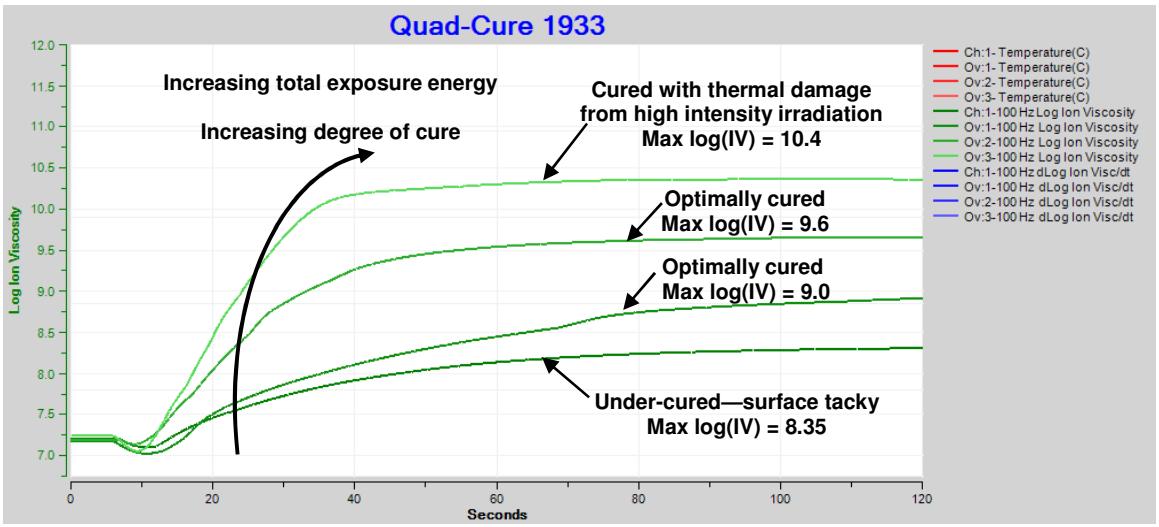

Figure 18-6
Comparison: Ion viscosity of Quad-Cure™ 1933, single exposures with increasing total energies

Instead of a single high-intensity exposure, multiple low-intensity exposures can drive cure to higher degrees without the damage from excessive heating. How would the relationship between ion viscosity and final material state change in this case? For quickly reacting resins like those used in UV curing, the value of dielectric cure monitoring lies in its ability to gather real-time information and answer questions like this in ways not possible with other methods.

References:

1. Quad-Cure 1933™, manufactured by Incure, Inc., New Britain, CT USA. www.uv-incure.com

2. SunSpot 2™, manufactured by Uvitron International, Inc., West Springfield, MA USA. www.uvitron.com

3. Quarto-Varicon sensor, manufactured by Lambient Technologies, Cambridge, MA USA. https://lambient.com

4. LT-631 High Speed Dielectric Cure Monitor, manufactured by Lambient Technologies, Cambridge, MA USA

Chapter 19—Electrode Polarization with AC and DC Cure Monitoring

History

Dielectric cure monitoring uses AC signals to measure the electrical properties of a thermoset or composite. Under certain circumstances with very conductive materials, a phenomenon called *electrode polarization* (EP) may create boundary layers on sensor electrodes and distort data. As a result, early researchers did not understand their measurements were sometimes erroneous and often struggled to explain the results.

The plot of Figure 19-1 is from a 1977 Air Force Materials Laboratory report of cure monitoring for adhesive bonding. At the time sensors were typically parallel plates; measurement of dissipation was preferred because the result is insensitive to changes in the spacing between electrodes.

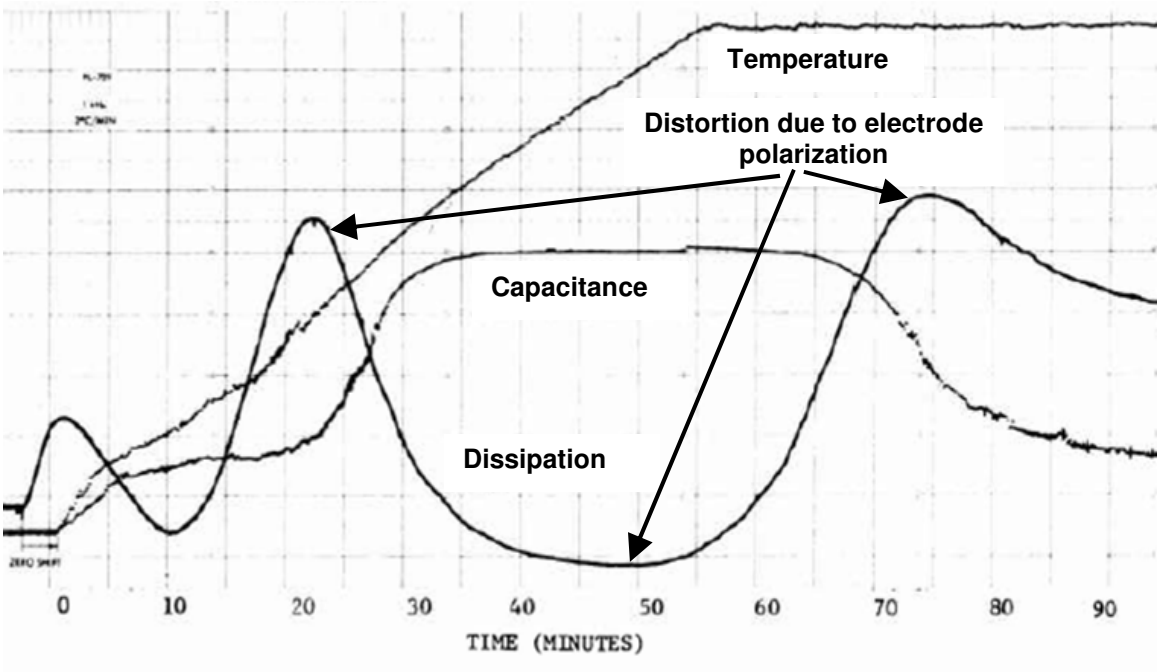

Figure 19-1
Cure data with distortion caused by electrode polarization[1] (1977)

Two significant dissipation peaks appeared during the test (invert the shape of the dissipation curve to relate its behavior to ion viscosity). The study's author attributed the first peak to "major softening of the adhesive" and the following dissipation minimum to "a region of minimum viscosity." The second

peak was simply described as a "cure associated dissipation peak which reflects the Tg of the adhesive at that particular stage of cure." In fact, only minimum viscosity correlated with a feature of the curve—the minimum in dissipation—and the two dissipation peaks were artifacts with no physical significance.

Electrode polarization during cure monitoring was first explained in 1982[2] and now it is possible to recognize its influence and avoid the misinterpretation of dielectric measurements. Furthermore, a mathematical model of the boundary layer effect allows the calculation of dielectric properties even when data have considerable distortion.

Electrode polarization and boundary layers

Electrode polarization is the accumulation of charge against the electrodes, which occurs when the material under test:

- Has low ion viscosity (high ionic conduction) at low frequency

  AND

- Has a non-conductive film, an oxide layer or an electrochemical potential barrier, resulting in an insulating boundary layer

Figure 19-2 is the electrical model of an electrode with a boundary layer and Material Under Test (MUT).

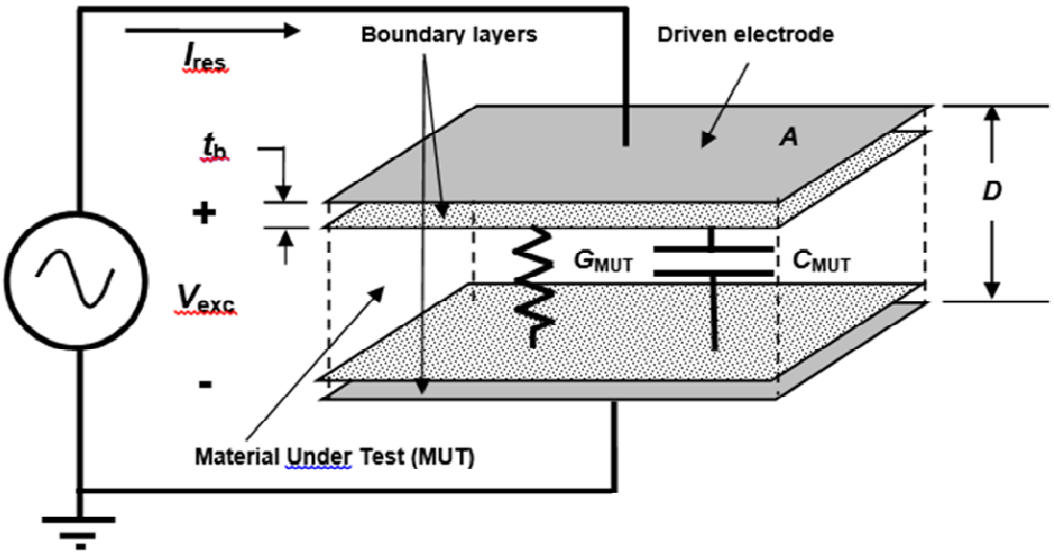

Figure 19-2
Electrical model of material on sensor with boundary layer

The boundary layer is an insulator that introduces a pair of capacitors in series between the electrodes and the MUT. Because capacitors pass only AC signals, measurements of the MUT are not possible with DC methods.

When the Material Under Test is very conductive, usually around the time of minimum viscosity, the boundary layers may introduce errors in ion viscosity measurements.[3] Note that insulating release films or vacuum bags can also act as boundary layers on sensors and can produce effects similar to electrode polarization.

AC cure monitoring of five-minute epoxy

Figure 19-3 shows a Mini-Varicon[4] dielectric/conductivity sensor, which was used for AC and DC measurements of "5-minute" epoxy with the LT-451 Dielectric Cure Monitor.[5] This sensor has electrodes with equal width and separation of 0.004".

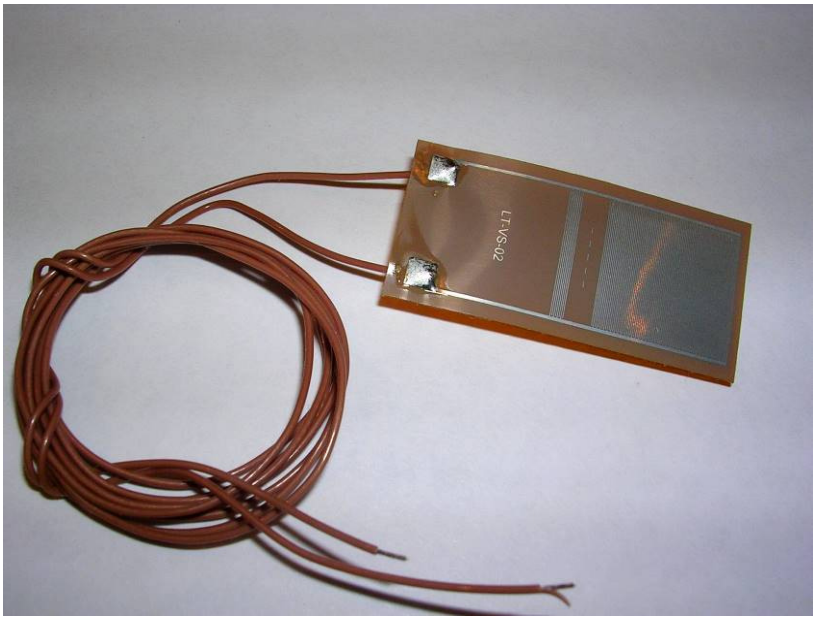

Figure 19-3
Mini-Varicon dielectric/conductivity sensor

The LT-451 monitored dielectric properties at multiple excitation frequencies from 1 Hz to 10 kHz during a 30-minute cure. Although primarily used for AC measurements, with a frequency range from 0.001 Hz to 100 kHz, a new DC option allows the LT-451 to simultaneously measure both the AC and DC response

Figure 19-4 is a plot of resistivity, which has both frequency independent (ρ_{DC}) and frequency dependent (ρ_{AC}) components, from AC measurements of

five-minute epoxy. Even though the strict definition of ion viscosity is frequency *independent* resistivity, for convenience all resistivity data are plotted against an axis labeled *ion viscosity* and may collectively be called ion viscosity.

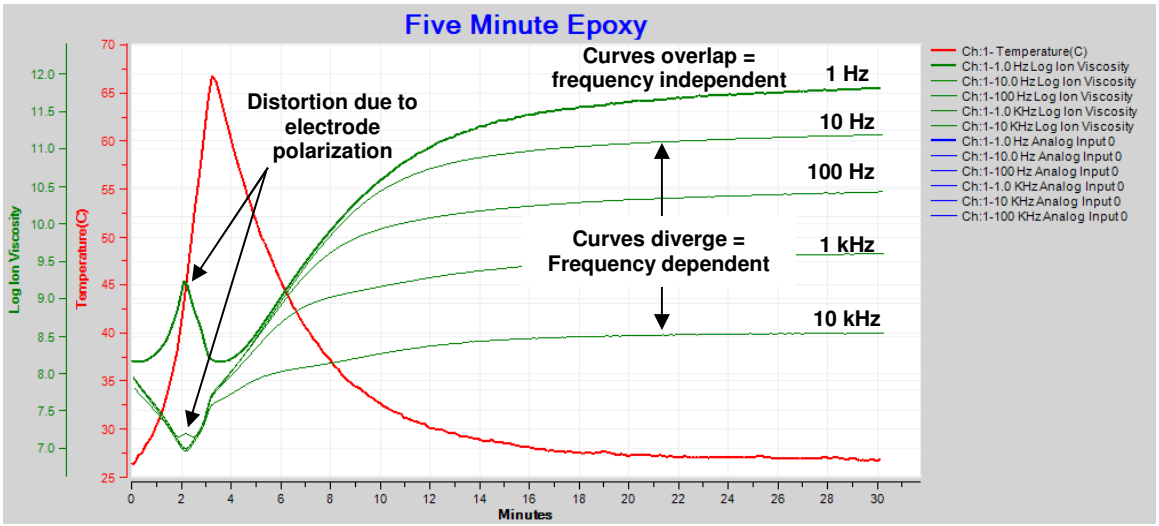

Figure 19-4
Ion viscosity / resistivity during cure of five-minute epoxy

Three features are apparent in the plot of Figure 19-4:

- Curves that overlap or nearly overlap, indicating the dominance of frequency independent resistivity (ρ_{DC})
    - Caused by flow of mobile ions—true ion viscosity
    - Correlates with cure state
- Curves that diverge, indicating the dominance of frequency dependent resistivity (ρ_{AC})
    - Caused by rotation of dipoles
    - Does not correlate well with cure state
- Distortion of 1 Hz and 10 Hz curves around 2 minutes due to electrode polarization and the boundary layer effect

Preliminary testing showed frequency independent resistivity dominates 1 Hz data at the end of cure. As a result, 1 Hz measurements may be used to determine cure state of this epoxy.

At the beginning of cure, however, electrode polarization causes considerable distortion in the 1 Hz data, shown in the expanded plot of Figure 19-5. This distortion changes the expected single minimum in resistivity/ion viscosity to a peak with *two* local minima.

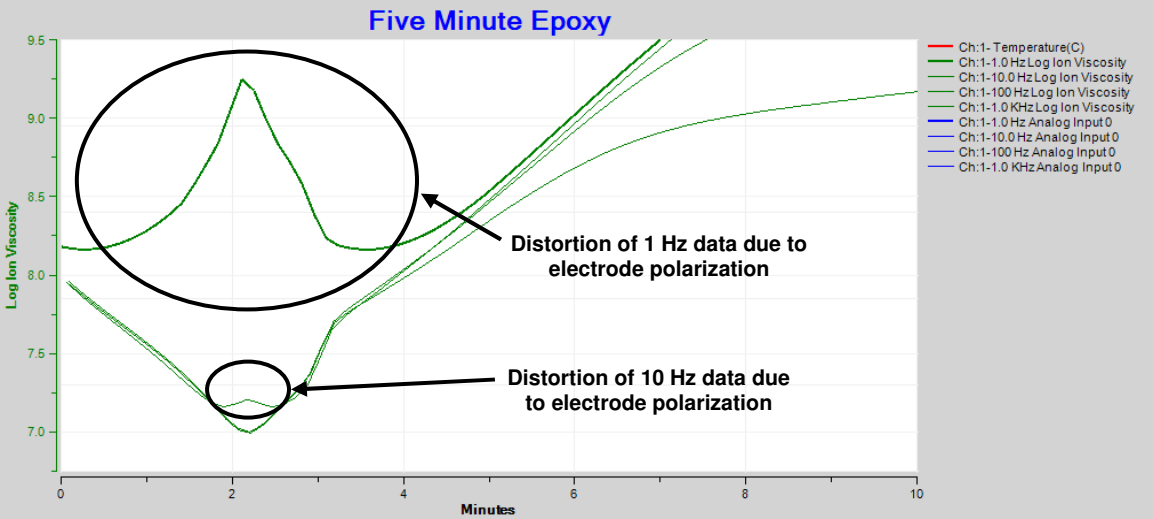

Figure 19-5
Expanded ion viscosity / resistivity around time of minimum viscosity

In the past the first minimum had been attributed to softening, and the second to gelation—but they are both artifacts of the boundary layer effect and do not describe actual dielectric or material events. In fact, the expected—but unseen—single minimum of ion viscosity corresponds to minimum mechanical viscosity, an event that would be completely lost if these data were misinterpreted.

Data from 10 Hz measurements also show distortion, though to a much lesser degree because the boundary layer effect decreases with increasing frequency. Furthermore, measurements at the higher excitation frequencies—1 kHz to 10 kHz—show no distortion and correctly identify the ion viscosity minimum.

In many cases it is possible to mathematically correct the distortion and restore information about the cure. Figure 19-6 shows how boundary layer correction—also called *electrode polarization* (EP) correction—recovers affected data. After EP correction, 1 Hz and 10 Hz ion viscosity correctly show a minimum, consistent with the higher frequency data.

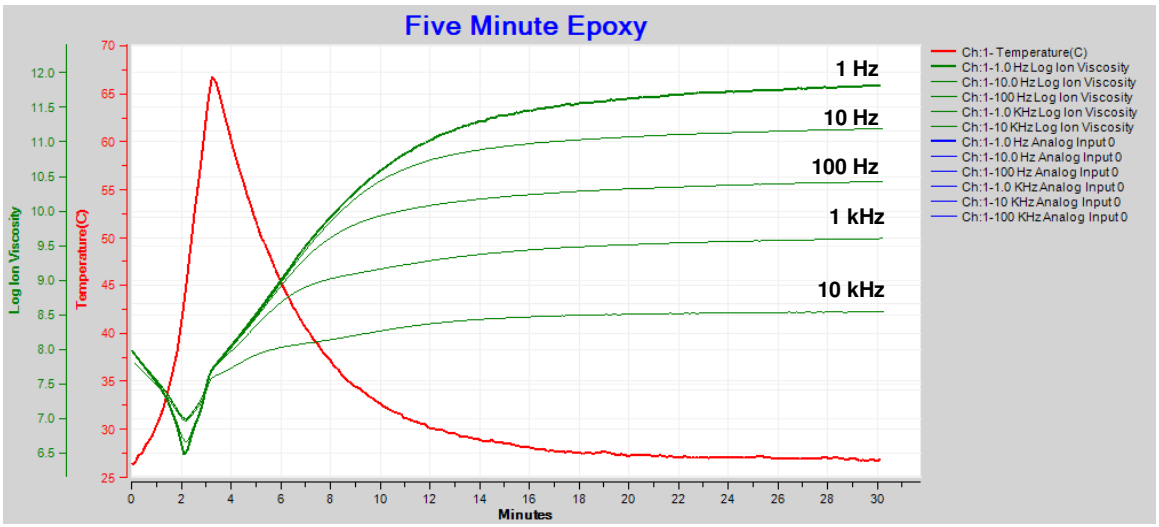

Figure 19-6
Resistivity / ion viscosity with boundary layer (EP) correction

After applying boundary layer correction, it is possible to use only the 1 Hz ion viscosity to follow the entire five-minute epoxy cure, as shown in Figure 19-7.

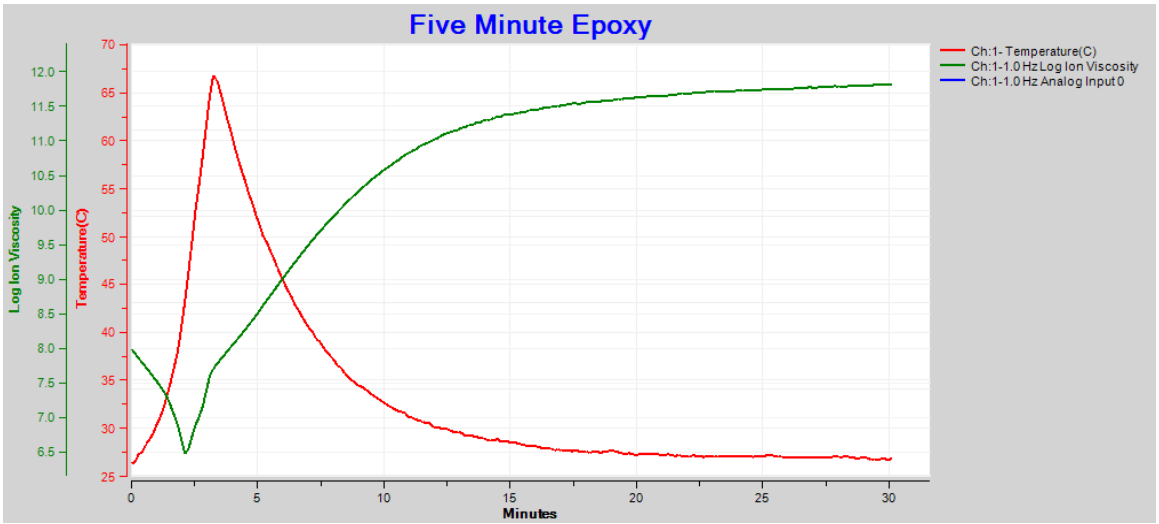

Figure 19-7
1 Hz ion viscosity with boundary layer (EP) correction

DC Cure monitoring of five-minute epoxy

DC measurement of resistance or ion viscosity is a simple method of probing cure state; however, it may have considerable distortion around the time of the ion viscosity minimum, when material is most conductive. As shown in

Figure 19-5, the boundary layer effect decreases with increasing frequency. *Conversely, the boundary layer effect and distortion of data increase with decreasing frequency*, having maximum consequence with DC (0 Hz) measurements.

The LT-451 Dielectric Cure Monitor has a DC option, which was used to study the cure of five-minute epoxy with the Mini-Varicon sensor. Figure 19-8 compares the results of simultaneous DC and AC measurements of ion viscosity.

Toward the end of cure, AC and DC results are similar and overlap. This overlap indicates that data for excitations of 1 Hz or less represent frequency independent resistivity (ρ_{DC}), which correlates with cure state.

Around the time of the ion viscosity minimum, the DC data show distortion caused by electrode polarization. As expected, this distortion for DC measurements is much greater than for the 1Hz AC measurements. While it is possible to correct this boundary layer effect with AC data (see Figure 19-6), it is not possible to correct DC data.

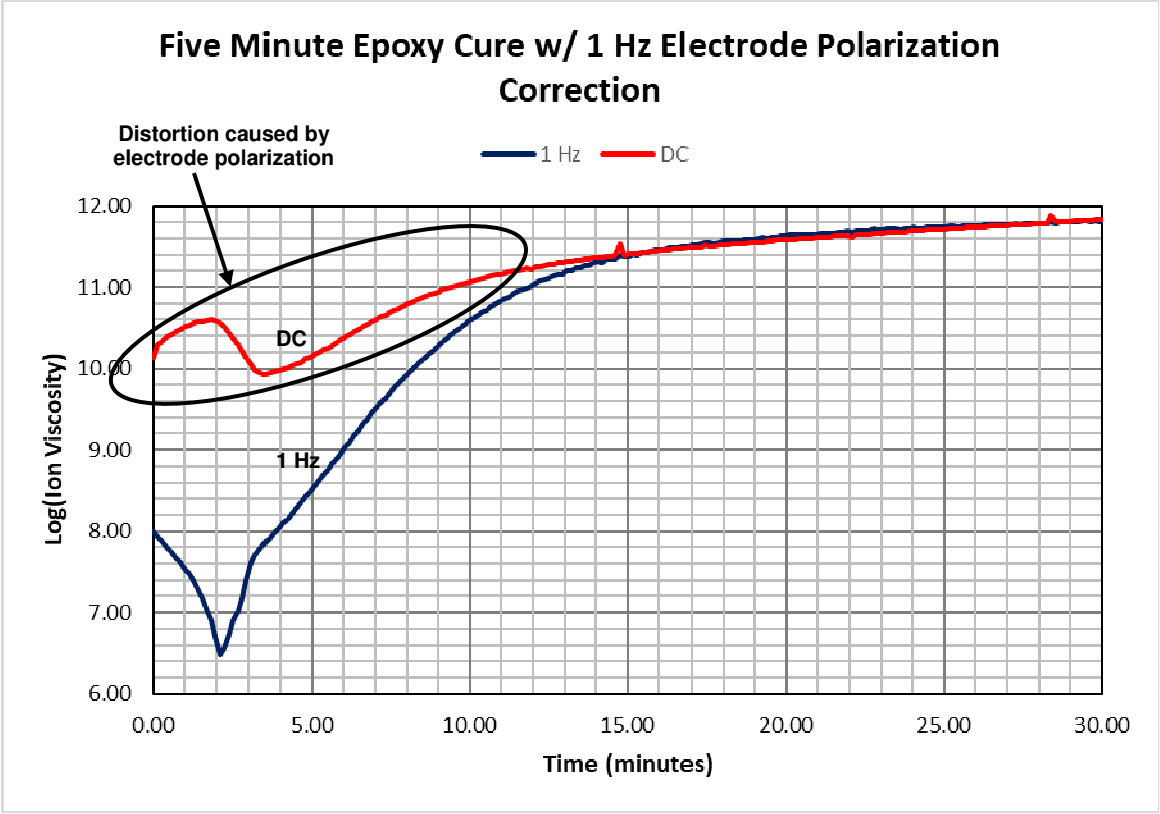

Figure 19-8
DC and 1 Hz ion viscosity of five-minute epoxy cure

Figure 19-9 is a plot of DC and AC measurements for a longer period of 120 minutes for five-minute epoxy. Ideally, frequency independent resistivity would produce a complete overlap of data, but non-ideal behavior is often present, resulting in a close but not complete overlap. As Figure 19-9 shows, the curves do closely overlap throughout the end of cure, indicating frequency independent resistivity that correlates with cure state.

Figure 19-10 shows another example of electrode polarization, this time for the cure of an epoxy-fiberglass prepreg. Again, the distortion increases as frequency decreases and is greatest for DC measurements.

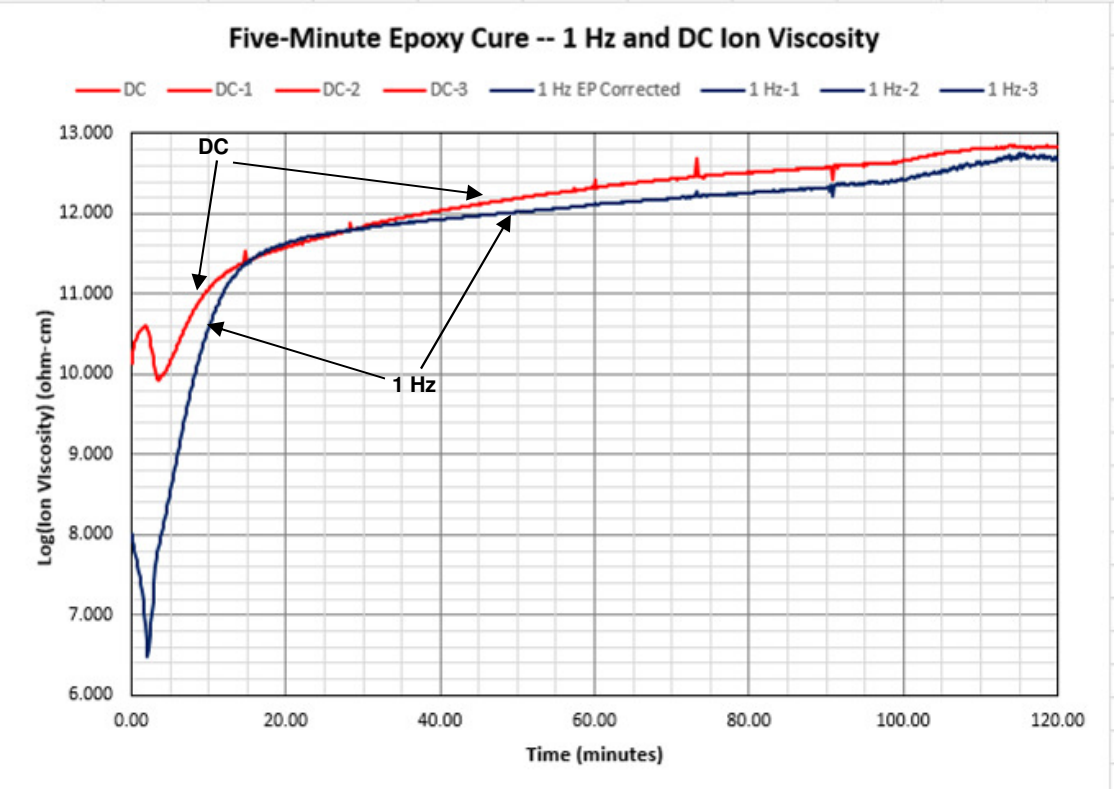

Figure 19-9
DC and 1 Hz ion viscosity of five-minute epoxy cure

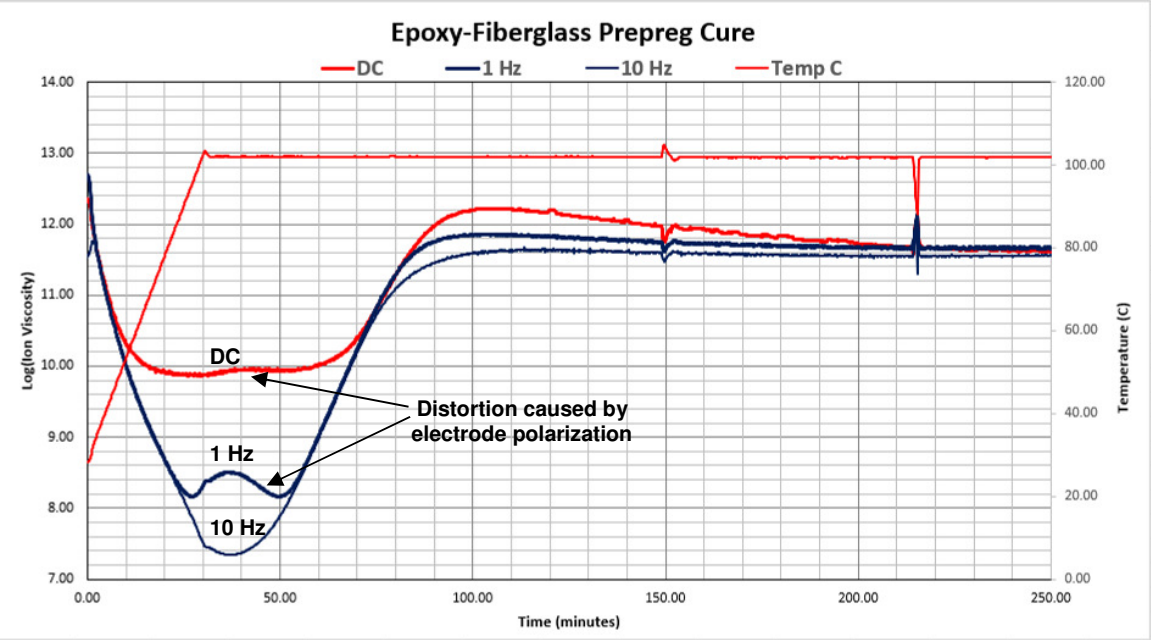

Figure 19-10
DC ,1 Hz and 10 Hz ion viscosity of epoxy-fiberglass prepreg cure

Under conditions of very high bulk conductivity, electrode polarization may create boundary layers on sensors used for dielectric cure monitoring. Electrode polarization most commonly appears around the time of minimum mechanical viscosity, when the material under test is most conductive. In this case, the boundary layer effect produces abnormally high *apparent* ion viscosities that can cause misinterpretation of cure state.

The distortion due to boundary layers increases as excitation frequency decreases and DC (0 Hz) measurements can have significant error around the time of minimum viscosity. While it is possible to mathematically correct AC data and calculate the true ion viscosity, correction of DC data is not possible. Consequently, when electrode polarization is present, DC cure monitoring is limited to the later portions of cure.

References

1. "Cure Monitoring Techniques for Adhesive Bonding Processes", Lockheed Missiles and Space Company, Technical Report AFML-TR-77-58 (March 1977)

2. Lee, H.L., "Optimization of a Resin Cure Sensor", S.M and E.E. thesis, Massachusetts Institute of Technology (1982)

3. Day, D.R.; Lewis, J.; Lee, H.L. and Senturia, S.D., "The Role of Boundary Layer Capacitance at Blocking Electrodes in the Interpretation of Dielectric Cure Data in Adhesives," *Journal of Adhesion*, V18, p.73 (1985)

4. Mini-Varicon sensor, manufactured by Lambient Technologies, Cambridge, MA USA. https://lambient.com

5. LT-451 Dielectric Cure Monitor, manufactured by Lambient Technologies, Cambridge, MA USA

Chapter 20—Cure Monitoring Through Release Films and Vacuum Bags

Release films and vacuum bags in manufacturing

In manufacturing, release films prevent the adhesion of molded parts to a tool and vacuum bags enable atmospheric pressure to compress composite material in the Vacuum Assisted Resin Transfer Molding (VARTM) process. Dielectric sensors typically must have direct contact with the material under test but both release films and vacuum bags prevent contact and create challenges for dielectric cure monitoring (DEA).

In fact, a suitably designed sensor, such as the 1-inch Single Electrode[1] reusable sensor, can measure cure state through thin films and enable the use of DEA in a wider range of applications.

AC Cure monitoring with direct contact

Figure 20-1 shows how a 1-inch Single Electrode sensor would be installed in a press or mold.

Figure 20-1
1" Single Electrode Sensor in press platen

For proper operation the tooling around the Single Electrode sensor must be grounded. This ground must be connected to the chassis of the instrumentation, illustrated schematically in Figure 20-2, to make a closed circuit

for the sensing current. If an upper platen or mold is used, it should also be grounded.

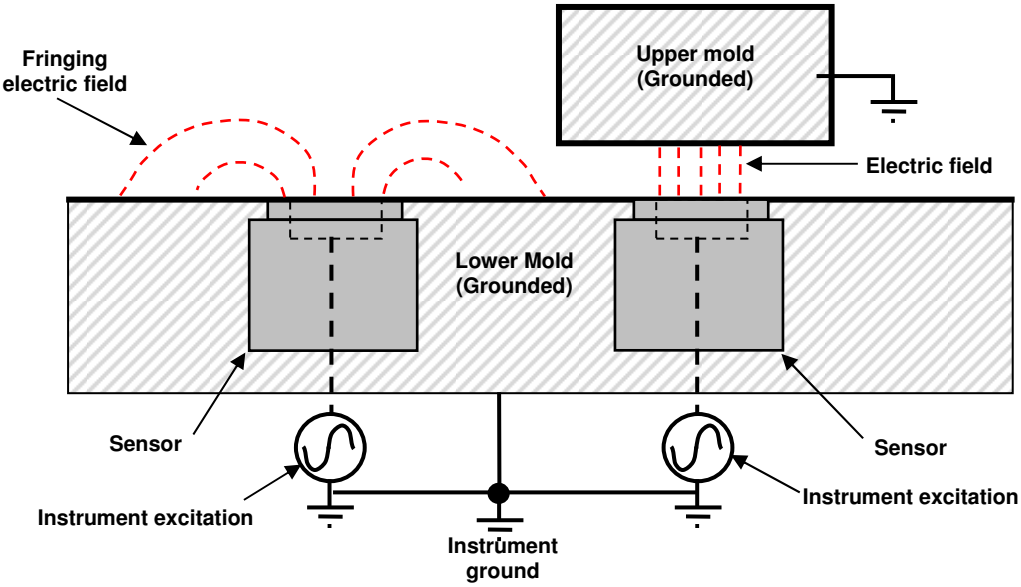

Figure 20-2
Proper grounding of platens or mold for single electrode sensors

For applications that do not use a release film or vacuum bag, resin flows upon heating and compression and makes direct contact with the sensor. Figure 20-3 shows the electrical model of this resin-sensor system.

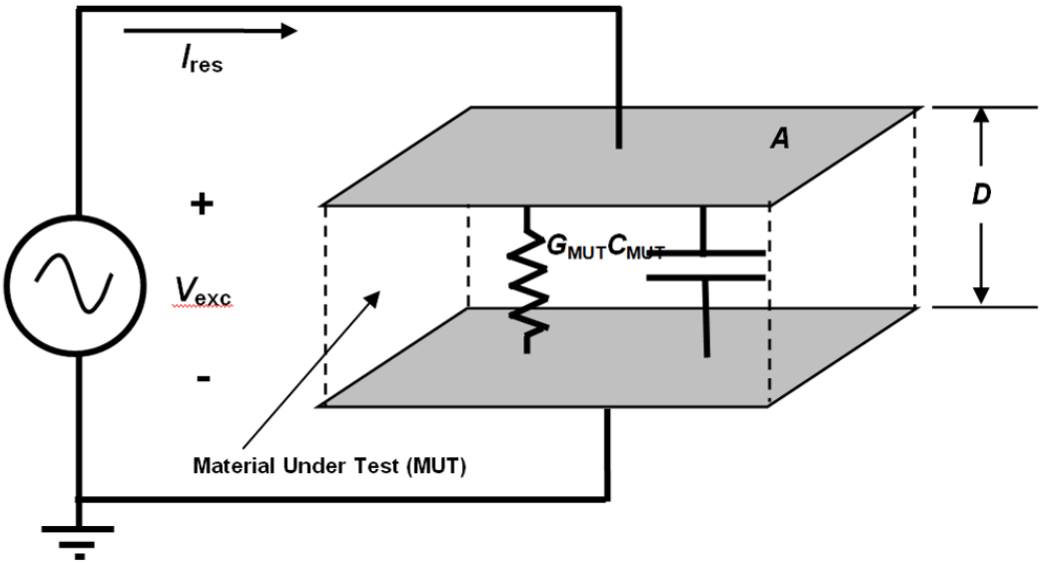

Figure 20-3
Electrical model of resin in direct contact with sensor

Figure 20-4 shows ion viscosity during a 130 °C cure of bulk molding compound (BMC). The BMC was in direct contact with the 1-inch Single Electrode sensor and an LT-451 Dielectric Cure Monitor[2] made measurements with a 100 Hz excitation. The response follows typical behavior for thermosets. As temperature increases, the resin's mechanical viscosity decreases, as does its ion viscosity. Then the material is at minimum mechanical and ion viscosity until the curing reaction dominates and they both increase.

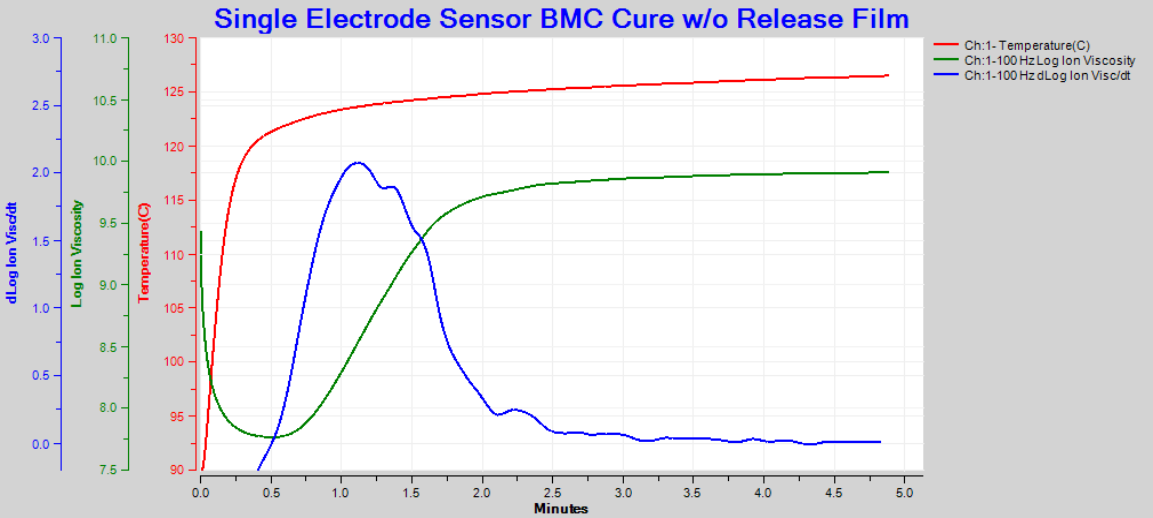

Figure 20-4
Cure of BMC in direct contact with 1-inch Single Electrode Sensor, 100 Hz AC measurement

At gelation, mechanical viscosity increases rapidly until it becomes unmeasurable. After gelation ion viscosity diverges from mechanical viscosity and often correlates with modulus until the end of cure. Because gelation is a mechanical—not an electrical—event, no dielectric feature indicates the gel point. Instead, ion viscosity continues to increase past gelation, enabling the continual measurement of material state to the end of cure

As the reaction ends, the ion viscosity curve flattens and its slope approaches zero. In practice, end of cure is a user defined slope that depends on the requirements of the application.

AC Cure monitoring with release films

Figure 20-5 illustrates a dielectric sensor in a mold with release films. When the mold is closed, the applied pressure ensures close contact between the

sensor and the release film and between the release film and the composite material.

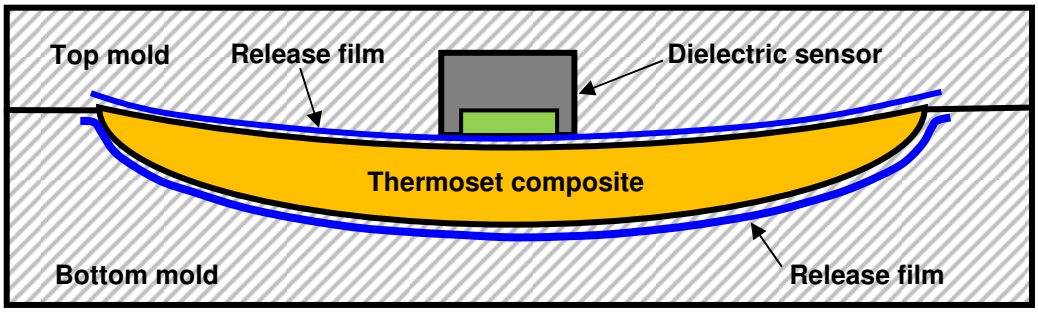

Figure 20-5
Cross section of mold with release film and dielectric sensor

Figure 20-6 shows a dielectric sensor positioned for cure monitoring of material inside a vacuum bag. Once a vacuum is pulled, the bag is in close contact with the composite and dielectric measurements are possible.

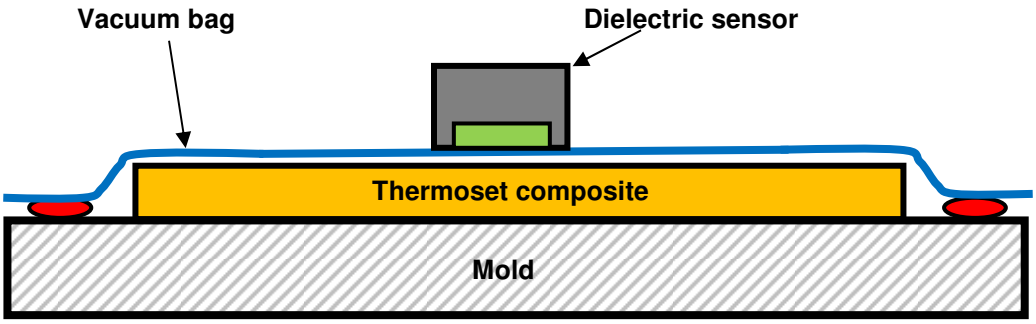

Figure 20-6
Cross section of lay-up with vacuum bag and dielectric sensor

Figure 20-7 is a cross-section of these configurations with a release film or vacuum bag, showing how the electric field from the sensor's electrode passes through an insulating layer into the composite and to the mold.

Figure 20-8 is an electrical model of the composite-insulator-sensor system. The insulator introduces a pair of capacitors in series between the electrodes and the Material Under Test (MUT). These capacitors act as boundary layers, an extra element not included in the model of Figure 20-3. Because capacitors pass only AC signals, cure monitoring is not possible with DC methods

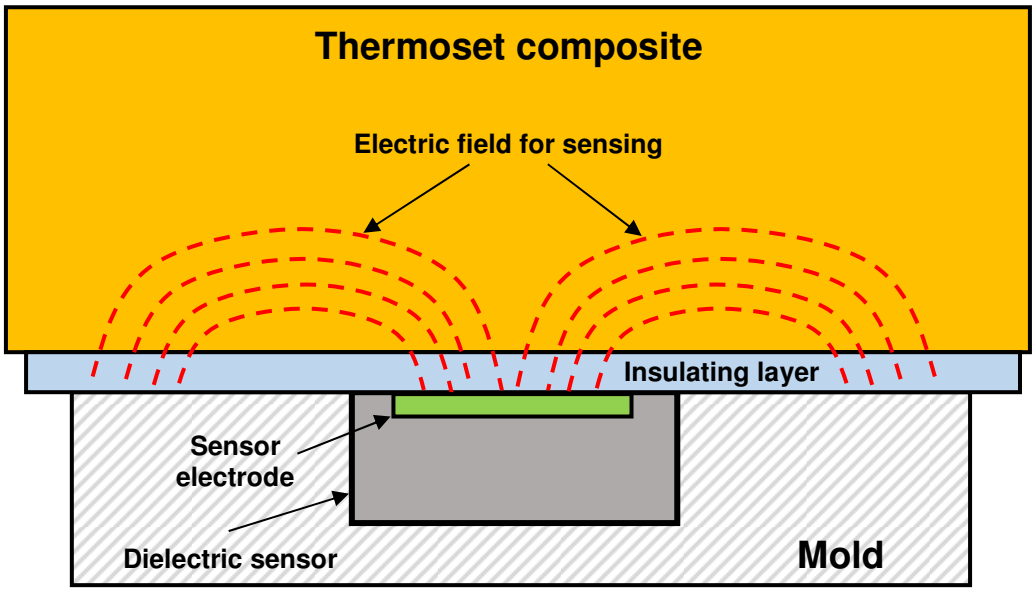

Figure 20-7
Cross section of lay-up with insulating layer, showing electric field

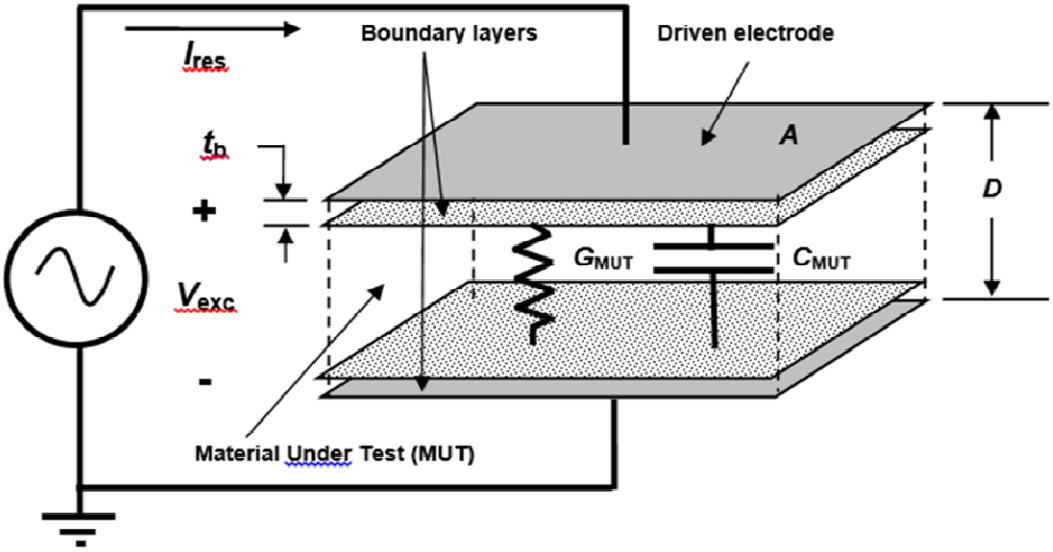

Figure 20-8
Electrical model of resin on sensor with insulating layer

When the Material Under Test is very conductive, usually around the time of minimum viscosity, the presence of boundary layers may distort ion viscosity measurements. To minimize the boundary layer effect, an insulating film must be thin compared to the separation between electrodes.[3,4,5]

Figure 20-9 shows the 1-inch Single Electrode sensor covered with HTF-621, a PTFE-based release film from Northern Composites. The HTF-621 layer is only 0.001" thick, is chemically inert and non-conductive.

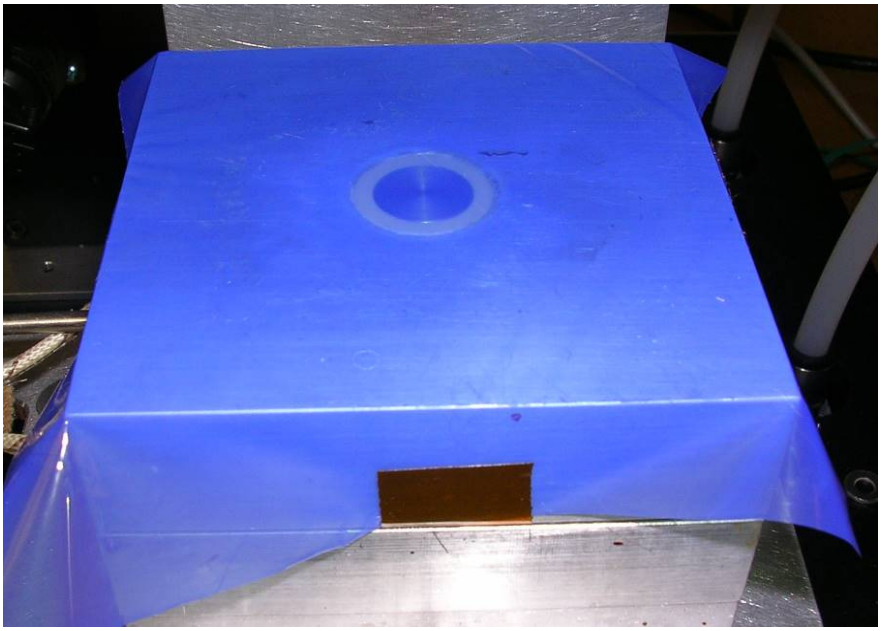

Figure 20-9
1" Single Electrode Sensor in press platen with HTF-621 release film

Figure 20-10 compares ion viscosity with and without a release film during the 130 °C cure of BMC. The curves are substantially the same except around the time of minimum ion viscosity, when the boundary layer effect distorts measurements through the release film. In many cases it is possible to mathematically correct this distortion and restore information about the cure.

Figure 20-11 shows how boundary layer correction—also called *electrode polarization* (EP) correction—recovers affected data. After EP correction, ion viscosity measured with the release film correctly follows ion viscosity measured without the release film. The minor discrepancy between curves is largely due to temperature differences in the tests.

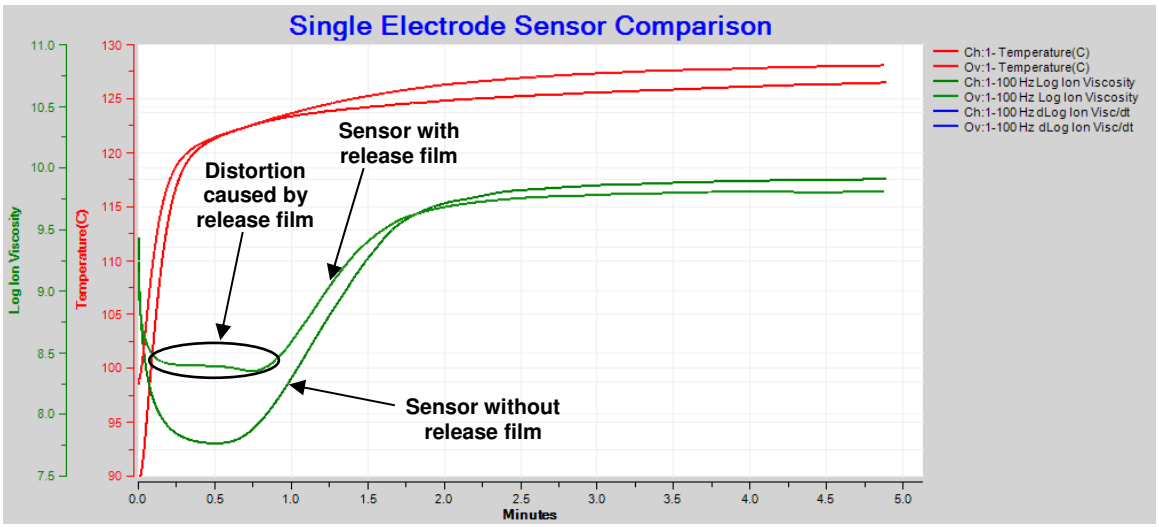

Figure 20-10
Comparison of BMC cure with and without release film, 100 Hz AC measurement

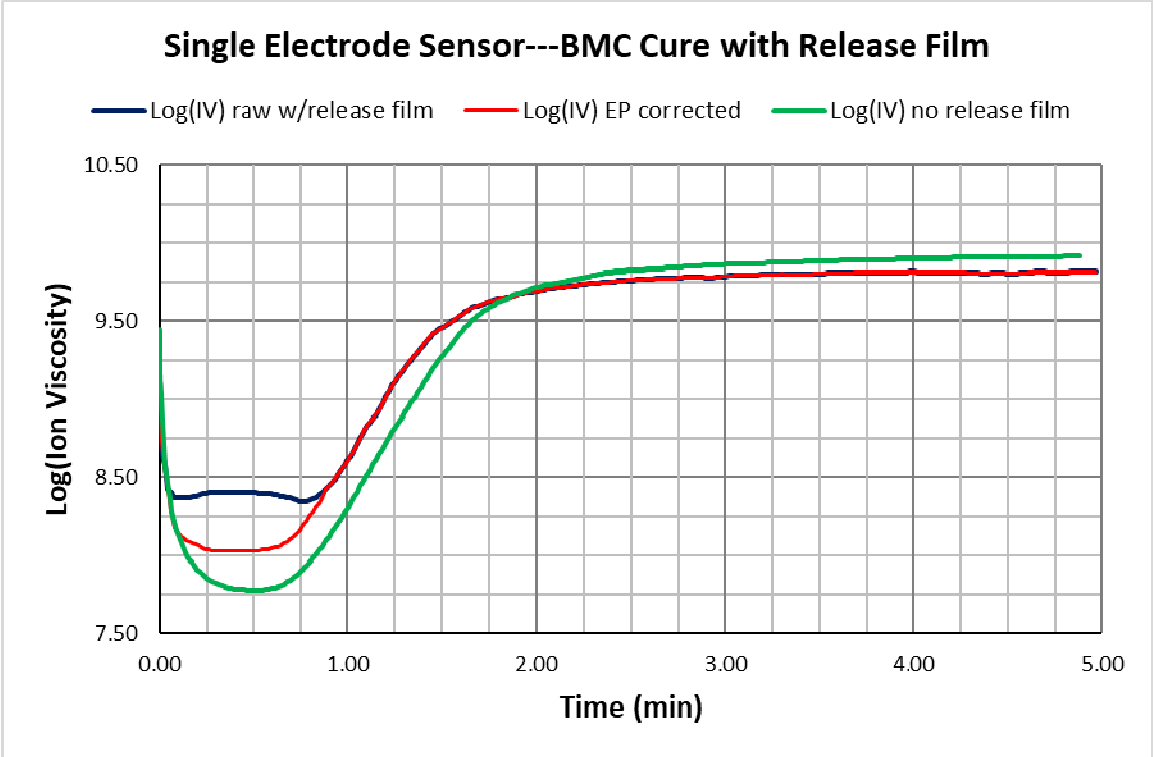

Figure 20-11
Comparison of raw ion viscosity and ion viscosity with EP (boundary layer) correction

Figures 20-12 and 20-13 show the correspondence between Critical Points detected by sensors with and without a release film.

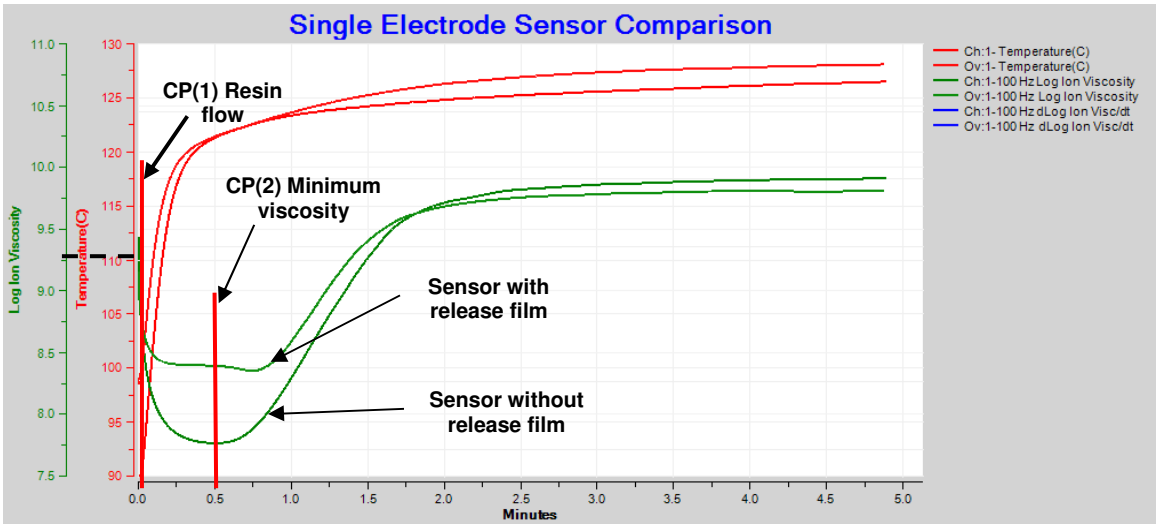

Figure 20-12
Comparison of ion viscosity with and without release film, 100 Hz AC measurement

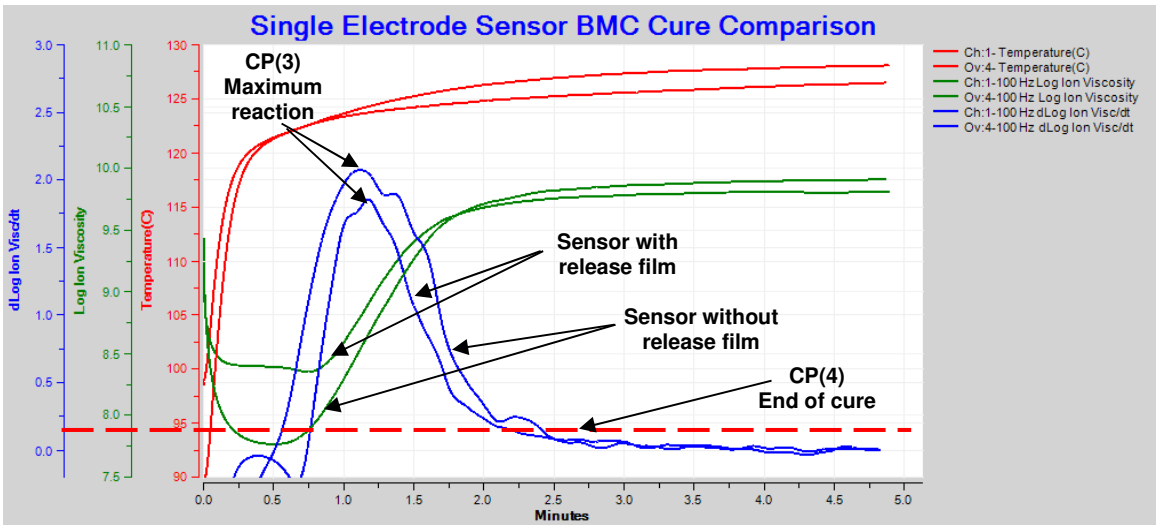

Figure 20-13
Comparison of slope with and without release film, 100 Hz AC measurement

The slope for CP(4) was arbitrarily chosen to illustrate the determination of end of cure. In reality, the user selects a slope based on the requirements of the application. Because AC measurements through a release film correspond to cure

state, Figure 20-13 shows that the appropriate slope enables reliable detection of end of cure.

DC Cure monitoring with release films

DC measurement of resistance or ion viscosity is a simple method of probing cure state; however, it has the following limitations:

- Possible distortion of data, due to electrode polarization, around the time of the viscosity minimum
- Inability to measure cure state through non-conductive release films or vacuum bags

Typical high temperature release films are made from PTFE or similar non-conductive materials. As a result, they act like the capacitive blocking layers of Figure 20-8 and prevent the passage of DC signals.

Some low-grade release films are conductive; however, the conductivity varies with temperature and may not be consistent from batch to batch. While it is possible to make DC measurements through such films, the results unpredictably combine the resistivity of the film and the material under test. Furthermore, the data depend on temperature, are unreliable and therefore not useful.

The LT-451 Dielectric Cure Monitor has a DC measurement option, which was used with the Single Electrode sensor to monitor BMC cure at 130 °C. Figure 20-14 compares DC results with no release film, with the non-conductive HTF-621 release film and with a conductive release film. For reference, data from 100 Hz AC measurements without a release film are also plotted.

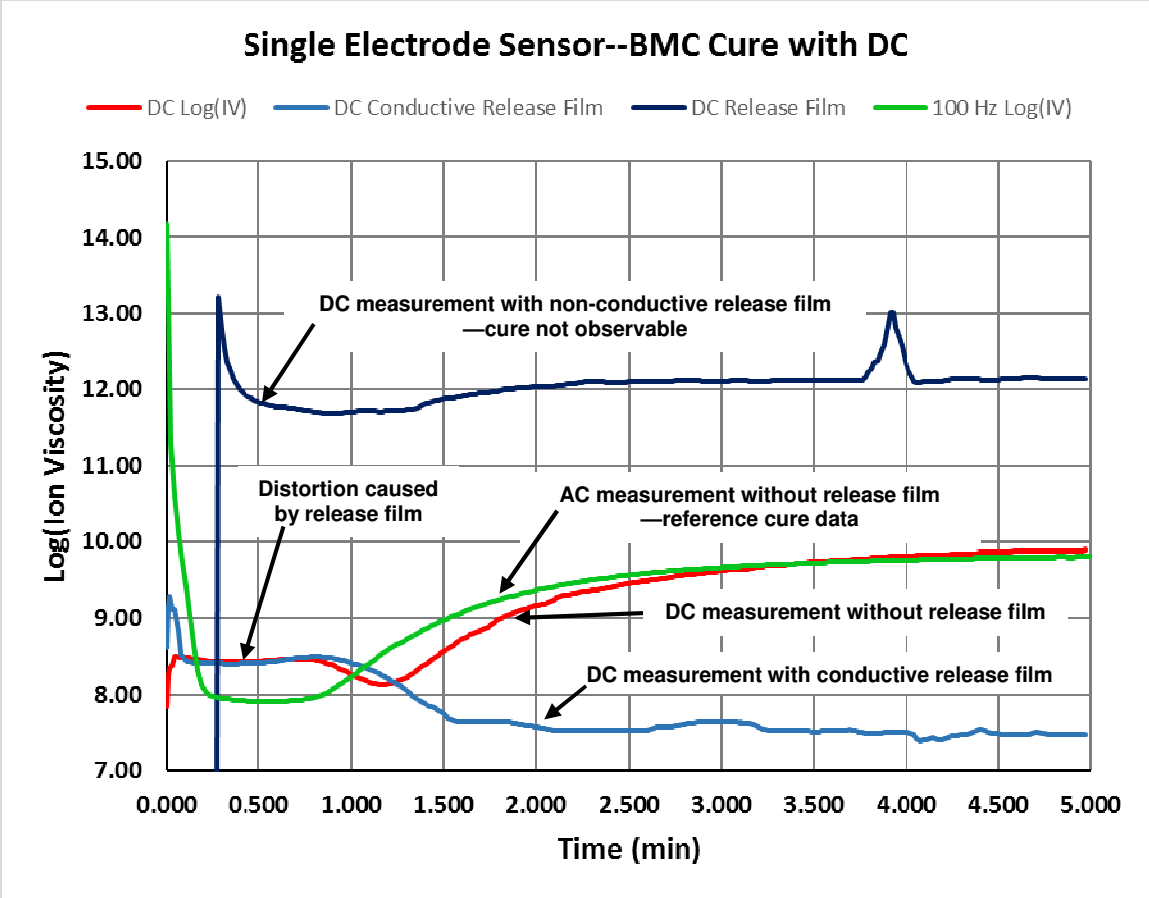

Figure 20-14
Comparison of AC and DC measurements of ion viscosity

Toward the end of cure, AC and DC measurements without a release film are similar. However, DC measurements with no release film show distortion caused by electrode polarization around the time of the ion viscosity minimum. While it is possible to correct this distortion with AC data (see Figure 20-11), it is not possible to correct DC data.

DC measurements through the conductive release film are possible, as shown, but still subject to distortion due to electrode polarization. Toward the end of cure the release film's conductivity dominates and prevents useful probing of cure state.

DC measurements through the non-conductive HTF-621 release film are not possible at all, as shown by very high, essentially constant ion viscosity at the measurement limit under these conditions.

With a suitable sensor, AC measurements through a release film or vacuum bag can follow cure and provide the same information as a sensor in direct contact with the material under test. The insulating layer distorts ion viscosity data around the time of the viscosity minimum, when the material is most conductive, but in many cases software can mathematically correct this distortion. DC measurements, however, are not possible through a release film and are a serious limitation of DC cure monitoring techniques.

References

1. 1" Single-Electrode sensor, manufactured by Lambient Technologies, Cambridge, MA USA. https://lambient.com

2. LT-451 Dielectric Cure Monitor, manufactured by Lambient Technologies, Cambridge, MA USA

3. Day, D.R.; Lewis, J.; Lee, H.L. and Senturia, S.D., "The Role of Boundary Layer Capacitance at Blocking Electrodes in the Interpretation of Dielectric Cure Data in Adhesives," *Journal of Adhesion*, V18, p.73 (1985)

4. Lambient Technologies application note AN2.16, "Electrode Polarization and Boundary Layer Effects"

5. Lambient Technologies application note AN2.40, "Electrode Polarization and Boundary Layer Effects with AC and DC Cure Monitoring"

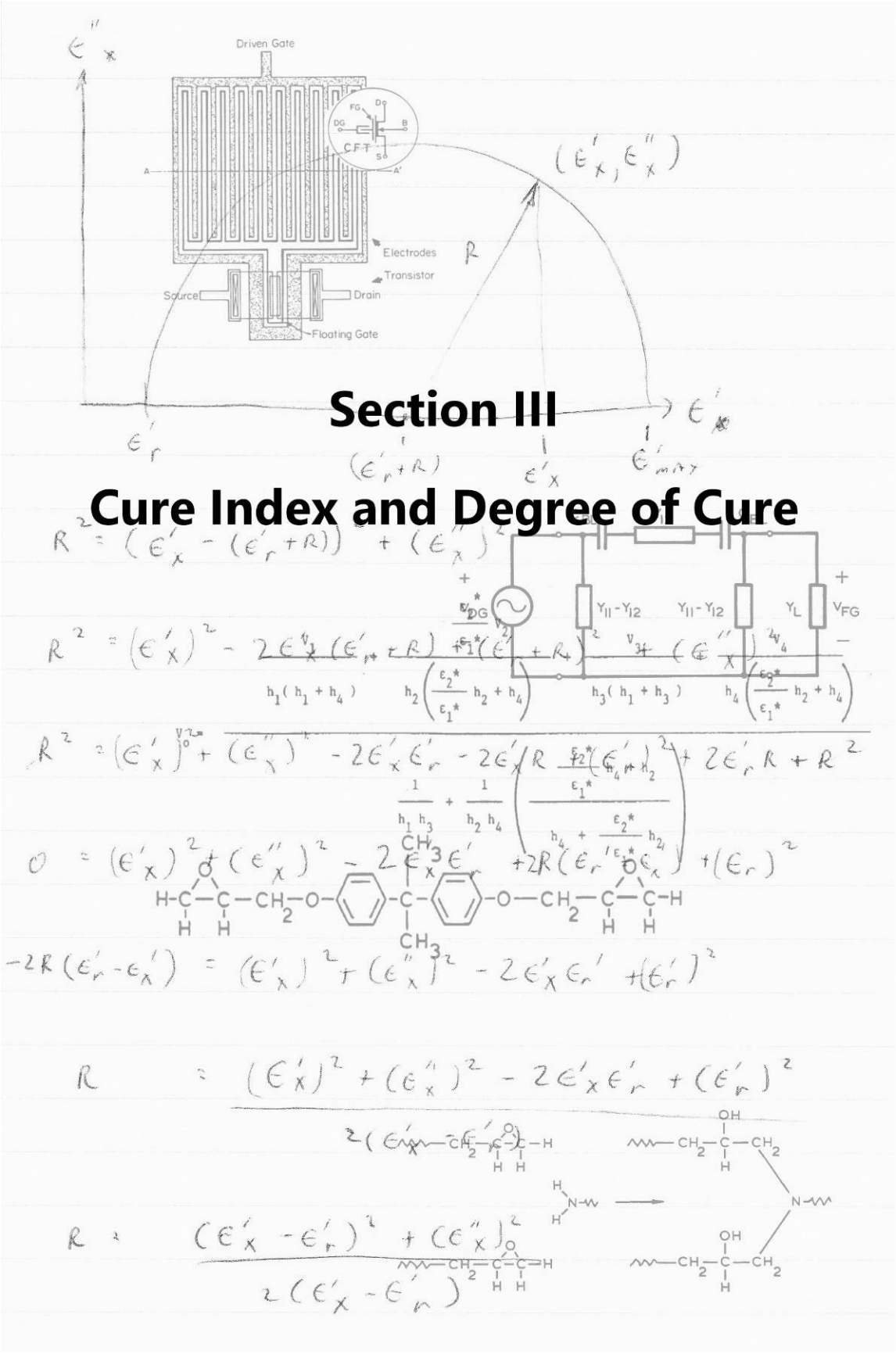
Driven Gate
Electrodes
Transistor
Source
Drain
Floating Gate
Section III
Cure Index and Degree of Cure

Chapter 21—Measuring Degree of Cure with DEA

Dependence of ion viscosity on temperature and cure state

When temperature is constant, it is easy to understand how dielectric measurements indicate cure state—only the degree of cure affects the ion viscosity of a thermoset or composite. However, ion viscosity actually depends on *both* degree of cure *and* temperature, and accounting for temperature is necessary to correctly interpret non-isothermal tests. Two rules can sum up the behavior of ion viscosity:

1. At constant degree of cure, increasing (or decreasing) temperature decreases (or increases) ion viscosity

2. At constant temperature, increasing (or decreasing) degree of cure increases (or decreases) ion viscosity

Because these rules have opposite effects, the net result depends on which dominates at a particular moment. Figure 21-1 plots data from the cure of an epoxy-fiberglass prepreg.

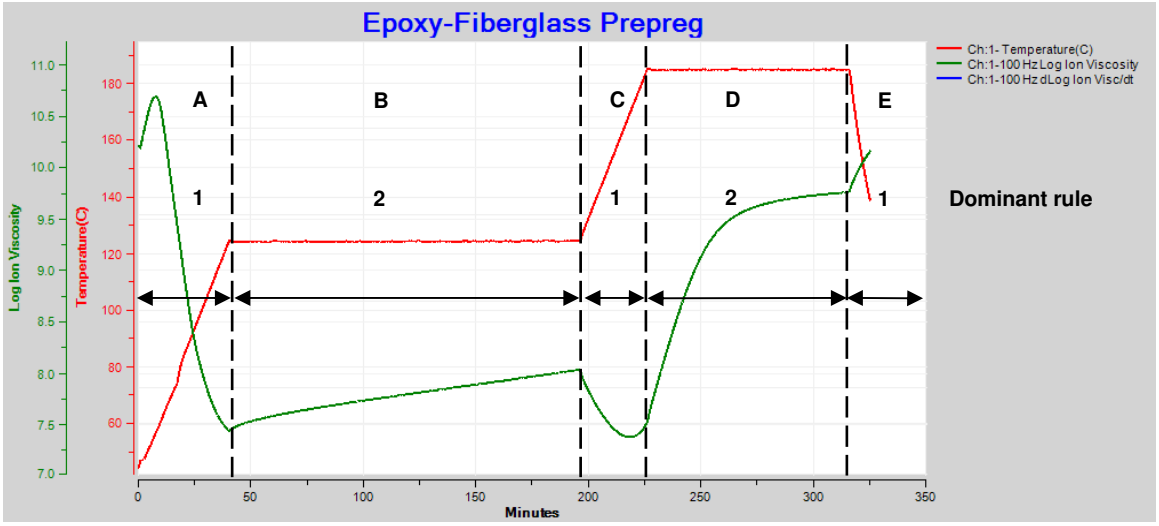

Figure 21-1
Epoxy-fiberglass prepreg cure with ramps and holds

Here ion viscosity changes as temperature goes through two ramp and hold steps then a final cooling:

A. Temperature increases but is too low to initiate significant reaction, so degree of cure is essentially constant and ion viscosity decreases (Rule 1 dominates).

B. Temperature is constant and the slow reaction slightly increases degree of cure, accompanied by a small increase in ion viscosity (Rule 2 dominates).

C. Temperature increases but is still too low for significant reaction or change in degree of cure, and ion viscosity decreases (Rule 1 dominates).

D. At this higher constant temperature, the reaction and degree of cure increase significantly, causing a large increase in ion viscosity (Rule 2 dominates).

E. Temperature decreases. Cure is complete by this time, degree of cure is constant and ion viscosity increases (Rule 1 dominates).

Sometimes the changing temperature and cure rate create a more complex ion viscosity curve, as shown in Figure 21-2. Why does ion viscosity rise then fall between 90 and 150 minutes? Shouldn't the reaction be accelerating because temperature is increasing during this time? Or is the cure somehow reversing?

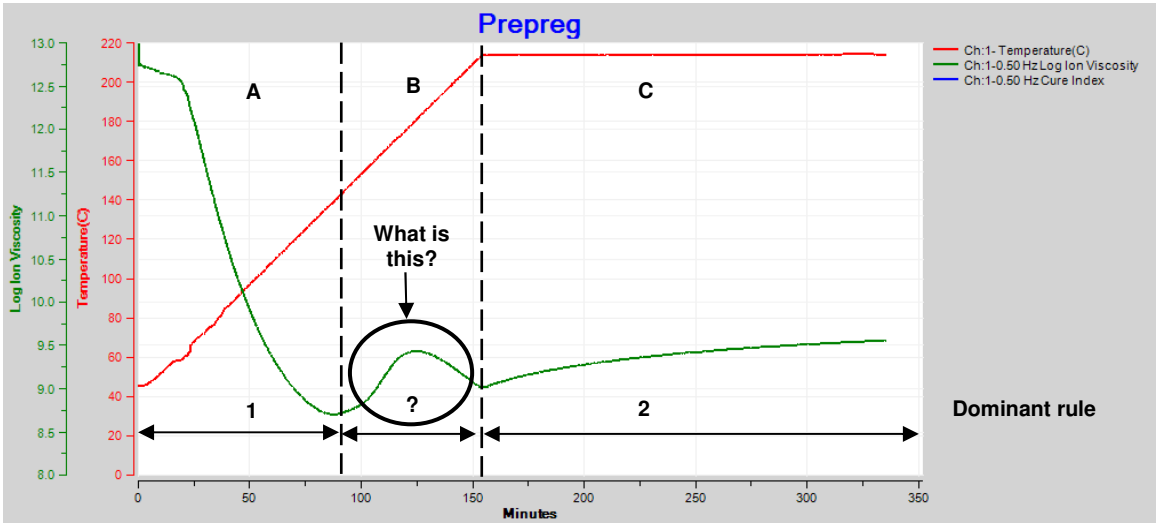

Figure 21-2
Epoxy-fiberglass prepreg cure with ramp and hold

Cure Index

For more insight, a parameter called *Cure Index* accounts for the effect of temperature and is closely related to degree of cure. Calculation of Cure Index requires two baselines that are characteristic of the material: one for the temperature dependence of ion viscosity at 0% cure and the second at 100% cure.

Any measurement of ion viscosity and the associated temperature now exists as a point between these baselines, as shown in Figure 21-3. Cure Index is the vertical distance between this point and the 0% baseline, expressed as a proportion of the vertical distance between the two baselines.

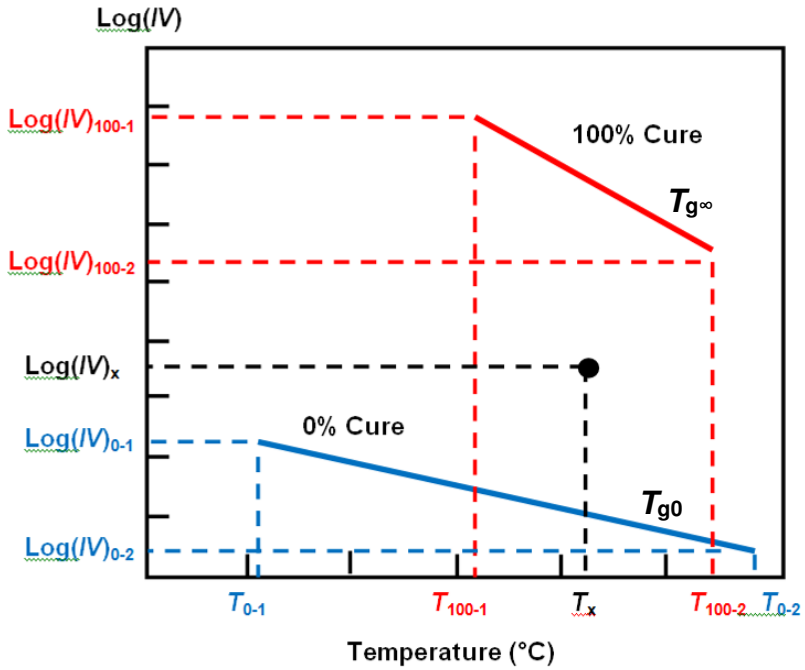

Figure 21-3
Cure Index baselines with ion viscosity-temperature data point

The 0% and 100% baselines are determined by measuring ion viscosity at different temperatures for uncured and fully cured material, respectively. Figure 21-4 shows the baselines obtained in this way for the prepreg of Figure 21-2. The ion viscosity-temperature data are plotted between them. The resulting Cure Index curve for this prepreg is shown in Figure 21-5 along with the original ion viscosity.

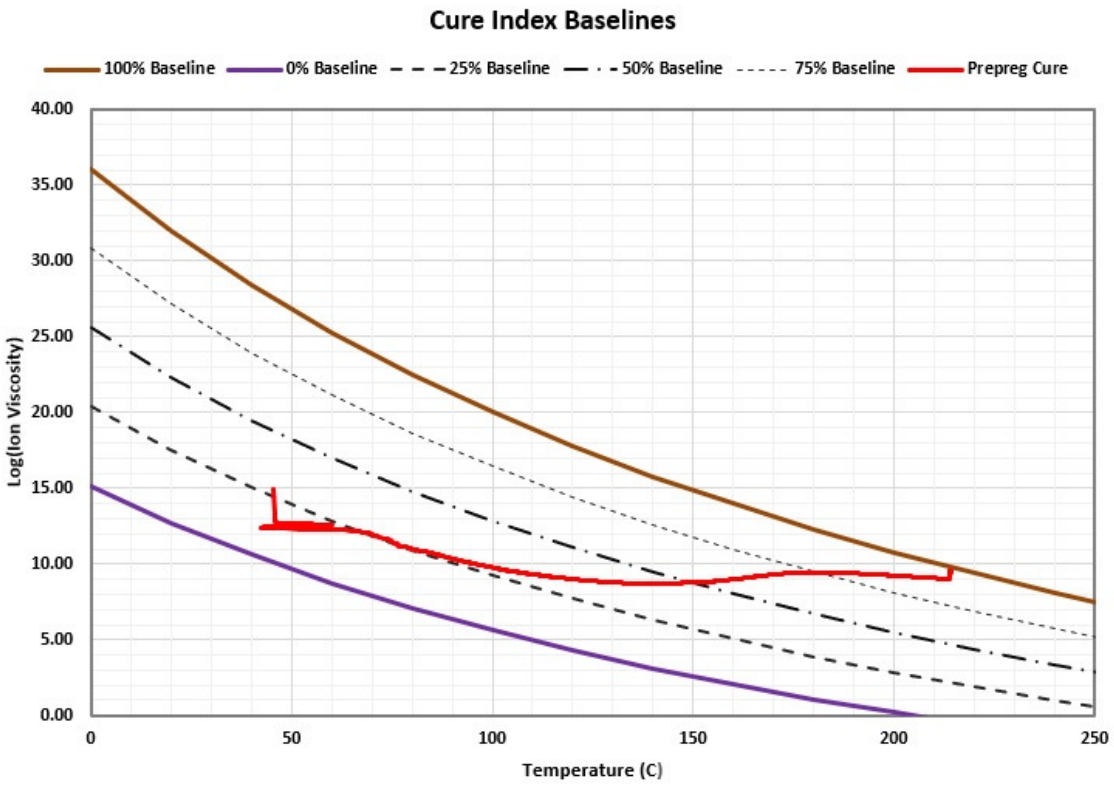

Figure 21-4
Prepreg data between Cure Index baselines

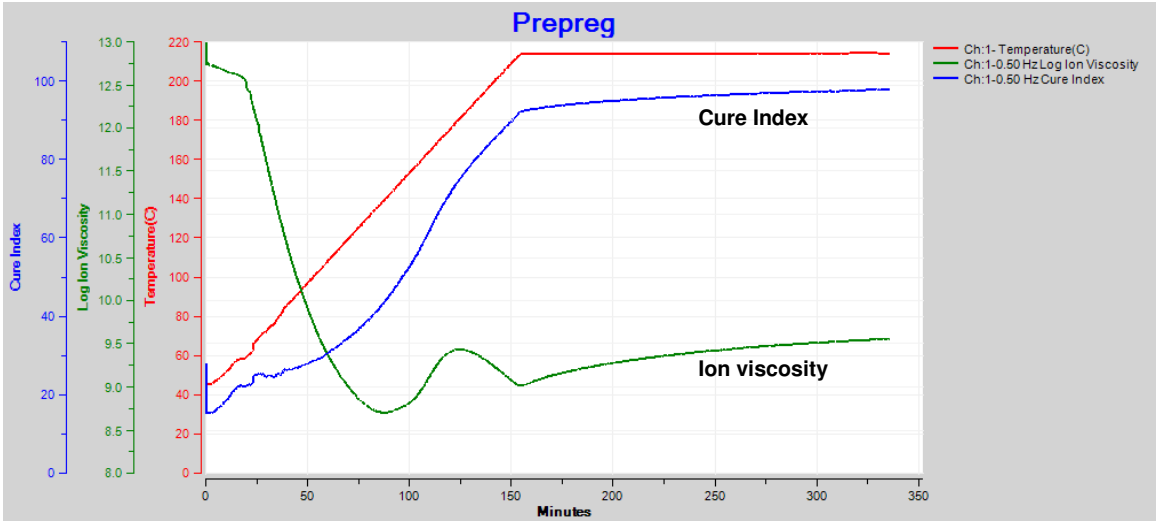

Figure 21-5
Epoxy-fiberglass prepreg ion viscosity and Cure Index

The reaction that drives polymerization is irreversible and the degree of cure always increases with time. The Cure Index of this prepreg shows a

continuous increase, consistent with irreversibility, even though ion viscosity peaks and falls between 90 and 150 minutes.

Cure Index reveals this behavior is simply the effect of curing dominating heating between about 90 and 125 minutes, then heating dominating curing between 125 and 150 minutes. To understand the bump in ion viscosity, consider these segments as two separate responses: a) resin during cure as shown in Figure 21-6 and b) resin after end of cure as shown in Figure 21-7.

At first, as temperature increases, ion viscosity decreases because the thermoset becomes more fluid and therefore less resistive. The reaction rate increases as the material becomes hotter. At some time the increase in ion viscosity due to polymerization overcomes the decrease in ion viscosity due to increasing temperature. This point is the ion viscosity minimum, which also occurs at the time of minimum mechanical viscosity.

After the minimum point, ion viscosity increases continuously until the concentration of unreacted monomers diminishes and the reaction rate decreases; consequently, the slope of ion viscosity also decreases and eventually ion viscosity will have zero slope when cure has stopped completely, as shown in Figure 21-6.

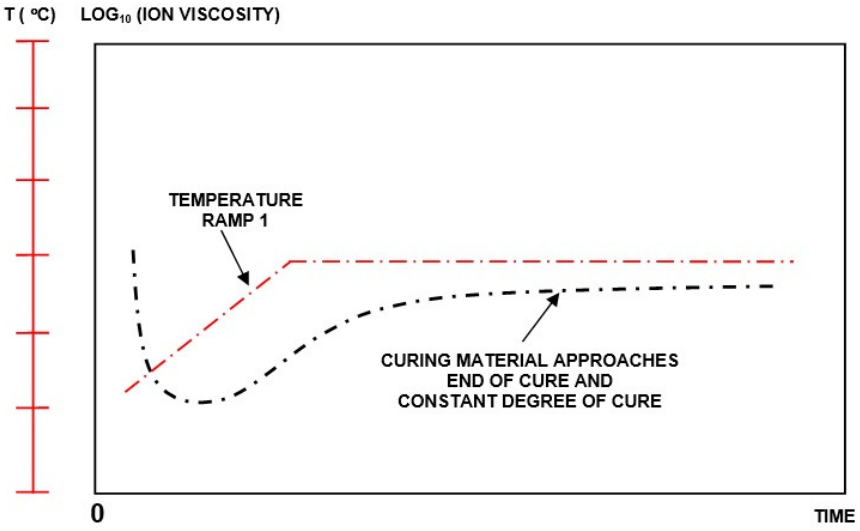

Figure 21-6
Ion viscosity during cure

The degree of cure is constant after the reaction has stopped, and under this condition Figure 21-7 shows ion viscosity remains constant during the first isothermal hold stage. When temperature increases during Ramp 2, ion viscosity

decreases according to Rule 1: *At constant degree of cure, increasing (or decreasing) temperature decreases (or increases) ion viscosity*. Finally, during the second isothermal hold stage, ion viscosity again becomes constant because both degree of cure and temperature are constant.

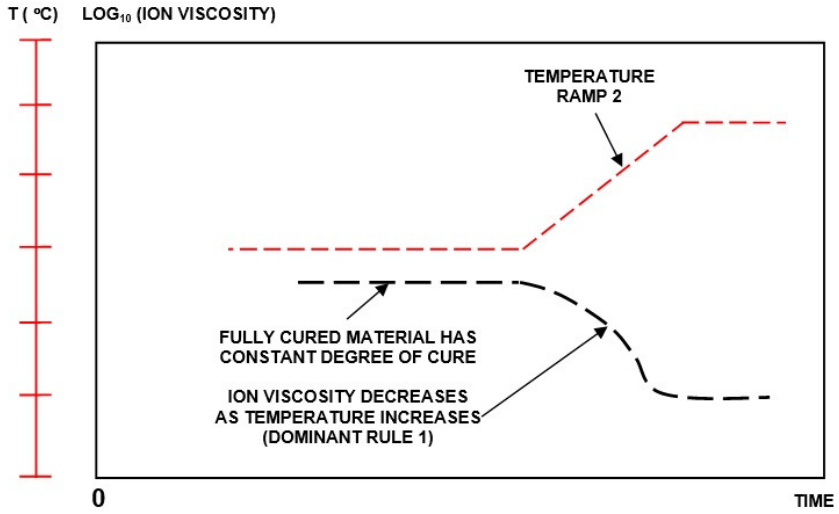

Figure 21-7
Ion viscosity during temperature ramp after end of cure

The behaviors of Figures 21-6 and 21-7 can be combined in Figure 21-8 to show how ion viscosity changes in response to two ramps and holds.

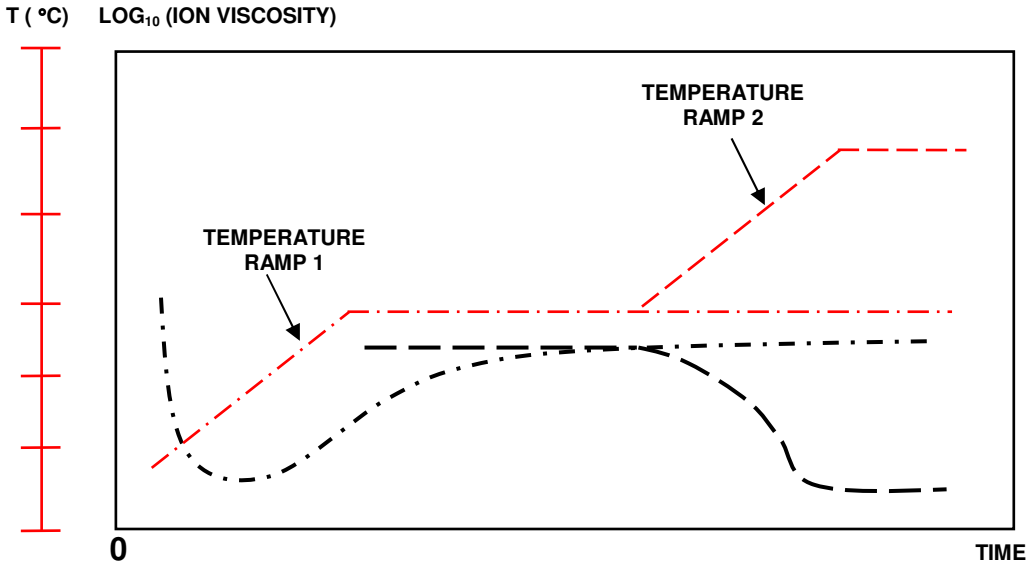

Figure 21-8
Ion viscosity response to two ramp and hold stages

If the time decreases between the two temperature ramps, the result looks like Figure 21-9.

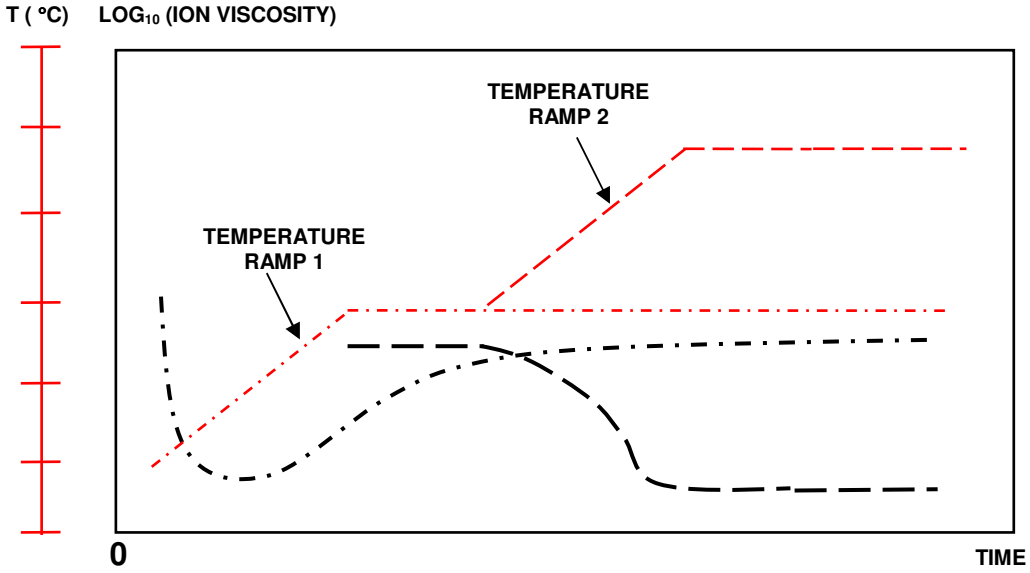

Figure 21-9
Ion viscosity response to two ramp and hold stages

Finally, with a single ramp of sufficient duration and magnitude, the combined behavior of ion viscosity produces the curve shown in Figure 21-10.

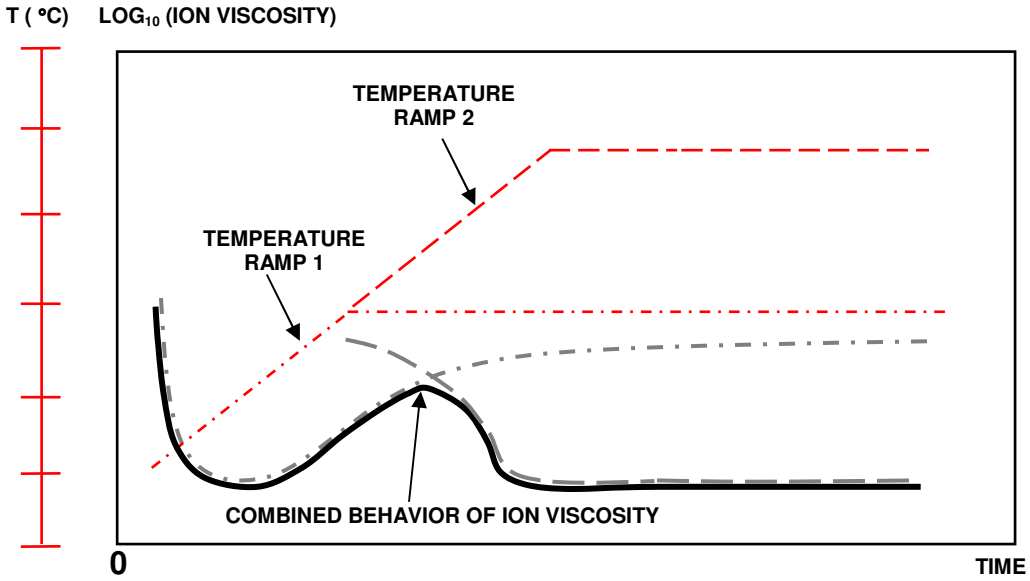

Figure 21-10
Ion viscosity response to a single ramp and hold step

When both cure state and temperature vary during thermoset processing, the progress of cure may not be clear and straightforward. Even worse, ion viscosity may present confusing behavior. Use of Cure Index can account for the effect of temperature on ion viscosity to yield a reproducible indicator of cure state. In fact, Cure Index is physically related to degree of cure and can be a valuable way to interpret the results of dielectric cure monitoring.

Chapter 22—Cure Index and Degree of Cure

Relating Cure Index to cure state

While it is easy to see how Cure Index *qualitatively* indicates cure state, in fact a *quantitative* relationship also exists between Cure Index and degree of cure. For a given material, any measurement of ion viscosity and the associated temperature exists as a point between two baselines: one representing the temperature dependence of ion viscosity at 0% cure and the other at 100% cure, as shown in Figure 22-1.

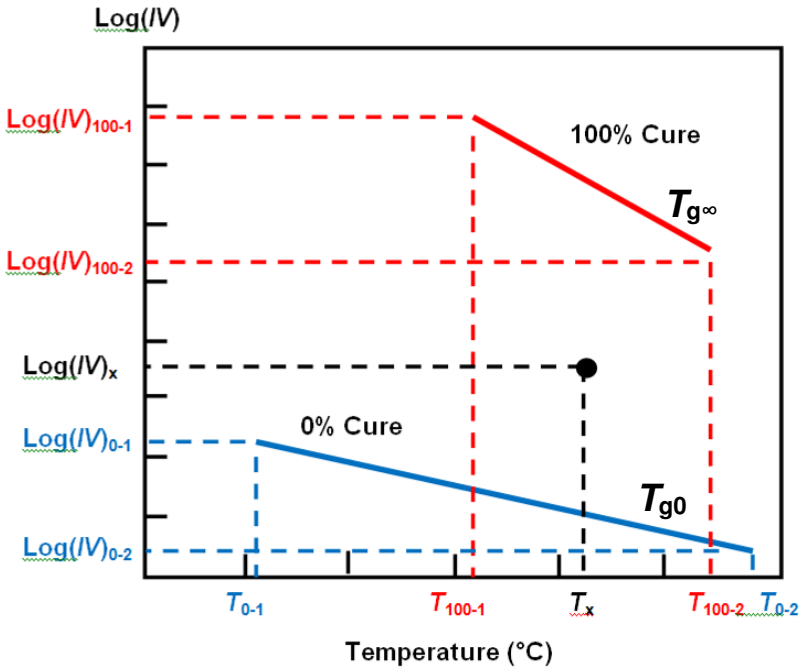

Figure 22-1
Cure Index baselines

Cure Index, given by Equation 22-1, is the vertical distance between this point and the 0% baseline, expressed as a proportion of the vertical distance between the two baselines.

(eq. 22-1)
$$\text{Cure Index} = \frac{\text{Log}(IV)_x - \text{Log}(IV(T_x))_0}{\text{Log}(IV(T_x))_{100} - \text{Log}(IV(T_x))_0}$$

How does Cure Index relate to degree of cure? As a thermoset reacts and polymerizes, each bond releases a fixed amount of heat. Degree of cure is defined as:

(eq. 22-2) $$\alpha = \Delta H \,/\, \Delta H_R$$

Where:

α = Degree of cure
ΔH = Total heat released
ΔH_R = Heat of reaction

Degree of cure therefore can indicate physical state because it measures the total amount of bond formation or crosslink density. Furthermore, Ueberreiter and Kanig[1] reported crosslink density is directly proportional to the change in glass transition temperature. This relationship between degree of cure and glass transition temperature is often expressed by the DiBenedetto[2] equation:

(eq. 22-3) $$\frac{(T_g - T_{g0})}{(T_{g\infty} - T_{g0})} = \frac{\lambda \bullet \alpha}{(1 - (1 - \lambda) \bullet \alpha)}$$

Where:

T_g = glass transition temperature
T_{g0} = glass transition temperature at 0% cure
$T_{g\infty}$ = glass transition temperature at 100% cure
λ = experimentally derived parameter
α = extent of conversion or degree of cure

Because ion viscosity increases with crosslink density, dielectric measurements should correlate with glass transition temperature as well. Early published data of an isothermal epoxy cure show such a relationship. In this test, T_g increased in proportion with log(resistivity), also known as log(*IV*), as shown in Figure 22-2.

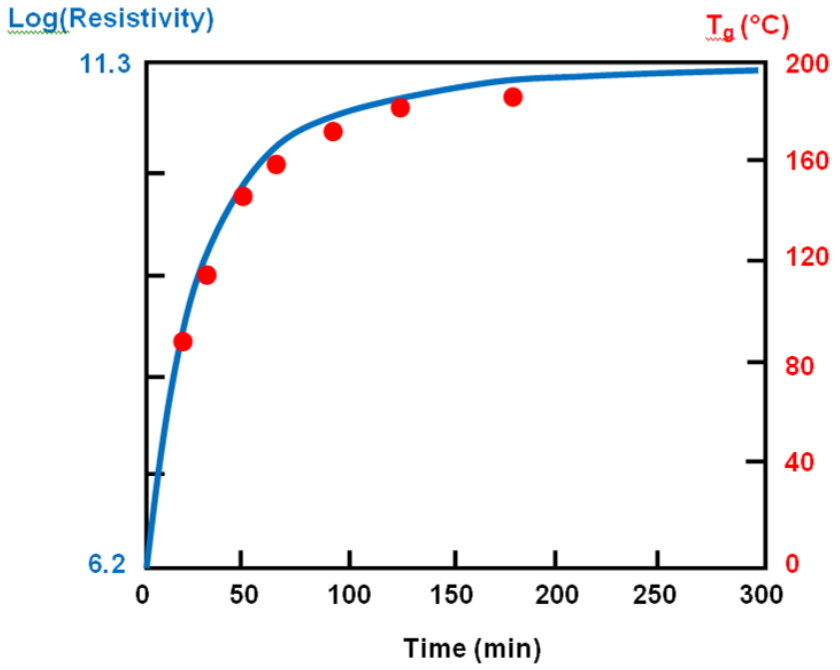

Figure 22-2
T_g and log(resistivity) vs. time during 200 °C isothermal epoxy cure[3]

Other published studies, such as the data of Figure 22-3, corroborate a linear relationship between log(*IV*) and T_g during isothermal cure.

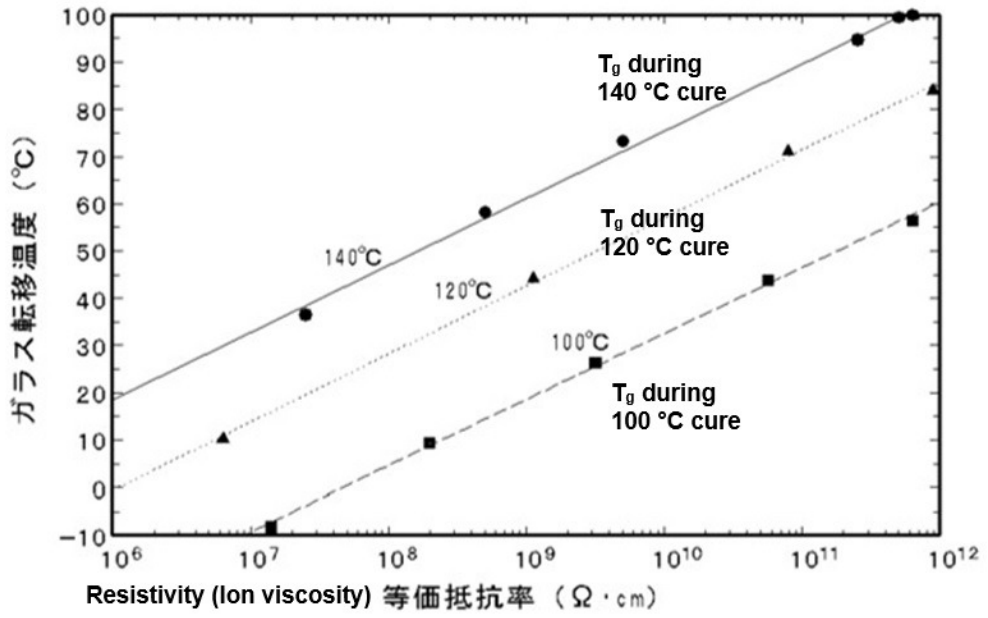

Figure 22-3
Glass transition temperature vs. resistivity (ion viscosity) for an epoxy [4]

Assuming the linear relationship between log(*IV*) and T_g shown in Figure 22-1, glass transition temperature as a function of Log(*IV*)x and *T*x can be calculated by linear interpolation:

$$T_g = T_{g0} + \frac{\text{Log}(IV)_x - \text{Log}(IV(T_x))_0}{\text{Log}(IV(T_x))_{100} - \text{Log}(IV(T_x))_0} [T_{g\infty} - T_{g0}] \quad \text{(eq. 22-4)}$$

Where:

T_g = glass transition temperature
T_{g0} = glass transition temperature at 0% cure
$T_{g\infty}$ = glass transition temperature at 100% cure

Figure 22-4 shows how resistivity varies with temperature for a particular epoxy resin. The dashed lines represent degree of cure determined by DSC and can be used to calculate glass transition temperature by interpolation of dielectric measurements. The solid lines approximate baselines for 0% and 100% degrees of cure.

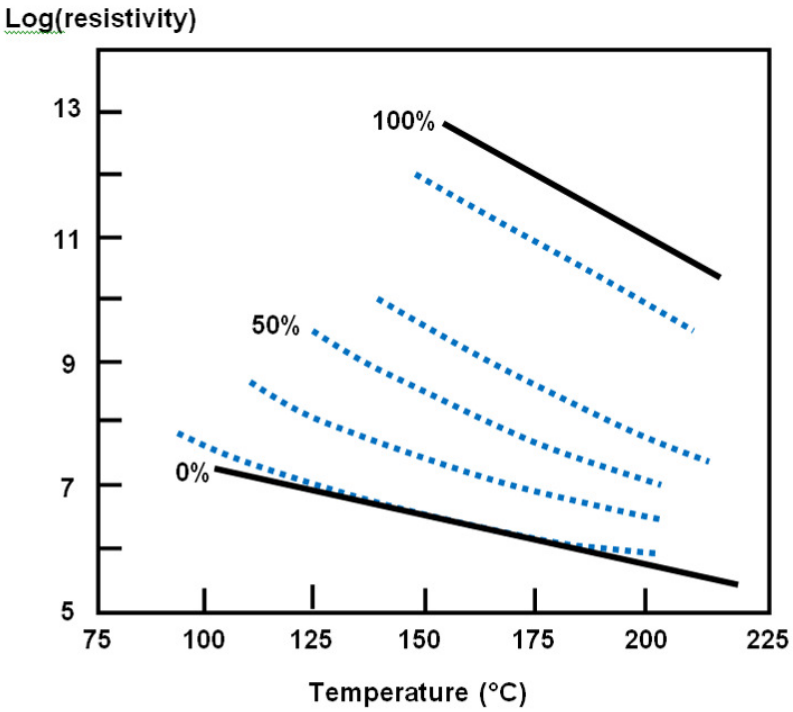

Figure 22-4
Variation in log(resistivity) with temperature for an epoxy[3]

Interpolation of dielectric data for non-isothermal cure of this epoxy yields glass transition temperatures as shown in Figure 22-5. For this particular material, T_g measured by DSC shows good agreement with values calculated from the linear T_g model.

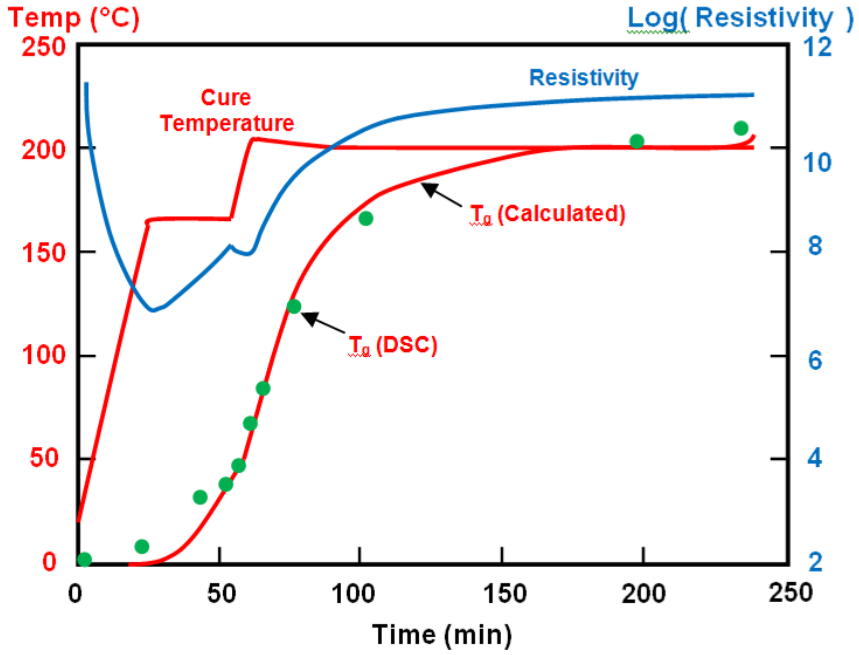

Figure 22-5
Calculated T_g during non-isothermal cure with linear T_g model[3]

By relating T_g and degree of cure, the DiBenedetto equation implies a similar linear correspondence between log(*IV*) and degree of cure. For isothermal processing, over limited degrees of reaction, the following expression often applies:

(eq. 22-5) $$\alpha = k \log(\rho_{DC}) + C$$

Where:

α = extent of conversion or degree of cure
ρ_{DC} = frequency independent resistivity or ion viscosity (*IV*)
k, C = experimental constants

For non-isothermal conditions, equation 22-5 is invalid because resistivity varies with temperature as well as cure state.

Equations 22-1 and 22-4 may be combined and rearranged to yield Cure Index, which is a reproducible indicator of cure state that does not rely on glass transition temperature—*but correlates with glass transition temperature*.

$$\text{(eq. 22-6)}\quad \text{Cure Index} = \frac{\text{Log}(IV)_x - \text{Log}(IV(T_x))_0}{\text{Log}(IV(T_x))_{100} - \text{Log}(IV(T_x))_0} = \frac{[T_g - T_{g0}]}{[T_{g\infty} - T_{g0}]}$$

Note this model may not apply in the presence of multiple reactions, loss of reaction products or loss of solvents. Results also may not be consistent from sample to sample of the same material if the background ion level varies too much. For most commercial or industrial thermosets, product composition is well controlled and differences in background ion concentration are typically not an issue.

Figure 22-6 plots Cure Index derived from the data of Figure 22-5, interpolated between the baselines of Figure 22-4.

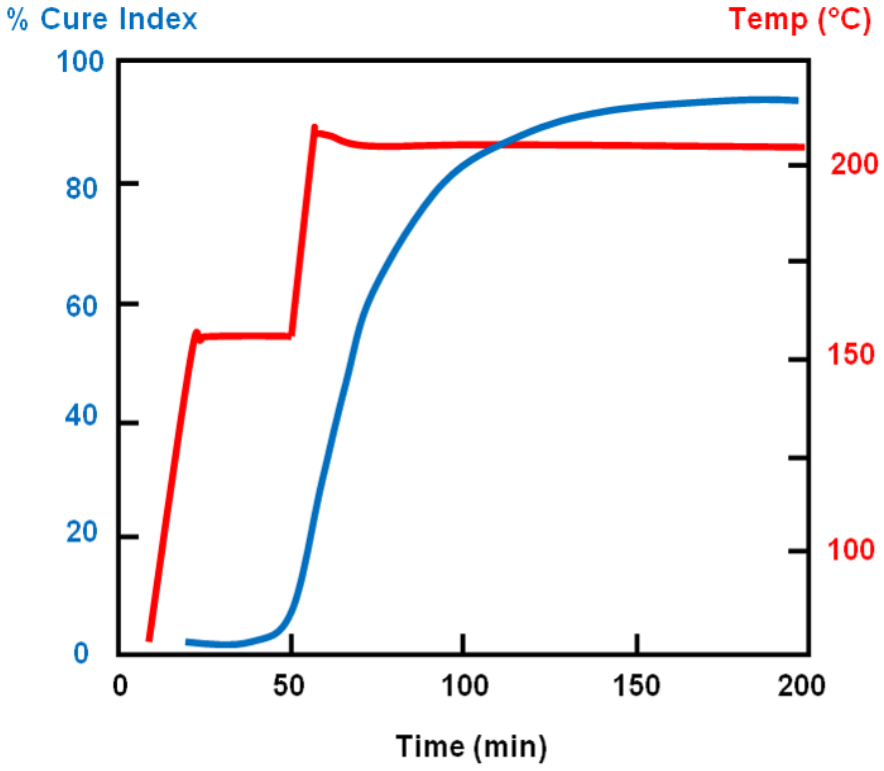

Figure 22-6
Percent Cure Index during non-isothermal cure with linear T_g model[3]

Figure 22-7 plots how the glass transition temperature of another epoxy changes with Cure Index during cure. As with other published data, a linear or near-linear relationship exists between Tg and Cure Index.

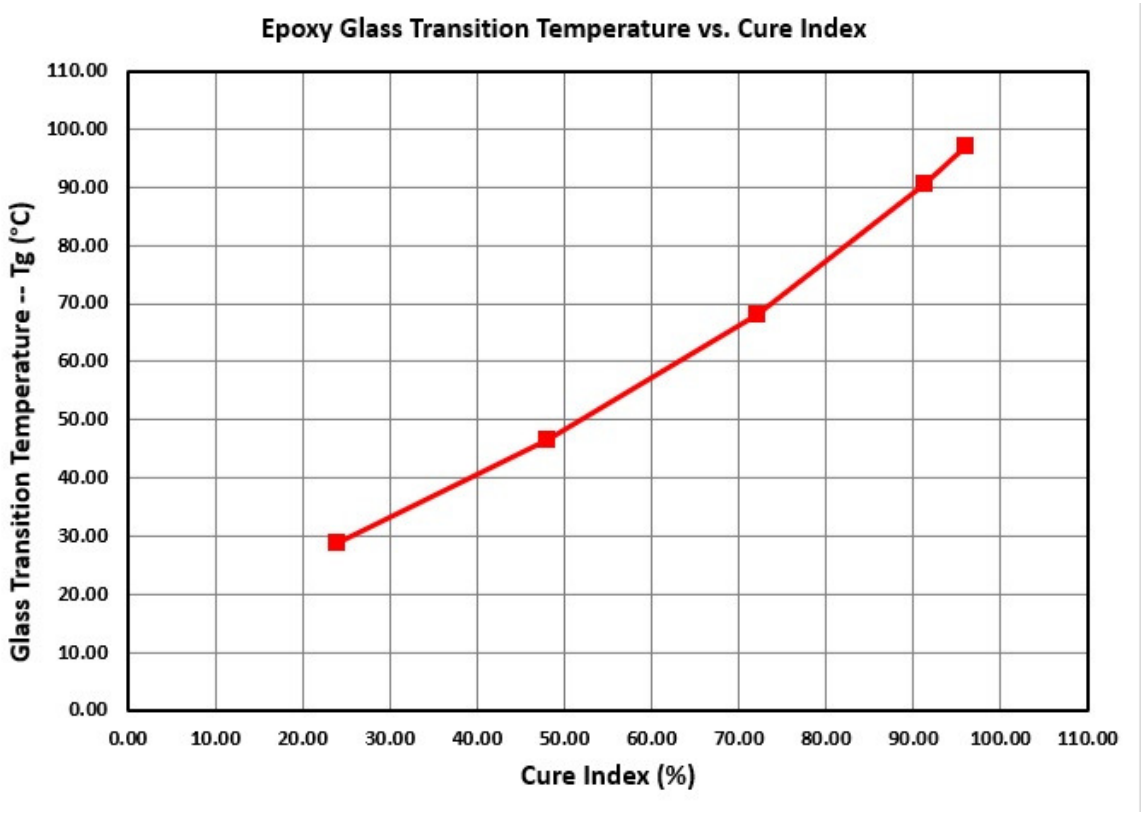

Figure 22-7
Glass transition temperature vs. Cure Index during cure of an epoxy resin

The DiBenedetto equation (eq. 22-3) can combined with the definition of Cure Index (eq. 22-6) and rearranged to express degree of cure in terms of Cure Index:

$$\alpha = \frac{\text{Cure Index}}{[\lambda + \text{Cure Index} \bullet (1 - \lambda)]} \quad \text{(eq. 22-7)}$$

Where:

λ = experimentally derived parameter
α = extent of conversion or degree of cure

Equation 22-7 shows degree of cure can be derived from Cure Index and therefore from ion viscosity and temperature. If the experimentally derived parameter $\lambda = 1$, then to first order equation 22-7 becomes simply:

(eq. 22-8) α = Cure Index

The term *Cure Index* was coined by D. R. Day[5] to distinguish it from *degree of cure*. Cure Index is derived from dielectric properties while degree of cure is defined by thermodynamics. However, they each are determined by the quantity of bond formation, a physical phenomenon they have in common, justifying the correlation between the two.

Unlike differential scanning calorimetry (DSC) or dynamic mechanic analysis (DMA), which can only be used in the laboratory, dielectric cure monitoring (DEA) works in molds, presses or manufacturing operations. With Cure Index, dielectric cure monitoring has the unique ability to make measurements that correlate with glass transition temperature and degree of cure during a process and in real time.

References

1. Ueberreiter, K.; Kanig, G., *Journal of Chemical Physics*, 18, 399 (1950).

2. Pascault, J.P. and Williams, R.J.J., "Glass transition Temperature vs. Conversion Relationships for Thermosetting Polymers," *J. of Polymer Science, Part B:Polymer Physics*, 28, 85-95 (1990).

3. Day, D.R., "Dielectric Properties of Polymeric Materials," Micromet Instruments, (1987). (Figures have been redrawn for clarity)

4. Makishima, S.; Nakano, T.; Koyama, M.; Inoue, Y., "Dielectric Property of Curing Epoxy Resin and Application for Casting Process," IEEE Electrical Electronics Insulation Conference, Sept. 18-21, 1995

5. Day, D.R., "Dielectric Determination of Cure State During Non-Isothermal Cure," *Polymer Engineering and Science*; 29(5):334-338, (August 2004).

Chapter 23—Cure Index Analysis of Five-Minute Epoxy

Cure of five-minute epoxy

A generic "five-minute epoxy" was tested under different thermal conditions to observe the effect on the progress of cure. For isothermal tests, ion viscosity measurements easily reveal cure state because temperature is not a variable; however, five-minute epoxy can generate a significant exotherm, making the typical reaction *non*-isothermal.

In this case, because ion viscosity depends on both cure state *and* temperature, reaction rate and degree of cure are not clear when analyzing ion viscosity alone. With Cure Index analysis, which accounts for the effect of temperature, dielectric measurements clearly show how cure time decreases and how degree of cure increases with greater peak exotherms, as expected for thermally driven reactions.

Procedure

The epoxy resin and catalyst were mixed according to the manufacturer's directions and placed on a Mini-Varicon[1] sensor, shown in Figure 23-1.

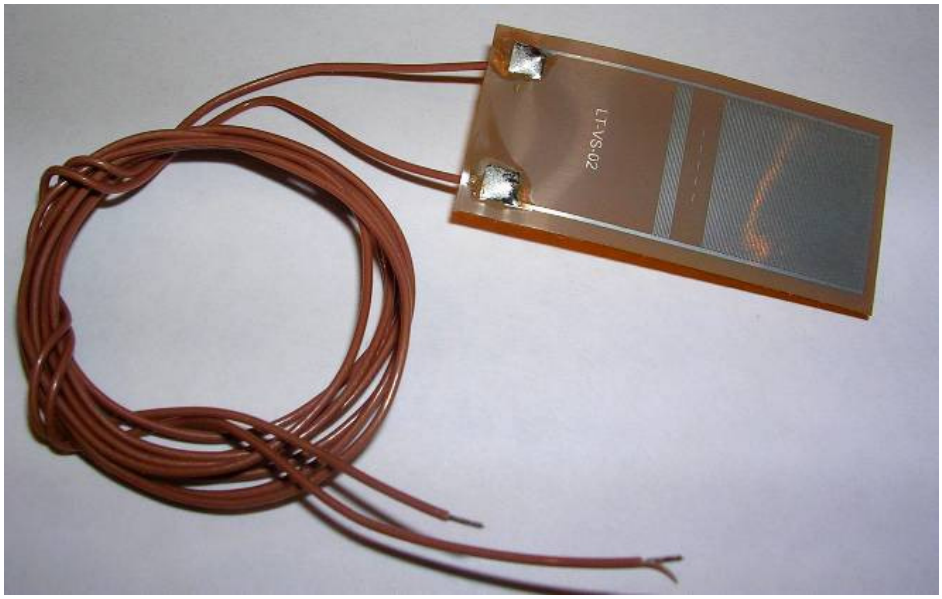

Figure 23-1
Mini-Varicon sensor

Three tests were performed under the following conditions:

Test Name	Amount Epoxy	Thermal Environment	Exotherm Peak
Cure 1	Thin Layer	Sensor on aluminum plate	28 °C
Cure 2	Medium Layer	Sensor on cardboard sheet	55 °C
Cure 3	Thick Layer	Sensor on cardboard sheet	80 °C

The Mini-Varicon sensor was trimmed to use the smaller electrode array, allowing ion viscosity measurements to remain in the optimal measurement range of the LT-451 Dielectric Cure Monitor[2] that was used for the tests.

For Cure 1 the aluminum plate acted as a heat sink, which reduced the exotherm to only 28 °C. In contrast, for Cure 2 and Cure 3 the cardboard sheet was a thermal insulator, which resulted in greater exotherms for these two tests. Thicker layers of epoxy also generated more heat and higher peak exotherms because of the greater mass of reacting material.

The LT-451 Dielectric Cure Monitor measured dielectric properties using 10 Hz, 100 Hz, 1.0 kHz and 10 kHz for 20 minutes. Later it was determined that 10 Hz was the optimum frequency because frequency independent resistivity—ion viscosity—dominated the dielectric response during the entire test. CureView[3] software acquired and stored the data, and performed post-analysis and presentation of the data.

Cure Index analysis

Cure Index analysis plots ion viscosity in relation to temperature between baselines representing 0% and 100% degrees of cure. This analysis proceeds with the following steps:

- Determine 0% Cure baseline
- Determine 100% Cure baseline
- Locate temperature – ion viscosity point between baselines
- Determine Cure Index by interpolating data location between baselines

Only two measurements of ion viscosity at different temperatures are required to define a baseline. CureView has a Cure Index parameter window for entering this information.

- To access the Cure Index parameter window, click **Edit** on the main menu bar. Then click the **Cure Index** tab in the **Data Parameters** window.

Determine 0% cure baseline

Depending on whether the MUT initially reacts slowly or quickly, determine the 0% Cure baseline with one of the following procedures.

Scenario 1—Preferred method if possible:

- Freshly mixed resin-catalyst does not cure significantly during parameter measurements at chosen temperatures
- More accurate to measure ion viscosity-temperature data on mix

1. Measure log(*IV*) for the mix of resin and catalyst at a known temperature
2. Measure log(*IV*) for the same mix at a different temperature
3. Enter the same temperature and *log*(*IV*) data for **Resin 0% Cure** and **Catalyst 0% Cure**, as shown in the example of Figure 23-2
4. Enter 50 for **Percent Resin** and 50 for **Percent Catalyst**
5. Enter 0.0 for **0% Baseline Offset**—this value may be adjusted later as necessary during Cure Index analysis

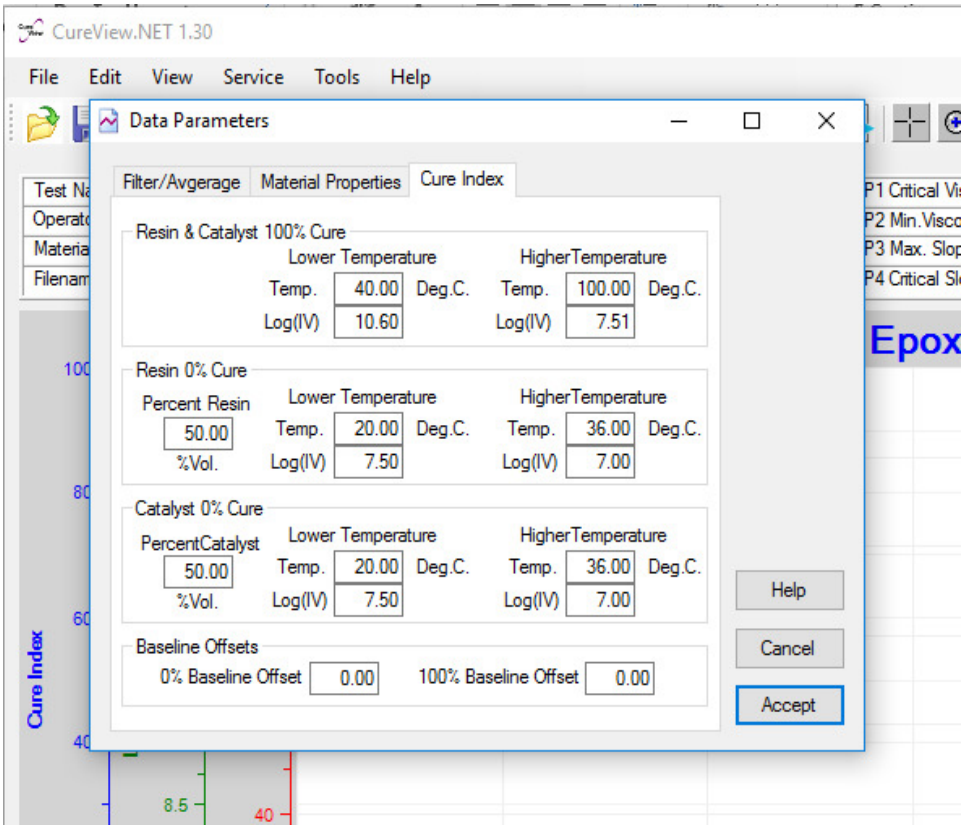

Figure 23-2
Cure Index parameter window
Example for resin-catalyst mix for 0% Cure baseline

Scenario 2—Alternative method

- Freshly mixed resin-catalyst would cure significantly during parameter measurements at chosen temperatures
- To avoid reaction, measure ion viscosity and temperature for resin and catalyst separately

1. Measure log(*IV*) for the resin at a known temperature
2. Measure log(*IV*) for the resin at a different temperature
3. Measure log(*IV*) for the catalyst at a known temperature
4. Measure log(*IV*) for the catalyst at a different temperature
5. Enter temperature-log(*IV*) data for **Resin 0% Cure** and **Catalyst 0% Cure**, as shown in the example of Figure 23-3
6. Enter **Percent Resin** and **Percent Catalyst** by volume
7. Enter 0.0 for **0% Baseline Offset**—this value may be adjusted later as necessary during Cure Index analysis

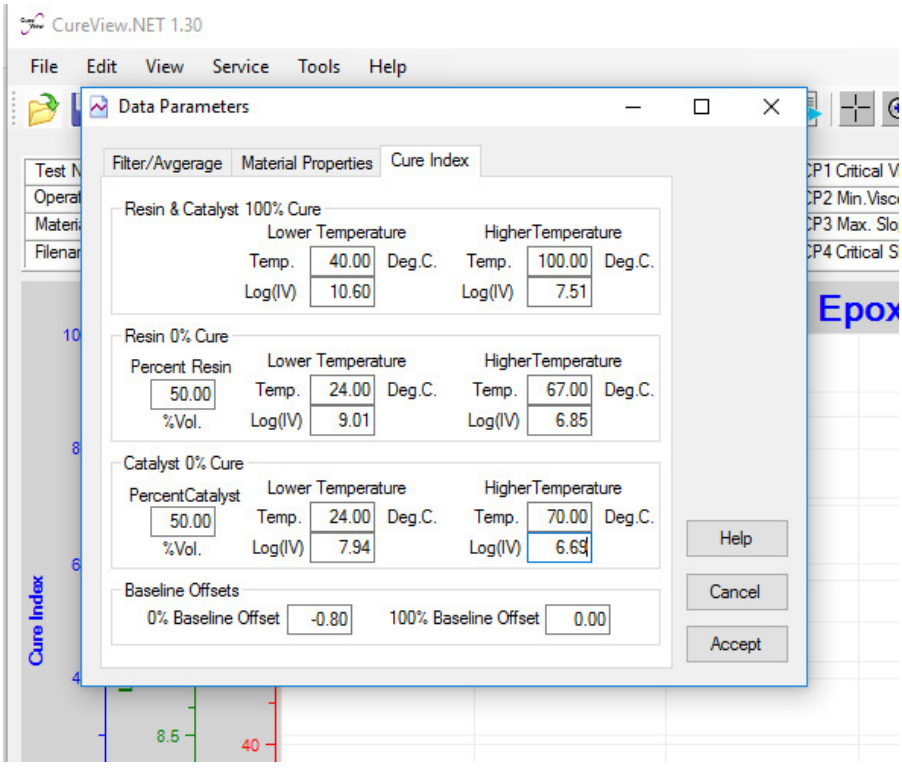

Figure 23-3
Cure Index parameter window
Example for separate resin and catalyst measurements for 0% Cure baseline

Determine 100% cure baseline

- Maximum degree of cure at a process temperature increases as temperature increases but is not necessarily 100% Cure
- Prepare the MUT by curing at elevated temperature to ensure material has reached 100% Cure

1. Measure log(*IV*) for the fully cured MUT at a known temperature
2. Measure log(*IV*) for the fully cured MUT at a different temperature
3. Enter the temperature and log(*IV*) data for **Resin & Catalyst 100% Cure**, as shown in the examples of Figure 23-2 or Figure 23-3
4. Enter 0.0 for **100% Baseline Offset**—this value may be adjusted later as necessary during Cure Index analysis

When plotted against log(*IV*) and temperature axes, the 0% Cure and 100% Cure baselines for these examples can be calculated as shown in Figure 23-4.

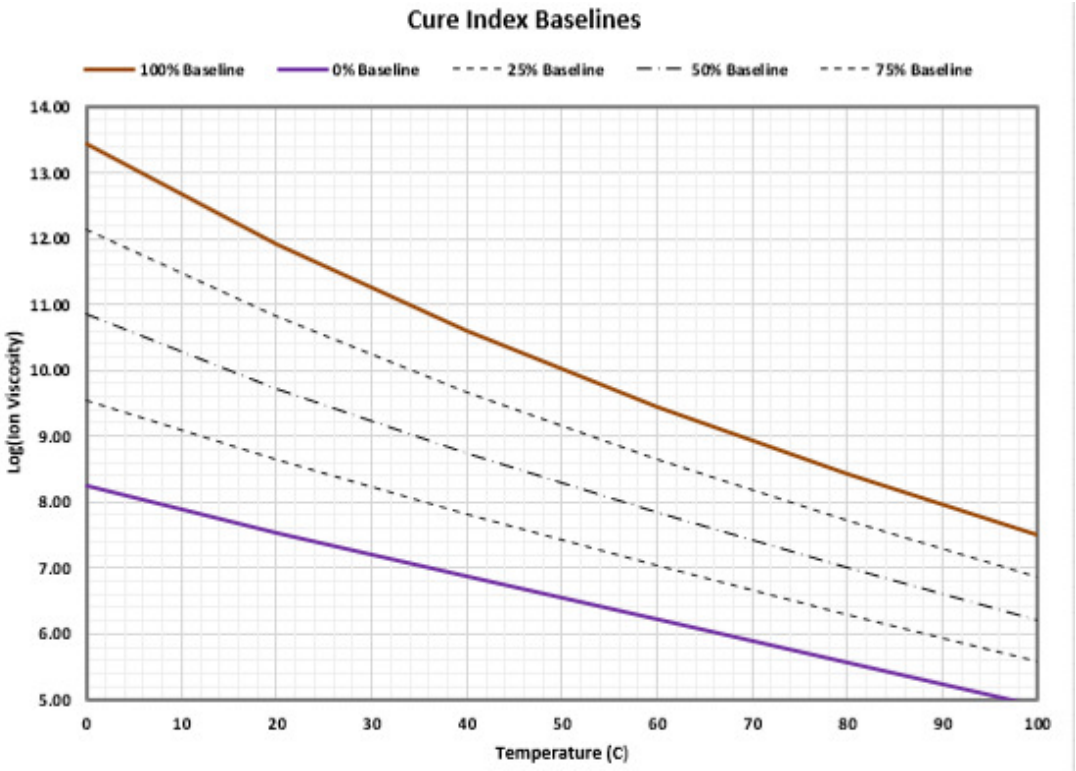

Figure 23-4
Cure Index baselines (Not displayed in CureView)

Locate temperature-ion viscosity point between baselines

Figure 23-5 shows 10 Hz ion viscosity and temperature during test *Cure 2*. The data trace the progress of a typical thermoset cure, with ion viscosity initially decreasing as temperature rises due to the exotherm. An ion viscosity minimum occurs when the viscosity increase due to accelerating cure dominates the viscosity decrease due to rising temperature.

At one point the exotherm peaks at about 55 °C then the reaction begins to slow and temperature decreases. In turn ion viscosity starts to become level, eventually flattening over time when the reaction ends.

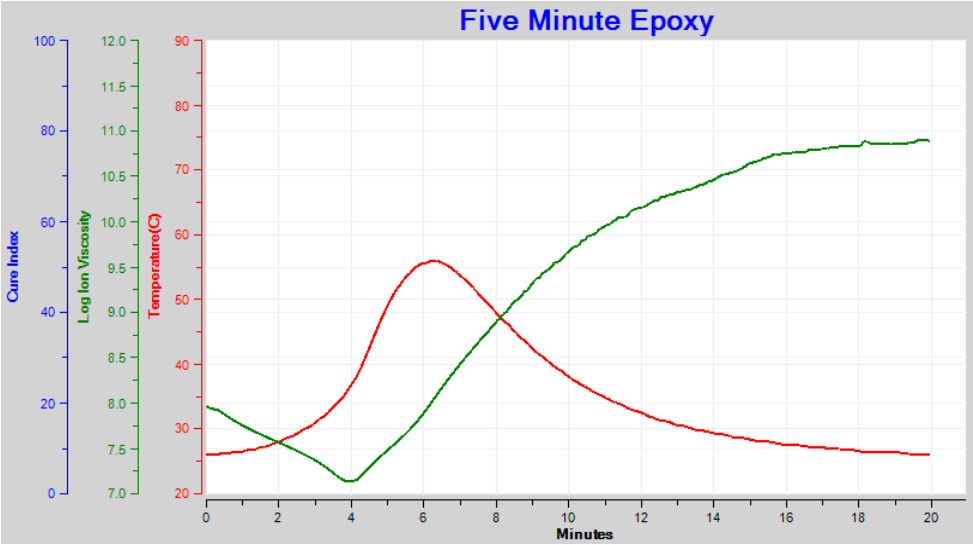

Figure 23-5
10 Hz ion viscosity and temperature for *Cure 2* of five-minute epoxy

Figure 23-6 shows data for *Cure 2* plotted between the 0% and 100% baselines.

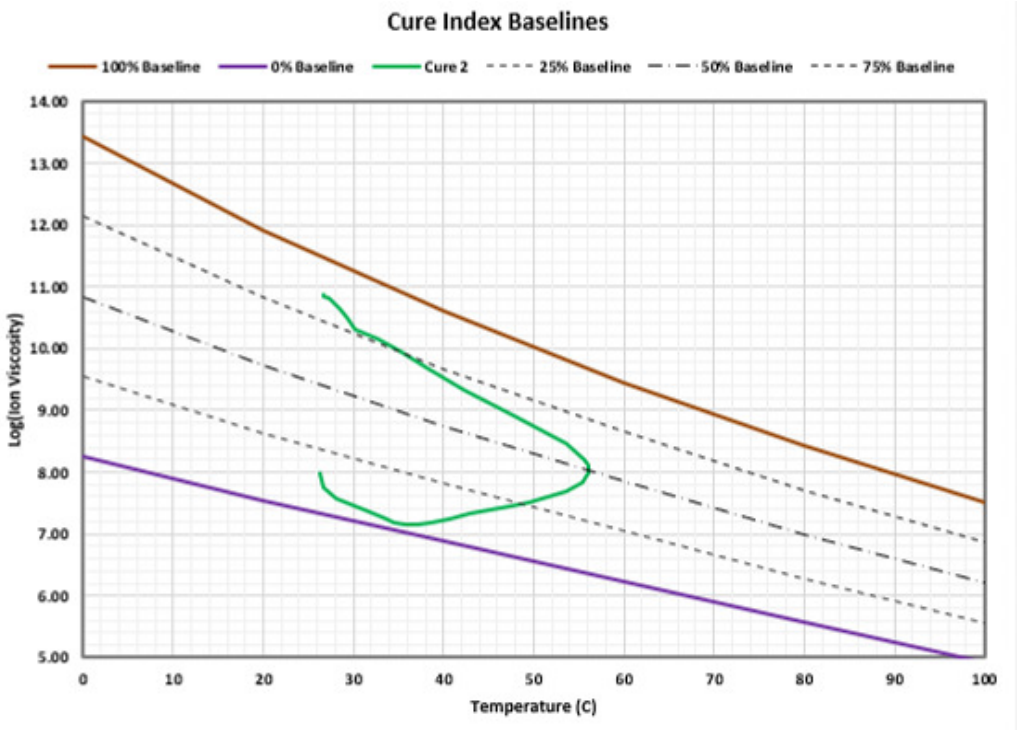

Figure 23-6
10 Hz ion viscosity and temperature for *Cure 2* plotted between baselines

Determine Cure Index by interpolating data location between baselines

For the example of *Cure 2*, interpolation of any ion viscosity-temperature point between the baselines determines Cure Index for that point. To perform Cure Index analysis on a data file, select the *Chart Configuration* icon as shown in Figure 23-7.

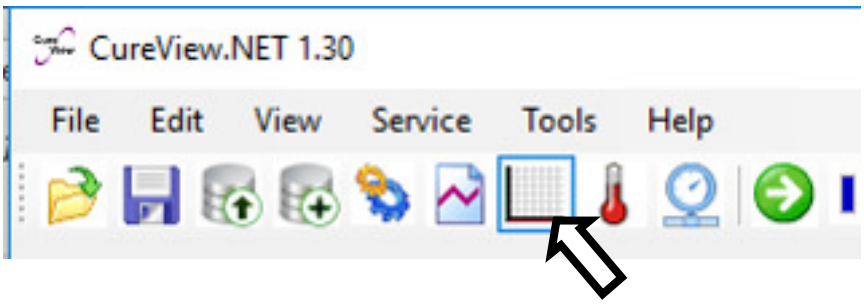

Figure 23-7
Select *Chart Configuration* icon for accessing Cure Index analysis

Then select *Cure Index* for the desired axis of the data plot as shown in Figure 23-8.

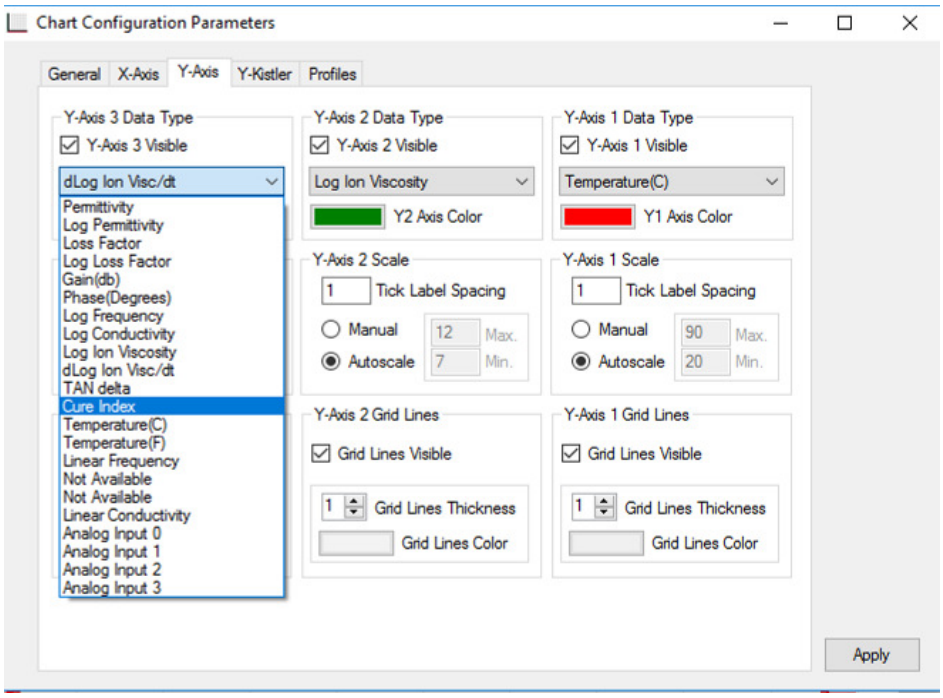

Figure 23-8
Select *Cure Index* plotting axis

After selection of the *Cure Index* axis, CureView plots Cure Index as shown in Figure 23-9.

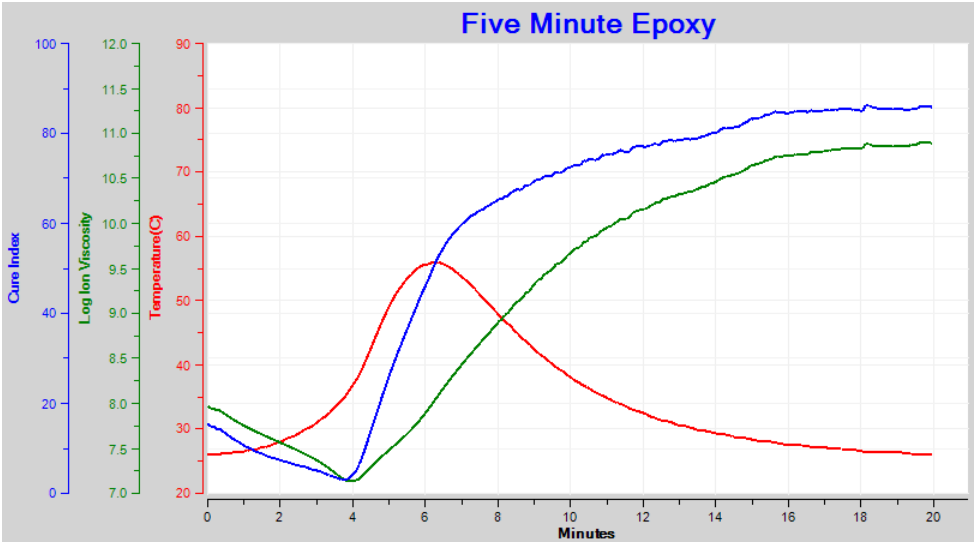

Figure 23-9
Cure Index, 10 Hz ion viscosity and temperature for *Cure 2*

Results

The term *Cure Index* was coined to distinguish it from *degree of cure*. Degree of cure has a formal definition based on the heat of reaction and is usually determined by glass transition temperatures (T_g). Cure Index is a reproducible measure of cure state that, depending on the material under test, can correlate very well with T_g. In many cases Cure Index can be a substitute for degree of cure even in the absence of glass transition temperature information.

Cure is an irreversible process, so Cure Index ideally increases continuously with time. The progress of Cure Index depends on the thermal environment but in general it takes the form shown in Figure 23-10. Curing and Cure Index are both minimal at sufficiently low temperatures. When temperature rises above a value that depends on resin chemistry, sufficient heat energy is available to drive the reaction and cure rate increases significantly.

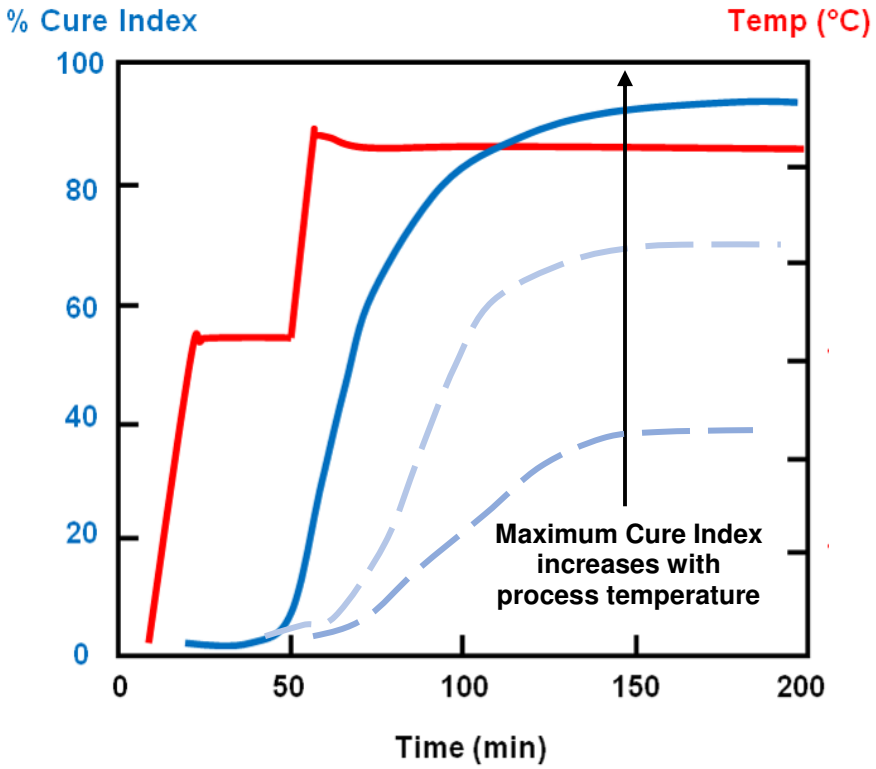

Figure 23-10
General profile of Cure Index during cure

As the reaction ends, the degree of cure and Cure Index reach a maximum value that depends on process temperature. Higher temperatures result in higher maximum degrees of cure. *Ultimate degree of cure* is the greatest amount of cure

possible for the material under test and may be defined as 100% degree of cure or 100% Cure Index.

Note that Cure Index data for *Cure 2* decreases between 0 and 4 minutes—unlike the expected continual increase. This behavior occurs because the viscous resin traps air bubbles during mixing with the catalyst. These fine air pockets refract light and turn the epoxy milky-white as shown in the photo on the bottom left of Figure 23-11. The trapped air also increases the volume of the sample. As a result, resistivity and ion viscosity increase compared to material without air.

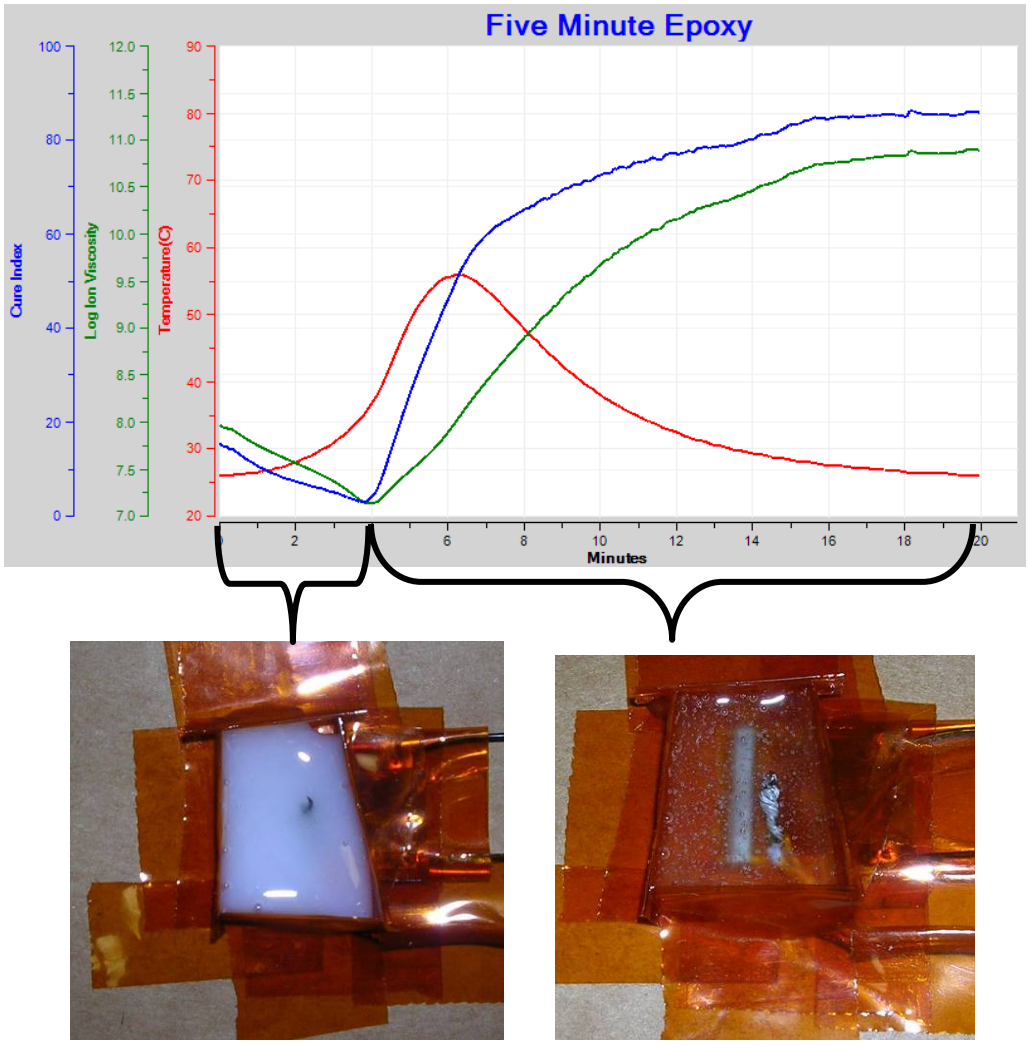

Figure 23-11
Appearance of five-minute epoxy during *Cure 2*

During early cure the epoxy gradually absorbs the air bubbles and becomes transparent, as shown in the photo on the bottom right of Figure 23-11. Volume also decreases, causing ion viscosity to decrease. At about 4 minutes the ion viscosity increase due to accelerating cure dominates the ion viscosity decrease due to air absorption, and the dielectric response shows an ion viscosity minimum.

Because volume changes during early cure, Cure Index data artificially decreases. Therefore, *for this five-minute epoxy, Cure Index information should be disregarded before the ion viscosity minimum*. After the ion viscosity minimum, Cure Index rises continuously as expected and reaches a maximum of about 87% for *Cure 2*.

Figure 23-12 shows ion viscosity and temperature data for *Cure 1*, *Cure 2* and *Cure 3*. Based on ion viscosity alone, it is not clear that *Cure 3* is significantly different from *Cure 2*, because the ion viscosity curves for both are very similar—even though their temperature profiles are very different.

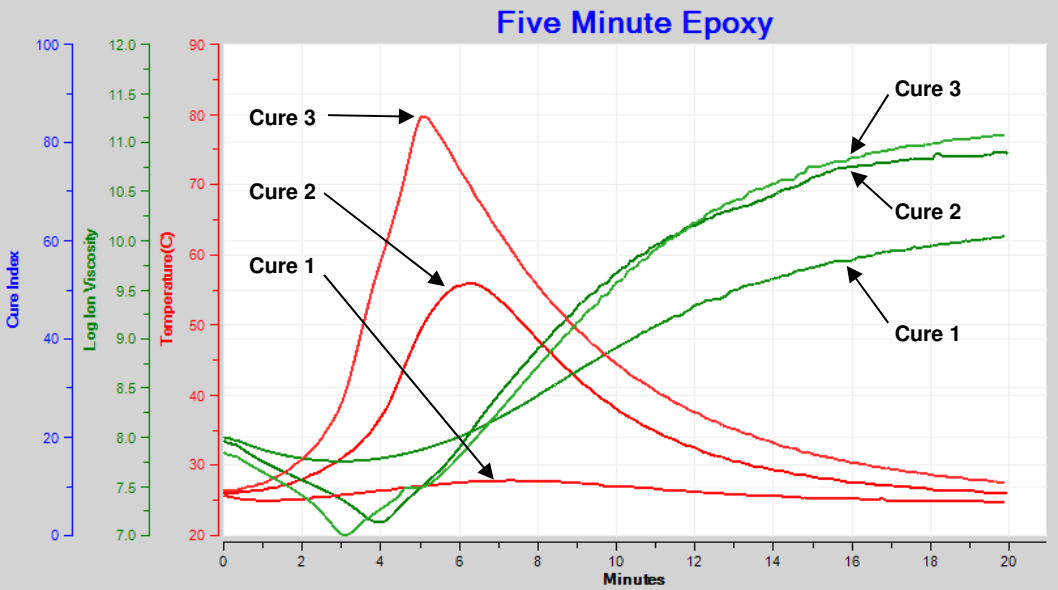

Figure 23-12
10 Hz ion viscosity and temperature for *Cure 1, Cure 2 and Cure 3*

Cures with higher exotherms should result in higher maximum degrees of cure and therefore higher maximum Cure Indexes. Figure 23-13 with the Cure Index analysis of these three tests shows this relationship is correct.

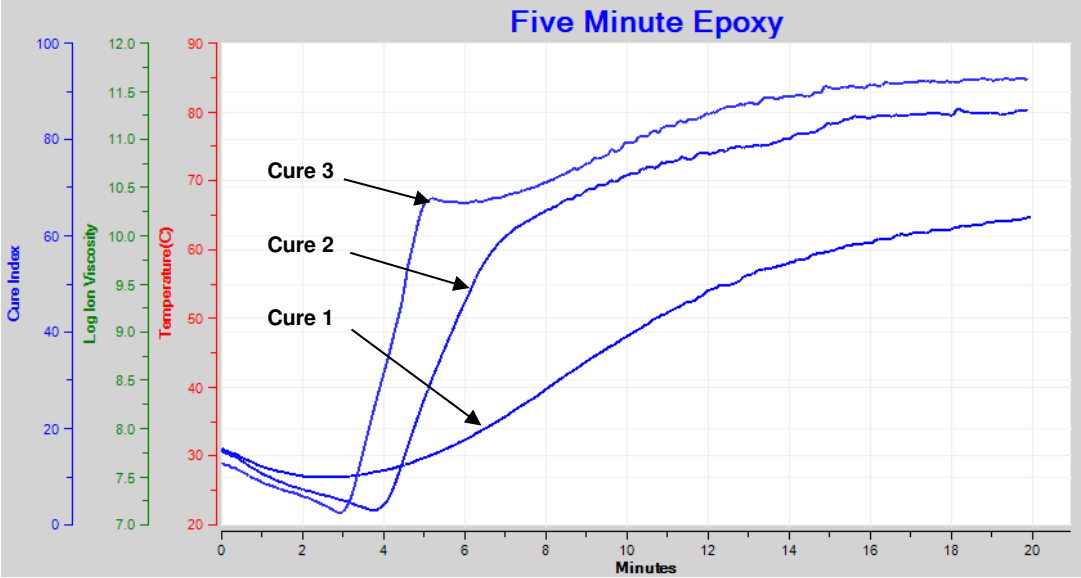

Figure 23-13
Cure Index for *Cure 1, Cure 2 and Cure 3*

Maximum Cure Index for the three tests of five-minute epoxy is shown below:

Test Name	Amount Epoxy	Thermal Environment	Exotherm Peak	Maximum Cure Index
Cure 1	Thin Layer	Sensor on aluminum plate	28 °C	64%
Cure 2	Medium Layer	Sensor on cardboard sheet	55 °C	87%
Cure 3	Thick Layer	Sensor on cardboard sheet	80 °C	92%

Ion viscosity depends on both cure state and temperature, and when used alone may provide uncertain information about degree of cure. Cure Index analysis accounts for the effect of temperature and allows greater insight into the cure state of materials under test, especially during non-isothermal conditions.

References

1. Mini-Varicon sensor, manufactured by Lambient Technologies, Cambridge, MA USA. https://lambient.com

2. LT-451 Dielectric Cure Monitor, manufactured by Lambient Technologies, Cambridge, MA USA

3. CureView software, manufactured by Lambient Technologies, Cambridge, MA USA

Chapter 24—Cure Index of Thermoplastic Polyimide

Thermoplastic polyimide

Thermoplastic polyimide (TPI) is a class of materials synthesized from a polyamic acid (PAA) solution. Polyamic acid is a linear, long chain polymer that undergoes a condensation reaction at elevated temperature to become polyimide. This process produces water as a byproduct and is called *imidization*. Typically the precursor solution is B-Staged to remove solvents and begin the reaction. Unlike thermosets, curing PAA does not crosslink. Polyimide has a much higher resistivity than PAA, however, and as a result dielectric cure monitoring can measure the conversion process.

A thermoplastic polyimide was cured in steps at higher and higher temperatures and dielectric measurements were converted to a quantity called *Cure Index*. Cure Index was then used to determine the relationship between maximum amount of cure and process temperature for TPI.

A thermoset's maximum degree of cure depends on cure temperature and is limited by the thermal energy available to drive polymerization. At higher temperatures a material cures to a greater degree than at lower temperatures. If the temperature is high enough, the thermoset can potentially reach the ultimate 100% degree of cure, which also corresponds to the highest achievable glass transition temperature (T_g) for that material.

Procedure

For this test a thin layer of PAA[1] solution was applied to a Mini-Varicon[2] dielectric sensor then heated to 150 °C to dry the solution and initiate imidization. Use of a thin coating was necessary for outgassing of evolved water.

This sample was cured isothermally until ion viscosity reached a constant value. An LT-451 Dielectric Cure Monitor[3] measured the dielectric properties of the TPI during each test.

The process was repeated for steps of 25 °C to the maximum of 300 °C. Figure 24-1 shows the resulting log(*IV*) and temperature data. Note when temperature *increases* at the step transitions, ion viscosity *decreases*. This behavior occurs because ion viscosity depends on both temperature and degree of cure. At the moment of each temperature step, cure state is essentially constant. In this case, ion viscosity changes only due to temperature, consequently decreasing as temperature increases. Then ion viscosity increases again as cure resumes and more PAA converts to polyimide.

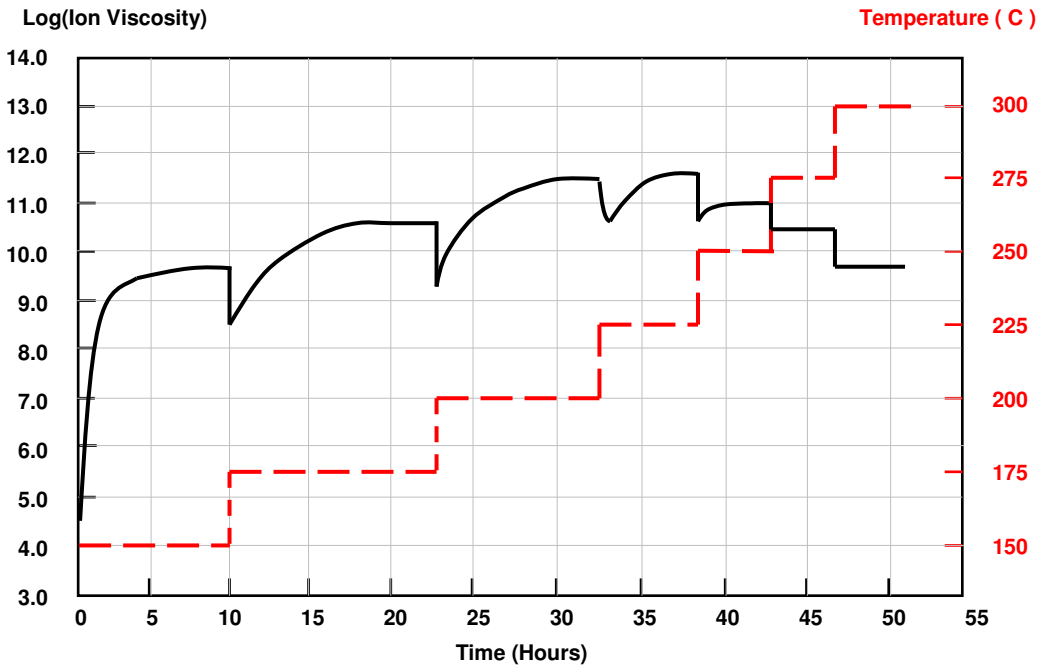

Figure 24-1
Thermoplastic polyimide cure

The use of Cure Index provides a simple way to determine how the polyimide cure advances. While Cure Index may not necessarily be proportional to degree of cure, it does yield a reproducible and consistent measure of polymerization.

Conversion of dielectric measurements to Cure Index requires baselines for the temperature dependence of ion viscosity at 0% and 100% cure. Figure 24-2 shows measurements of log(*IV*) for polymide at 0% cure when it is entirely PAA, and for polyimide cured at 300 °C, to guarantee 100% cure. Extended baselines for 0% and 100% cure were then calculated to fit the data.

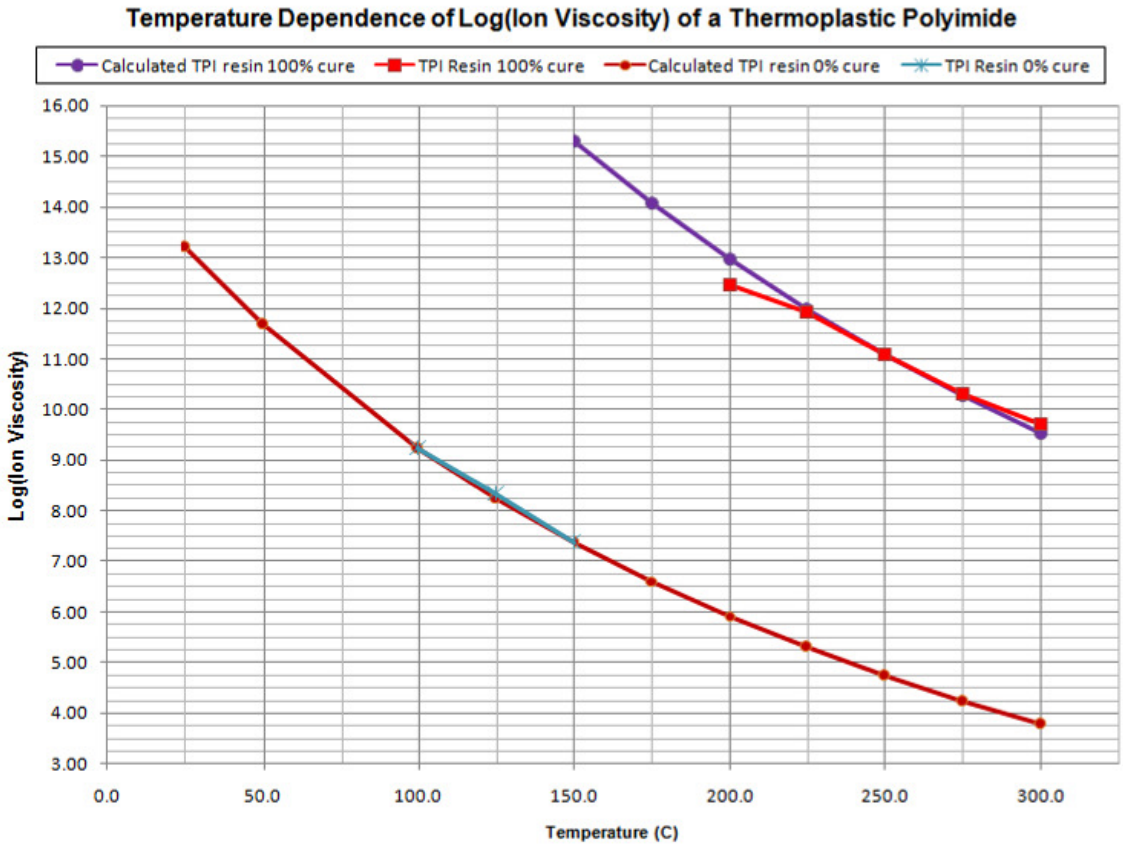

Figure 24-2
Experimental and calculated baselines for 0% and 100% TPI[1] cure

Figure 24-3 shows 0% and 100% Cure Index baselines as well as contours for 25%, 50% and 75% Cure Index, as calculated by interpolation. The end state value of log(*IV*) at each temperature step is plotted against these contours. The Cure Index for these data show that this polyimide has essentially reached 100% cure when processed at 225 °C.

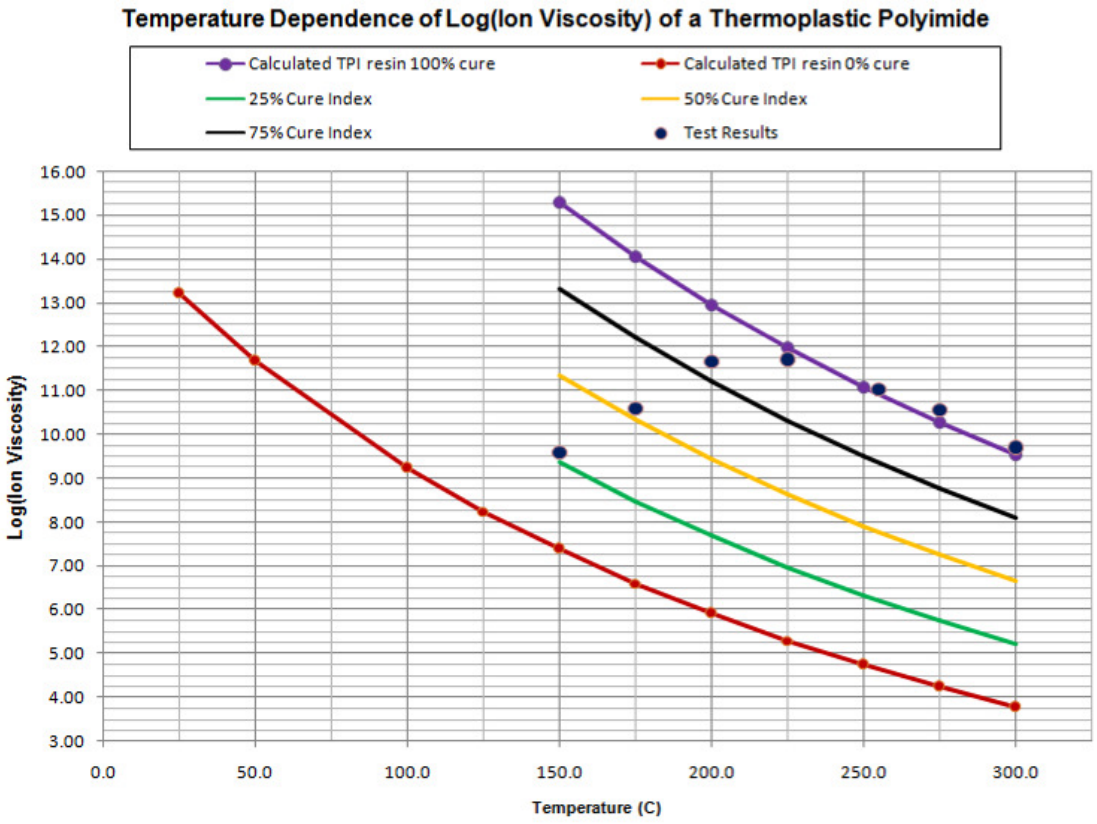

Figure 24-3
Thermoplastic polyimide[1] maximum cure state at isothermal cure temperature

Figure 24-4 shows the maximum Cure Index attainable at various process temperatures, as determined by the data of Figure 24-3. Values of Cure Index greater than 1.0 are the result of experimental error. The Cure Index data of Figure 24-4 are useful for determining optimum cure temperature for a particular application. It is not necessary to process this formulation of thermoplastic polyimide at 300 °C to achieve 100 % cure—225 °C is sufficient. Even lower process temperatures may be suitable, depending on the application.

Before relating Cure Index to degree of cure, it is important to validate this information with other analytical methods, such as differential scanning calorimetry. However, if Cure Index is proportional to degree of cure, then Cure Index also is a means of estimating the amount of cure remaining before reaching 100% cure, and therefore the amount of water remaining to be released.

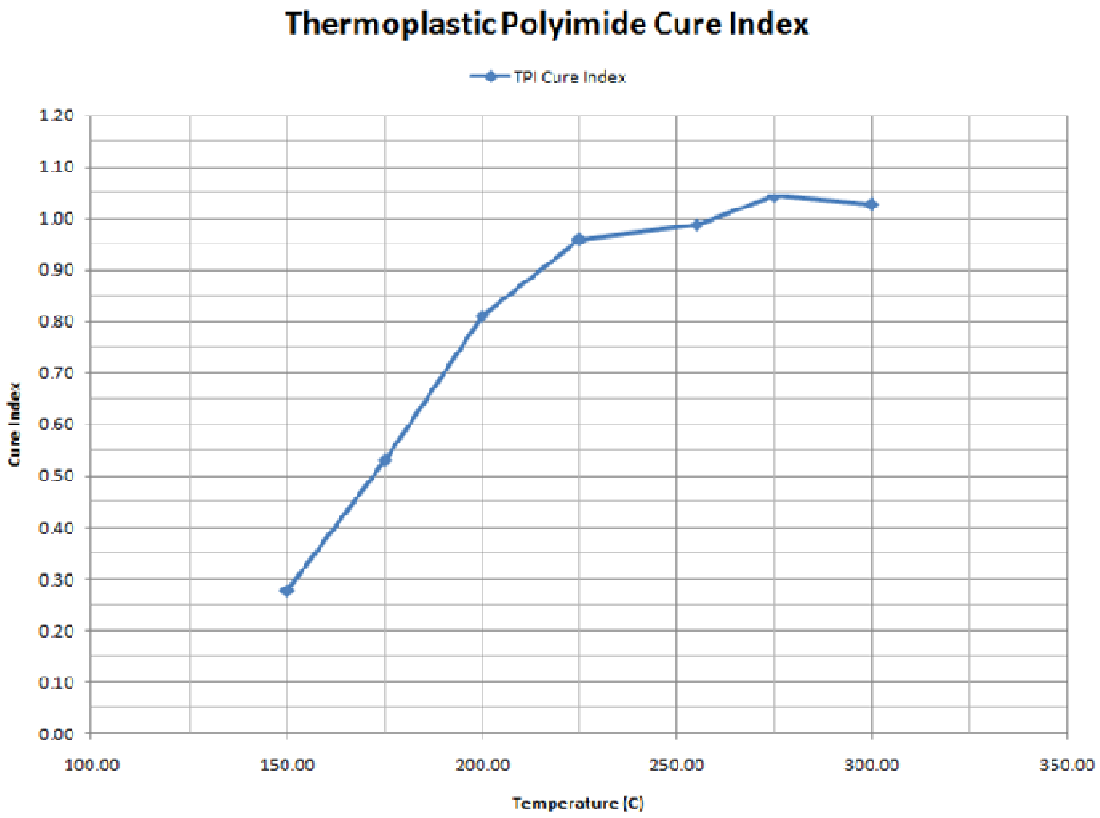

Figure 24-4
Maximum Cure Index of thermoplastic polyimide[1] vs. process temperature

References

1. Proprietary thermoplastic polyimide adhesive, derived from FM901 polyamic-acid polymer solution, provided by Fraivillig Technologies Company, Boston, MA. http://www.fraivillig.com/

2. Mini-Varicon sensor, manufactured by Lambient Technologies, Cambridge, MA USA https://lambient.com

3. LT-451 Dielectric Cure Monitor, manufactured by Lambient Technologies, Cambridge, MA USA

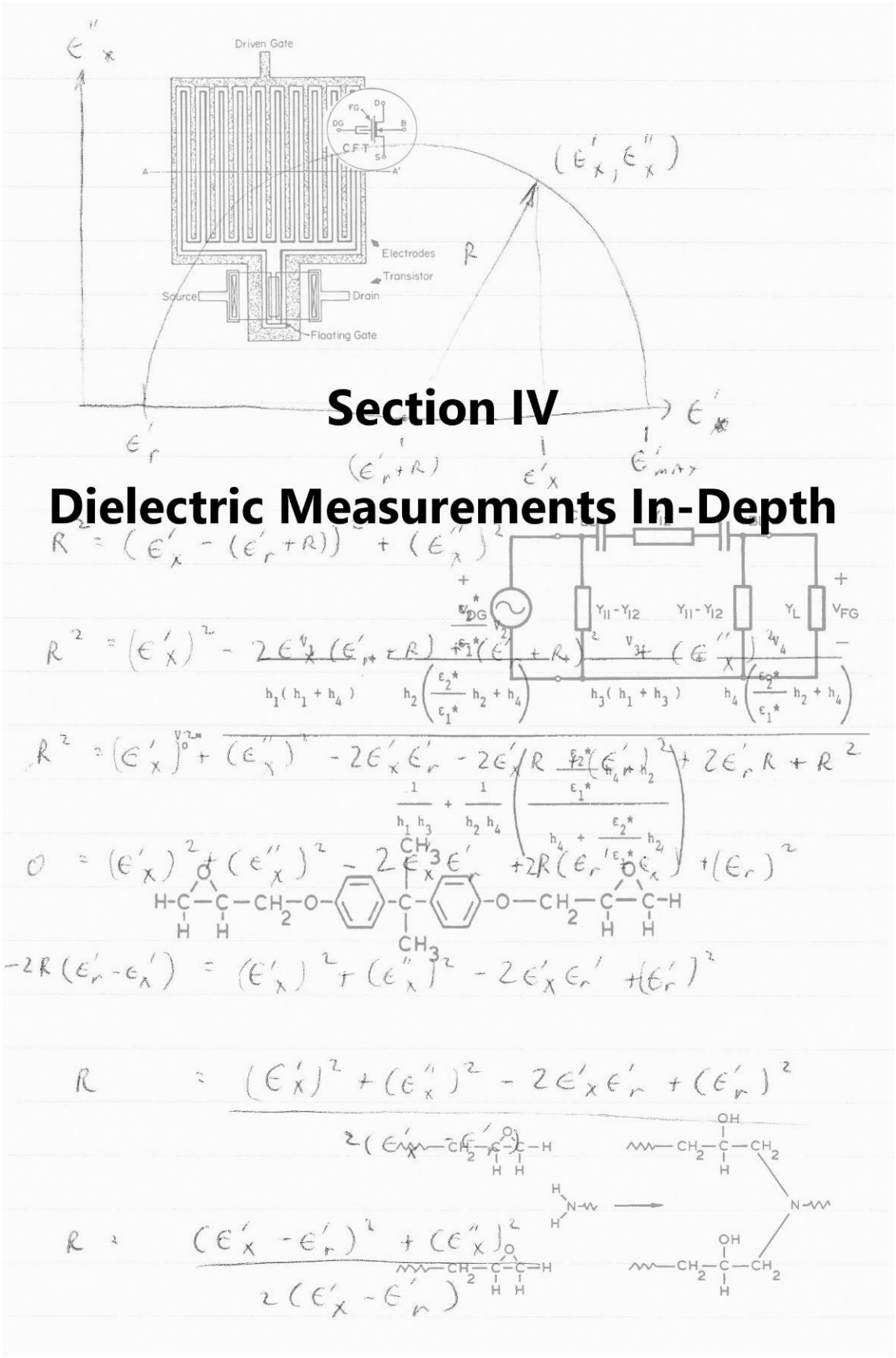
Driven Gate
Electrodes
Transistor
Source
Drain
Floating Gate
Section IV
Dielectric Measurements In-Depth

Chapter 25—Dielectric Measurement Techniques

Electrical model of sensor and thermoset

Dielectric instrumentation measures the conductance *G* (or resistance *R*) and capacitance *C* between a pair of electrodes at a given frequency. The Material Under Test (MUT) between a pair of electrodes can be modeled as a conductance in parallel with a capacitance, as shown in Figure 25-1.

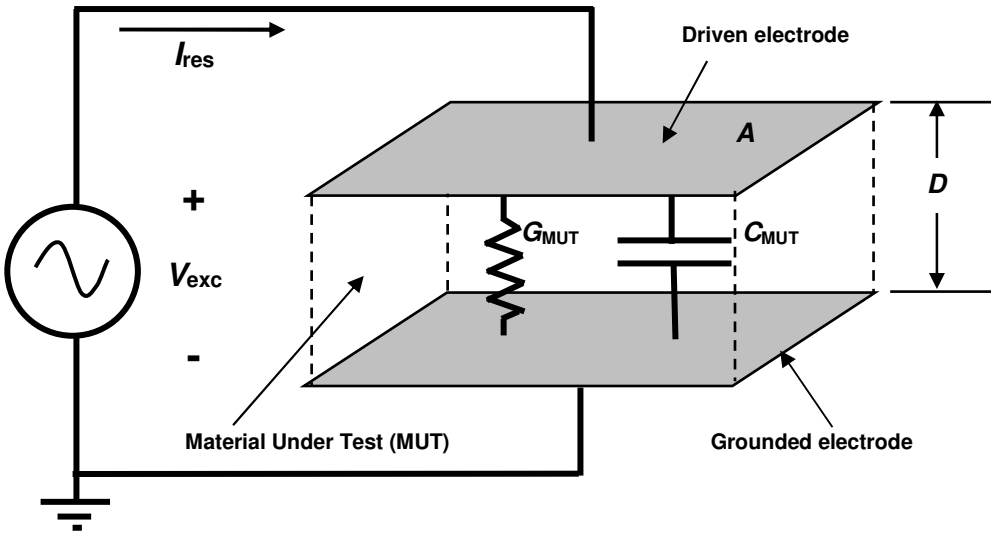

Figure 25-1
Electrical model of dielectric Material Under Test
(Grounded electrode configuration)

Grounded electrode configuration

Figure 25-1 also happens to depict a grounded electrode configuration for measuring the dielectric response. Note that one of the electrodes shares the ground of V_{exc}. An AC excitation voltage V_{exc} is applied between a pair of parallel plate electrodes, and the response current I_{res} is measured. Several methods exist for measuring current, but they all involve passing the current through a component such as a resistor, hall effect device, inductor or capacitor. The voltage induced across the component is measured and current is calculated from the component transfer function.

The amplitude of this current, and its phase shift relative to the excitation signal, are determined by the capacitive and conductive currents. The amplitude of the current and phase relationship between V_{exc} and I_{res} provide the information to calculate admittance *Y*, as shown in Figure 25-2.

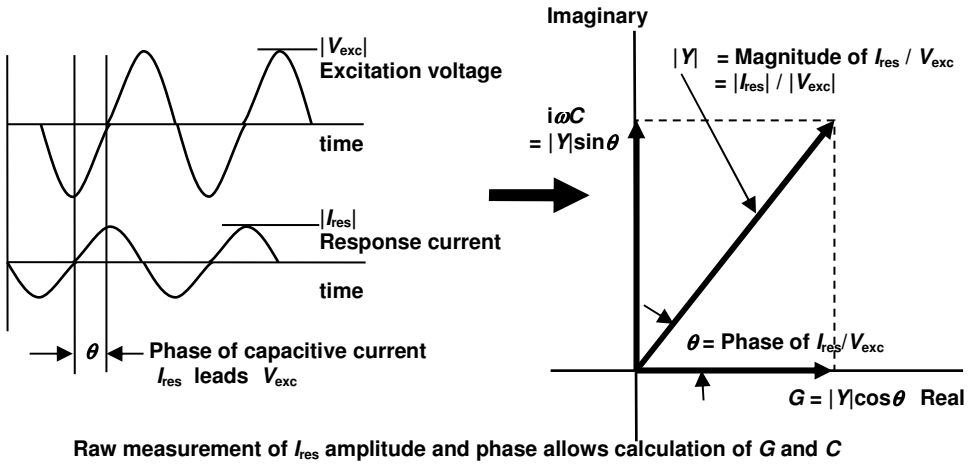

Figure 25-2
Signal relationships for grounded electrode configuration

Y, and therefore the conductance *G* and capacitance *C*, of the MUT is calculated by equation 25-1:

(eq. 25-1) $$Y_{MUT} = G_{MUT} + i\omega C_{MUT} = I_{res} / V_{exc}$$

where:

I_{res}	= AC current through MUT	(a complex number, amps)
V_{exc}	= AC voltage across MUT	(a complex number, volts)
C_{MUT}	= Capacitance of MUT	(a real number, Farads)
G_{MUT}	= Conductance of MUT	(a real number, ohms^{-1})
f	= Excitation frequency	(Hz)
ω	= 2πf	(angular frequency, radians/sec)

If the electrode *A/D* ratio is known, then the dimensionless material properties of σ / ε_o and relative permittivity ε' can be calculated from equations 25-2 and 25-3, as shown in Figure 25-3.

(eq. 25-2) $$\sigma / \varepsilon_o = G / (\varepsilon_o A/D)$$

(eq. 25-3) $$\varepsilon' = C / (\varepsilon_o A/D)$$

where:

ε_0 = 8.85 x 10^{-14} F/cm (permittivity of free space)

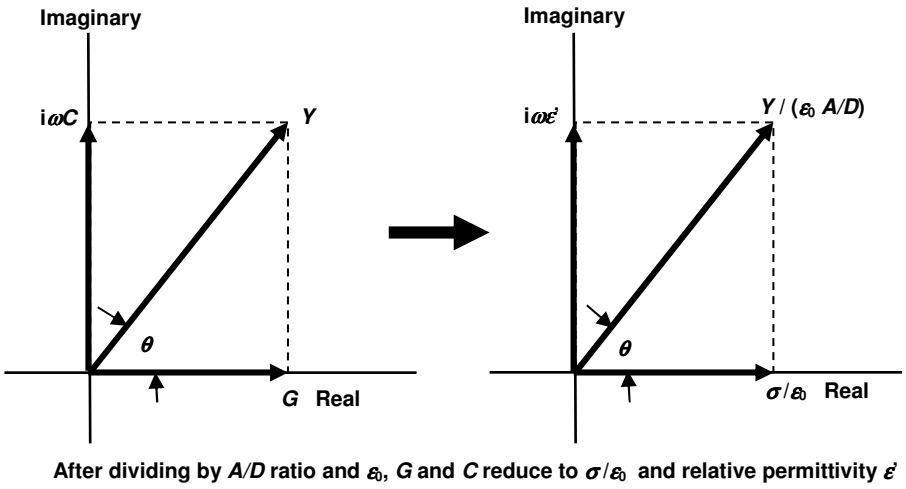

Figure 25-3
Real and imaginary components of bulk and material properties

In most implementations, the current through the MUT passes into the virtual ground of a current-to-voltage converter, as shown in Figure 25-4. An instrument can measure the voltage output, V_{out} , and current I_{res} can be calculated from the known value of R_{load}. Finally, from the amplitude of I_{res} and the phase of I_{res} relative to V_{exc}, the capacitance and conductance of the material between the electrodes can be calculated from equation 25-1.

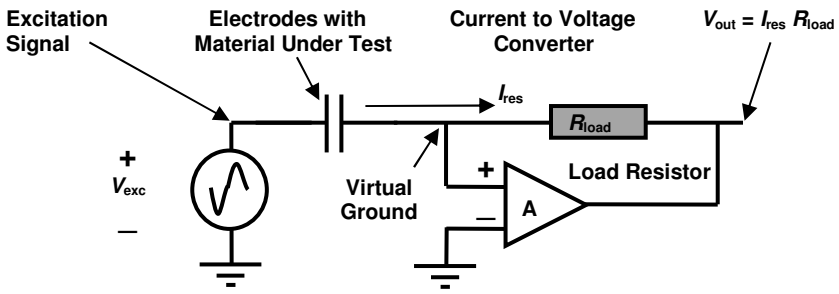

Figure 25-4
Current-to-voltage conversion of I_{res}

While simple, the circuit configuration of 25-4 has the disadvantage of low capacitive signal at low frequencies, and low conductive signal for highly insulating materials. These conditions can and do occur in thermosets at the end of cure, resulting in increased noise and reduced measurement accuracy during that period.

Kelvin (four-wire) connection

The circuit of Figure 25-4 can be modified to exclude the effect of wire resistance by using a Kelvin connection, as shown in Figure 25-5. As in Figure 25-4, a current-to-voltage converter outputs a signal for measurement of the current through the MUT. By Ohm's law, current I_{res} through wire resistances produces voltage drops that reduce the response voltage V_{res} across the electrodes.

In a Kelvin connection, a differential amplifier with high input impedence measures the voltage across these electrodes, using leads that pass no current and therefore produce no voltage drop from the wire resistance. With V_{res} and I_{res}, it is possible to calculate the capacitance and conductance of material between the electrodes using the following relationship:

(eq. 25-4) $$Y_{MUT} = G_{MUT} + i\omega C_{MUT} = I_{res} / V_{res}.$$

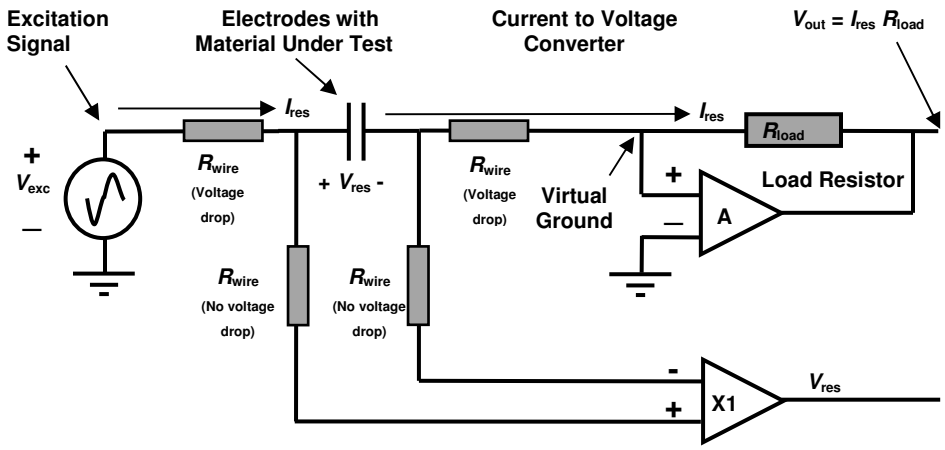

Figure 25-5
Kelvin (4-wire) connection for dielectric measurements

A Kelvin connection requires four wires and an extra amplifier, and is more complex than the configuration of Figure 25-4. It is most useful when the resistance being measured is small and comparable to the wire resistances. For example, 28 AWG wire has a resistance of 64.9 mΩ/ft (212.9 mΩ/m). A 20-foot cable has 40 feet of wire (20 feet to the electrode and 20 feet from the electrode), for a total resistance of 2.6 Ω. For a measurement error of 1%, the MUT must have a resistance of about 260 Ω across the electrodes.

For typical dielectric cure monitoring applications, the resistance of material on a sensor is on the order of 100,000 Ω or greater. Without a Kelvin connection, the error from a 20-foot cable to the sensor is 2.6 Ω / 100,000 Ω = 2.6 x 10^{-5} = 0.0026%. Thus, the extra complexity and cost of the Kelvin connection is difficult to justify for dielectric cure monitoring.

Floating electrode configuration

Dielectric measurements can also be made by driving one electrode with an AC excitation voltage without grounding the second electrode, also known as the floating electrode. This floating electrode configuration is shown in Figure 25-6. Note the load capacitor C_{load} between the floating electrode and ground.

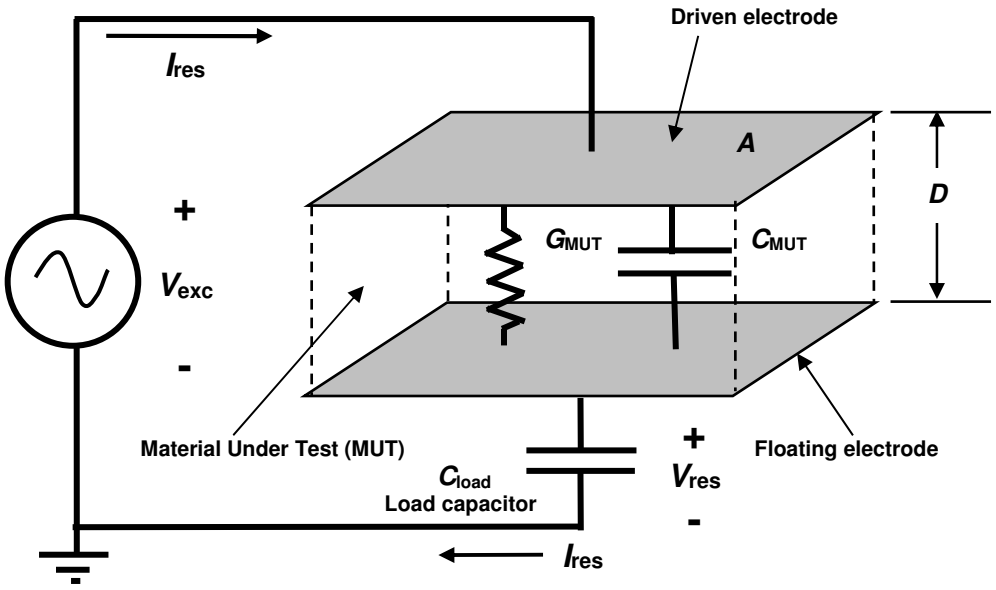

Figure 25-6
Electrical model of Material Under Test
(Floating electrode configuration)

The response voltage, V_{res}, across C_{load} depends on the load capacitance as well as the conductance and capacitance of the MUT. This load capacitance integrates current I_{res} to produce a large signal at low frequencies while also reducing noise. In effect, the current I_{res} is measured by the voltage it creates across the load capacitance, similar to the way the current-to-voltage converter of Figure 25-4 creates a voltage across a load resistance.

In practical implementations, a x1 amplifier buffers the voltage of the floating electrode, as shown in Figure 25-7. This buffer prevents cable capacitances from affecting the floating electrode and the response signal. The buffer also drives a reproduction of the response signal through cabling to the instrumentation.

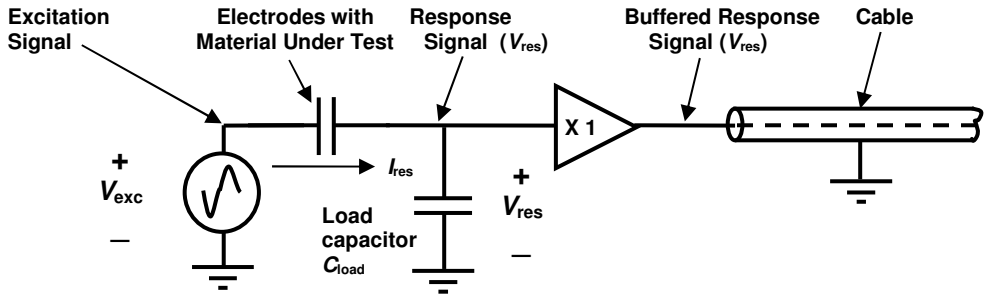

Figure 25-7
Floating electrode configuration

The output of the buffer is V_{res}, which has an amplitude that is attenuated and a phase that is shifted relative to V_{exc}. With a known load capacitance, the response amplitude and phase can be used to calculate the capacitance and conductance of the material between the electrodes. The load capacitance collects and integrates the current I_{res} through the MUT. As a result, the floating electrode configuration produces a larger signal with less noise compared to current to voltage conversion with a resistor. The advantages of the floating electrode configuration become especially apparent when making measurements in highly insulating materials at the end of cure.

Due to the added load capacitor, the equations to obtain conductance and capacitance for the floating electrode configuration are more complex than for the grounded electrode configuration. To span a wide dynamic range, the attenuation of the response signal is often expressed as "gain" on a logarithmic scale, as given by equation 25-5.

(eq. 25-5) $$Gain\ (\text{dB}) = 20 \log_{10}(|V_{res}| / |V_{exc}|)$$

The gain and phase of the response can be plotted in Gain-Phase space as shown in Figure 25-8. The use of Gain-Phase space is convenient for charting the changing response for curing thermosets, and provides insight into the state of cure.

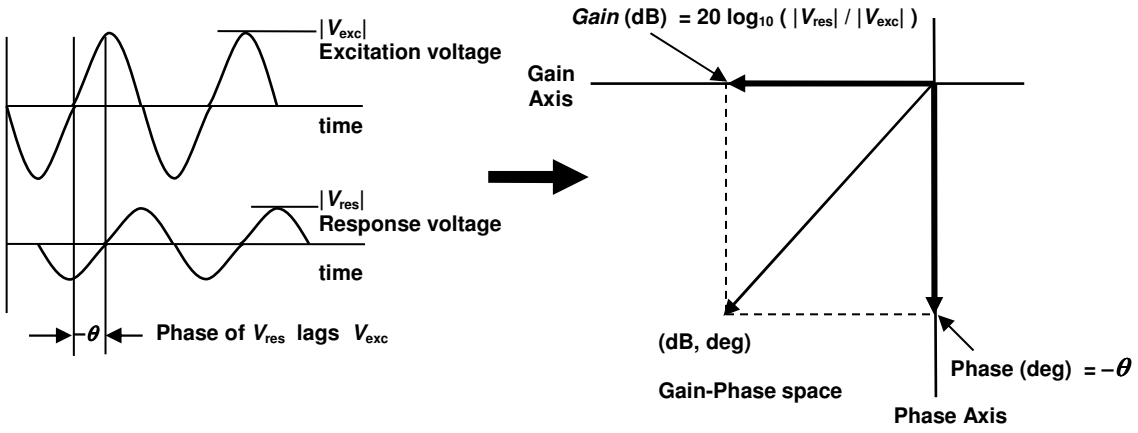

Figure 25-8
Signal relationships for floating electrode configuration

Given *gain* (dB), phase θ (deg), frequency f (Hz) and C_{load} (farad), conductance and capacitance for the floating electrode configuration can be calculated as follows:

(eq. 25-6) $$| V_{res} / V_{exc} | = 10^{(Gain/20)}$$

(eq. 25-7) $$A = \cos(-\theta) / | V_{res} / V_{exc} |$$

(eq. 25-8) $$B = \sin(-\theta) / | V_{res} / V_{exc} |$$

(eq. 25-9) $$G_{tot} = G_{MUT} = (2\pi f \ C_{load} B) / ((A - 1)^2 + B^2)$$

(eq. 25-10) $$C_{tot} = (C_{load} (A - 1)) / ((A - 1)^2 + B^2)$$

G_{tot} (G_{MUT})is the total conductance between the electrodes. C_{tot} is the total capacitance between the electrodes, including any stray, or base, capacitance contributed by various sources. *Note that this base capacitance must be subtracted from C_{tot} before further calculation to obtain conductivity and permittivity.*

Subtraction and non-subtraction mode interfaces

Figure 25-9 shows a dielectric sensor in the floating electrode configuration. When the response voltage V_{res} is directly buffered by a x1 amplifier, the interface operates in *non-subtraction* mode. In this arrangement, load capacitance C_{load} is grounded and any cable capacitance on the response signal is in parallel with C_{load}. If the load capacitance is very large compared to sensor capacitance C_{MUT}, then cable capacitance has relatively little effect on the response signal.

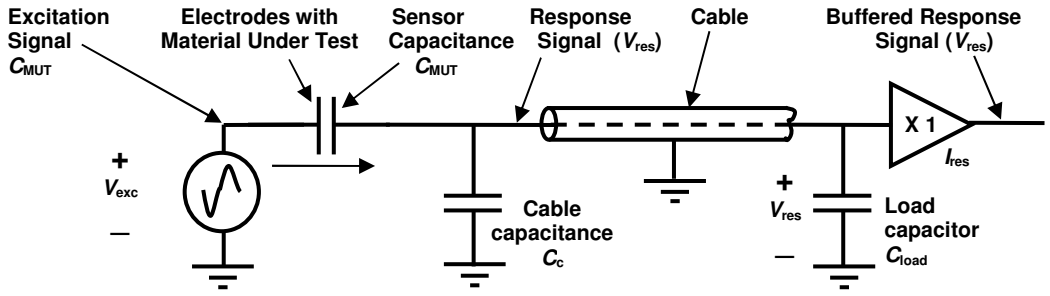

Figure 25-9
Non-subtraction mode interface

From basic circuit theory, the response with only capacitances is:

(eq. 25-11) $$V_{res} / V_{exc} = C_{MUT} / (C_{load} + C_{MUT} + C_c)$$

For example, if C_{load} is 2000 pF and C_{MUT} is 20 pF, for various cable capacitances the response for the interface of Figure 25-9 is shown in Table 25-1.

Table 25-1
Response of Non-subtraction Mode Interface

C_{load} (pF)	C_{MUT} (pF)	C_c (pF)	V_{res} / V_{exc}	Gain (dB)	V_{res} / V_{exc} / V_{res} / V_{exc} for C_c = 0 pF
2000	20	0	0.0099	–40.09	1.00
2000	20	20	0.0098	–40.17	0.99
2000	20	40	0.0097	–40.26	0.98
2000	20	60	0.0096	–40.34	0.97
2000	20	100	0.0094	–40.51	0.95

Even for relatively large cable capacitances, the effect on the response is small.

In contrast, Figure 25-10 shows a dielectric sensor interface operating in *subtraction mode*. Here the sensor capacitance C_{MUT}, not the load capacitance, is grounded. A differential amplifier subtracts the sensor signal from the excitation signal, resulting in a response that ideally is the same as for non-subtraction mode.

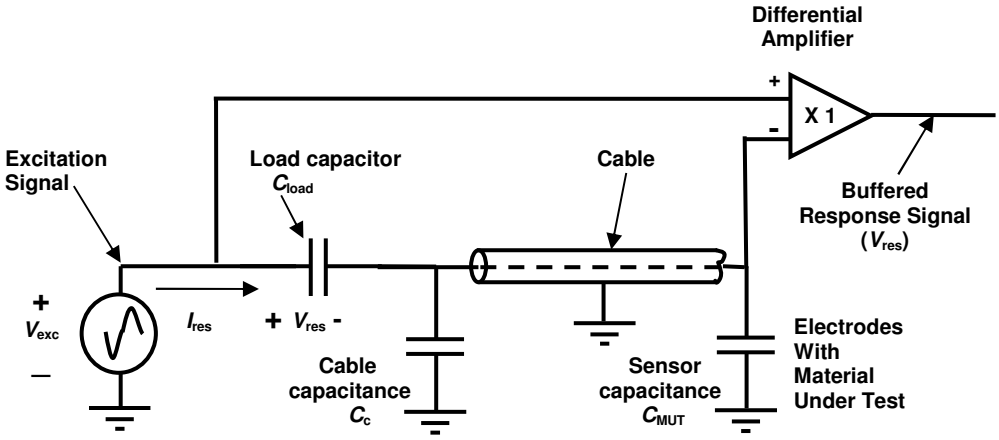

Figure 25-10
"Subtraction" mode interface

Both subtraction mode and non-subtraction mode circuits use equations 25-5 through 25-10 to convert the response signal to conductance and capacitance. Subtraction mode has the advantage of allowing a dielectric sensor to operate with a single electrode, such as the sensor of Figure 25-11.

Figure 25-11
Dielectric sensor with single electrode

A sensor with one electrode uses a nearby grounded surface as an effective second electrode. This surface may be a mold or the platen of a press, either surrounding the sensor or the opposite it as shown in Figure 25-12. Thus a single electrode sensor may be smaller than one that requires two electrodes.

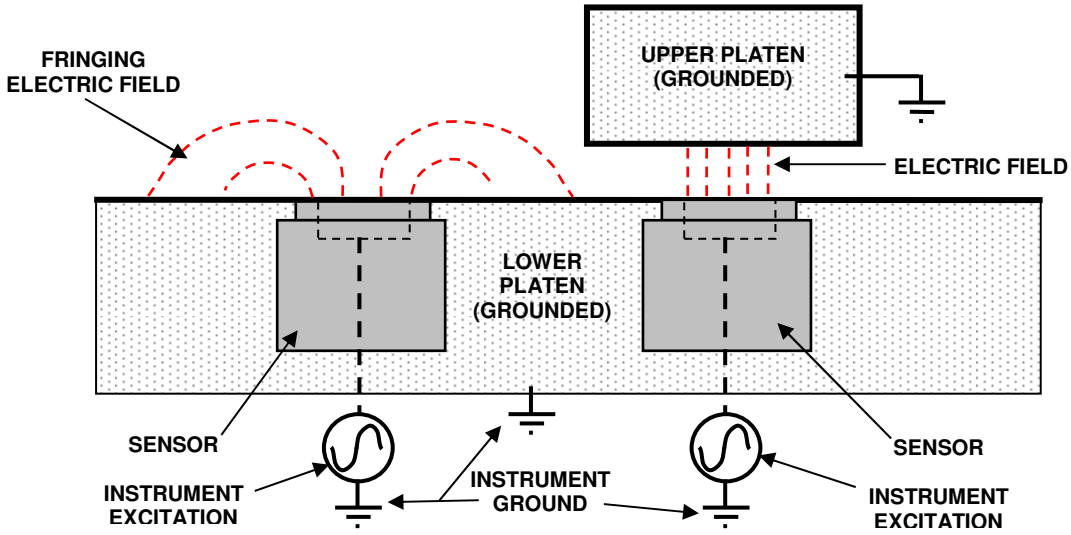

Figure 25-12
Single electrode sensor using nearby grounded surface as second electrode

Non-subtraction mode requires a sensor with two electrodes, while a subtraction mode interface may use sensors with either one or two electrodes. A subtraction mode interface, however, is more influenced by cable capacitance than a non-subtraction mode interface. As apparent in Figure 25-10, for a subtraction mode interface the cable capacitance is in parallel with the sensor capacitance.

From circuit theory, the response with capacitances only is:

(eq. 25-12) $$V_{RES} / V_{EXC} = (C_{MUT} + C_C) / (C_{LOAD} + C_{MUT} + C_C)$$

Again, for example, if C_{load} is 2000 pF and C_{MUT} is 20 pF, for various cable capacitances the response for the interface of Figure 25-10 is shown in Table 25-2.

Table 25-2
Response of Subtraction Mode Interface

C_{load} (pF)	C_{MUT} (pF)	C_c (pF)	V_{res} / V_{exc}	Gain (dB)	V_{res} / V_{exc} / V_{res} / V_{exc} for C_c = 0 pF
2000	20	0	0.0099	–40.09	1.00
2000	20	20	0.0196	–34.15	1.98
2000	20	40	0.0291	–30.71	2.94
2000	20	60	0.0385	–28.30	3.89
2000	20	100	0.0566	–24.94	5.72

Even for relatively small cable capacitances, the influence on the response is large. The effect of cable capacitance may be subtracted from the response, but uncertainty in the value of cable capacitance will correspondingly affect the accuracy of sensor capacitance measurements.

In subtraction mode, conductance measurement is not affected by cable capacitance. For dielectric cure monitoring, when conductance is the property of interest, subtraction mode offers flexibility in the choice of sensors. For measurements when capacitance is also important, then non-subtraction mode should be used.

DC measurements

Instruments for measuring only the conductance of the material under test have the advantage of simplicity compared to those measuring both conductance and capacitance. These conductance measurement instruments (essentially highly sensitive ohmmeters) use a DC voltage source to drive current through the MUT between the sensor electrodes. This current typically passes into the virtual ground of a current-to-voltage converter, as shown in Figure 25-13. A data acquisition system can measure the DC voltage output, V_{out} , and DC current I_{res} can be calculated from the known value of R_{load}. From the value of I_{res}, the frequency independent (DC) conductance of the material between the electrodes can be calculated from Ohm's law.

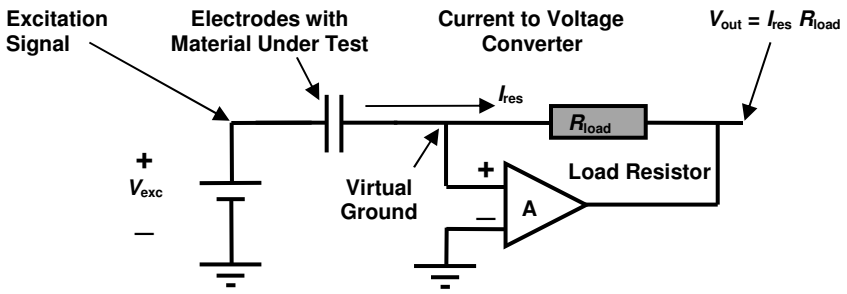

Figure 25-13
DC measurement of dielectric properties (conductance only)

The simplicity of the circuit of 25-13, however, comes at the expense of flexibility and possibly accuracy. DC methods can only measure the DC conductance; measurement of capacitance requires an AC excitation. DC measurements may be confounded by offset voltage drifts, thermal drifts and leakage currents in the interface electronics, which cannot be distinguished from the true DC signal.

Finally, DC measurements are not possible with release layers, which are very thin insulating sheets sometimes used to prevent material from adhering to a mold or platen. Release layers block DC current and therefore prevent measurements of DC conductance.

Digital sampled data system

Some dielectric measurement instruments use sampled data acquisition, as shown in the block diagram of Figure 25-14. A sampled data acquisition system analyzes the sensor response using digital signal processing (DSP), which can extract information from a very noisy signal. This ability results in more accurate, precise and repeatable data than from an instrument using analog computation, but with greater complexity and cost.

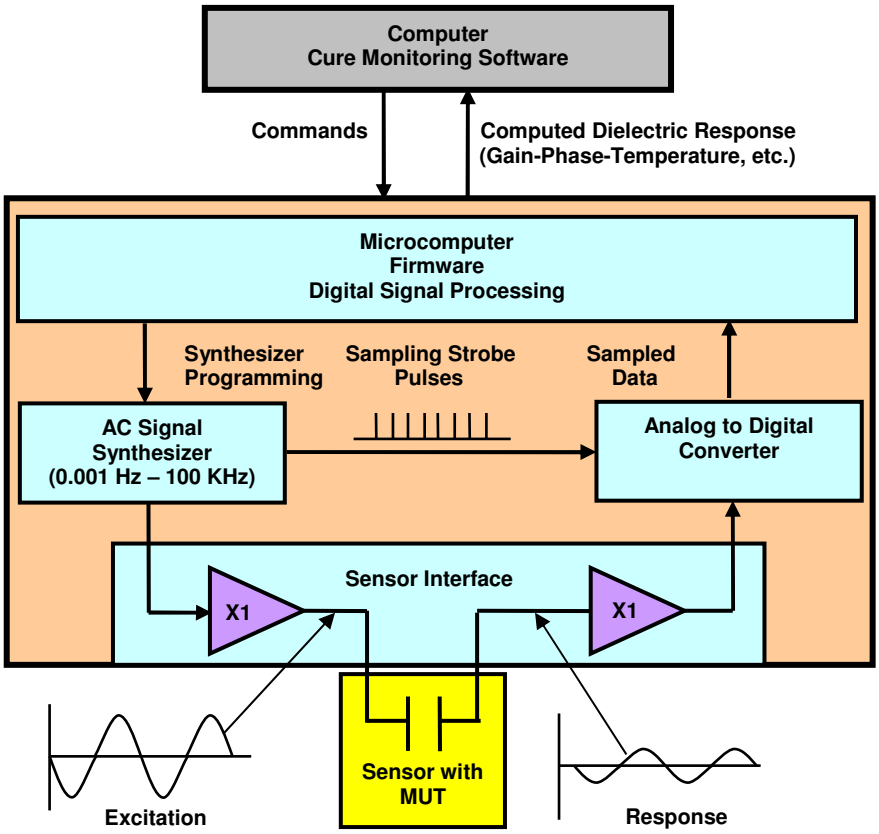

Figure 25-14
Block diagram of a sampled data acquisition system

Analog computation system

Analog measurement techniques are less expensive and much faster, but more noise sensitive and less accurate, than digital sampled data systems. However, analog instruments can perform well in applications where rapid data acquisition is a desired tradeoff for accuracy and precision. The block diagram of Figure 25-15 shows how an instrument can use analog computation to measure dielectric properties.

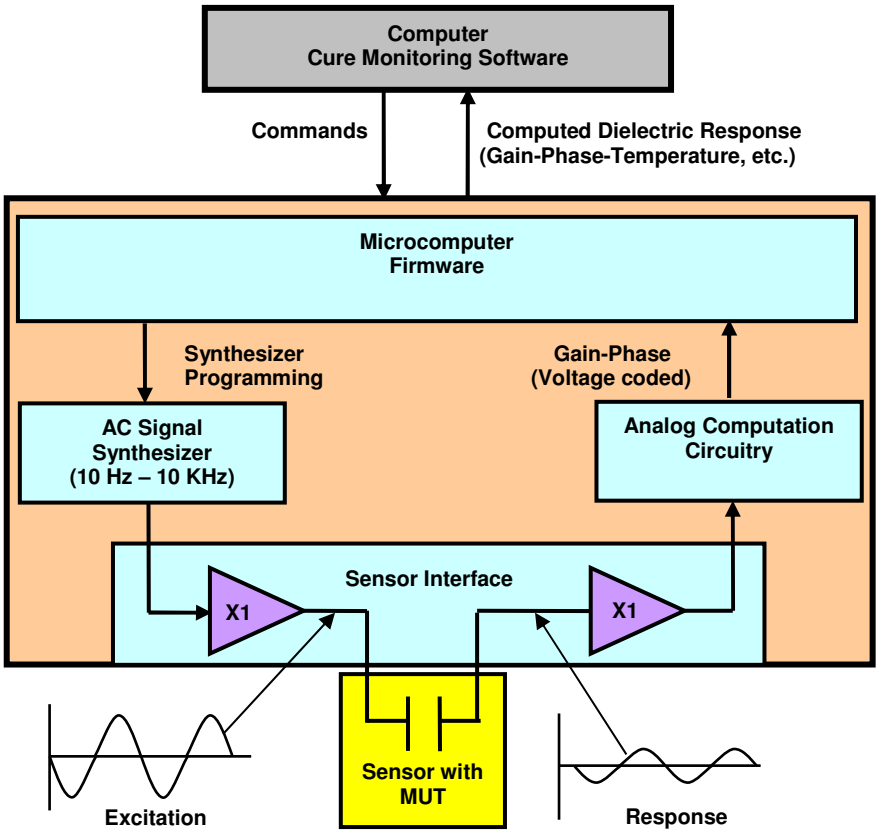

Figure 25-15
Block diagram of analog computation system

Chapter 26—Dielectric Measurements in Batch Reactors

The batch reaction process

The monitoring of dielectric properties is useful for controlling polymerization in a batch reactor. Previous work has shown that DEA could observe the free-radical polymerization of methyl methacrylate,[1] where the change of log(*ion viscosity*) correlated with fractional monomer conversion and physical viscosity.

Dielectric cure monitoring has the advantage of real time, in-process measurement of polymerization, unlike standard laboratory gravimetric methods, which must be performed off-line.

Resins processed in batch reactors typically start with a high concentration of monomers, as shown in Figure 26-1. At this stage mobile ions can move very easily through the material, resulting in very low ion viscosities (low resistivities).

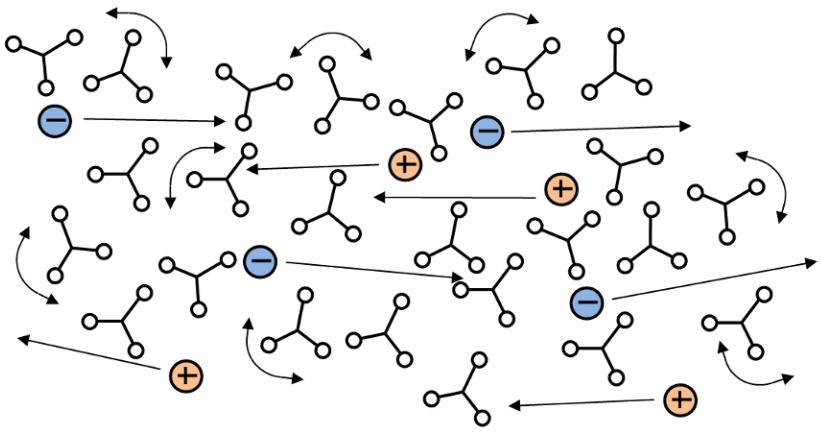

Figure 26-1
Unreacted monomers

When heated, these monomers react and bond to form polymer chains, represented in Figure 26-2. During this period the number of molecules decreases while their molecular weight increases. Mechanical viscosity also increases, as does resistance to the flow of mobile ions in an electric field. Dielectric cure monitoring measures this electrical resistance and is unique in enabling direct observation of material state in the reaction vessel.

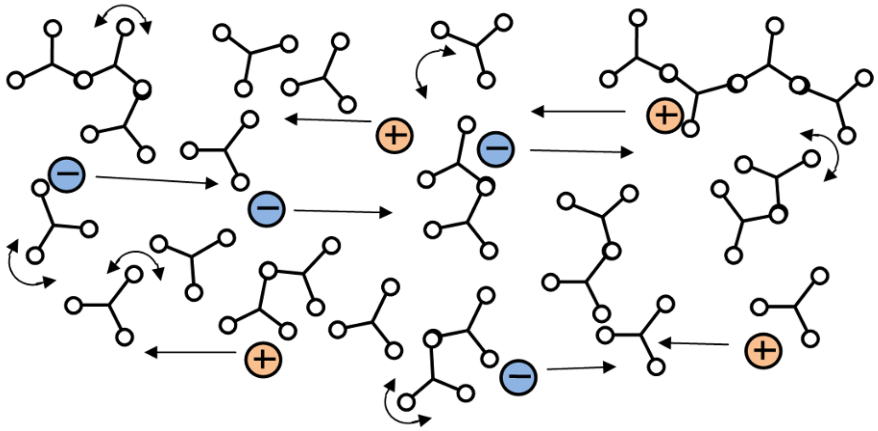

Figure 26-2
Early stage polymerization

As more and more monomers are polymerized, log(*ion viscosity*) increases in a fashion similar to the plot of Figure 26-3. *Note that only the change in log(ion viscosity) correlates with fractional monomer conversion*—the actual relationship and scaling factors must always be determined experimentally.

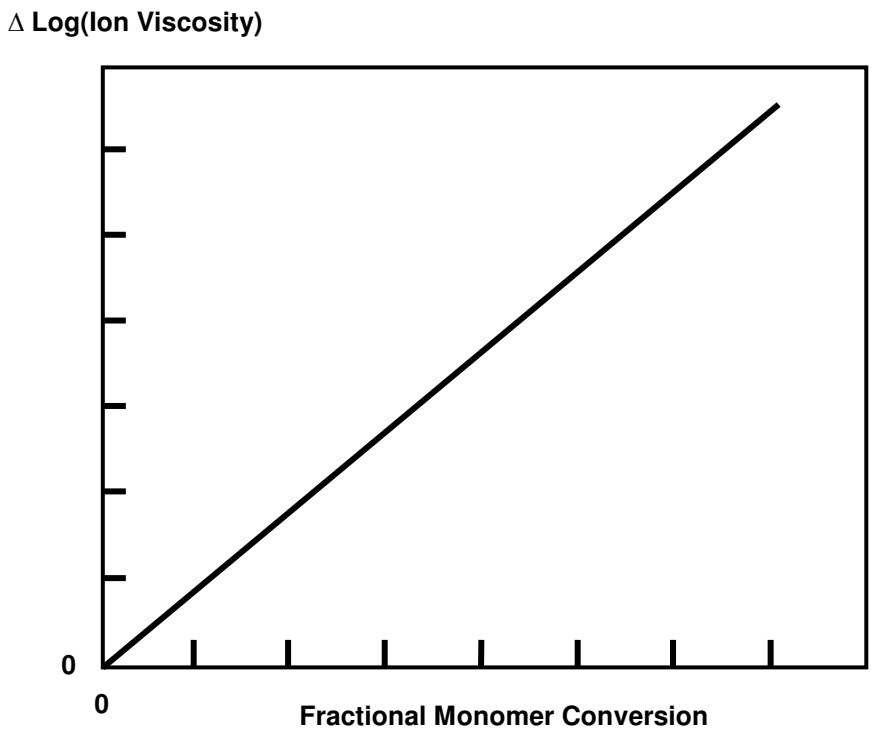

Figure 26-3
Change in log(*IV*) vs. Fractional Monomer Conversion

The value of log(*ion viscosity*) depends on the level of ions and impurities, and may not be the same from batch to batch. As a result, log(Ion Viscosity) alone is not a reliable measure of resin polymerization—only the *change* is useful.

Standard instrument configuration

A computer with data acquisition software connects to a dielectric cure monitor through an RS-232 or USB serial port. The instrument connects to a dielectric sensor and a thermocouple, which are immersed in the batch reactor. This standard configuration is shown in Figure 26-4.

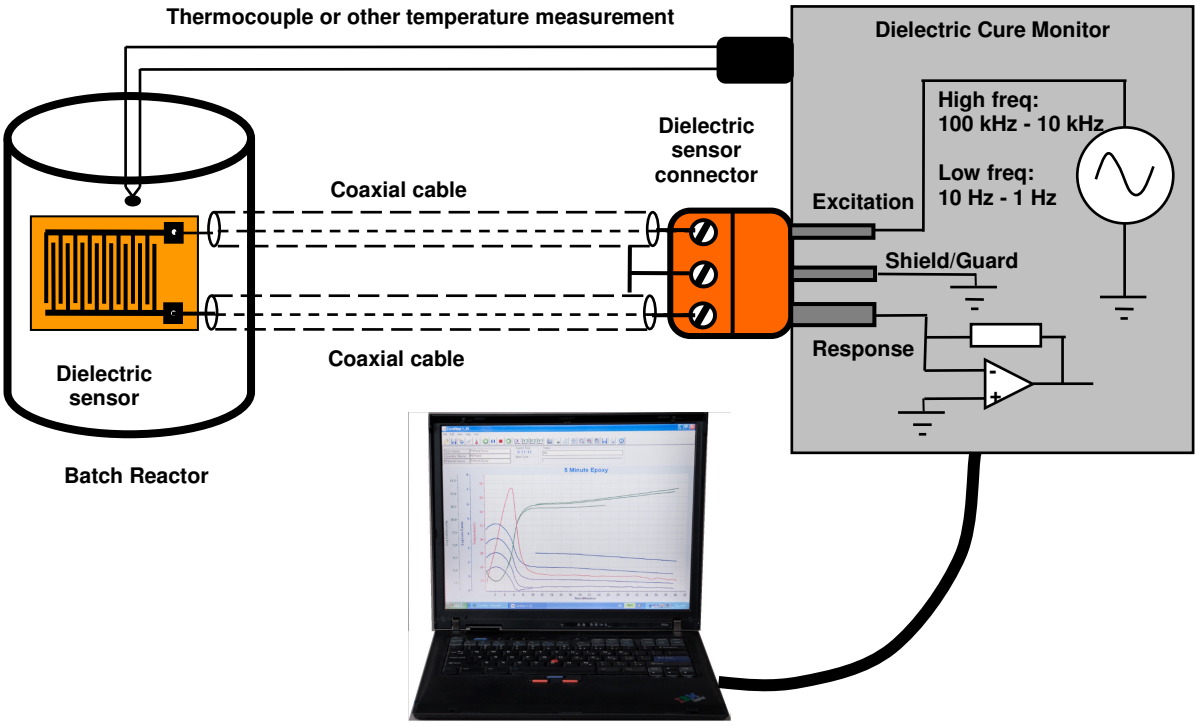

Figure 26-4
Dielectric cure monitoring system for a batch reactor

A dielectric sensor usually consists of a pair of interdigitated electrodes on a polyimide or ceramic substrate. A thermocouple measures the process temperature, which is important because dielectric properties vary with both the material's degree of conversion *and* temperature.

Simplified sensor for batch reactors

In many cases the resin in a batch reactor has low ion viscosity during the entire process. Consequently, it is often not necessary to use a sensor with interdigitated electrodes. Because the electrodes occupy a large area and are close together, this type of sensor is very sensitive.

Thermosets at the end of cure have very high ion viscosities, so studying materials at this stage requires a sensor with correspondingly high sensitivity. However, when ion viscosity is low, the large signal from interdigitated electrodes can exceed the range of the dielectric cure monitor, resulting in bad measurements.

For batch reactors it may be better to use a simple electrode design with an output level more suitable to the instrument. Figure 26-5 shows how a pair of wires with exposed ends becomes a low sensitivity dielectric sensor.

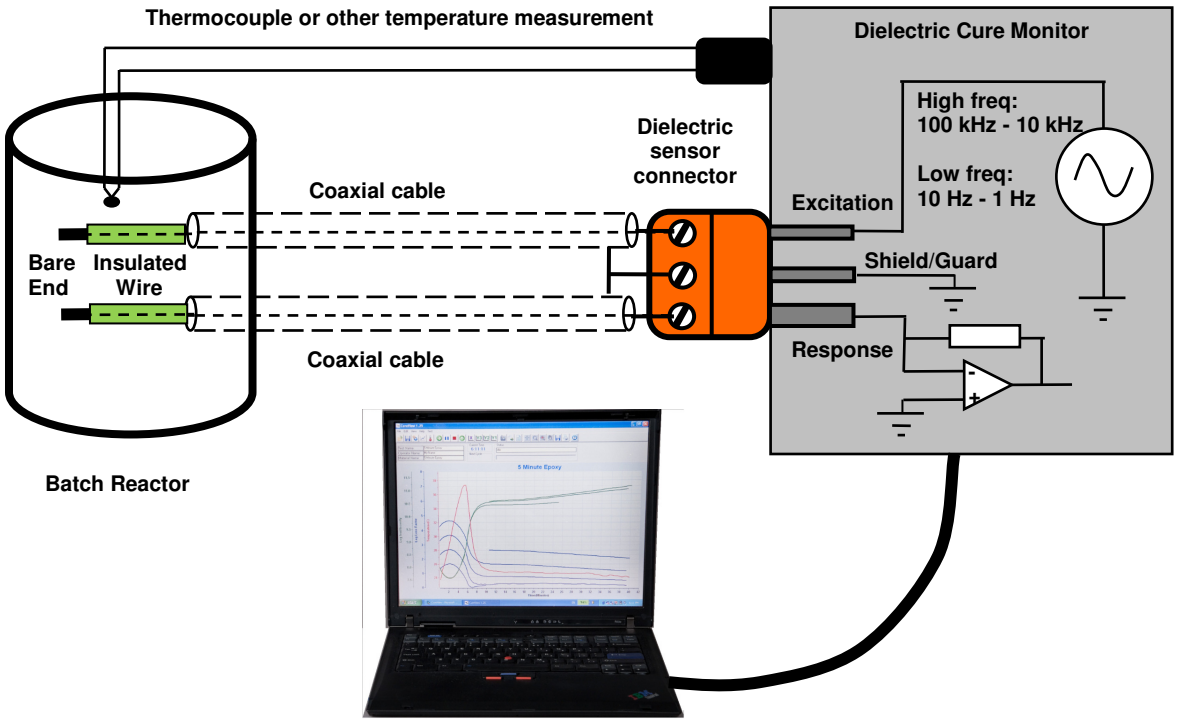

Figure 26-5
Simplified sensor for use with a batch reactor process

The optimum configuration must be determined by trial and error, but a reasonable design could start with 5 mm of exposed wire and 5 mm separation

between the bare ends, as in Figure 26-6. Use solid wire 24 AWG or thicker, so it may easily formed and remains rigid after shaping. The insulation should be Teflon for ruggedness and chemical resistance, and the ends should be secured so their separation cannot change.

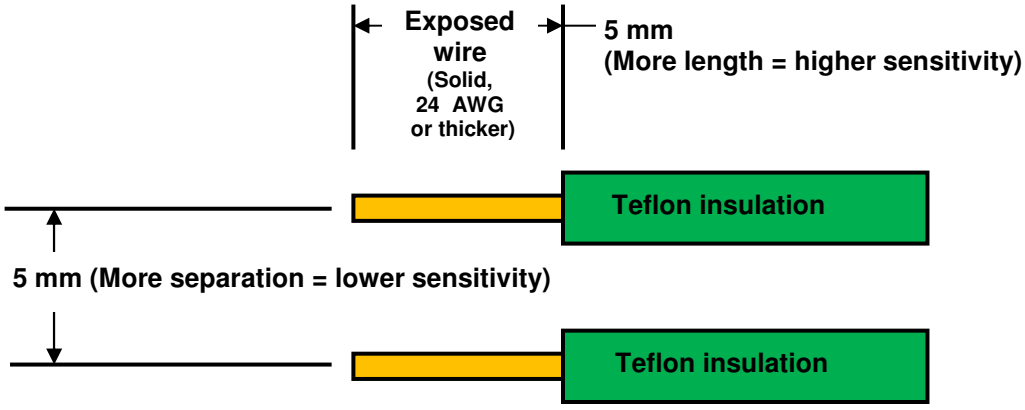

Figure 26-6
Simplified dielectric sensor for low ion viscosity, example configuration

Test the sensor by making a measurement in the material under test at the process temperature. Adjust the configuration of the sensor as necessary using the following guidelines:

- If the signal level is too low, decrease the separation or increase the length of the exposed wire
- If the signal level is too high, increase the separation or decrease the length of exposed wire

Hazardous environments around batch reactors

Batch reaction processes use large volumes of resin and may produce volatile, flammable gases. The National Fire Protection Association (NFPA) Publication 70, the NEC and CEC categorize hazardous environments by *Class*, *Division* and *Group* as follows:

- **Class**—Type of flammable substance
    - **Class I**—Locations where flammable vapors or gases may be present
    - **Class II**—Locations where combustible dust may be present
    - **Class III**—Locations where easily ignitable fibers or flyings may be present
- **Division**—Area classification
    - **Division 1**—Ignitable substances exist under normal operating condition and/or caused by frequent maintenance or repair work or frequent equipment failure
    - **Division 2**—Ignitable substances are handled or used but normally in closed containers or systems, with escape only under abnormal operating conditions such as rupture of the container or breakdown of the system
- **Group**—Gas group, or flammability
    - **Group A**—*Example*: Acetylene
    - **Group B**—*Examples*: Hydrogen, butadiene, ethylene oxide, propylene oxide
    - **Group C**—*Examples*: Ethylene, cyclopropane, ethyl ether
    - **Group D**—*Examples*: Propane, acetone, ammonia, benzene, butane, ethanol, gasoline, methanol, natural gas

Preventing ignition or explosion in hazardous environments

In hazardous locations, electrical equipment such as a dielectric cure monitor often requires *intrinsically safe barriers* in-line with sensors to prevent the ignition or explosion of flammable gases. Intrinsically safe barriers (I.S. barriers) are protective circuits designed to limit voltage and current to electrical devices. The limitations prevent dangerous energy discharge and depend on the classification of the hazardous environment and the requirements of the device.

Intrinsically safe barriers consist of a resistor, a fuse and one or two zener diodes, and must be connected to a ground point. Intrinsically safe barriers may handle positive, negative or AC signals, with configurations shown in Figure 26-7.

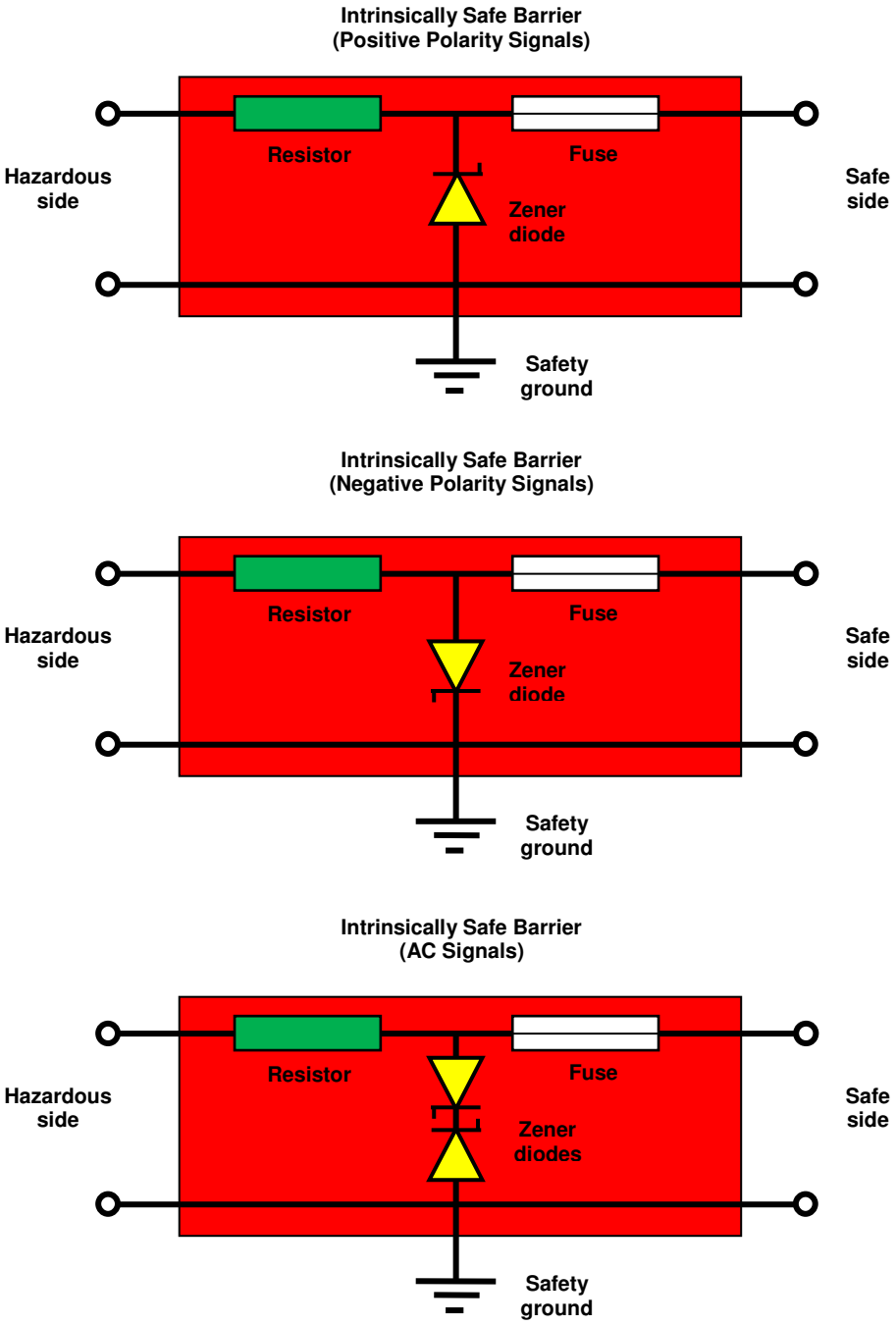

Figure 26-7
Intrinsically safe barrier configurations

Explosion-Proof Enclosures

By ensuring that the available energy is insufficient to ignite the hazardous substance that may be present, intrinsically safe barriers remove the need for special *explosion-proof* enclosures around measurement circuitry. Article 100 of the NEC defines Explosion-Proof Apparatus as follows:

Apparatus is enclosed in a case that is capable of withstanding an explosion of a specified gas or vapor that may occur within it and of preventing the ignition of a specified gas or vapor surrounding the enclosure by sparks, flashes, or explosion of the gas or vapor within, and which operates at such an external temperature that a surrounding flammable atmosphere will not be ignited thereby.

NEMA Type 7 enclosures are designed to meet explosion-proof requirements in indoor Class I, Group A, B, C or D locations. They can withstand the pressures from an internal explosion of specified gases, and are able to contain the explosion and prevent ignition of a surrounding explosive atmosphere.

While intrinsically safe barriers can eliminate use of explosion-proof enclosures, *the user should always consult with the local or company safety authority to confirm equipment meets safety requirements*.

Implementing Intrinsically Safe Barriers into a Batch Reaction Process

Identifying the category of hazardous environment is the first step to implementing dielectric cure monitoring in a batch reaction process. Then select appropriate intrinsically safe barriers for use with thermocouples and dielectric sensors. Install these barriers in an enclosure to support connectors to the sensors and connectors for cabling to the instrumentation.

For example, a batch reactor is in a Class I, Division 2, Group D hazardous environment. The company R. Stahl[2] is a manufacturer of intrinsically safe barriers and the following components may be used to assemble an Intrinsically Safe Interface:

- For thermocouples: R. Stahl 9001/01-050-150-101 I.S. barrier
  (Ω = 42 – 49, V = 1 – 3 VDC, I_{MAX} = 20 – 61 mA)
- For dielectric sensors: R. Stahl 9001/02-093-390-101 I.S. barrier
  (Ω = 31 – 36, V = ±6 VAC, I_{MAX} = 110 mA)
- Enclosure: R. Stahl 8150/5-0200-0300-150-3321 stainless steel enclosure

- **Note that the enclosure is not explosion-proof** but is safe and suitable when used with intrinsically safe barriers for Class I, Division 2, Group D environments

This enclosure with the intrinsically safe barriers is the *Intrinsically Safe Interface* and is shown schematically with the dielectric cure monitoring system in Figure 26-8. Because of the added circuitry in the I.S. barriers, dielectric measurements may have frequency or accuracy limitations compared to the base instrument.

IMPORTANT: For safe operation, the Intrinsically Safe Interface and the Dielectric Cure Monitor must both be connected to the same electrical ground.

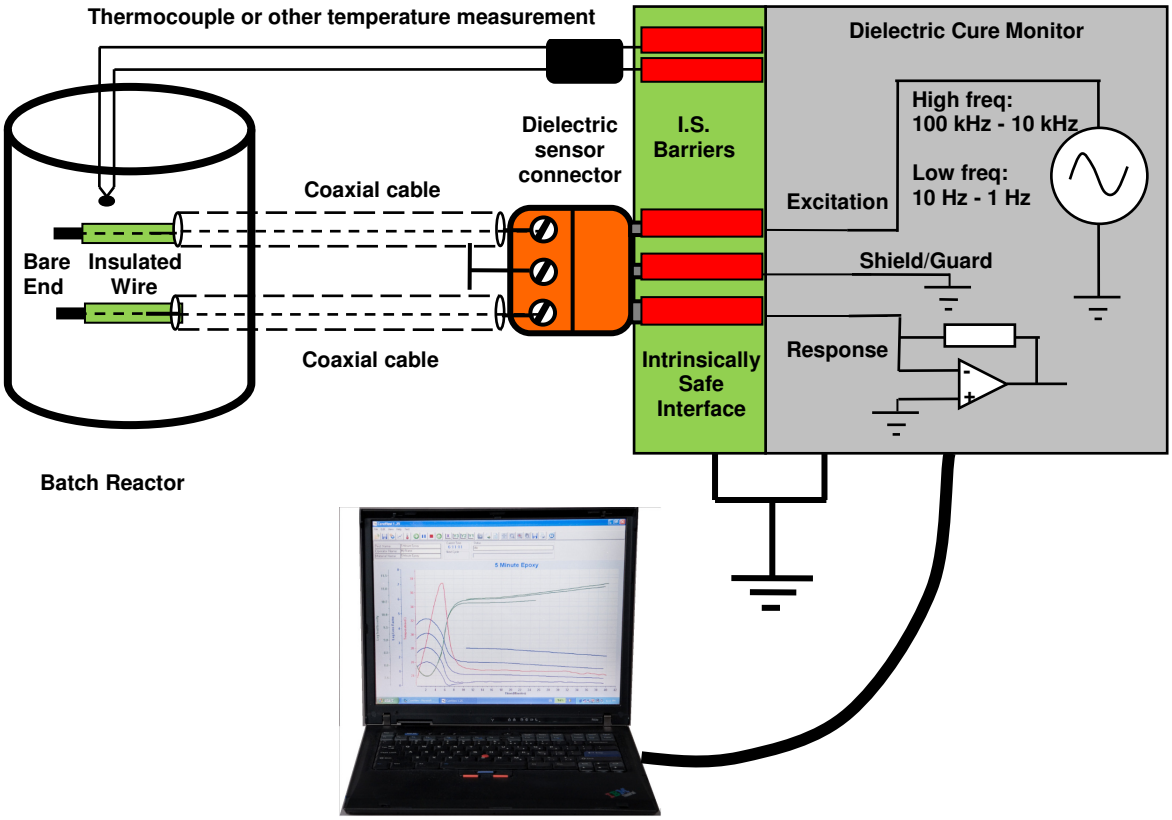

Figure 26-8
Apparatus for single channel of intrinsically safe process monitoring in a batch reactor

Figure 26-9 schematically shows a full, four-channel system with cabling, using an LT-451C Dielectric Cure Monitor.[3]

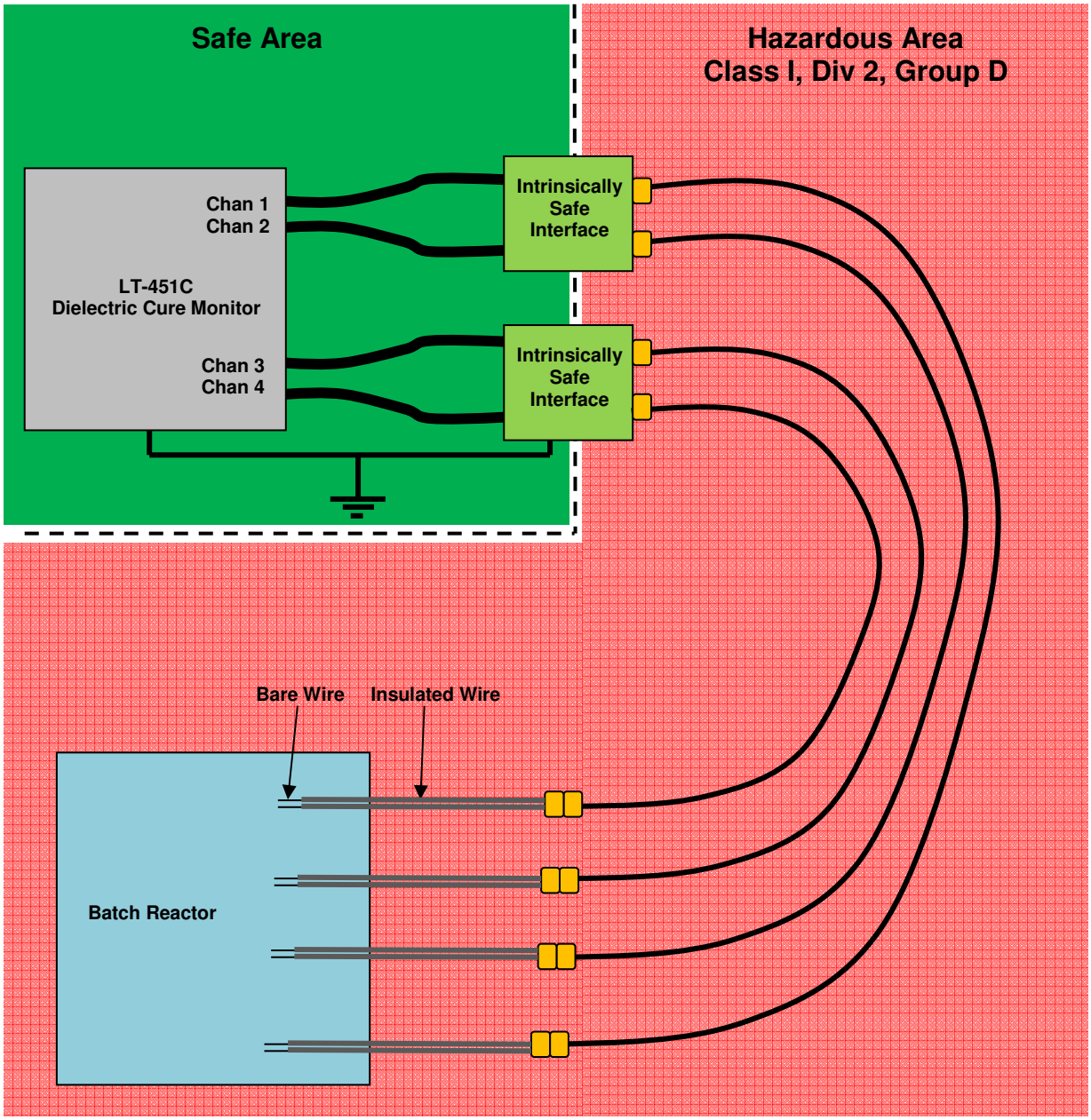

Figure 26-9
Four-channel dielectric cure monitoring system
with intrinsically safe barriers
(Computer and thermocouples not shown for clarity)

The intrinsically safe barriers require a ground reference and the enclosure must be grounded to ensure their protective function. For good measurements, the LT-451C Dielectric Cure Monitor must have the same ground as the barriers. Figure 26-10 shows the ground connection points of the Intrinsically Safe Interface and the LT-451C. These points must be connected to the ground reference. **This ground reference must be the same as the safety ground of the AC Mains supply.**

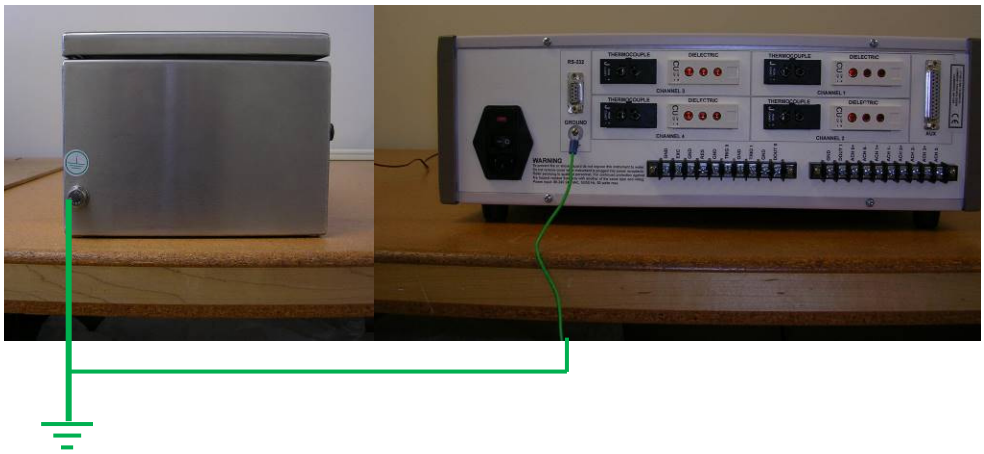

Figure 26-10
Grounding points of the Intrinsically Safe Interface and LT-451C Dielectric Cure Monitor

Dielectric cure monitoring can provide on-line, real time information about the polymerization in a batch reaction process. Batch reactors, however, often operate in hazardous environments with flammable gases. Intrinsically safe barriers can be used with thermocouples and dielectric sensors to limit energy below the ignition point of these gases and prevent explosion. A dielectric cure monitoring system with an Intrinsically Safe Interface can enable valuable process control of batch reactions in large scale resin production.

References

1. Crowley, Timothy J. and Choi, Kyu Yong, In-line dielectric monitoring of monomer conversion in a batch polymerization reactor, *Journal of Applied Polymer Science*, Feb. 28, 1995, pp 1361-1365

2. R. Stahl, Inc., Stafford, TX USA. https://www.rstahl.com/

3. LT-451C Dielectric Cure Monitor, manufactured by Lambient Technologies, Cambridge, MA USA. https://lambient.com

Chapter 27–Parallel Plate Measurements

Electrical model of thermosets

Dielectric instrumentation measures the electrical properties of the Material Under Test (MUT) between a pair of electrodes, which can be modeled as a conductance in parallel with a capacitance, as shown in Figure 27-1.

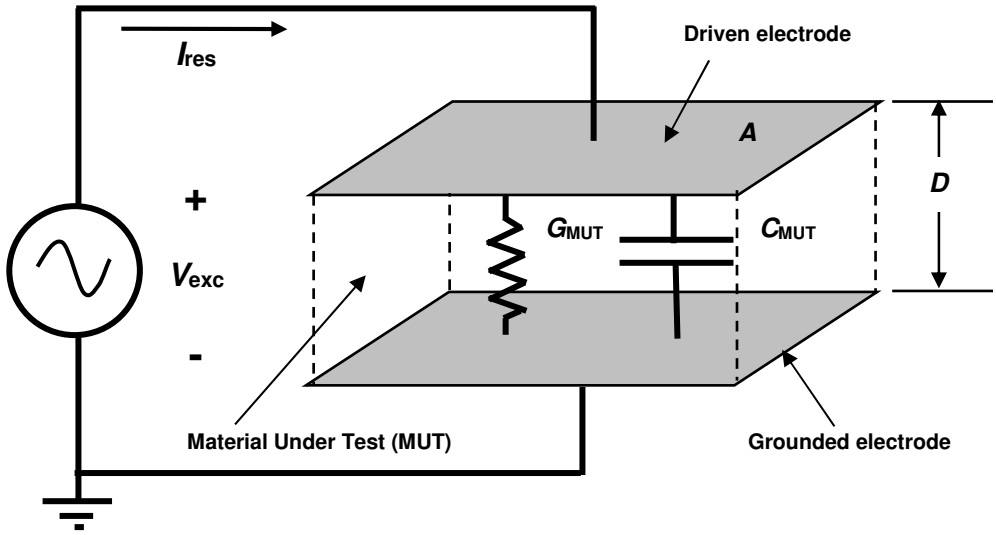

Figure 27-1
Electrical model of dielectric Material Under Test

Raw dielectric measurements at frequency f are conductance G_{MUT} (ohm^{-1}) and capacitance C_{MUT} (farads). Resistance and other material properties are given by equations 27-1 through 27-5:

(eq. 27-1)	R_{MUT}	$= 1/G_{MUT}$	(resistance)
(eq. 27-2)	ρ	$= R_{MUT}\, A/D$	(resistivity or ion viscosity)
(eq. 27-3)	σ	$= G_{MUT} / (A/D)$	(conductivity)
(eq. 27-4)	ε'	$= C_{MUT} / (\varepsilon_o\, A/D)$	(relative permittivity)
(eq. 27-5)	ε''	$= \sigma / (\varepsilon_o\, \omega)$	(loss factor)

Where:

$\omega = 2\pi f$
$\varepsilon_0 = 8.85 \times 10^{-14}$ F/cm
A/D = ratio of area to distance for electrodes

Dissipation, or tanδ, at measurement frequency *f* is the ratio of a material's relative loss to its relative permittivity, and is given by the relationship:

(eq. 27-6) $$\tan\delta = \varepsilon''/\varepsilon' = 1 / (\omega C_{MUT} R_{MUT})$$

Dielectric properties can be measured in a test cell, and parallel plate electrodes are usually used for solid material in the form of a laminate or panel. Some test cells have cylindrical geometries for measuring fluids or tubular solids, and many other configurations are possible. In general the *A/D* ratio may also be called the *cell constant*.

ASTM standard for parallel plate dielectric measurements

The ASTM standard D150-98 (Reapproved 2004) **Standard Test Methods for DAC Loss Characteristics and Permittivity (Dielectric Constant) of Solid Electrical Insulation** describes general configurations of electrodes, circuits and instruments. For measurements that do not require best accuracy, unshielded two-electrode systems with corrections may be convenient, but exacting measurements require guarded three-electrode fixtures.

An unshielded two-electrode arrangement produces fringing electric fields between the electrodes and through the sample and surrounding media, as shown in Figure 27-2. These fringe fields create stray capacitance that introduces uncertainty in the *A/D* ratio, or cell constant, and reduces measurement accuracy.

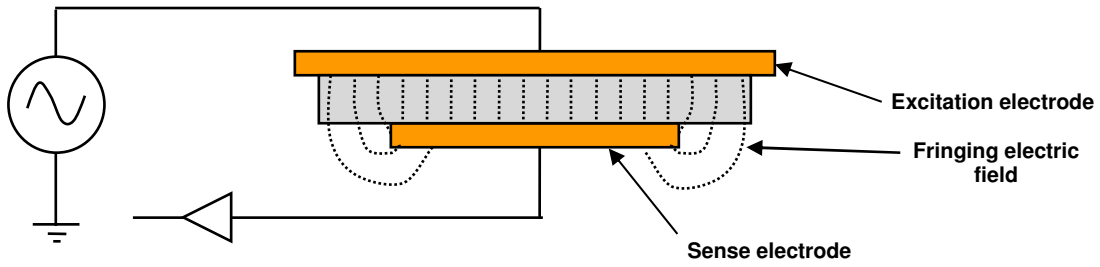

Figure 27-2
Unguarded parallel plate electrodes with fringing electric field

Guarded three-electrode fixtures are the standard for accurate dielectric measurements. In this configuration, a guard electrode surrounds the response electrode. Additional circuitry drives the guard electrode with a reproduction of the response voltage. Most impedence measurement instruments, such as LCR

meters, connect the response electrode to a virtual ground; in this case the guard electrode is also grounded.

Figure 27-3 shows how the guard electrode creates a uniform electric field that extends beyond the sample. This configuration eliminates fringing fields and allows exact definition of the *A/D* ratio or cell constant, based on the dimensions of the electrodes alone. Also, because the electric field between excitation and response electrodes is confined to the sample, the medium beyond the sample does not influence the measurement.

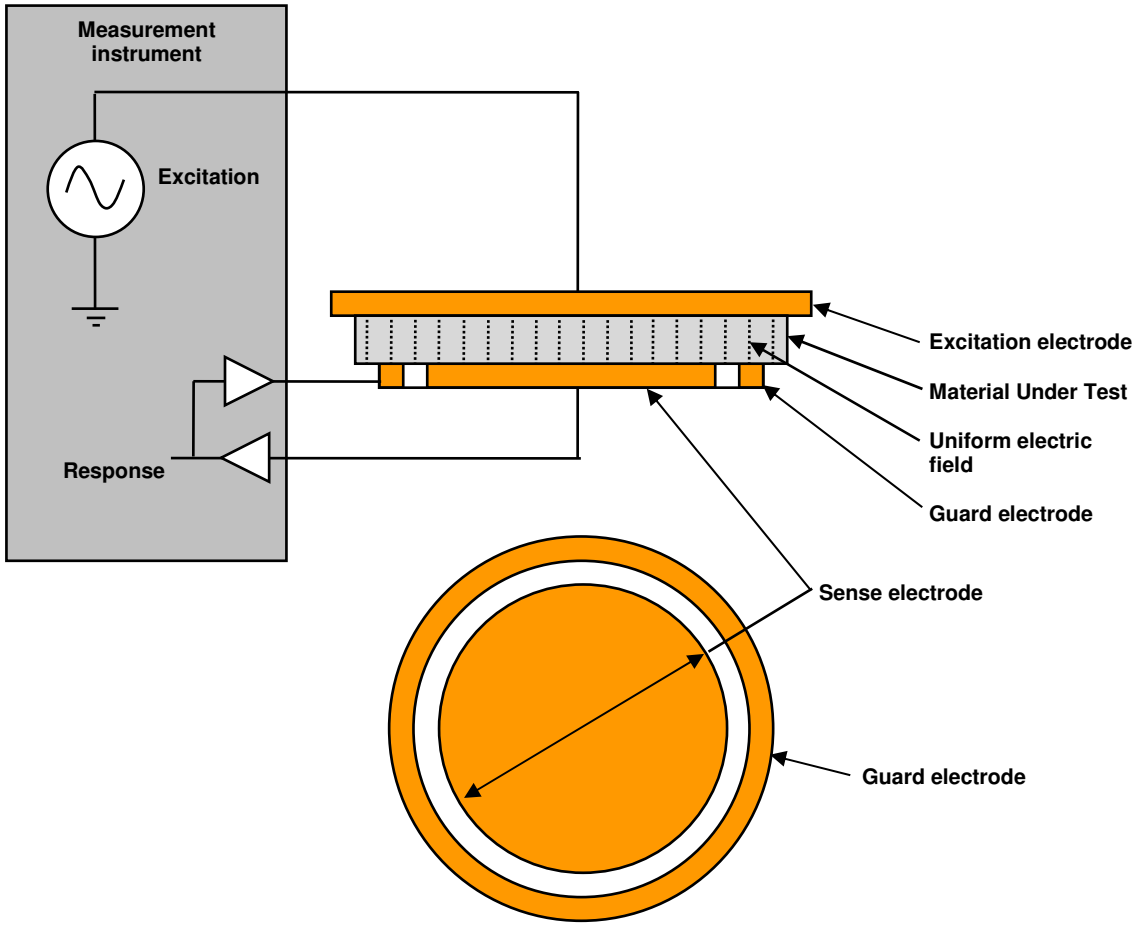

Figure 27-3
Guarded parallel plate electrodes with uniform electric field

Cabling to instruments

For accurate measurements, good cabling is important. Figure 27-4 shows the typical connection of an instrument to a parallel plate test fixture. The excitation line uses a coaxial cable and the response line uses a triaxial cable. The shield of the coaxial cable is grounded to prevent coupling of the excitation to the response signal. The inner shield of the triaxial cable is driven by a buffered version of the response signal; this method of signal *guarding* reduces the effect of input and cable capacitance for small voltages at high impedence levels. The guard output also drives the guard electrode of the test fixture. The outer shield of the triaxial cable is grounded to prevent transmission of noise to the guard signal. When the response line is a virtual ground, which is the case for most LCR meters, a coaxial cable with grounded shield is sufficient for the response signal.

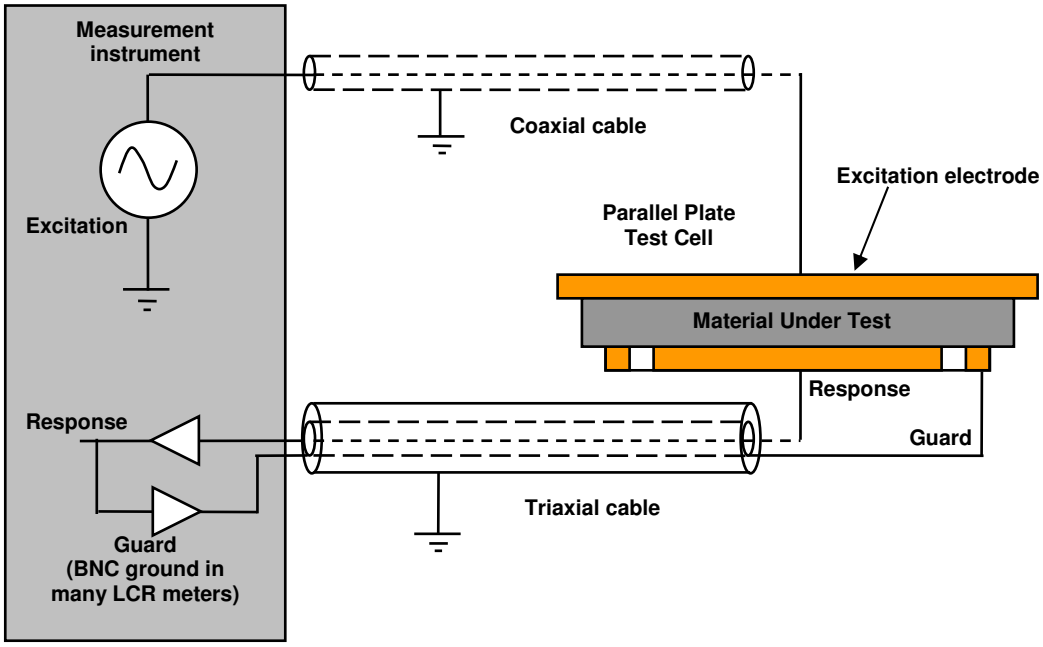

Figure 27-4
Typical excitation and response cabling to a parallel plate test fixture

Contacting electrode measurements

The contacting electrode method requires only one measurement with the electrodes in direct contact with the MUT as shown in Figure 27-5. The surface of the MUT must be flat to prevent an air gap between the sample and electrodes. The MUT should also be incompressible so the separation between the electrodes is the same as the true thickness of the sample.

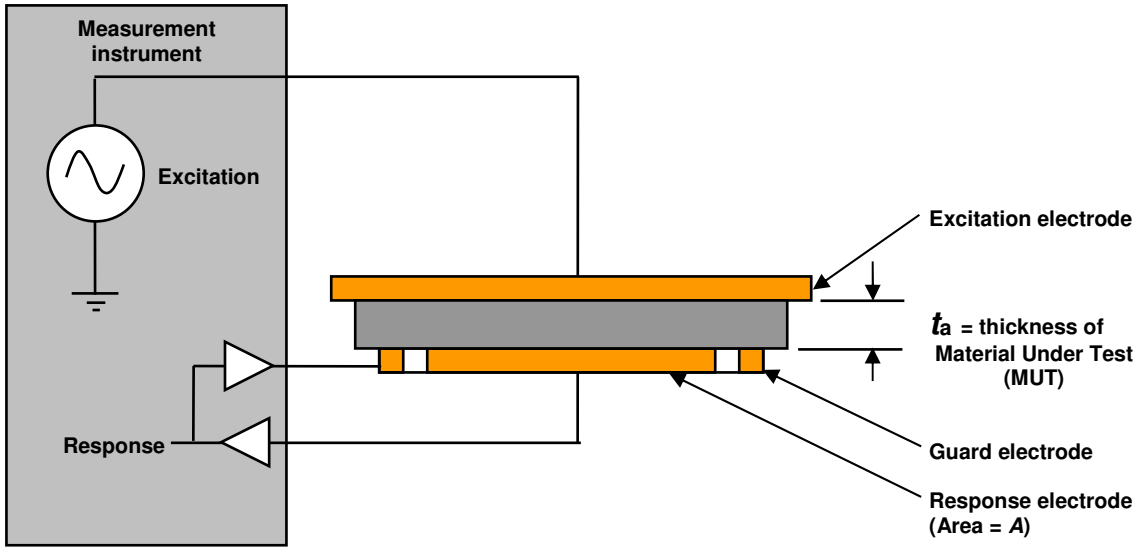

Figure 27-5
Configuration for contacting electrode measurements

Dielectric properties at *f*, the frequency of measurement, are calculated below:

(eq. 27-7) $\varepsilon' = C_P / (\varepsilon_0 A / t_a)$

(eq. 27-8) $\tan\delta = \varepsilon'' / \varepsilon' = 1 / (\omega C_P R_P)$

(eq. 27-9) $\varepsilon'' = \varepsilon' \tan\delta$

Where: $\omega = 2\pi f$
$\varepsilon_0 = 8.85 \times 10^{-14}$ F/cm
C_P = Capacitance of measurement (farad)
R_P = Resistance of measurement (ohm)

Non-contacting electrode measurements

The non-contacting electrode method can obtain accurate results for dielectric properties in the presence of an air gap, but requires two measurements. The first measurement determines the capacitance and dissipation of the test fixture at a known separation with only air between the electrodes, as shown in Figure 27-6a. The second measurement determines the capacitance and dissipation at the same separation with the sample inserted between the electrodes, as shown in Figure 27-6b. For this method the air gap and the compressibility of the MUT do not affect the results.

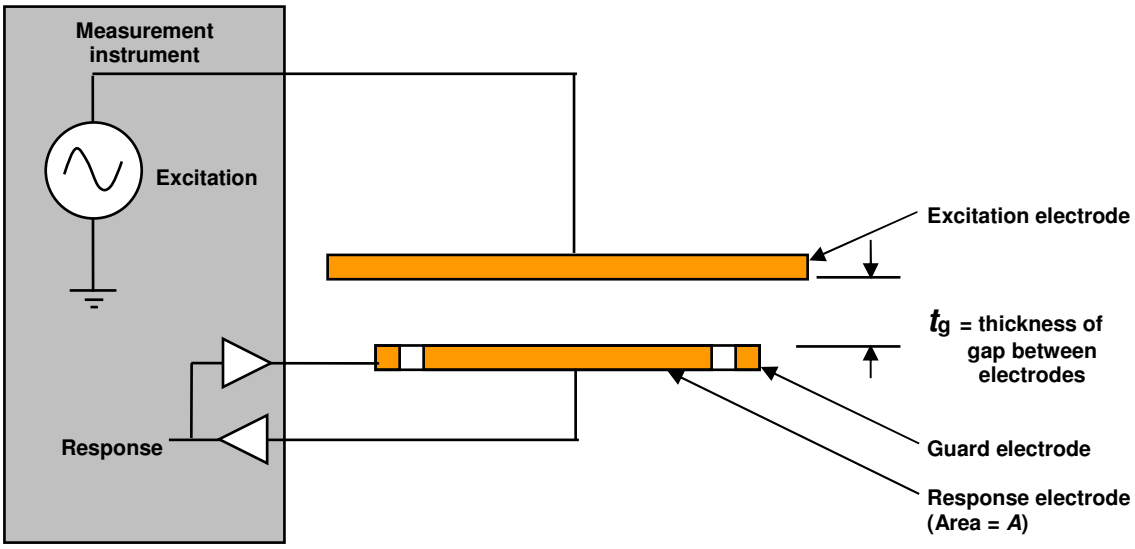

Figure 27-6a
Non-contacting electrode measurement with air only between electrodes (First measurement)

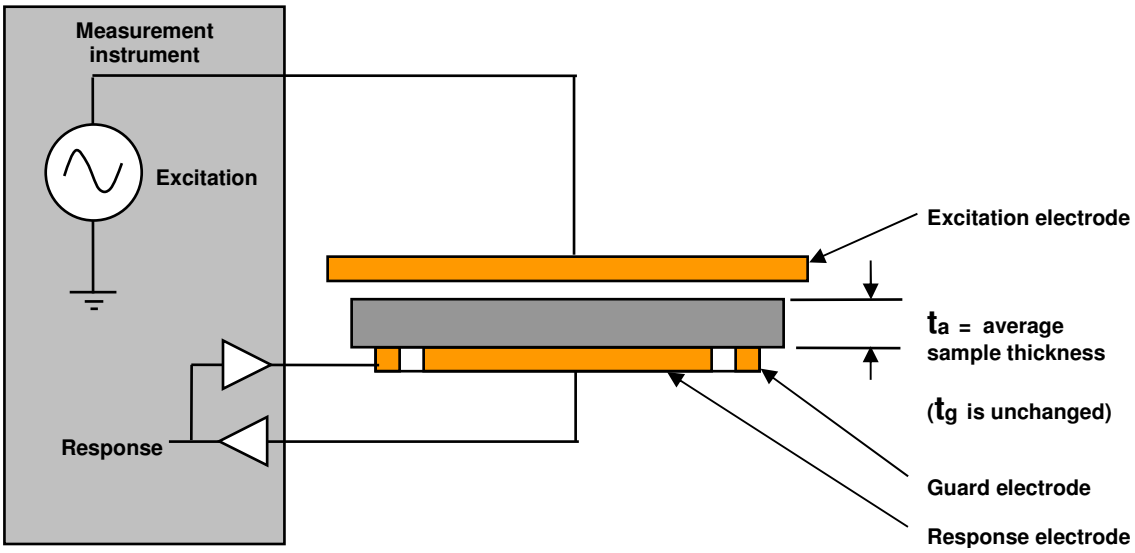

Figure 27-6b
Non-contacting electrode measurement with sample between electrodes (Second measurement)

For low dissipation the dielectric properties at *f*, the frequency of measurement, are calculated below:

For $(\tan\delta)^2 << 1$

(eq. 27-10) $\varepsilon' = 1 / [1 - (a\ b)]$

(eq. 27-11) $\tan\delta = \tan\delta_{P2} + [\varepsilon' c\ d]$

(eq. 27-12) $\varepsilon'' = \varepsilon' \tan\delta$

Where:

$\omega = 2\pi f$

C_{P1} = Capacitance (F) without MUT inserted (Fig. 27-6a)

R_{P1} = Resistance (Ω) without MUT inserted (Fig. 27-6a)

$\tan\delta_{P1} = 1 / (\omega C_{P1} R_{P1})$ = Dissipation without MUT inserted (Fig. 27-6a)

C_{P2} = Capacitance (F) with MUT inserted (Fig. 27-6b)

R_{P2} = Resistance (Ω) with MUT inserted (Fig. 27-6b)

$\tan\delta_{P2} = 1 / (\omega C_{P2} R_{P2})$ = Dissipation with MUT inserted (Fig. 27-6b)

t_g = Separation (m) between electrodes

t_a = Average sample thickness (m)

$a = 1 - (C_{P1} / C_{P2})$

$b = t_g / t_a$

$c = \tan\delta_{P2} - \tan\delta_{P1}$

$d = (t_g / t_a) - 1$

Results for non-contacting electrode measurements can only be as accurate as the measurements of electrode separation and sample thickness. For situations where the air gap is a large fraction of the sample thickness, calculations for relative permittivity, ε', and dissipation, $\tan\delta$, are very sensitive to uncertainties in t_g and t_a . Consequently, non-contacting electrode measurements are best used for thicker samples where the air gap can be relatively small.

Chapter 28–Calculating A/D Ratio and Base Capacitance

Sensor capacitances

The cross section of the planar electrodes shown in Figure 28-1 shows that the total capacitance C_{tot} is the sum of C_{MUT} from the Material Under Test above electrodes and C_{base} from the substrate beneath the electrodes. This second component C_{base} is called the base capacitance.

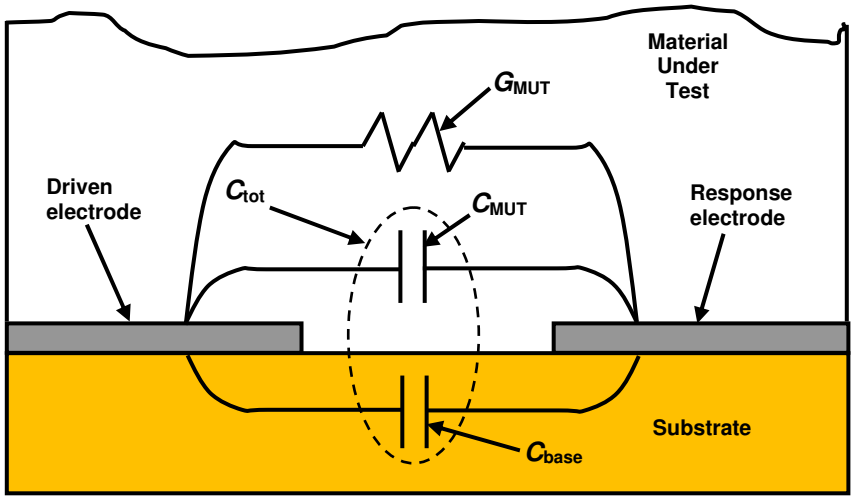

Figure 28-1
Cross section of interdigitated electrode structure

The total capacitance measured by the interdigitated electrodes is:

(eq. 28-1) $$C_{tot} = C_{MUT} + C_{base}$$

The capacitance of the Material Under Test is calculated as shown below:

(eq. 28-2) $$C_{MUT} = \varepsilon_o \, \varepsilon'_{MUT} \, A/D$$

Calculating Base Capacitance with Known *A/D*

It is possible to determine the base capacitance of a sensor by measuring its response in two different, non-conducting materials of known permittivity. To determine base capacitance, measure the sensor capacitance in air.

(eq. 28-3) $$C_{tot\text{-}air} = C_{MUT\text{-}air} + C_{base}$$

Then measure the sensor capacitance in a second, non-conducting fluid. Food grade mineral oil is a good second fluid because it is readily available, has very low conductivity and uniform characteristics. The relative permittivity of food-grade mineral oil is about 2.2.

(eq. 28-4) $$C_{TOT\text{-}oil} = C_{MUT\text{-}oil} + C_{base}$$

Sum together equations 28-3 and 28-4.

(eq. 28-5) $$C_{tot\text{-}air} + C_{tot\text{-}oil} = C_{MUT\text{-}oil} + C_{MUT\text{-}oil} + 2\,C_{base}$$

C_{tot} is measured in each case, and C_{MUT} is calculated in each case from equation 28-2 using the known permittivity of each Material Under Test and the *A/D* ratio of the sensor. Then C_{base} can be calculated using equation 28-6:

(eq. 28-6) $$C_{base} = 1/2\,[(C_{tot\text{-}air} + C_{tot\text{-}oil}) - (C_{MUT\text{-}air} + C_{MUT\text{-}oil})]$$

Calculating Base Capacitance and *A/D* When Both are Unknown

Both the *A/D* ratio and the base capacitance are required to fully describe a sensor. If they are both unknown then the two measurements described previously can be used to create a system of two equations in two unknowns which can be solved with basic algebra. Equations 28-3 and 28-4 are repeated below:

(eq. 28-3) $$C_{tot\text{-}air} = C_{MUT\text{-}air} + C_{base}$$
(eq. 28-4) $$C_{TOT\text{-}oil} = C_{MUT\text{-}oil} + C_{base}$$

The capacitance for the Material Under Test for equations 28-3 and 28-4 can be rewritten using equation 28-2:

(eq. 28-7) $$C_{TOT\text{-}air} = (\varepsilon'_{MUT\text{-}air}\,\varepsilon_o)\,A/D + C_{base}$$
(eq. 28-8) $$C_{TOT\text{-}oil} = (\varepsilon'_{MUT\text{-}oil}\,\varepsilon_o)\,A/D + C_{base}$$

Equations 28-7 and 28-8 make up a system of two equations in two unknowns, where the unknowns are the *A/D* ratio and C_{base}. First, these equations can be solved for the *A/D* ratio:

(eq. 28-9) $$A/D = (C_{TOT\text{-}air} - C_{TOT\text{-}oil}) / (\varepsilon_o \ (\varepsilon'_{MUT\text{-}air} - \varepsilon'_{MUT\text{-}oil}))$$

Knowing the *A/D* ratio, C_{base} can then be calculated from equation 28-6 and equation 28-2.

Chapter 29–Electrode Polarization and Boundary Layer Effects

Causes of electrode polarization

When the incorrect model is used to determine dielectric properties, low frequency measurements of highly conductive materials may appear to have unusually low conductivity. This phenomenon is caused by electrode polarization, the accumulation of charge against the electrodes, which occurs when the material under test:

- Has high loss factor (high ionic conduction at low frequency)

  AND

- Has a non-conductive film, an oxide layer or an electrochemical potential barrier, resulting in an insulating boundary layer

If the effects of electrode polarization and boundary layers are properly considered, then it is possible to account for their influence and correctly calculate bulk permittivity and conductivity.

Effects of electrode polarization

Electrode polarization distorts dielectric data by artificially increasing *apparent* relative permittivity (ε') and decreasing *apparent* loss factor (ε''). When plotted against time, loss factor curves may display anomalous behavior as shown in Figure 29-1.

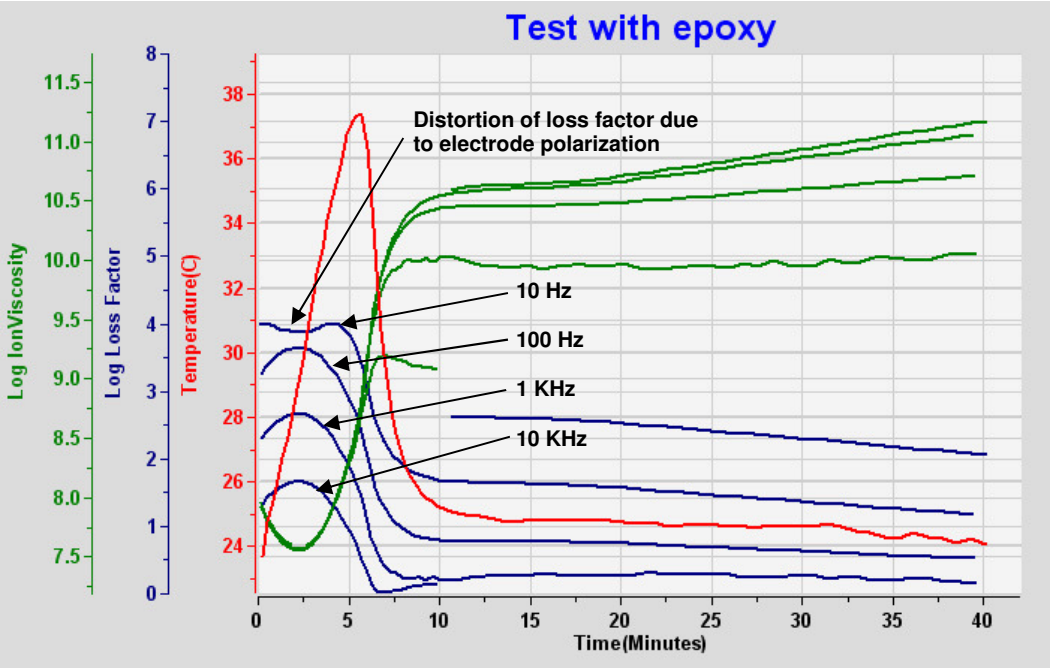

Figure 29-1
Plot showing distortion of loss factor due to electrode polarization

This distortion increases as loss factor increases. In addition, lower frequencies correspond to higher loss factors for a given conductivity, and therefore display even greater distortion. As a result, the 10 Hz loss factor data of Figure 29-1 shows a double hump—a depression with two satellite peaks instead of a single peak. The first satellite peak has been attributed to softening, and the second satellite peak to gelation—but they both are artifacts from use of an incorrect model and do not describe actual dielectric events. In fact, the expected—but unseen—single loss factor peak corresponds to the point of minimum viscosity, an event that would be completely lost if the data were misinterpreted.

The loss factor data of Figure 29-1 can be plotted against permittivity to highlight the nature of these relationships, as shown in Figure 29-2.

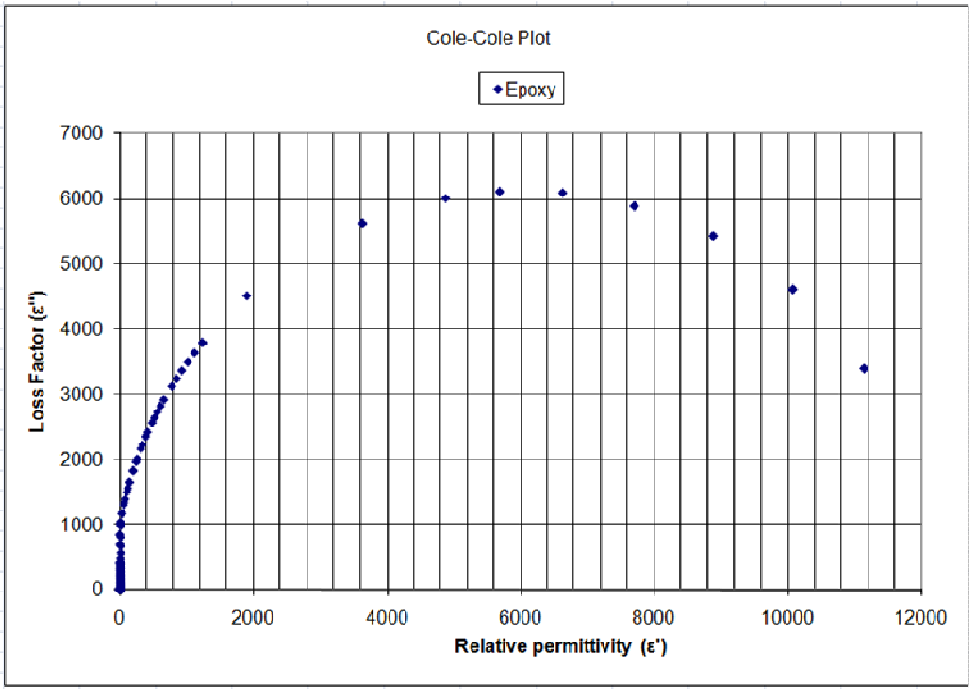

Figure 29-2
Cole-Cole plot of epoxy cure data distorted by electrode polarization

In older literature this Cole-Cole plot behavior has been erroneously explained by a large dipole relaxation response.

Basic Circuit Model of a Dielectric Material

The basic model of a dielectric Material Under Test consists of a conductance G_{MUT} in parallel with a capacitance C_{MUT} as shown below in Figure 29-3. This configuration has a simple relationship between the excitation voltage V_{exc} across the material and the response current I_{res} through the material, given by equation 29-1:

(eq. 29-1) $$I_{res} / V_{exc} = G_{MUT} + i\omega C_{MUT} = Y_{MUT}$$

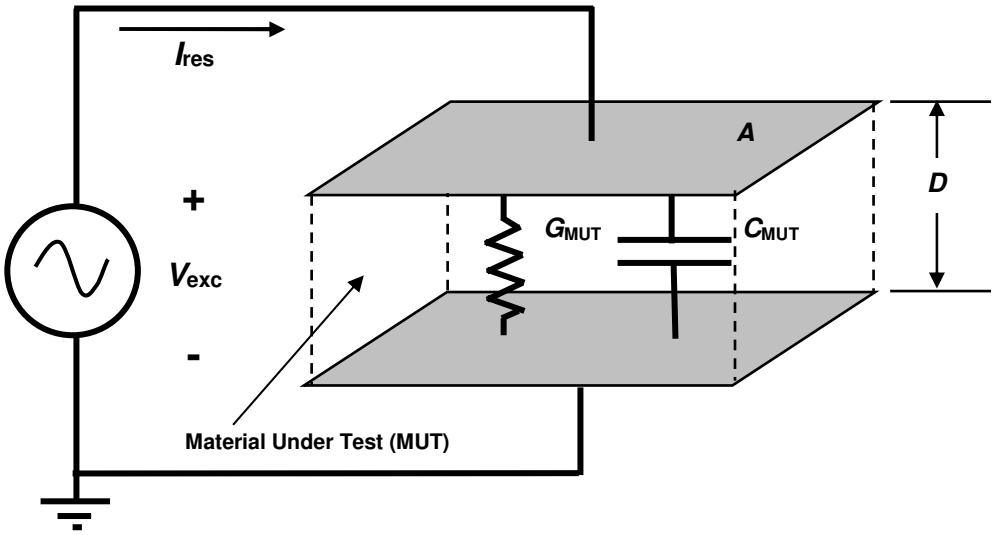

Figure 29-3
Basic model of a dielectric material

Boundary Layers

Electrode polarization creates a boundary layer at the interface with the material and changes the model to that of Figure 29-4:

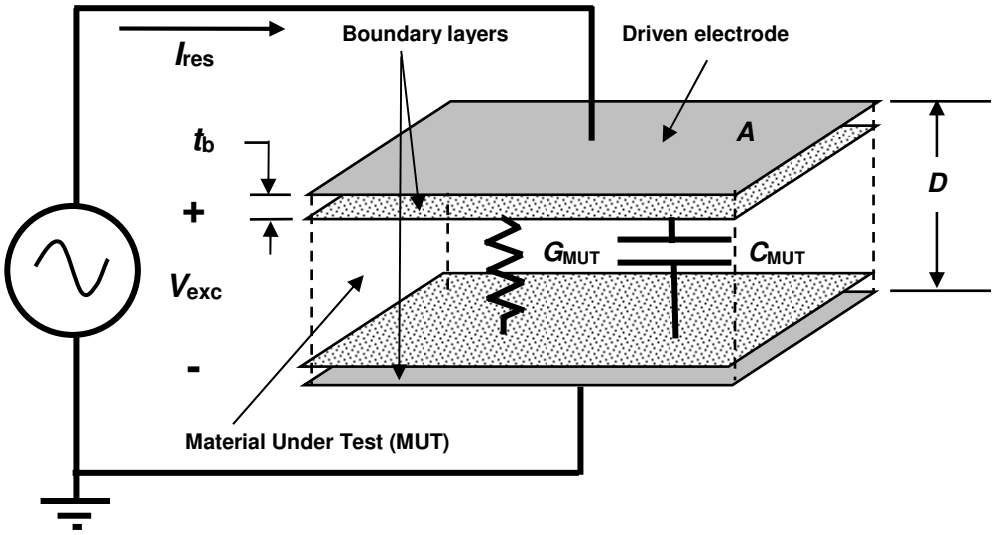

Figure 29-4
Model of dielectric material with boundary layer

Boundary layers are very thin (thickness = t_b) and have the surface area of the electrodes. Consequently they have a very large *A/D* ratio, resulting in a large

capacitance C_B in series with the bulk material. This arrangement is shown in the circuit model of Figure 29-5.

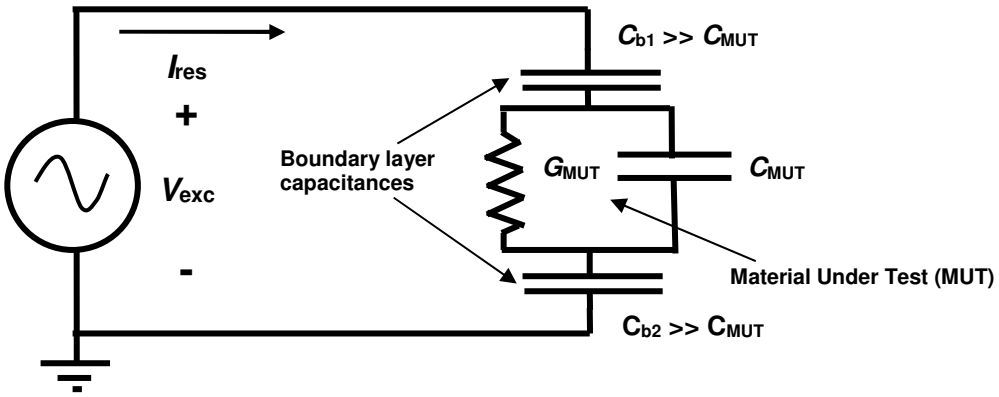

Figure 29-5
Circuit model of dielectric with boundary layer capacitances

Analysis of the boundary layer model is much more complicated than for the basic model, but it is possible to quickly understand the circuit behavior in certain limiting cases.

Low Frequency Response of Boundary Layers

For situations with low excitation frequency or high bulk conductivity, the boundary layer capacitances dominate the circuit response and the model of Figure 29-5 reduces to Figure 29-6. Capacitances act as open circuits at low frequencies, so the boundary layer blocks DC current. Measurements of DC conductance are impossible in this case and the material appears primarily insulating or capacitive.

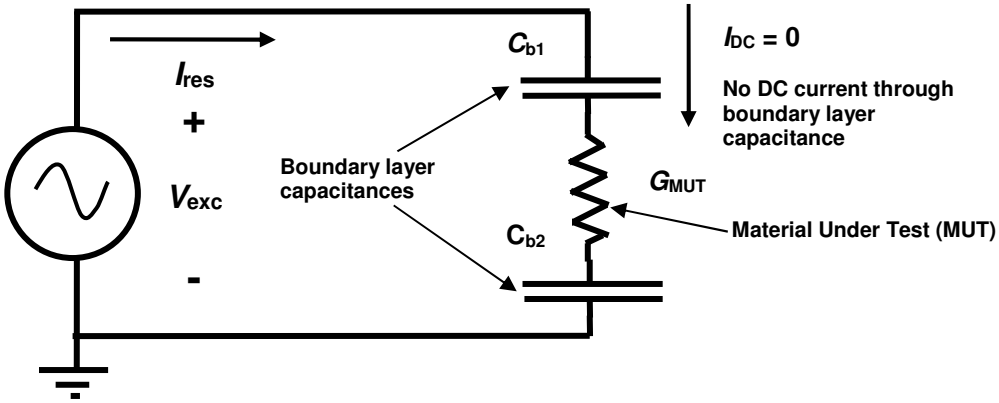

Figure 29-6
Low frequency circuit model with boundary layer capacitances

High Frequency Response of Boundary Layers

For the limit of high frequency or low bulk conductivity, boundary layer admittance is high compared to the Material Under Test, and boundary layer capacitances act like short circuits. In this case the circuit of Figure 29-5 reduces to the simpler one of Figure 29-7, which is identical to the basic model of a dielectric material. Therefore, at sufficiently high frequency, the behavior of a dielectric material is the same with or without boundary layers.

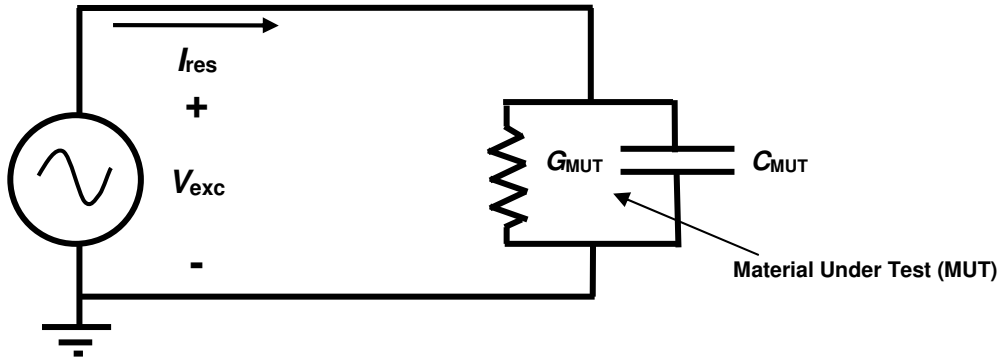

Figure 29-7
High frequency circuit model with boundary layer capacitances
(Also applies to low bulk conductivity)

Boundary Layer Effect on Dielectric Cure Monitoring

It is possible to calculate the following dielectric material properties from measurements of a material's conductance and capacitance:

(eq. 29-2) $\sigma = G_{MUT} / (A/D)$ (conductivity)
(eq. 29-3) $\varepsilon' = C_{MUT} / (\varepsilon_o A/D)$ (relative permittivity)
(eq. 29-4) $\varepsilon'' = \sigma / (\varepsilon_o \omega)$ (loss factor)
(eq. 29-5) $\rho = (A/D) / G_{MUT}$ (resistivity)

Where:

$\omega = 2\pi f_{exc}$
$\varepsilon_0 = 8.85 \times 10^{-14}$ F/cm
A/D = ratio of area to distance for electrodes

A common convention describes the cure of a polymeric material in terms of relative permttivity, ε', and loss factor, ε''. The boundary layer model of Figure 29-6 can be solved using these terms as follows:[1]

(eq. 29-6) $$\varepsilon'_x = \varepsilon' \, (D / 2t_b) \frac{(\varepsilon''/\varepsilon')^2 + (D / 2t_b)}{(\varepsilon''/\varepsilon')^2 + (D / 2t_b)^2)}$$

(eq. 29-7) $$\varepsilon''_x = \varepsilon'' \, (D / 2t_b) \frac{(D / 2t_b) - 1}{(\varepsilon''/\varepsilon')^2 + (D / 2t_b)^2)}$$

(eq. 29-8) $$\tan \delta_x = \varepsilon''_x / \varepsilon'_x = \tan \delta \, [((D / 2t_b) - 1) / ((\tan \delta)^2 + (D / 2t_b))]$$

Where:

t_b	= boundary layer thickness
D	= distance between electrodes or plate separation
ε'_x	= uncorrected (apparent) permittivity
ε''_x	= uncorrected (apparent) loss factor
ε'	= actual permittivity
ε''	= actual loss factor
$\tan \delta$	= $\varepsilon''/\varepsilon'$

Figure 29-8 shows how boundary layer thickness, temperature, frequency and state of cure influence the Cole-Cole plot of a curing material. With no boundary layer, loss factor decreases with advancing cure, while permittivity remains constant at the value ε_r, called the relaxed permittivity. Thicker boundary layers cause the Cole-Cole plot to develop a curvature which in extreme cases can become a complete semi-circle.

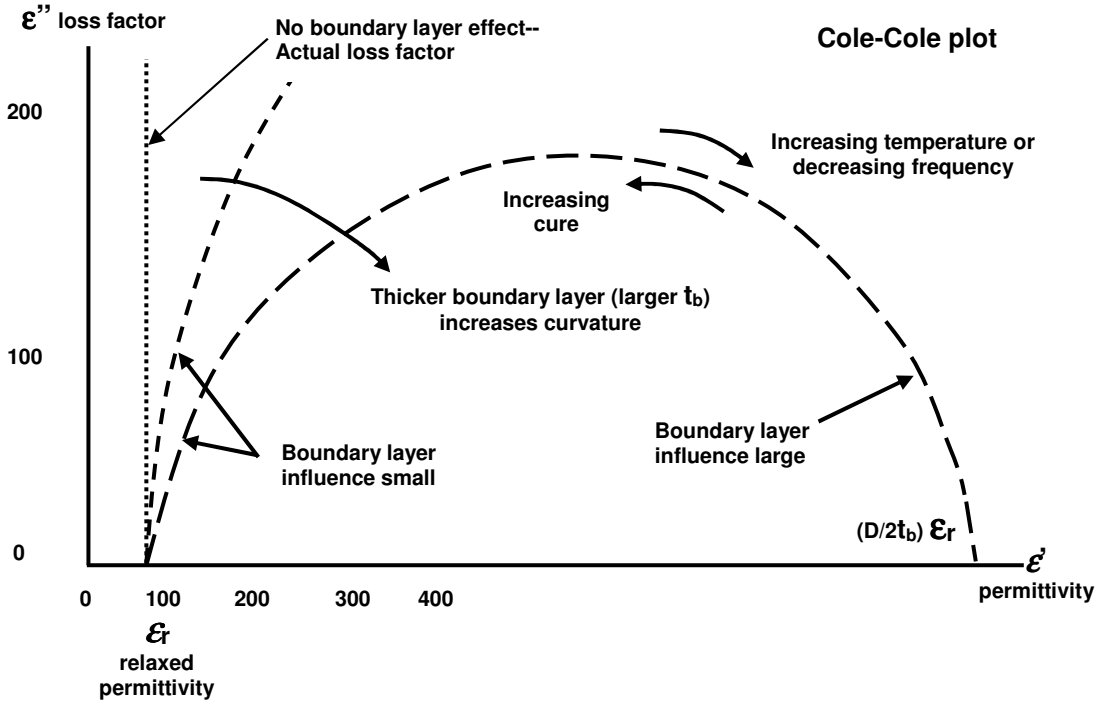

Figure 29-8
Cole-Cole plot of curing material with boundary layer effect

The left intercept of the semi-circle is the relaxed permittivity ε_r, and the right intercept is determined by both ε_r and the ratio $D/2t_b$. This information can be used to calculate the boundary layer thickness t_b. In the absence of an artificial blocking layer such as an applied insulator or an oxide coating, the boundary layer thickness can be used to calculate an approximate mobile ion concentration [*C*] and ion mobility μ:[2]

(eq. 29-9) $$[C] = (t_b^2 \, q^2) / (2kT\varepsilon' \varepsilon_0)$$

(eq. 29-10) $$\mu = \sigma / ([C] \, q)$$

Where : k = Boltzmann's constant (eV/K)
T = temperature in degrees Kelvin (K)
q = magnitude of electronic charge (coulombs)
μ = free ion mobility (cm^2 / (V-s))

Electrode Polarization Correction

It is possible to manipulate equations 29-6, 29-7 and 29-8 to correct the effect of electrode polarization in certain cases. Figure 29-9 shows data that has been adjusted in this manner.

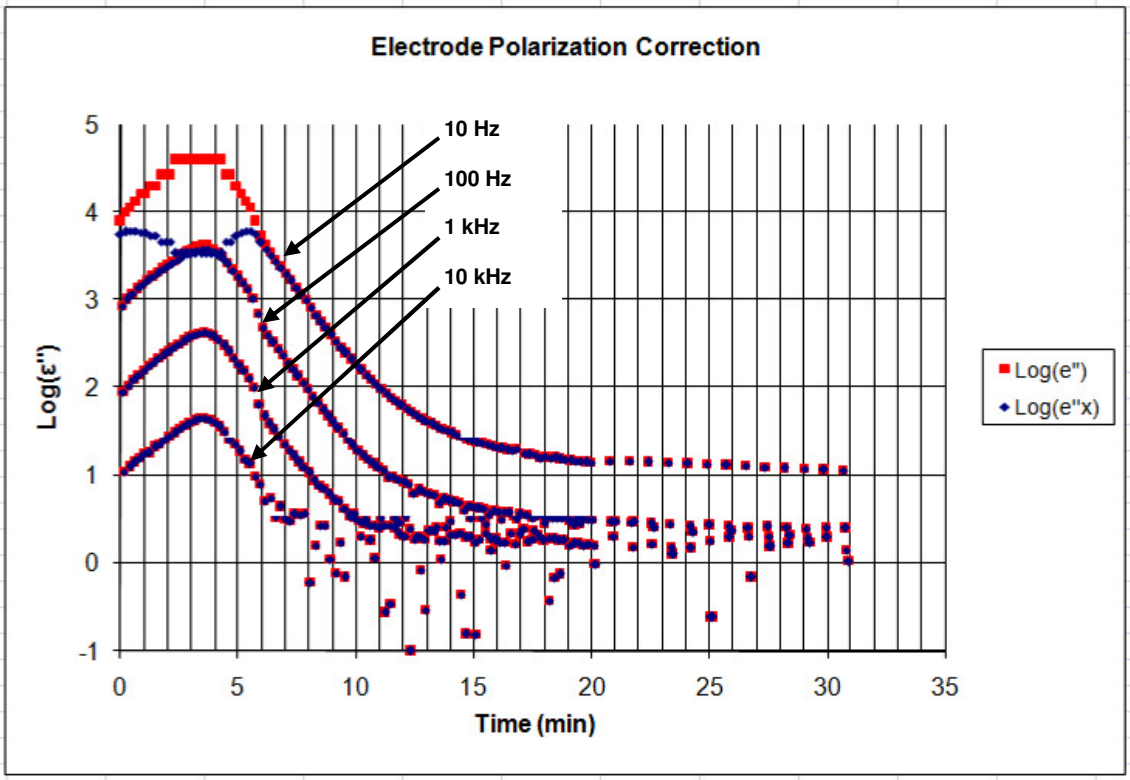

Figure 29-9
Correction of the boundary layer effect

Log(*e"x*) is the logarithm of the original loss factor *e"x*, which was acquired during cure of an epoxy resin. Log(*e"x*) data at 10 Hz shows distortions and the characteristic double hump from the boundary layer effect. This anomaly occurs at the time of maximum loss factor—maximum conductivity—as indicated by peaks from data at the higher frequencies of 100 Hz, 1.0 kHz and 10 kHz. Log(*e"*) is the logarithm of the corrected loss factor *e"*, and the corrected 10 Hz curve shows a loss factor peak consistent with peaks for higher frequencies.

Figure 29-10 compares data from the cure of this epoxy both before and after boundary layer correction.

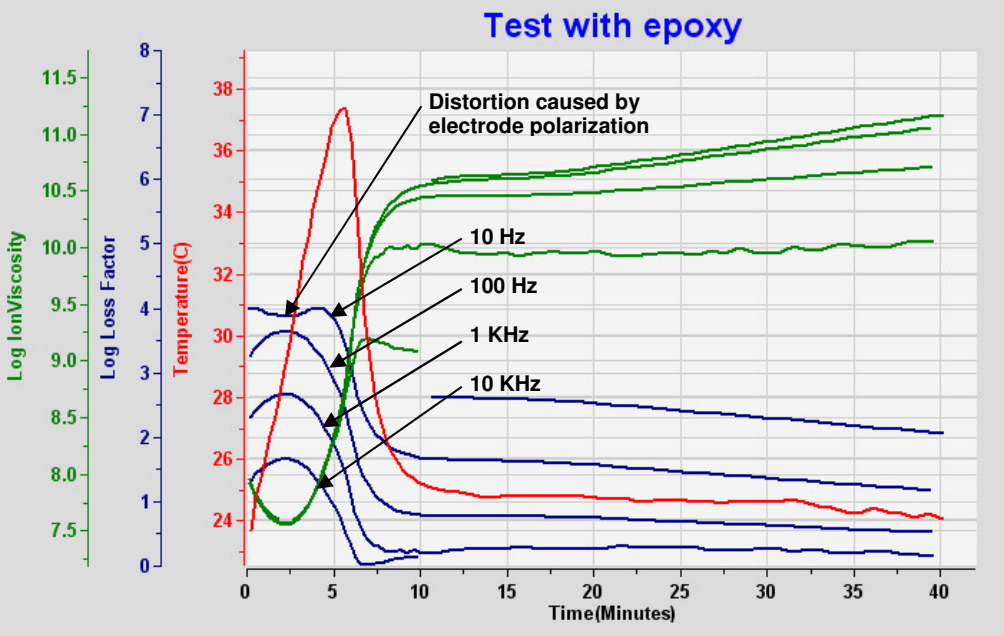

Epoxy cure data showing distortion due to boundary layers

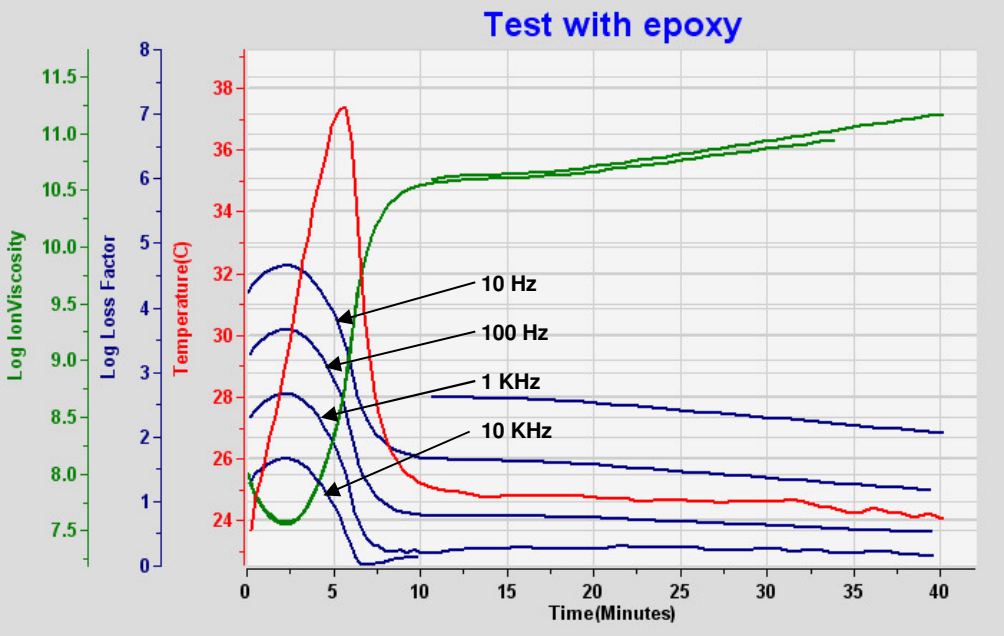

Epoxy cure data after electrode polarization correction

Figure 29-10
Comparison of data before and after electrode polarization correction

Note loss factor is inversely proportional to frequency, as given by equation 29-4, repeated below:

(eq. 29-4) $$\varepsilon'' = \sigma' / (\varepsilon_o \omega)$$

During the early portion of cure, frequency independent DC conductivity (σ_{DC}) typically dominates loss factor. For the epoxy of this example, the corrected curves for 10 Hz, 100 Hz, 1 kHz and 10 kHz are all parallel and separated by factors of 10, as expected.

References

1. Day, D.R.; Lewis, J.; Lee, H.L. and Senturia, S.D., "The Role of Boundary Layer Capacitance at Blocking Electrodes in the Interpretation of Dielectric Cure Data in Adhesives," *Journal of Adhesion*, V18, p.73 (1985)

2. MacDonald, J.R., *Phys. Rev*., v92, p.4 (1953)

Chapter 30—Electrical Modeling of Polymers

Dielectric properties

The dielectric—literally "two-electric"—properties of conductivity σ, and permittivity ε, arise from ionic current and dipole rotation in bulk material. For polymers, mobile ions are often due to impurities and additives, while dipoles result from the separation of charge on nonpolar bonds or across a molecule. When analyzing dielectric properties, it is possible and convenient to separate the influence of ions from dipoles, as shown in Figure 30-1.a., to consider their individual effects.

Ions and Dipoles

The flow of ions in an electric field is called current, and is determined by conductivity σ or its inverse, resistivity ρ. The bulk effect of mobile ions can be modeled as a conductance G, shown in Figure 30-1.b, which varies with material state—its viscosity when liquid or its modulus when solid.

The term *ion viscosity* was coined to describe resistivity ρ and emphasize its relationship to mechanical viscosity. More specifically, ion viscosity is *frequency independent* resistivity ρ_{DC}. During thermoset cure, the change in ion viscosity is often proportional to the change in mechanical viscosity or the change in modulus. Thus ion viscosity can provide valuable insight throughout cure.

The current through a conductance is in phase with the voltage across it, as shown in Figure 30-1.c. Admittance Y is given by equations 30-1 and 30-2:

(eq. 30-1) $$Y = I/V$$

(eq. 30-2) $$Y = G + i\omega C$$

Where:
I = current (A)
V = voltage (V)
G = conductance (ohm^{-1})
C = capacitance (F)
ω = $2\pi f$ (s^{-1})
f = frequency (Hz)

Current *I* and voltage *V* in general are complex quantities. An admittance consisting only of conductance *G* can be represented as a vector along the Real axis in the complex plane, as shown in Figure 30-1.d.

The rotation of dipoles is a second material phenomenon, as shown in Figure 30-1.a, and gives rise to permittivity ε. As dipoles change their orientation in response to an electric field, they store energy which is released when their orientation returns to the relaxed state. This energy storage can be modeled as a capacitor, as shown in Figure 30-1.b.

The sinusoidal current through a capacitance leads the voltage across it by 90° as shown in Figure 30-1.c. An admittance consisting only of ωC can be portrayed on the complex plane as a vector along the Imaginary axis, as shown in Figure 30-1.d.

Raw dielectric measurements are conductance *G* (ohms^{-1}) and capacitance *C* (farads). Resistance and other material properties are given by equations 30-3 through 30-7:

(eq. 30-3)	$R = 1/G$	(resistance)
(eq. 30-4)	$\rho = R\,A/D$	(resistivity or ion viscosity)
(eq. 30-5)	$\sigma = G / (A/D)$	(conductivity)
(eq. 30-6)	$\varepsilon' = C / (\varepsilon_o\, A/D)$	(relative permittivity)
(eq. 30-7)	$\varepsilon'' = \sigma / (\varepsilon_o\, \omega)$	(loss factor)

Where: $\varepsilon_0 = 8.85 \times 10^{-14}$ F/cm (permittivity of free space)
A/D = ratio of area to distance for electrodes

Although A/D is classically applied to parallel plate geometries, it may be generalized to other configurations as a scaling factor, or cell constant, which makes equations 30-4, 30-5 and 30-6 true. In this case, *A* is not necessarily the area of the electrodes and *D* is not necessarily the distance between them. Two dimensional numerical simulations of electrodes in lossy media have validated this generalization across a wide range of conductivity.

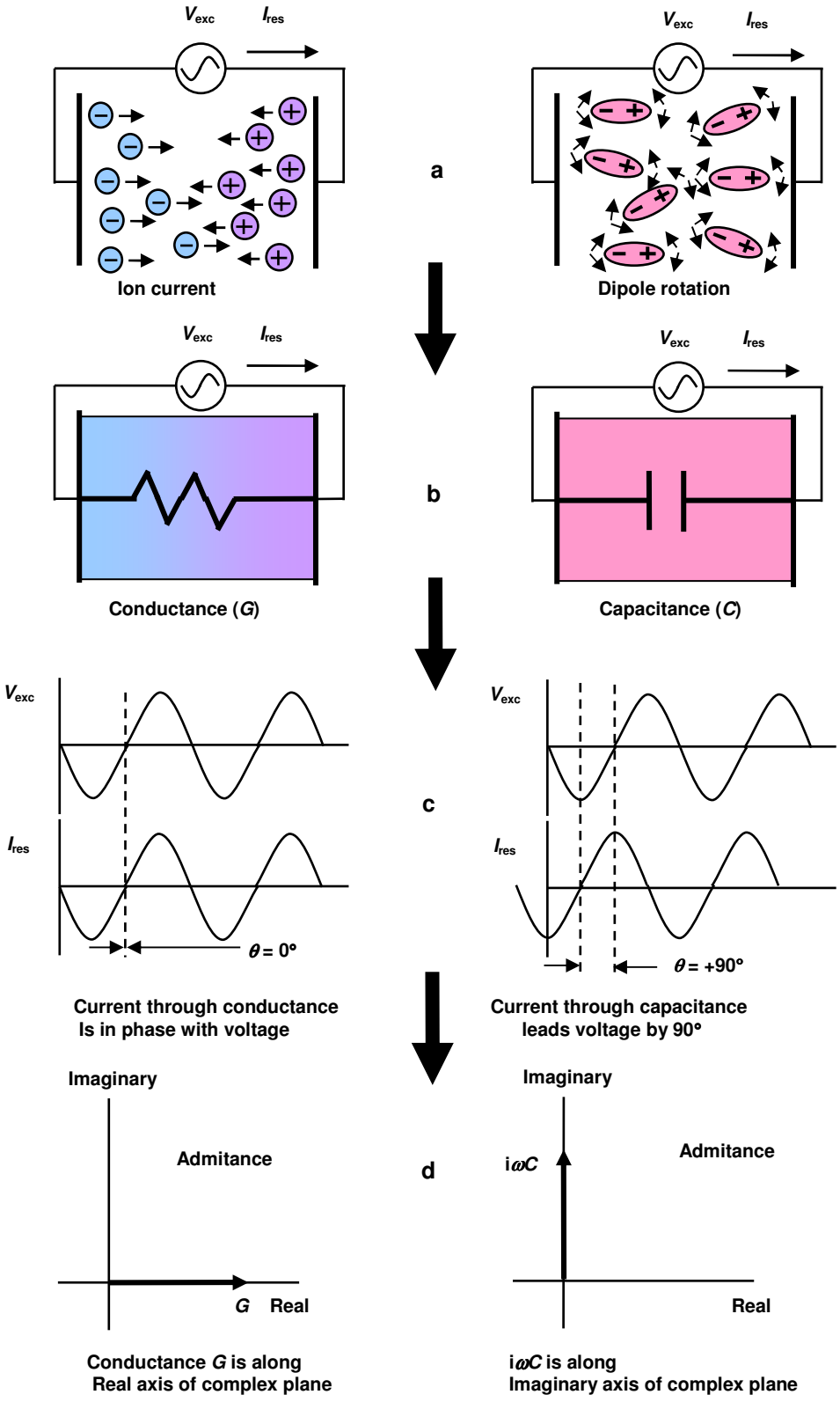

Figure 30-1
Relationships between physical and electrical behavior

The combined quantities *G* and *C* may be visualized on the complex plane as shown in Figure 30-2, where *G* is the real component of the admittance and ωC is the imaginary component. After bulk quantities *G* and *C* are divided by *A*/*D* and ε_0, the material properties of σ/ε_0 and relative permittivity ε' remain, resulting in rescaled values on the complex plane.

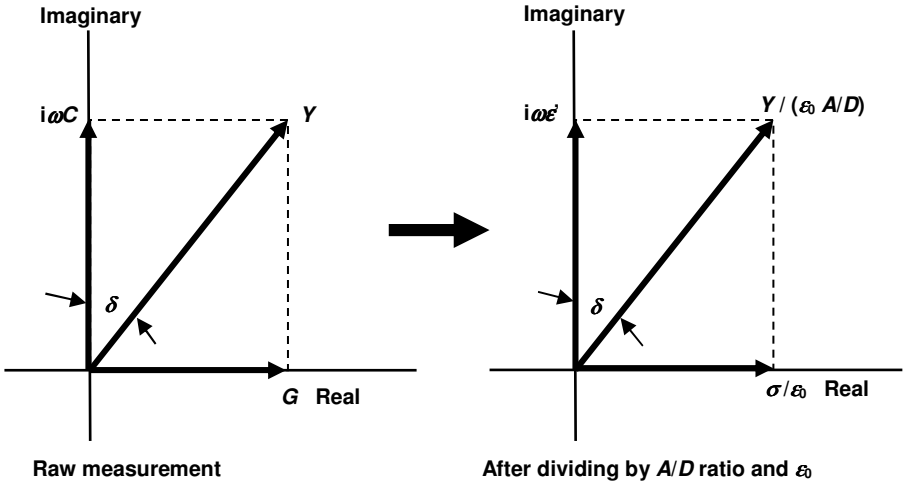

Figure 30-2
Relationship between bulk and material properties

The angle δ between *Y* and the imaginary axis may be incorporated into a quantity called dissipation factor, or loss tangent, tan δ, given by equation 30-8:

(eq. 30-8) $$\tan \delta = \sigma/(\omega \varepsilon_0 \varepsilon')$$

Use of loss factor in equation 30-8 yields the more common expression for loss tangent:

(eq. 30-9) $$\tan \delta = \varepsilon''/\varepsilon'$$

If a material has low conductivity or the frequency is very high, then ε'' and the ratio $\varepsilon''/\varepsilon'$ are small. In this case $\tan \delta \sim \delta$ and δ may be approximated by equation 30-10:

(eq. 30-10) $$\delta \sim \varepsilon''/\varepsilon'$$

Electrical model of Material Under Test (MUT)

Dielectric measurements of a Material Under Test (MUT) yield a bulk conductance G_{MUT} in parallel with a bulk capacitance C_{MUT}, which can be used in the electrical model of Figure 30-3. In general, both components have frequency dependent and frequency independent terms. Similarly, the material properties of conductivity σ and permittivity ε have frequency dependent and independent behavior.

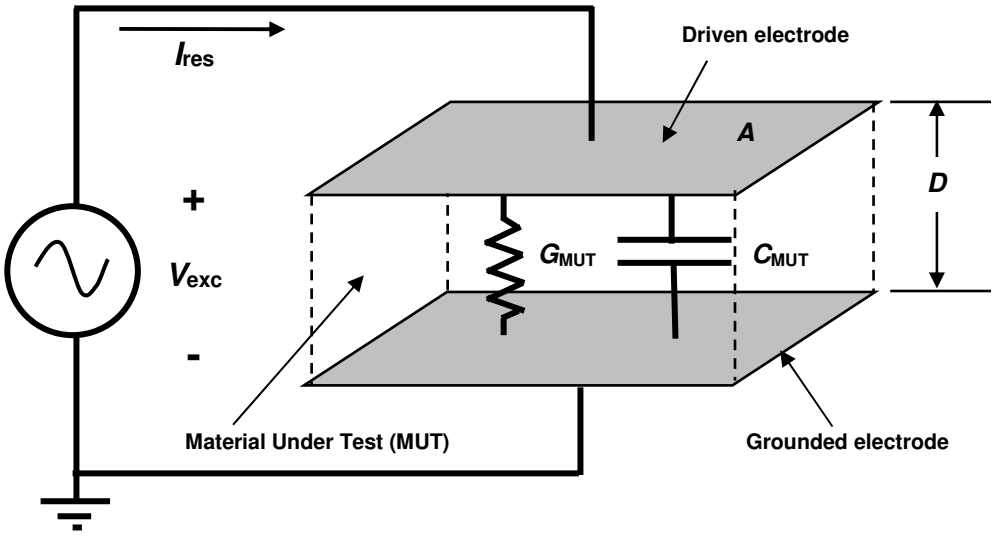

Figure 30-3
Electrical model of a polymer

It is easier to understand the electrical behavior of a polymer by considering Figure 30-4, which uses circuit components corresponding to the following physical phenomena:

- Flow of ions
    - Ion current in an electric field is determined by mobility in the polymer network
    - Current is frequency independent to first order in common polymers
    - Modeled by conductance G_{ion}

- Rotation of induced dipoles
  - Induced dipoles result from charge separation on nonpolar bonds
  - Induced dipoles rotate in an electric field without energy loss
  - Rotation has a frequency independent response
  - Modeled by capacitance $C_{induced}$
- Rotation of static dipoles
  - Static dipoles result from charge separation on molecules
  - Static dipoles rotate in an electric field with energy loss from friction
  - Rotation has a frequency dependent response with relaxation time τ
  - Modeled by conductance G_{static} in series with capacitance C_{static}

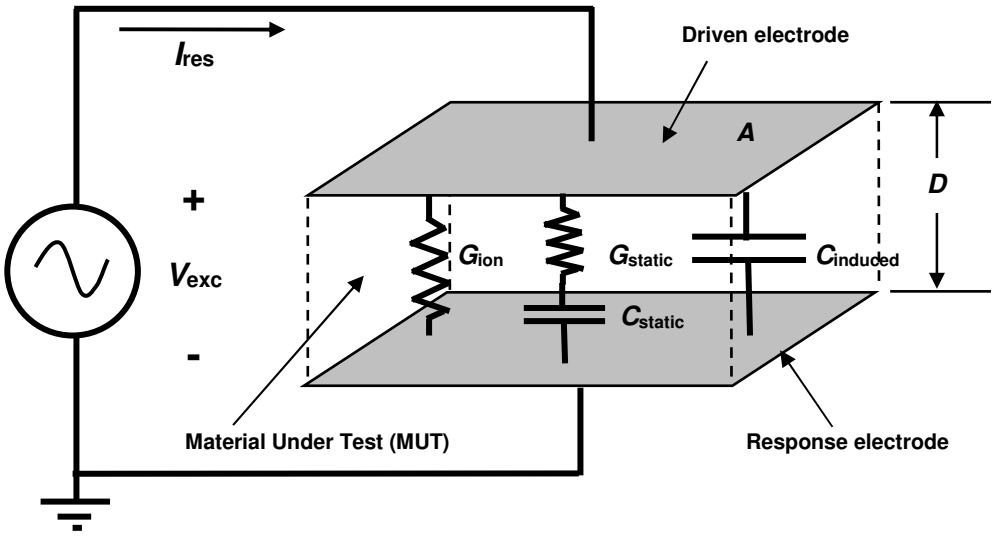

Figure 30-4
Electrical model of polymer physical behavior

It is possible to interpret the model of Figure 30-4 in terms of the measured quantities of conductance G_{MUT} and C_{MUT}. From circuit theory, the admittance of Figure 30-4 is given by equation 30-11:

(eq. 30-11) $Y_{MUT} = G_{ion} + i\omega C_{induced} + i\omega C_{static} /(1 + i\omega\tau)$

Where: $\tau = R_{static} C_{static}$ (dipole relaxation time)
$R_{static} = 1/G_{static}$

Admittance can be expressed by keeping real and imaginary terms together:

(eq. 30-12) $$Y_{MUT} = [G_{ion} + \omega^2\tau C_{static}/(1 + (\omega\tau)^2)] + i\omega[C_{induced} + C_{static}/(1 + (\omega\tau)^2)]$$

Combining equations 30-2 and 30-12 yields the following expressions for the measured bulk quantities:

(eq. 30-13) $G_{MUT} = G_{ion} + C_{static} [\omega^2 \tau /(1 + (\omega\tau)^2)]$

(eq. 30-14) $C_{MUT} = C_{induced} + C_{static}/(1 + (\omega\tau)^2)$

Combining equations 30-5, 30-6, 30-7 and 30-13 results in the expressions for conductivity, loss factor and relative dielectric constant:

(eq. 30-15) $\sigma_{MUT} = \sigma_{ion} + \varepsilon_{static} [\omega^2 \tau /(1 + (\omega\tau)^2)]$

(eq. 30-16) $\varepsilon''_{MUT} = \sigma_{ion}/(\omega\varepsilon_0) + [\varepsilon_{static} /\varepsilon_0][\omega \tau /(1 + (\omega\tau)^2)]$

(eq. 30-17) $\varepsilon'_{MUT} = (\varepsilon_{induced} /\varepsilon_0) + (\varepsilon_{static} /\varepsilon_0) /(1 + (\omega\tau)^2)$

At low frequencies the *relaxed relative permittivity* is the sum of dielectric constants due to both static and induced dipoles. At high frequencies the *unrelaxed relative permittivity* is due only to induced dipoles. They are defined as follows:

(eq. 30-18) $\varepsilon'_r = (\varepsilon_{static} + \varepsilon_{induced})/\varepsilon_0$ (relaxed relative permittivity)

(eq. 30-19) $\varepsilon'_u = \varepsilon_{induced} /\varepsilon_0$ (unrelaxed relative permittivity)

The relative dielectric constant resulting from static dipoles may be expressed in terms of the relaxed and unrelaxed relative dielectric constants by using equations 30-18 and 30-19:

(eq. 30-20) $$\varepsilon_{static}/\varepsilon_0 = \varepsilon'_r - \varepsilon'_u$$

Combining equations 30-16, 30-17, 30-19 and 30-20 yields equations for the dielectric response:

(eq. 30-21) $$\varepsilon''_{MUT} = \sigma_{ion}/\omega\varepsilon_0 + (\varepsilon'_r - \varepsilon'_u)\frac{\omega\tau}{1 + (\omega\tau)^2}$$

(eq. 30-22) $$\varepsilon'_{MUT} = \varepsilon'_u + \frac{\varepsilon'_r - \varepsilon'_u}{1 + (\omega\tau)^2}$$

Where: ε'_u = Unrelaxed (high frequency) relative permittivity
ε'_r = Relaxed (low frequency) relative permittivity
$\omega = 2\pi f$ (radians/s)
$\tau = R_{static} C_{static}$ (s)

Debye equations for dipolar rotation

Neglecting the ionic conductivity term, equations 30-21 and 30-22 also happen to be the loss factor and permittivity as expressed by the Debye equations, which describe the behavior of rotating dipoles. General admittance *Y* is given by equation 30-2, presented earlier:

(eq. 30-2) $$Y = G + i\omega C$$

Equation 30-2 may be rearranged to define admittance as a complex admittance $i\omega C^*$:

(eq. 30-23) $$i\omega C^* = i\omega(C - iG/\omega)$$

Dividing both sides of equation 30-23 by $i\omega\varepsilon_0$ and the *A*/*D* ratio yields a complex permittivity ε^*:

(eq. 30-24) $$\varepsilon^* = \varepsilon' - i(\sigma/\varepsilon_0\omega)$$

Finally, from the definition of loss factor (eq. 30-7), the complex permittivity may be expressed as follows:

(eq. 30-25) $$\varepsilon^* = \varepsilon' - i\varepsilon''$$

The classic Debye equation for dielectric relaxation, as a complex number and function of frequency, is:

(eq. 30-26) $$\varepsilon^*(\omega) = \varepsilon'_u + \frac{\varepsilon'_r - \varepsilon'_u}{1 + i\omega\tau}$$

Where: ε'_u = Unrelaxed (high frequency) relative permittivity
ε'_r = Relaxed (low frequency) relative permittivity
$\omega = 2\pi f$ (radians/s)
τ = Dipole relaxation time (s)

Separating real and imaginary components of equation 30-26 yields the Debye equations for loss factor and relative permittivity:

(eq. 17-27) $$\varepsilon'' = \mathrm{Im}(\varepsilon^*(\omega)) = \frac{(\varepsilon'_r - \varepsilon'_u)\,\omega\tau}{1 + (\omega\tau)^2}$$

(eq. 17-28) $$\varepsilon' = \mathrm{Re}(\varepsilon^*(\omega)) = \varepsilon'_u + \frac{\varepsilon'_r - \varepsilon'_u}{1 + (\omega\tau)^2}$$

Loss factor ε'' and relative permittivity ε' are plotted as a function of $\omega\tau$ in Figure 30-5. The loss peak and the inflection point of relative permittivity both occur at $\omega\tau = 1$.

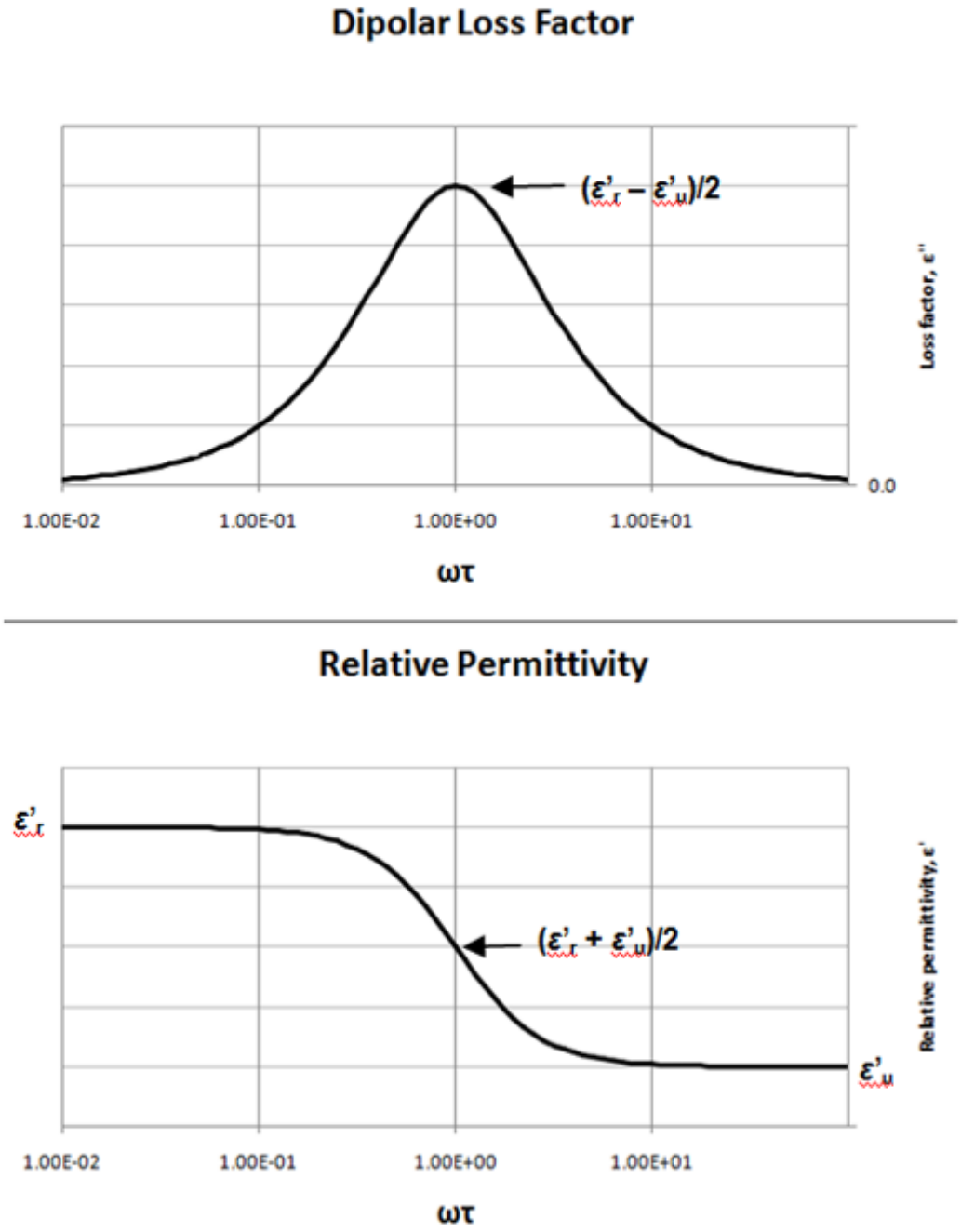

Figure 30-5
Debye relaxation behavior for loss factor and relative permittivity

A common diagram is the Cole-Cole plot shown in Figure 30-6. When loss factor is plotted vs. permittivity, the Debye equations form a semi-circle. This

ideal behavior results from the assumption of a single dipolar time constant τ. In reality, a single relaxation time does not account for the effect of molecular weight distributions, varying locations along a polymer chain or the environment .

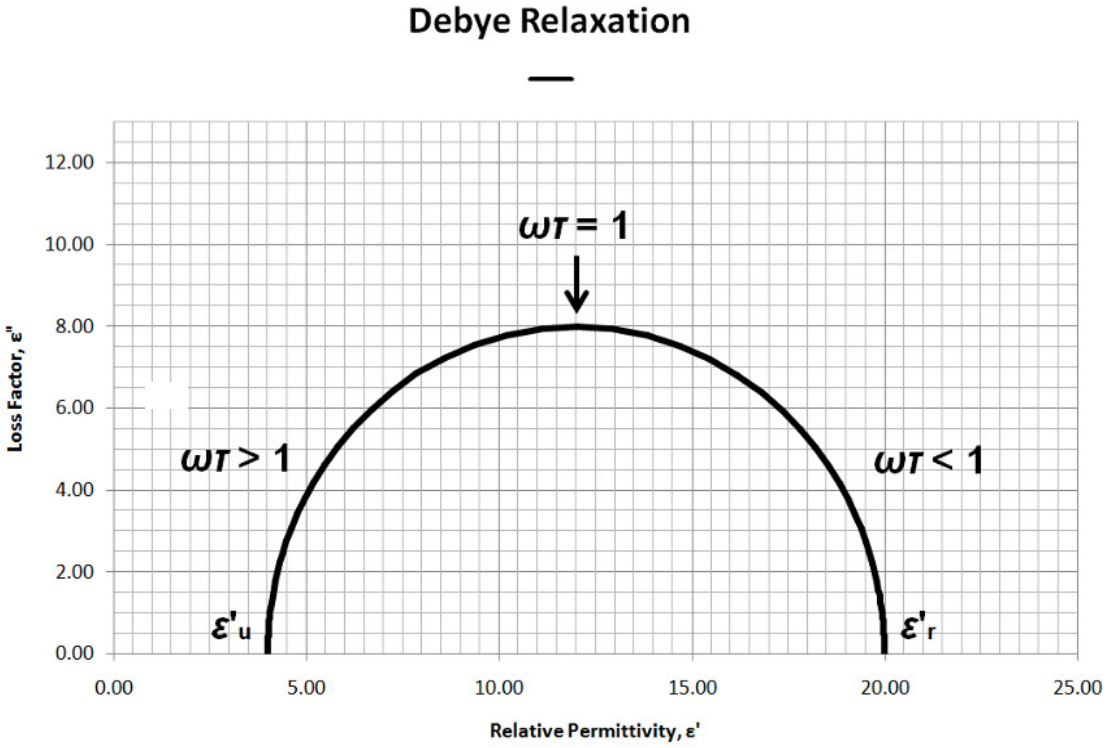

Figure 30-6
Cole-Cole plot of Debye relaxation

Variants of the Debye equations

In polymers and thermosets, it is common to find non-ideal dipole relaxation behavior, resulting in Cole-Cole plots that are squashed compared to the semi-circle of the Debye equations. This response has been attributed to the superposition of a range of relaxation times. The Cole-Cole plot may also be asymmetric, supposedly corresponding to asymmetric distributions of relaxation times.

Three common variants of the Debye equations attempt to empirically model non-ideal dipole behavior:

- Cole-Cole relaxation[1,2] (squashed plots)

(eq. 30-29)
$$\varepsilon^*(\omega) = \varepsilon'_u + \frac{\varepsilon'_r - \varepsilon'_u}{1 + (i\omega\tau)^{1-\alpha}} \qquad (0 \le \alpha \le 1)$$

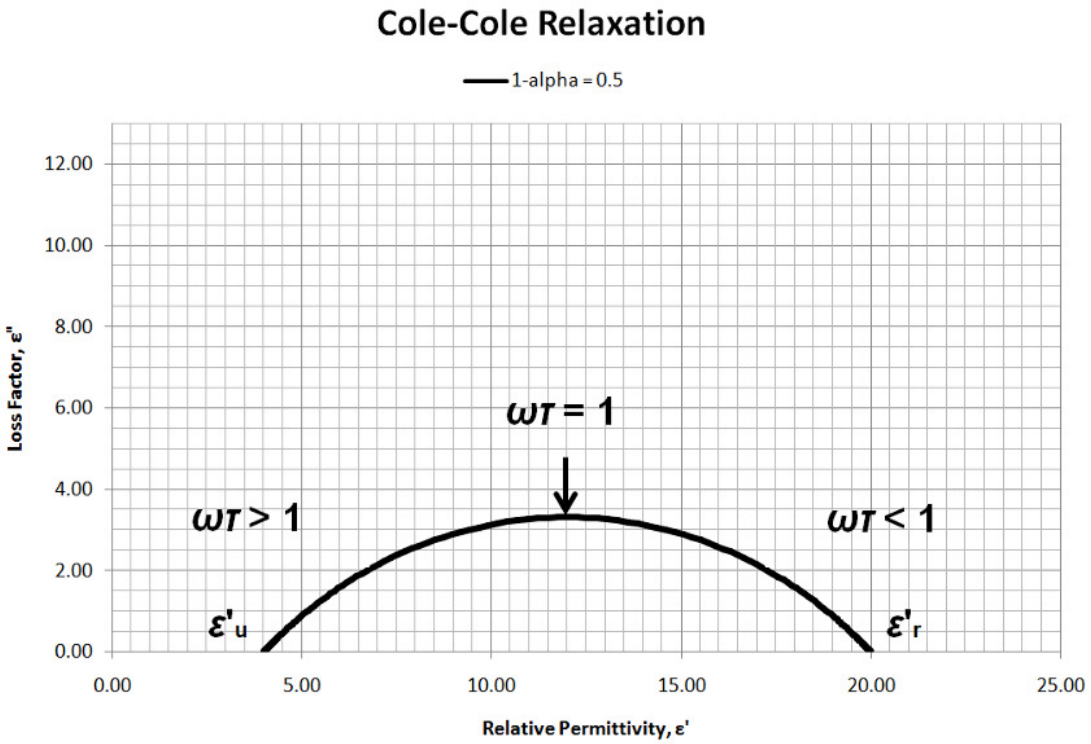

Figure 30-7
Cole-Cole plot of Cole-Cole relaxation

- Cole-Davidson[3] relaxation (asymmetric plots)

(eq. 30-30) $$\varepsilon^*(\omega) = \varepsilon'_u + \frac{\varepsilon'_r - \varepsilon'_u}{(1 + i\omega\tau)^\beta} \qquad (0 \le \beta \le 1)$$

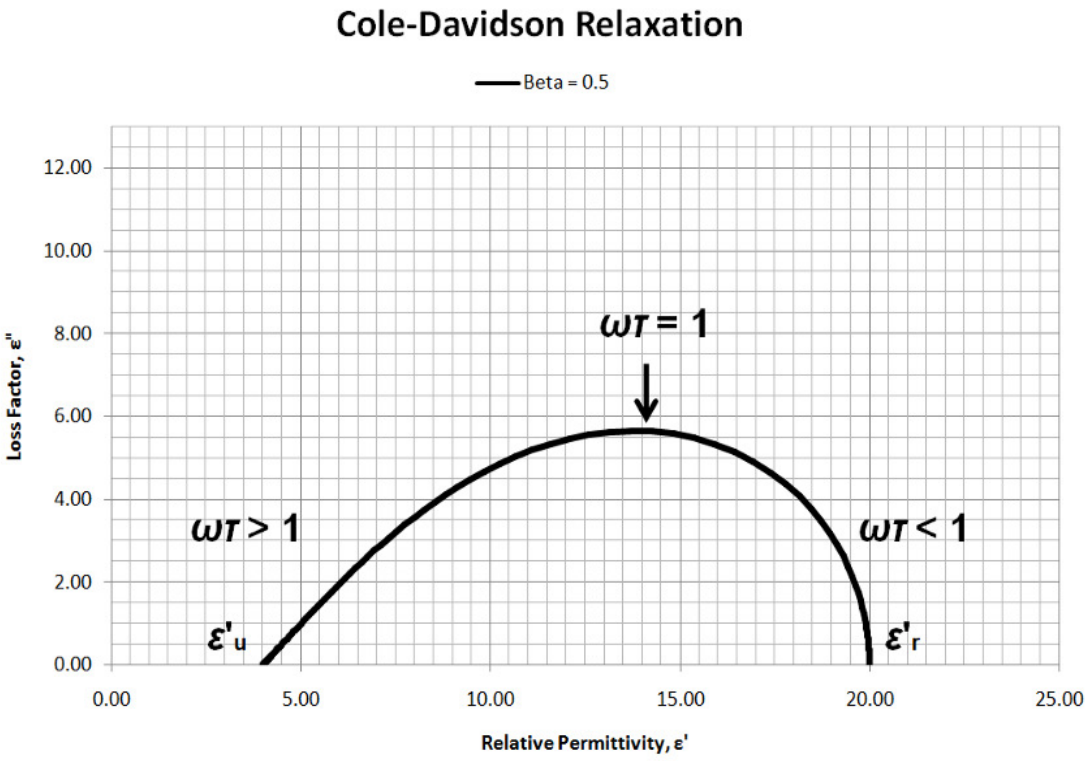

Figure 30-8
Cole-Cole plot of Cole-Davidson relaxation

- Havriliak-Negami relaxation[4] (squashed and asymmetric plots)

(eq. 30-31)
$$\varepsilon^*(\omega) = \varepsilon'_u + \frac{\varepsilon'_r - \varepsilon'_u}{(1 + (i\omega\tau)^{\alpha})^{\beta}} \qquad \begin{matrix} (0 \le \alpha \le 1) \\ \text{and} \\ (0 \le \beta \le 1) \end{matrix}$$

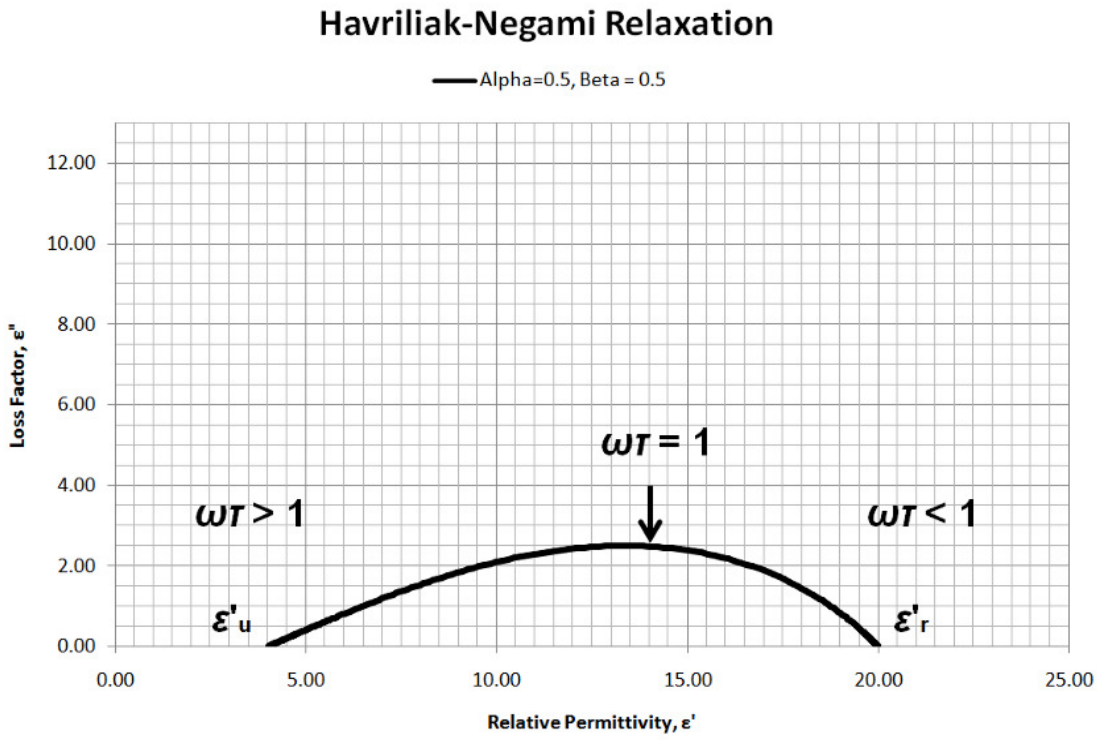

Figure 30-9
Cole-Cole plot of Havriliak-Negami relaxation

The Havriliak-Negami equation is simply a combination of the Cole-Cole and Cole-Davidson equations. If β = 1, then the result is Cole-Cole behavior. If α = 1, then the result is Cole-Davidson behavior. If both α =1 and β = 1, then the Havriliak-Negami relaxation reduces to Debye relaxation.

The Havriliak-Negami relaxation of equation 30-31 may be factored into imaginary and real terms to yield expressions for loss factor and relative permittivity:

(eq. 30-32) $\varepsilon'' = (\varepsilon'_r - \varepsilon'_u)\,(1 + 2(\omega\tau)^{\alpha}\cos(\pi\alpha/2) + (\omega\tau)^{2\alpha})^{-\beta/2}\sin(\beta\theta)$

(eq. 30-33) $\varepsilon' = \varepsilon'_u + (\varepsilon'_r - \varepsilon'_u)\,(1 + 2(\omega\tau)^{\alpha}\cos(\pi\alpha/2) + (\omega\tau)^{2\alpha})^{-\beta/2}\cos(\beta\theta)$

Where:

(eq. 30-34) $\theta = \tan^{-1}[(\omega\tau)^{\alpha}\sin(\pi\alpha/2) / (1 + (\omega\tau)^{\alpha}\cos(\pi\alpha/2))]$

α = Empirical "broadness" parameter

β = Empirical "asymmetry" parameter

ε'_u = Unrelaxed (high frequency) relative permittivity

ε'_r = Relaxed (low frequency) relative permittivity

ω = $2\pi f$ (radians/s)

τ = Dipole relaxation time (s)

Contribution of ionic conduction to loss factor

Pure dielectric materials show only the Debye-type dipolar relaxation behavior; however, in reality almost all materials have some ionic content or impurity. The presence of mobile ions adds an ionic conduction term to loss factor, as seen in equation 30-21, repeated below:

(eq. 30-21) $$\varepsilon''_{MUT} = \sigma_{ion}/\omega\varepsilon_0 + (\varepsilon'_r - \varepsilon'_u)\frac{\omega\tau}{1 + (\omega\tau)^2}$$

In the case of equation 30-21, dipole relaxation is expressed with the Debye equation. More generally, loss factor may be expressed as the sum of ionic and dipolar loss factors, which is plotted in Figure 30-10:

(eq. 30-35) $$\varepsilon''_{MUT} = \varepsilon''_{ion} + \varepsilon''_{dipole}$$

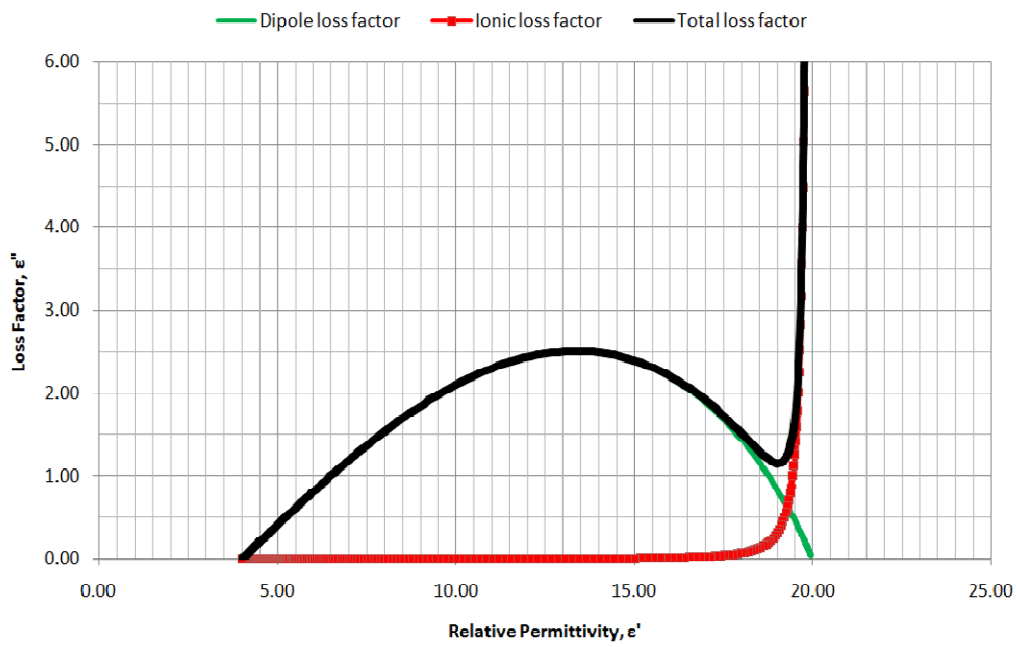

Figure 30-10
Addition of ionic and dipolar loss factors

Alternatively, the total loss factor is the sum of terms with frequency independent conductivity (σ_{DC}) and frequency dependent conductivity (σ_{AC}):

(eq. 30-36) $$\varepsilon''_{MUT} = (\sigma_{DC} + \sigma_{AC})/\omega\varepsilon_0$$

Where:

$$\sigma_{DC} = \sigma_{ion}$$

$$\sigma_{AC} = \varepsilon_0 (\varepsilon'_r - \varepsilon'_u) \frac{\omega^2 \tau}{1 + (\omega\tau)^2}$$

As ionic conductivity increases, the effect on a Cole-Cole plot is shown in Figure 30-11:

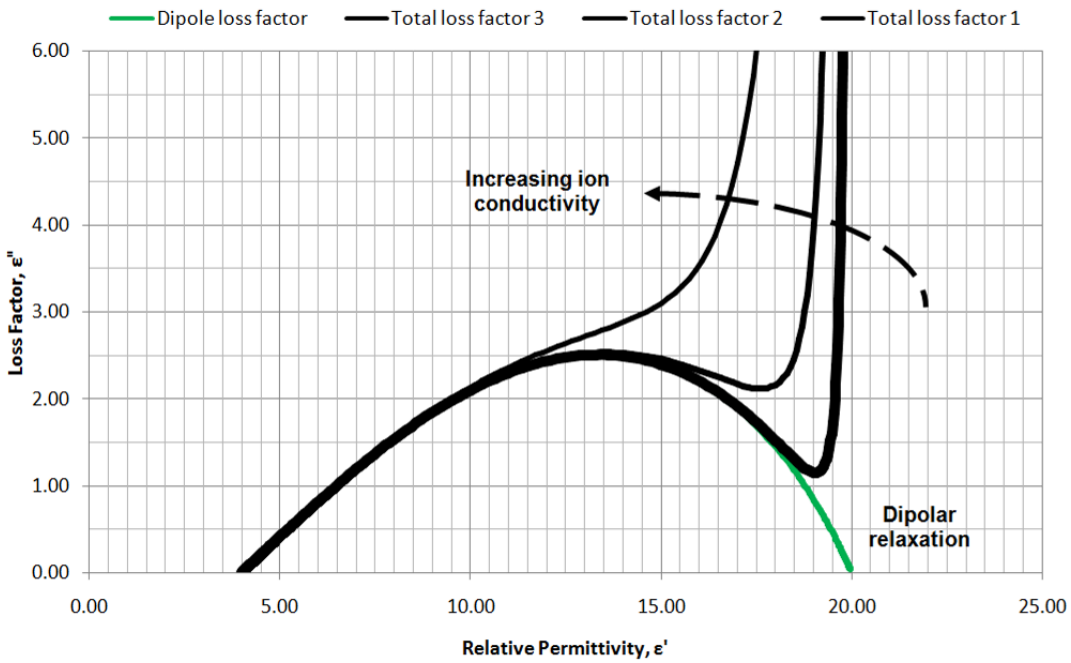

Figure 30-11
Total loss factor as a function of increasing ionic conductivity

When loss factor is plotted as a function of frequency, it is easier to see the relative contributions from ionic conductivity and dipolar relaxation. Dielectric measurements measure total loss factor, and information from a single frequency cannot separate the effects of ions and dipoles. If conductivity is sufficiently low, however, a frequency sweep can reveal the dipole loss peak, as shown in Figures 30-12a,b for low and intermediate conductivities. Note that high conductivity in Figure 30-12c has hidden the dipole peak.

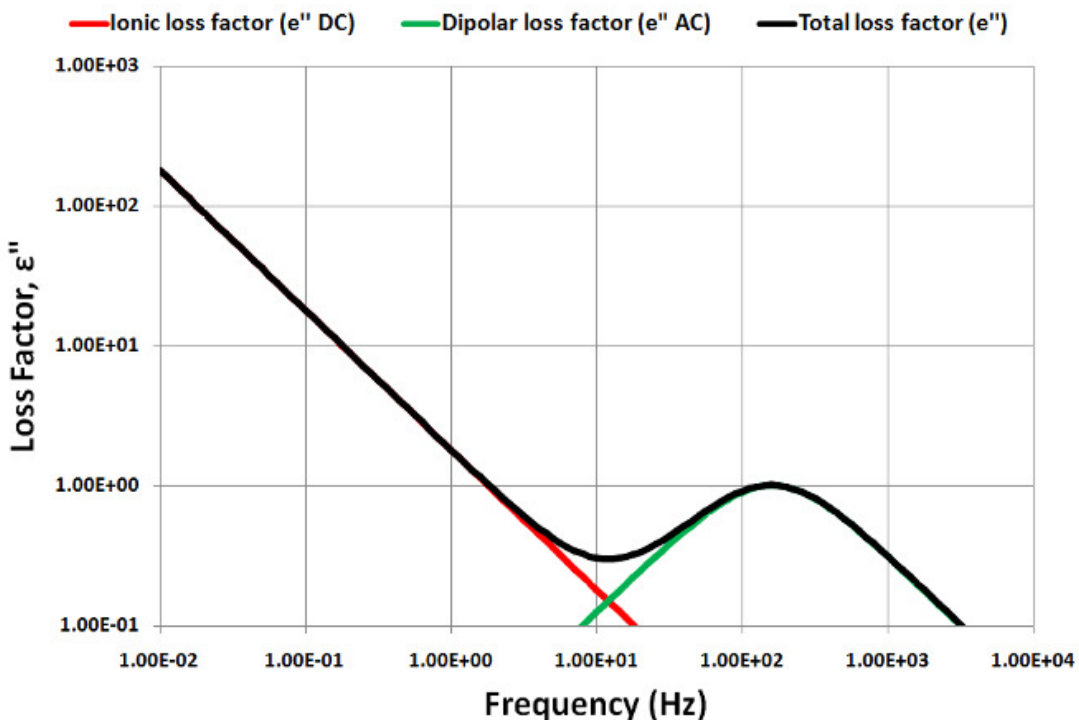

Figure 30-12a
Effect of low conductivity on loss factor (modeled)

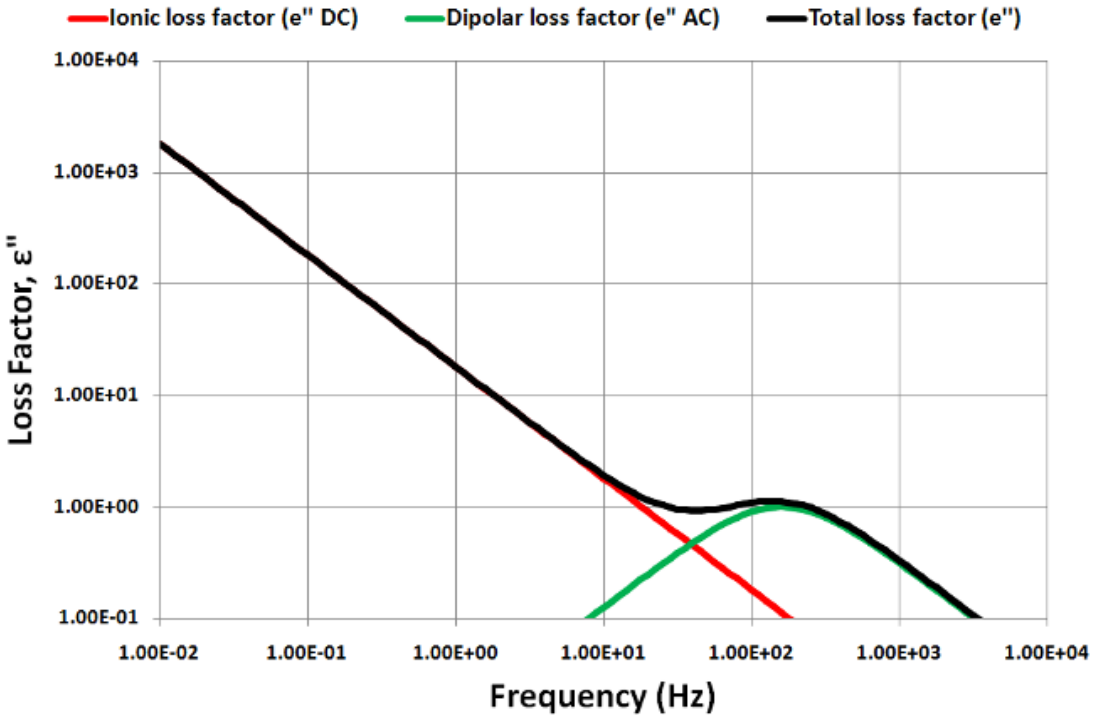

Figure 30-12b
Effect of intermediate conductivity on loss factor (modeled)

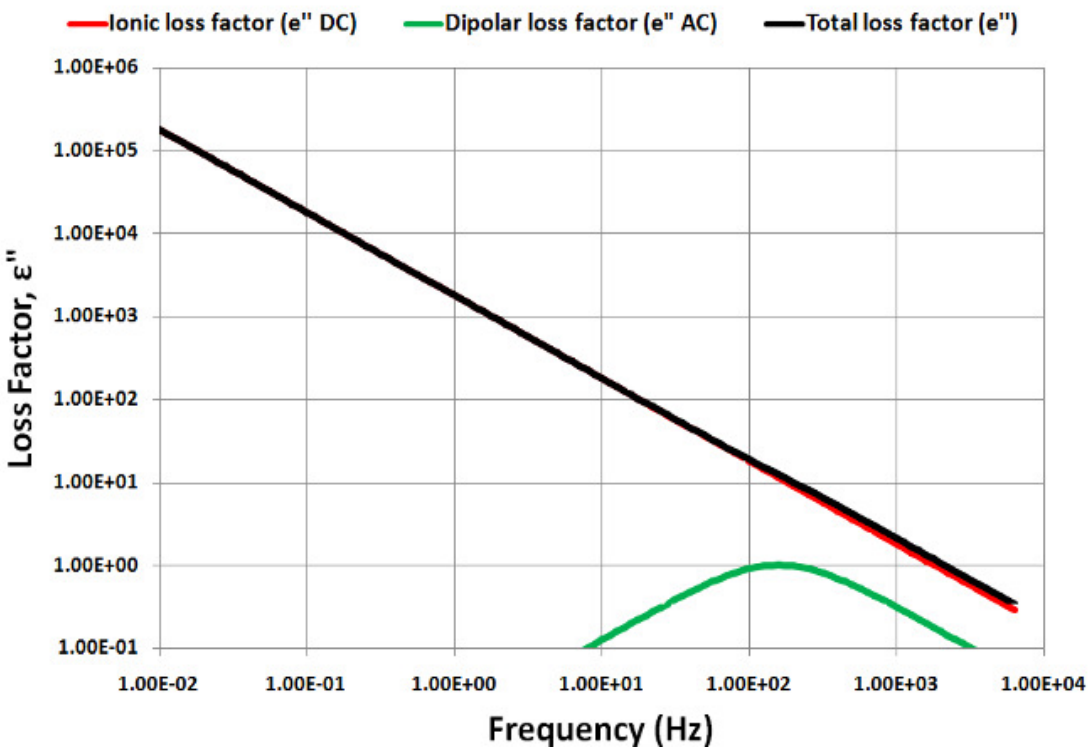

Figure 30-12
Effect of high conductivity on loss factor (modeled)

As these plots illustrate, loss factor due to ions always dominates the response at sufficiently low frequencies. Dielectric cure monitoring takes advantage of this behavior to measure ionic conductivity without the influence of dipoles.

The amount of polymerization determines mechanical viscosity, free ion mobility and therefore electrical conductivity up to the gel point. The amount of crosslinking determines modulus and continues to affect conductivity after the gel point. As a result, measurements of frequency independent conductivity σ_{DC} can probe the cure state of a material. Uniquely, dielectric measurements can observe the state of cure in-situ and in real time.

Electrode polarization and the low frequency response of boundary layers

The presence of mobile ions in a polymer does not affect how its dipoles rotate. Therefore the frequency response of relative permittivity should not depend on the amount of ionic conductivity. Figure 30-13 shows this ideal behavior for relative permittivity—which is the same at low, intermediate and high conductivities—for the example modeled in Figure 30-12.

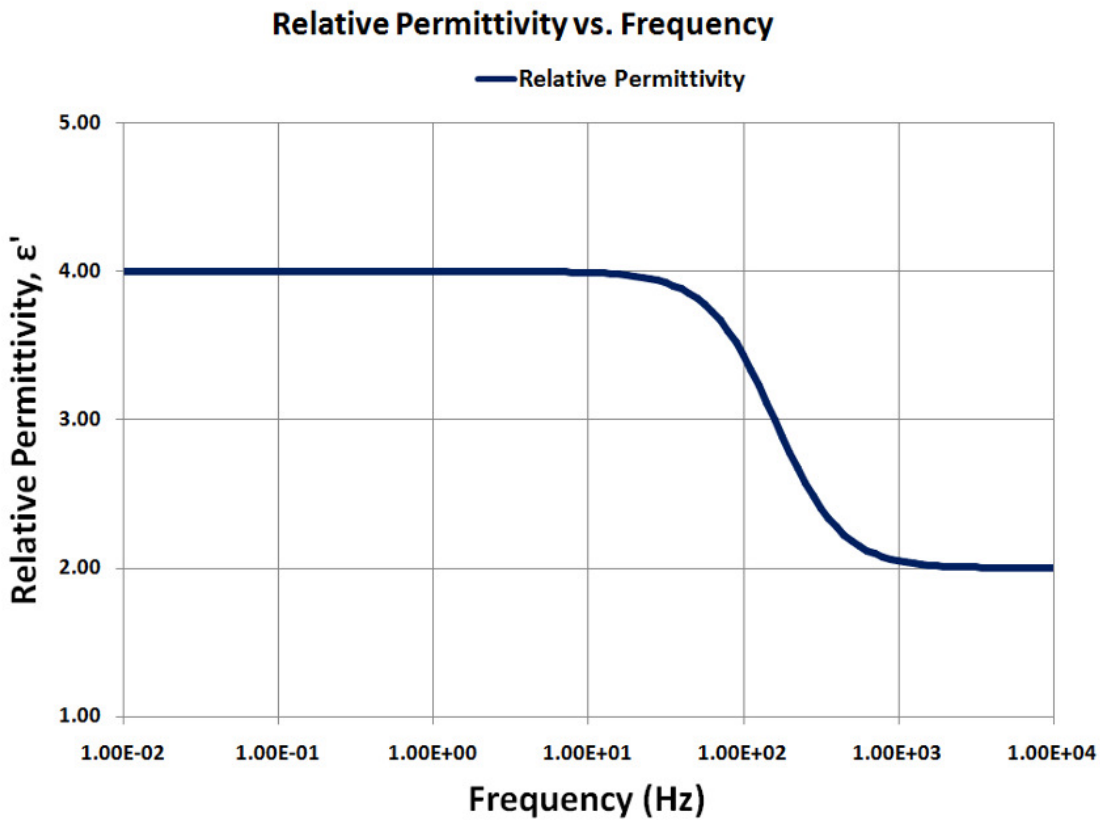

Figure 30-13
Ideal frequency response of relative permittivity
(Corresponding to example modeled in Figure 30-12)

Actual dielectric measurements of polymers usually reveal very large increases in permittivity at low frequencies or high conductivities. This behavior differs significantly from the Debye response and is *not* caused by a true change in permittivity. Instead, it is the result of an interaction between the material and the electrodes used to make measurements.

When a polymer has very high loss factor, ions accumulate at the electrode, where they are not exchanged because of an electrically insulating layer, such as a film or oxide or electrochemical potential barrier. This phenomenon is called *electrode polarization*. A boundary layer forms, depleted of ions, and only the dipolar response remains. As a result, the boundary layer acts as a capacitor in series with the bulk material.

In the presence of electrode polarization, very high permittivities result from use of the model of Figure 30-4, which is incorrect for the situation. The correct model of Figure 30-14 and the corresponding circuit of Figure 30-15 must be used, instead.

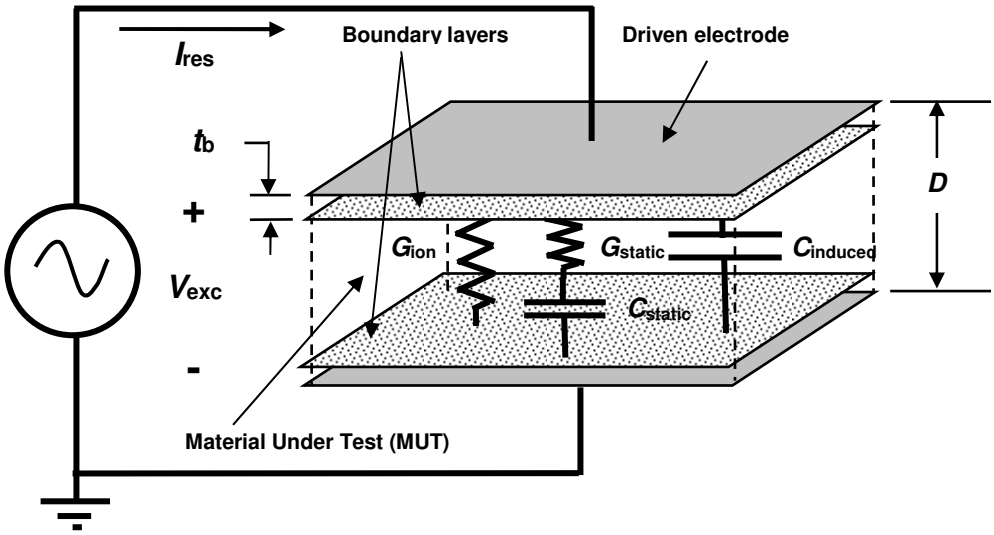

Figure 30-14
Boundary layer capacitances resulting from electrode polarization

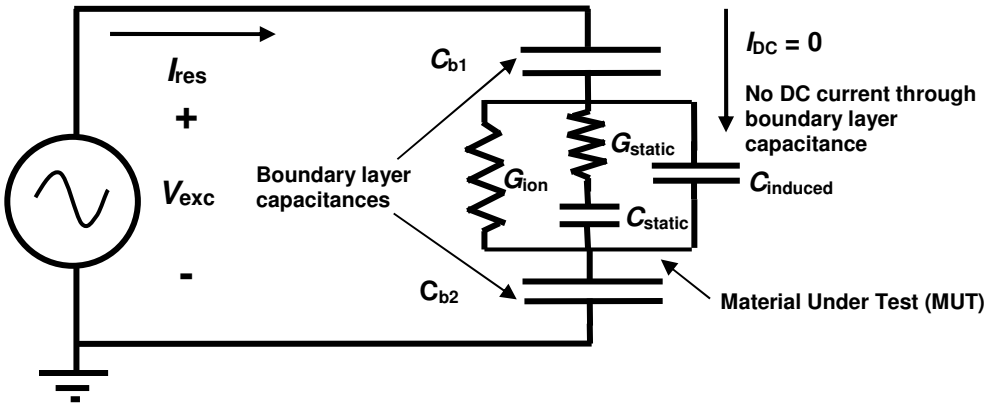

Figure 30-15
Circuit model of polymer with boundary layer capacitances

The boundary layer is very thin compared to the separation between electrodes. Consequently, boundary layer capacitance is much larger than bulk capacitance. The boundary layer capacitance dominates the circuit response and acts as an open circuit to block DC current. Measurements of DC conductance are impossible in this case and the material appears insulating or capacitive.

The low frequency electrical circuit of Figure 30-16 may be used to understand the resulting dielectric response. Here the two boundary layer

capacitances, which are in series, have been combined into a single component with half the capacitance $C_b/2$. At low frequencies the admittances of capacitances due to static and induced dipoles are very low and only the conductive component G_{ion} contributes significantly to the response. This configuration is the same as the circuit representing the behavior of dipoles (G_{static} in series with C_{static} of Figure 30-4), and would have behavior similar to Debye relaxation.

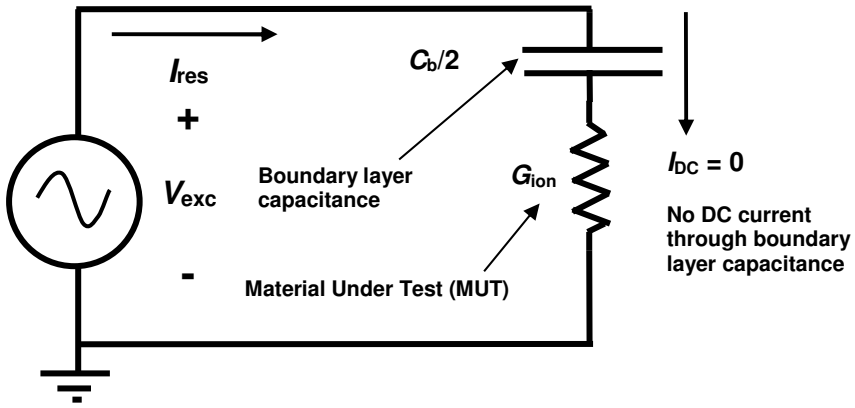

Figure 30-16
Low frequency circuit model with boundary layer capacitance

The uncorrected relative permittivity and loss factor resulting from electrode polarization are given by the following equations[5]:

(eq. 30-37) $$\varepsilon'_x = \varepsilon' \left(D / 2t_b\right) \frac{(\varepsilon''/\varepsilon')^2 + (D / 2t_b)}{(\varepsilon''/\varepsilon')^2 + (D / 2t_b)^2)}$$ Apparent relative permittivity

(eq. 30-38) $$\varepsilon''_x = \varepsilon'' \left(D / 2t_b\right) \frac{(D / 2t_b) - 1}{(\varepsilon''/\varepsilon')^2 + (D / 2t_b)^2)}$$ Apparent loss factor

Where:
- t_b = boundary layer thickness
- D = distance between electrodes or plate separation
- ε' = actual permittivity
- ε'' = actual loss factor

At low loss factors (high frequencies or low conductivities), electrode polarization has little effect on either the measured permittivity or loss factor. At

sufficiently high loss factors, however, the apparent permittivity begins to increase, causing loss factor on the Cole-Cole plot of Figure 30-17 to deviate from its ideal, vertical trajectory.

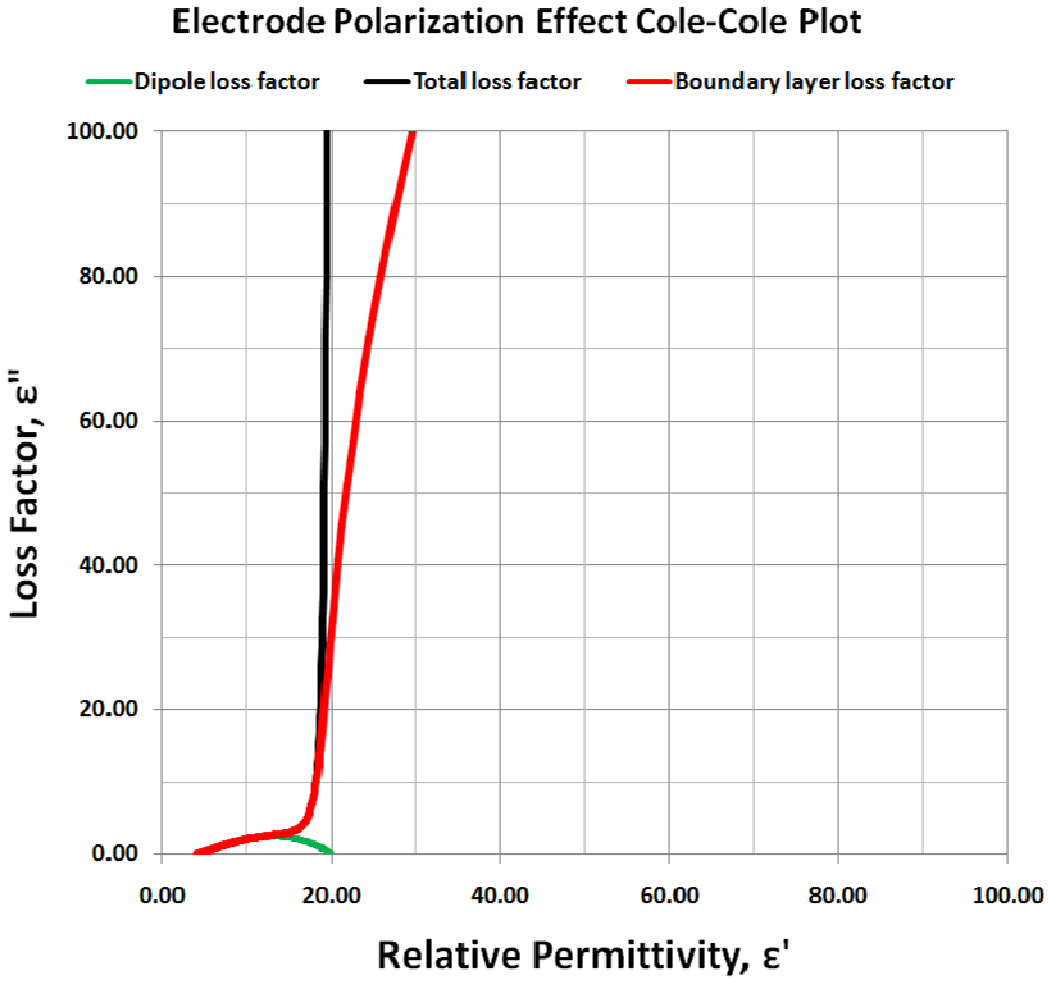

Figure 30-17
Deviation of Cole-Cole plot trajectory caused by electrode polarization

As the *true* material loss factor increases even further, the *apparent* permittivity continues to increase and at some point the *apparent* loss factor actually begins to decrease. The Cole-Cole plot becomes the arc of Figure 30-18. Eventually, when the true loss factor is high enough (i.e. frequency is sufficiently low or conductivity is sufficiently high), the apparent permittivity reaches a very high limit and the apparent loss factor approaches zero. The result is a semi-circle on the Cole-Cole plot like that produced by the Debye relaxation, but with a much larger radius. This radius depends on the thickness of the boundary layer relative to the separation between electrodes.

Because of electrochemical potential barriers, electrode polarization almost always occurs. If the resulting boundary layer is very thin, the effect on loss factor is reduced, and the radius of the Cole-Cole plot is very large. While the change in apparent loss factor may be small, the change in apparent relative permittivity usually remains significant.

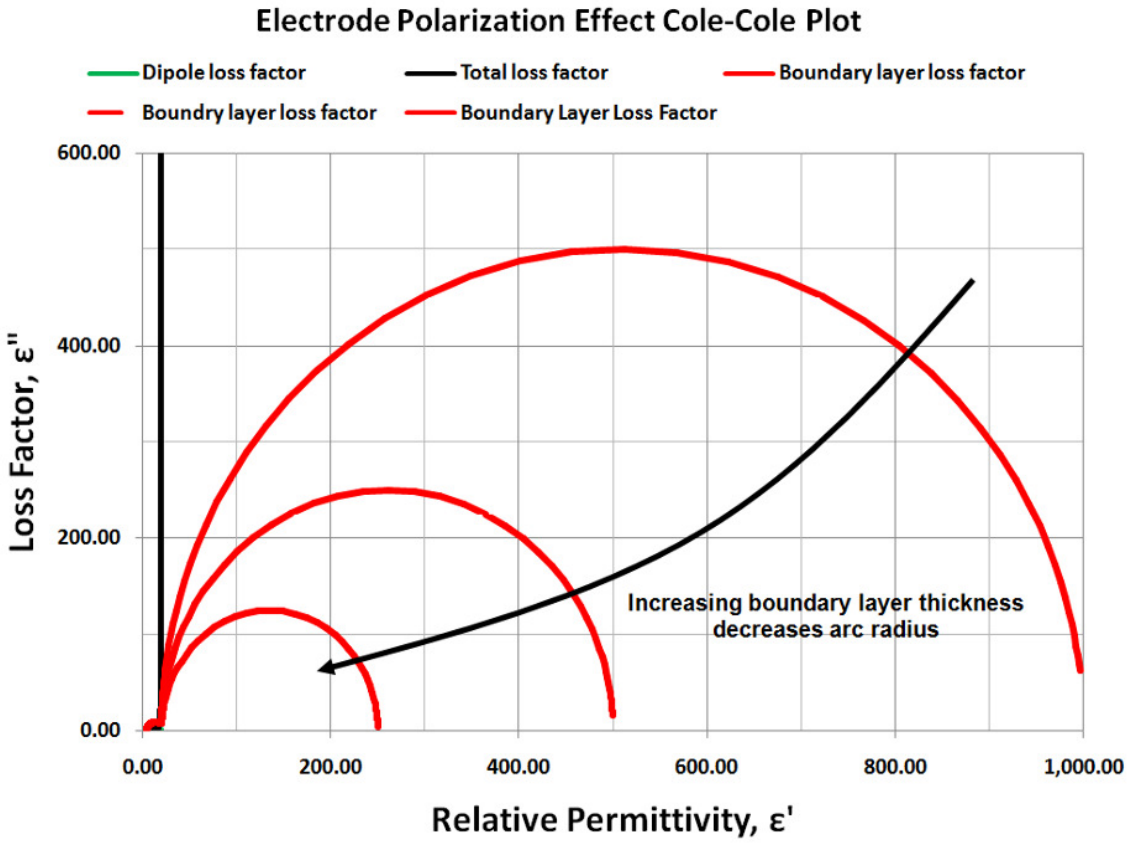

Figure 30-18
Cole-Cole plot trajectories caused by electrode polarization

Figure 30-19 compares the frequency response of true permittivity, which has a Debye-type relaxation, with the apparent permittivity resulting from a boundary layer. In this case the modeled behavior demonstrates how the relative relationship between the dipolar and the boundary layer time constants determines visibility of the dipole relaxation.

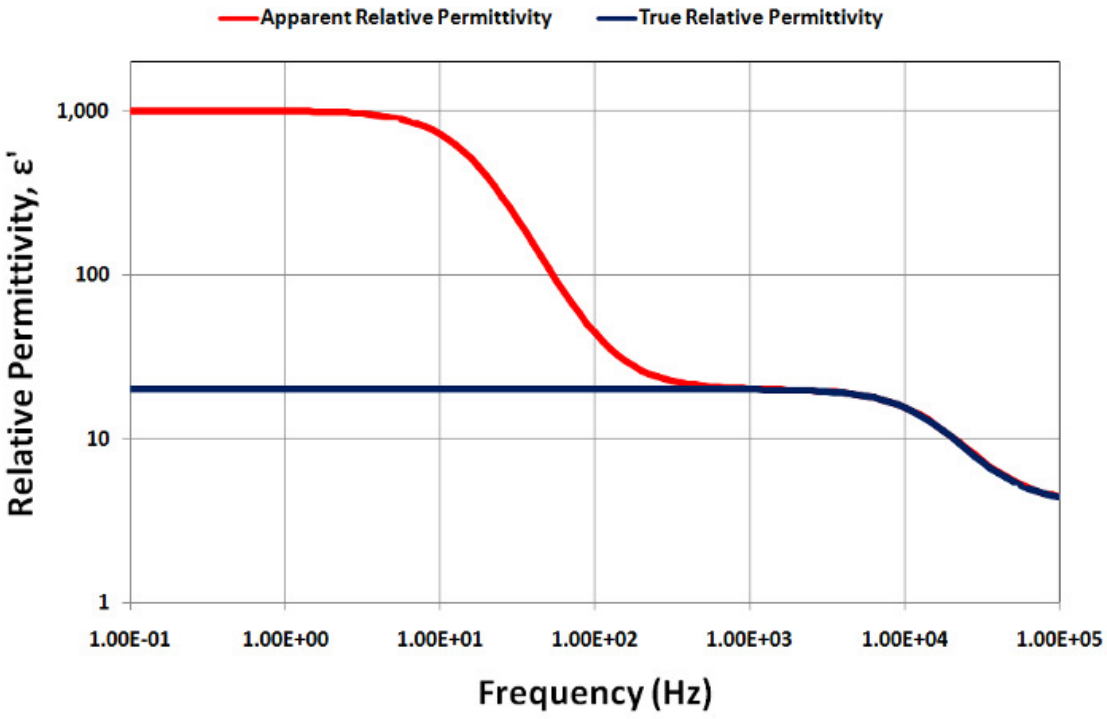

Figure 30-19a

ε′ with electrode polarization and small dipole time constant

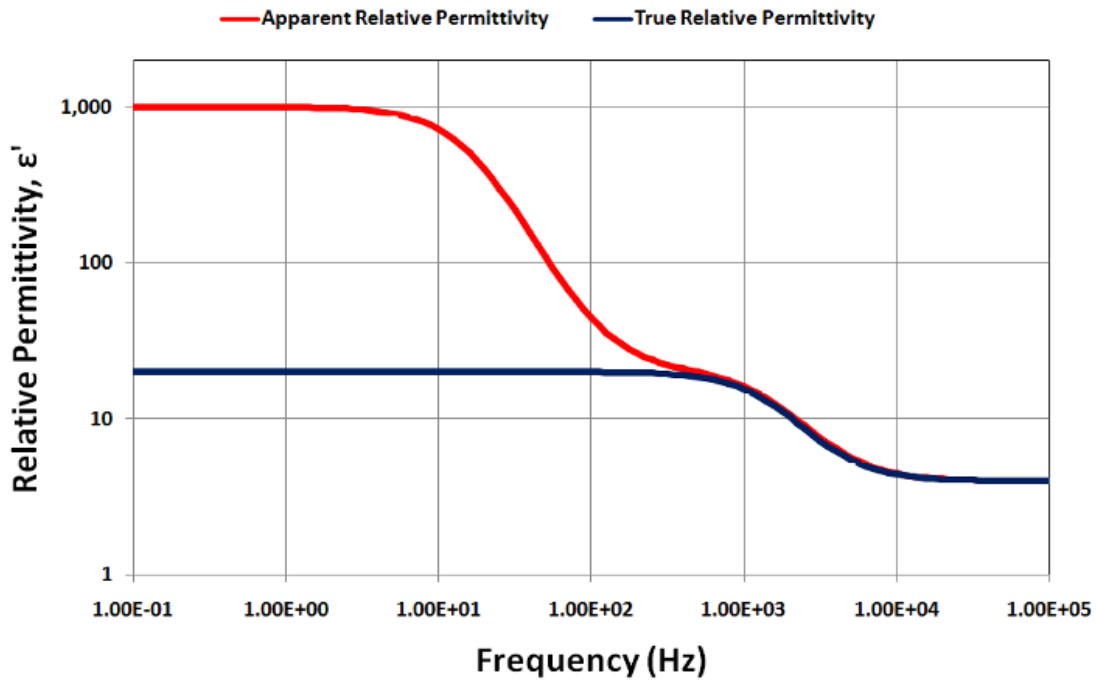

Figure 30-19b

ε′ with electrode polarization and intermediate dipole time constant

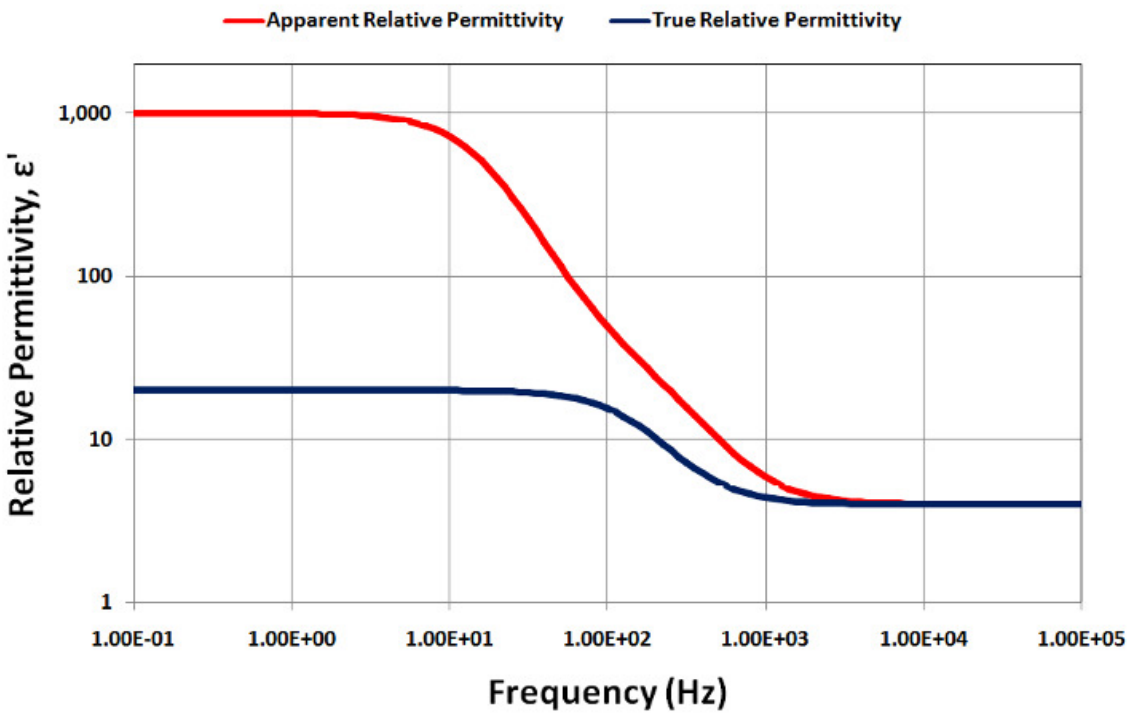

Figure 30-19c

ε′ with electrode polarization and large dipole time constant

Under the same conditions modeled in Figure 30-19, Figure 30-20 compares the frequency response of true loss factor with the apparent loss factor resulting from a boundary layer. Note that the apparent loss factor has a peak with very high value at very low frequency, while true loss factor does not. In the past this artificial loss peak has been attributed to a large dipole relaxation. The differences between dipole and boundary layer loss peaks are:[6]

- Dipole loss peaks for most polymers are rarely greater than 3 and almost never greater than ~10
- Boundary layer loss peaks are usually greater than ~100
- Boundary layer loss peaks vary with electrode separation, while dipole loss peaks do not

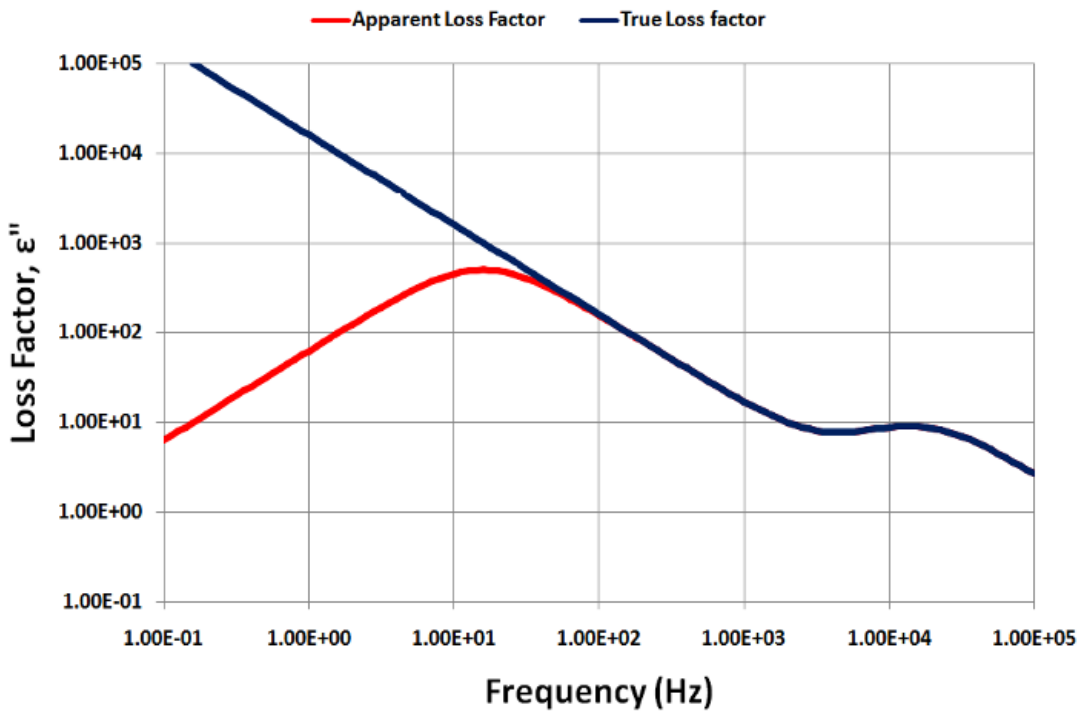

Figure 30-20a

ε″ with electrode polarization and small dipole time constant

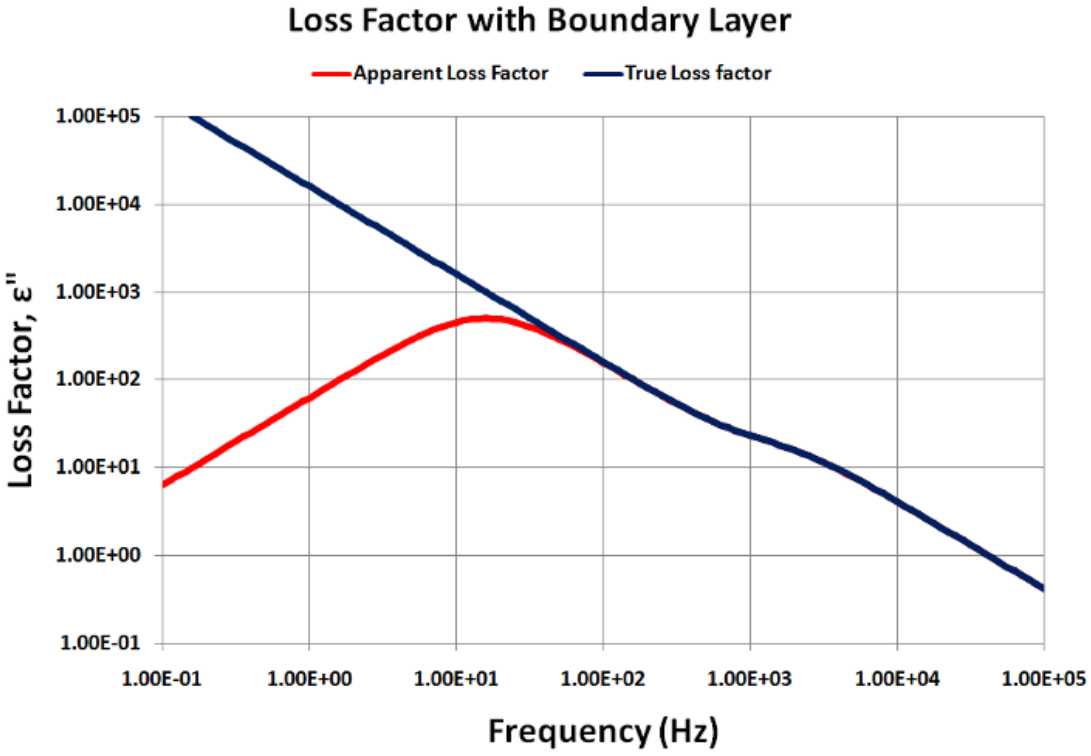

Figure 30-20b

ε″ with electrode polarization and intermediate dipole time constant

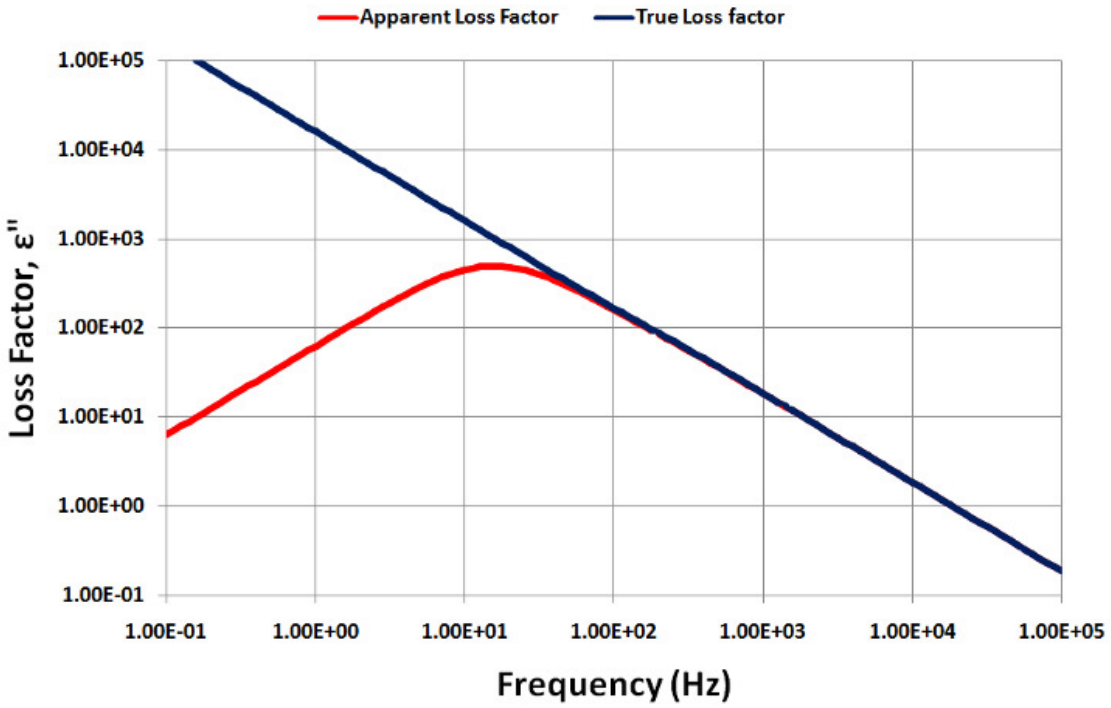

Figure 30-20c

ε″ with electrode polarization and large dipole time constant

Figures 30-21 and 30-22 show the effect of boundary layers on apparent dielectric properties during cure of "five-minute" epoxy. In this case, unlike for Figures 30-19 and 30-20, permittivity and loss factor are changing with both time and temperature.

The curing reaction is exothermic and temperature increases at first, which causes viscosity to decrease. Consequently, both conductivity and loss factor increase during this initial period. After a certain time, temperature is high enough for the accelerating reaction rate to dominate—viscosity begins to increase because the amount of polymerization overcomes the decrease in viscosity due to temperature. At this point conductivity and loss factor also decrease.

After loss factor reaches its peak, it declines to approach a constant value at the end of cure. For frequencies of 10 Hz or greater, this peak in loss factor is well behaved. For 1 Hz, however, the boundary layer effect distorts loss factor by depressing the peak and creating two satellite peaks in its place. Before researchers understood electrode polarization in polymers, the second satellite peak was thought to coincide with gelation. In fact, these peaks are artifacts of an incorrect electrical model. Fortunately, in many cases it is possible to

mathematically correct the distortion caused by boundary layers (See Chapter 29, *Electrode Polarization and Boundary Layer Effects*).

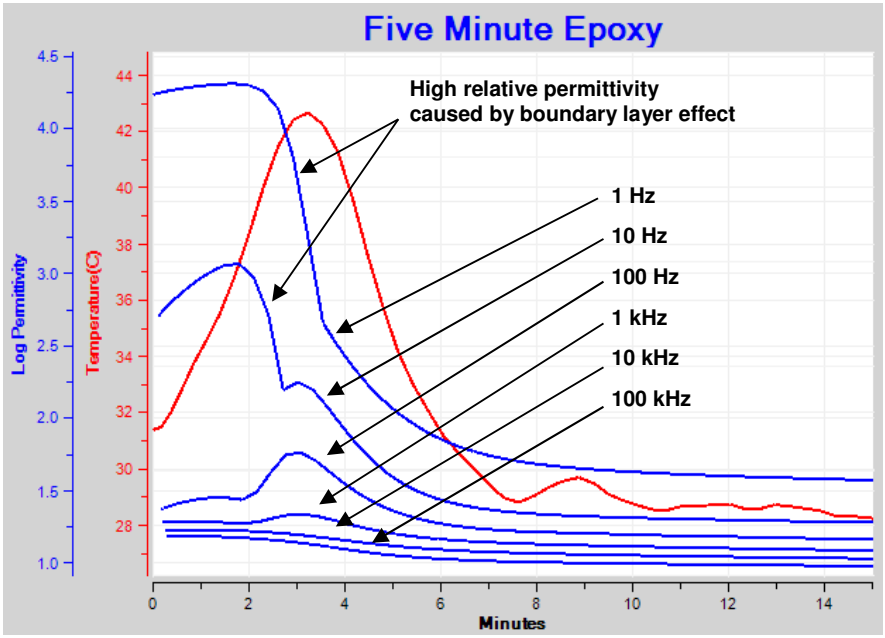

Figure 30-21
Relative permittivity of curing epoxy, showing effect of boundary layer

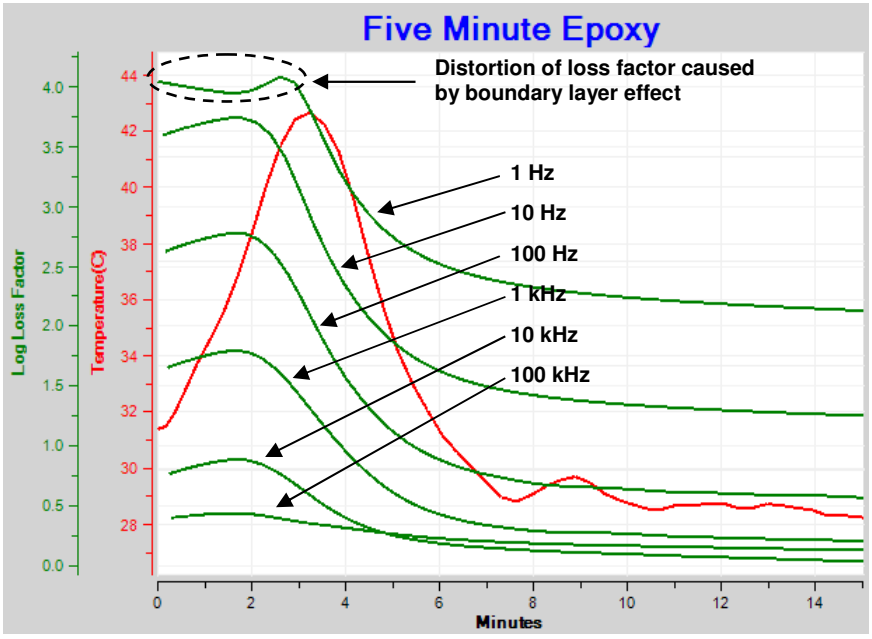

Figure 30-22
Loss factor of curing epoxy, showing effect of boundary layer

For this epoxy, relative permittivity has a clear Debye-type relaxation visible at 100 kHz and 10 kHz. At 1 kHz and 100 Hz, relative permittivity displays a peak, which is caused by the temperature response of permittivity. Note that maximum permittivity coincides with the maximum temperature of this test. At 10 Hz the boundary layer effect artificially increases apparent permittivity and partially hides this peak in permittivity. Finally, at 1 Hz the boundary layer dominates completely and relative permittivity exceeds 10,000 at its maximum—a completely unrealistic value.

Inhomogeneities and Maxwell-Wagner-Sillars polarization

Until now this chapter has discussed only homogeneous polymers. The electrical response, however, is not as straightforward with multi-layer films, fiberglass composites or materials with several phases. The Maxwell-Wagner-Sillars[7,8] effect (sometimes simply called the Maxwell-Wagner effect) describes dielectric behavior resulting from charge accumulation at the boundaries of inhomogeneities. The Maxwell-Wagner-Sillars model uses small spheres embedded in an infinite dielectric as shown in Figure 30-23. In essence, Maxwell-Wagner-Sillars polarization is the same as electrode polarization, resulting in a large parasitic capacitance in series with bulk material.

This model has a dielectric response like that of a boundary layer, with very high *apparent* permittivities and distortions in *apparent* loss factor. Depending on the nature of the inhomogeneity, the Maxwell-Wagner-Sillars effect can become very complicated. In the case of multi-layer films, the dielectric behavior can be identical to that of a boundary layer because the geometries are the same.

Some analysis of insulating fibers in a conductive material has attempted to simulate the cure of fiberglass or Kevlar epoxy composites. For reasonable fiber geometries, permittivity is affected but loss factor is not, which agrees with experimental evidence.[6] In some cases loss factor increases, possibility because of an increase in ion concentration from the fibers.

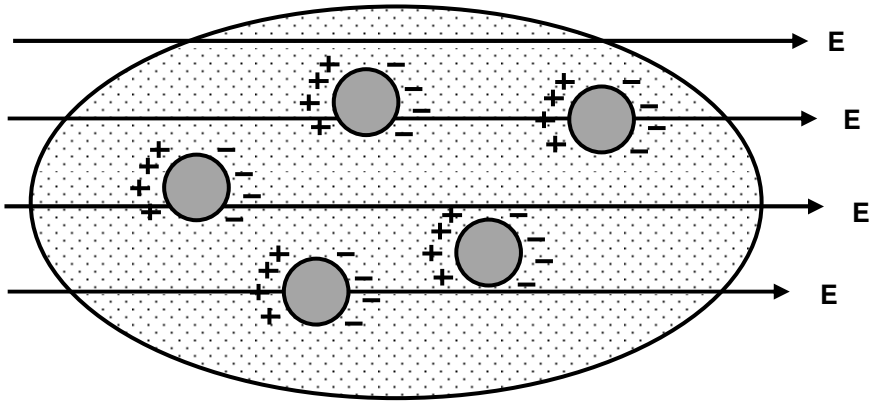

Figure 30-23
Maxwell-Wagner-Sillars polarization

Summary of the electrical model of polymers

- Induced dipole rotation
  - Modeled by $C_{induced}$, bulk capacitance from induced dipoles on nonpolar bonds
  - Frequency independent response
- Static dipole rotation
  - Modeled by C_{static} in series with G_{static}, capacitance and conductance from molecular dipoles
  - Frequency dependent response
  - Cole-Cole plot is an arc between relaxed and unrelaxed permittivity limits
  - Dipole loss factor peaks rarely greater than 3 and almost never greater than ~10
- Ionic conduction
  - Modeled by G_{ion}, bulk conductance from mobile ions
  - Frequency independent response
  - Cole-Cole plot is a vertical line
- Electrode polarization
  - Modeled by C_b, boundary layer capacitance on electrodes
  - Frequency dependent response in combination with G_{ion}
  - Cole-Cole plot is an arc over unrealistically large permittivities
  - Boundary layer loss factor peaks usually greater than ~100
- Maxwell-Wagner-Sillars polarization
  - Modeled by spheres in a dielectric material
  - Frequency dependent response in combination with G_{ion}
  - Cole-Cole plot similar to result from electrode polarization

References

1. Cole, K.S.; Cole, R.H., "Dispersion and Absorption in Dielectrics - I Alternating Current Characteristics". *Journal of Chemical Physics,* **9**: 341–352 (1941).

2. Cole, K.S.; Cole, R.H., "Dispersion and Absorption in Dielectrics - II Direct Current Characteristics". *Journal of Chemical Physics,* **10**: 98–105 (1942).

3. Davidson, D.W. and Cole, R.H., "Dielectric relaxation in glycerol, propylene glycol, and normal-propanol". *Journal of Chemical Physics*, 19(12):1484–1490 (1951).

4. Havriliak, S.; Negami, S., "A complex plane representation of dielectric and mechanical relaxation processes in some polymers". *Polymer*, **8**:161-210 (1967).

5. Day, D.R.; Lewis, J.; Lee, H.L. and Senturia, S.D., "The Role of Boundary Layer Capacitance at Blocking Electrodes in the Interpretation of Dielectric Cure Data in Adhesives," *Journal of Adhesion*, V18, p.73 (1985)

6. Day, D.R., *Dielectric Properties of Polymeric Materials*, Micromet Instruments, (1988).

7. Wagner, K.W., *Arch. Elektrotech*. 2:378 (1914).

8. Sillars, R.W., *J. Inst. Elm. Engrs* (London) 80:378 (1937).

Chapter 31—Using Ion Viscosity for Cure Monitoring

Definition of ion viscosity

The dielectric properties of a thermoset or composite are permittivity and conductivity. Conductivity has a frequency independent component (σ_{DC}) due to mobile ions and a frequency dependent component (σ_{AC}) due to dipole rotation. The inverse of conductivity is resistivity ρ, which also has frequency independent (ρ_{DC}) and frequency dependent terms (ρ_{AC}).

Frequency independent resistivity is also called ion viscosity (*IV*), which correlates with the cure state of thermoset materials. For dielectric cure monitoring it is important to recognize ion viscosity and understand how to isolate it from other factors.

Loss factor during cure

The loss factor of a Material Under Test, ε''_{MUT}, is given by equation 31-1:

(eq. 31-1) $$\varepsilon''_{MUT} = (\sigma_{DC} + \sigma_{AC})/\omega\varepsilon_0$$

Where: $\varepsilon_0 = 8.85 \times 10^{-14}$ F/cm (permittivity of free space)
$\omega = 2\pi f$ (s^{-1})
f = frequency (Hz)

Figure 31-1 shows loss factor for the cure of a "five-minute" epoxy. When σ_{DC} dominates dielectric measurements, loss factor is inversely proportional to frequency. For example, if $\sigma_{DC} >> \sigma_{AC}$ then loss factor at 10 Hz would be ten times greater than loss factor at 100 Hz.

In the early part of this cure, loss factor is inversely proportional to frequency for 10 kHz and less, and σ_{DC} dominates at these frequencies. Loss factor for 1 Hz shows distortions characteristic of a boundary layer caused by electrode polarization. As cure progresses, the relative influence of dipoles grows, σ_{AC} increases and after a time loss factor is no longer inversely proportional to frequency for 1 kHz, 10 kHz and 100 kHz. At the end of cure, loss factor for these frequencies almost overlap, indicating the strong influence of dipole relaxation.

At the end of cure, loss factors for 1 Hz and 10 Hz still show the inversely proportional relationship associated with frequency independent conductivity, and these two frequencies are suitable to redefine as ion viscosity.

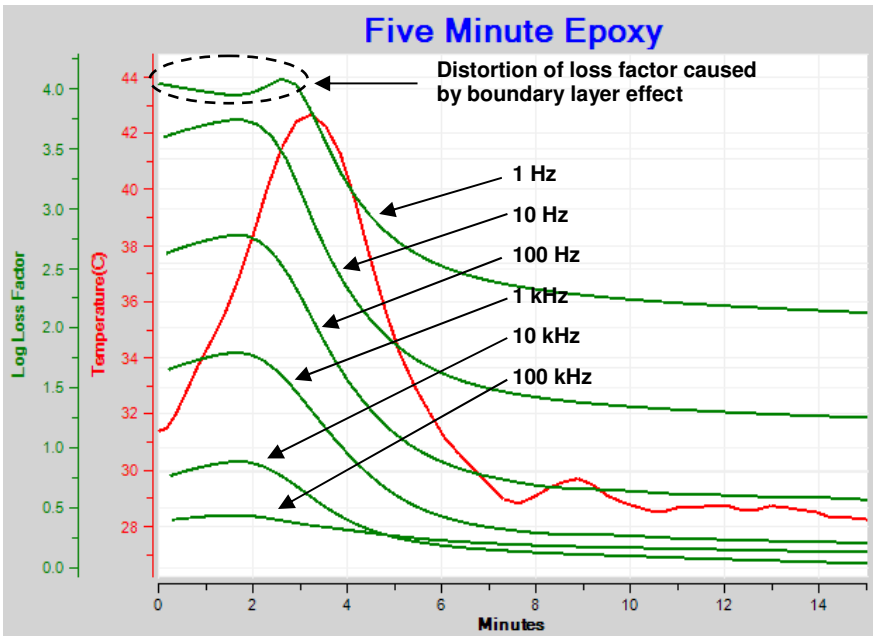

Figure 31-1
Loss factor of curing epoxy, showing effect of boundary layer

Figure 31-2 shows resistivity ρ derived from the loss factor data of Figure 31-1, using equation 31-2.

(eq. 31-2) $$\rho = 1/(\omega \varepsilon_0 \varepsilon''_{MUT})$$

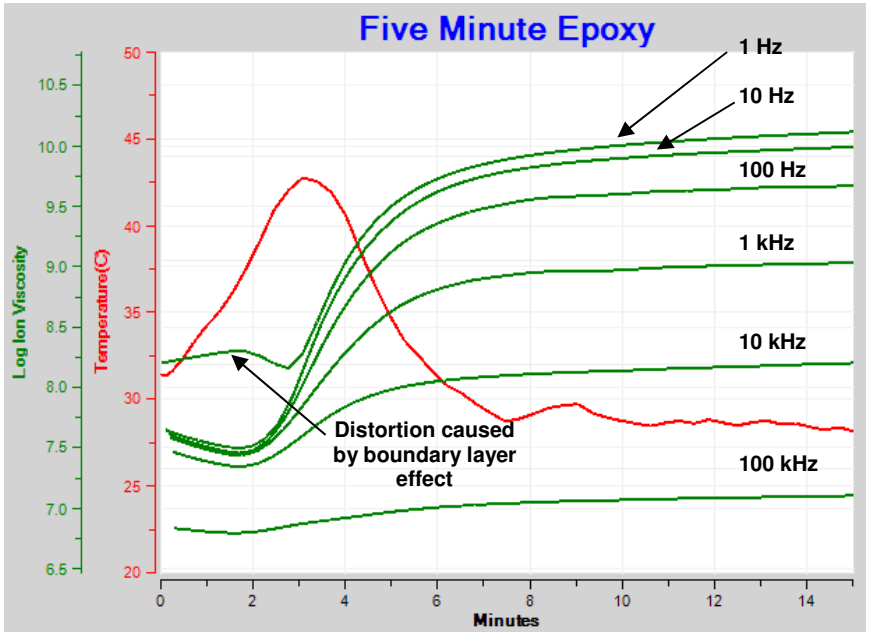

Figure 31-2
Resistivity of curing epoxy (plotted against log(ion viscosity) axis)

Here, resistivity has both frequency independent and frequency dependent terms, given by equations 31-3, 31-4 and 31-5. In this case, ionic conductivity σ_{DC} is dominant where curves overlap, and dipolar response is dominant where they do not.

(eq. 31-3) $$\rho = 1/(\sigma_{DC} + \sigma_{AC})$$

(eq. 31-4) $$\sigma_{DC} = \sigma_{ion}$$

(eq. 31-5) $$\sigma_{AC} = \varepsilon_0 \omega \frac{(\varepsilon'_r - \varepsilon'_u)}{1 + (\omega\tau)^2}$$

Where: ε'_u = Unrelaxed (high frequency) relative permittivity
ε'_r = Relaxed (low frequency) relative permittivity
$\omega = 2\pi f$ (radians/s)
τ = Dipole relaxation time (s)

Finally, ion viscosity (*IV*) is defined as the frequency independent resistivity, given by equation 31-6:

(eq. 31-6) $$IV = \rho_{DC} = 1/\sigma_{DC}$$

Distinguishing ion viscosity from resistivity

In the CureView[1] data acquisition and analysis software for dielectric cure monitoring, it is possible to use two adjustable, empirical parameters to define whether loss factor—and consequently conductivity and resistivity—are dominated by ionic conduction. These parameters are called *Loss Factor Cut*off and *Permittivity Cutoff*, and are used in algorithms to automatically distinguish ion viscosity from resistivity in general.

- **Loss Factor Cutoff (see Figures 31-3 and 31-4)**
  - Sometimes called *Dipole Cutoff*
  - Maximum loss factor showing the influence of dipole relaxation
  - Below Loss Factor Cutoff, frequency dependent conductivity (σ_{AC}) dominates the dielectric response
  - Above Loss Factor Cutoff, frequency independent conductivity (σ_{DC}) dominates the dielectric response
  - ε'' is converted to ion viscosity only for ε'' > Loss Factor Cutoff

Figures 31-3 and 31-4 show the relationship between dielectric data and a Loss Factor Cutoff with the value of 3.0.

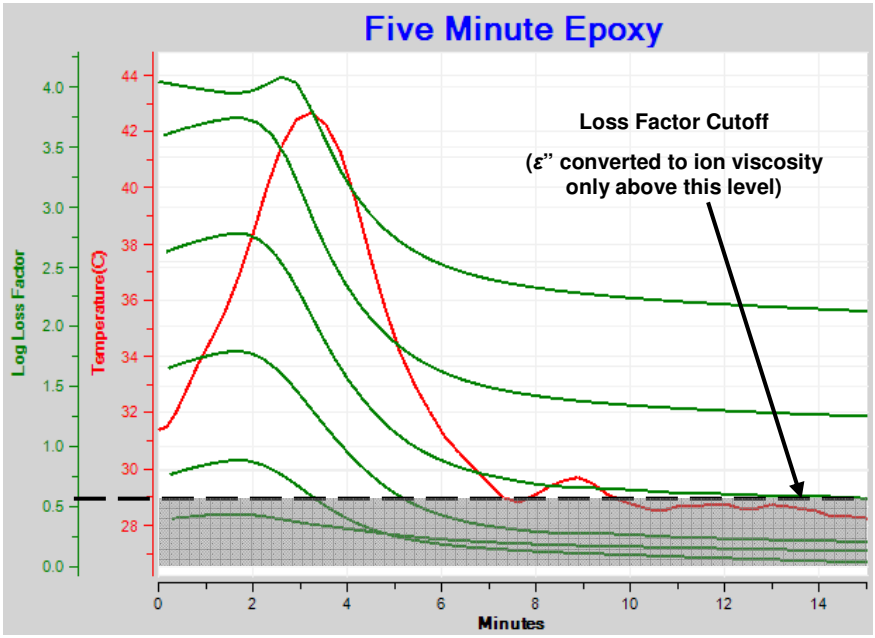

Figure 31-3
Loss factor cutoff applied to Five Minute Epoxy cure data

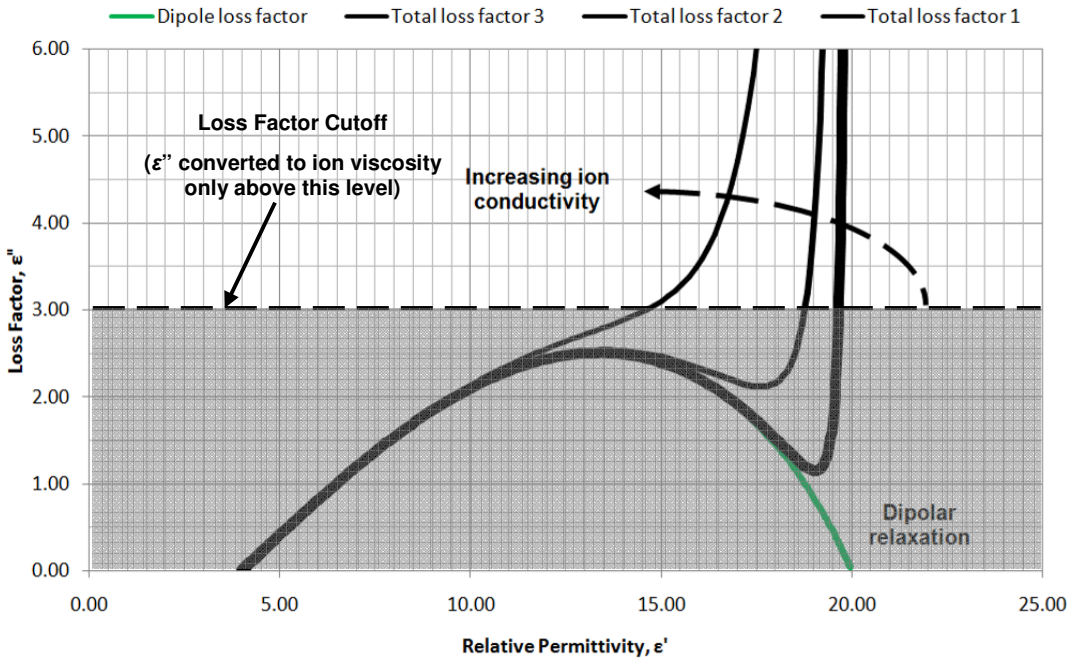

Figure 31-4
Loss factor cutoff on Cole-Cole plot (example)

Figure 31-5 shows multiple ion viscosity curves when the Loss Factor Cutoff is too low. As a result, some curves do not overlap and do not indicate clearly which data correlate with cure state. Note the distortion in the 1 Hz curve from the boundary layer effect.

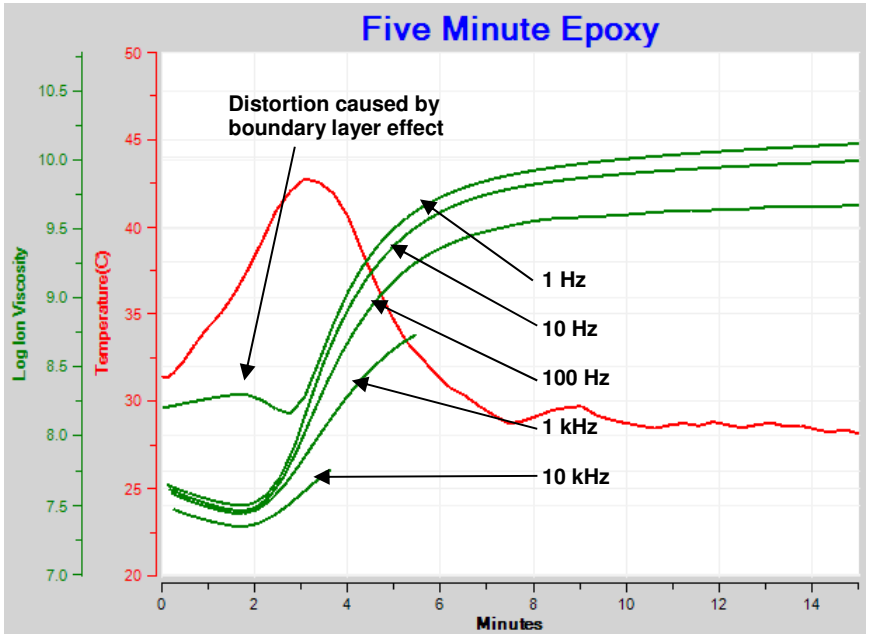

Figure 31-5
Ion viscosity data when Loss Factor Cutoff is too low

Results with an appropriate value of Loss Factor Cutoff are shown in Figure 31-6.

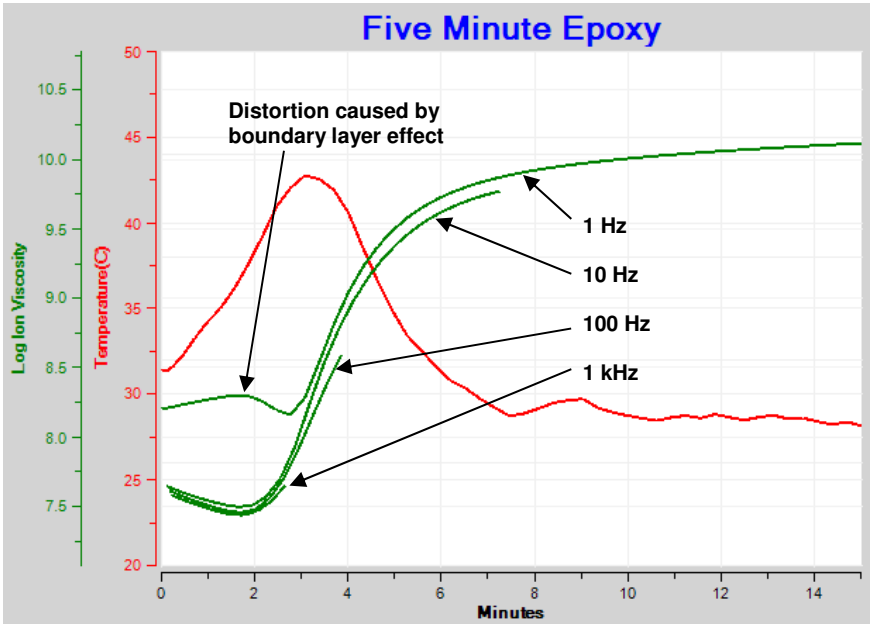

Figure 31-6
Ion viscosity data with appropriate Loss Factor Cutoff

Now the plotted ion viscosity curves largely overlap, indicating data dominated by frequency independent conductivity, which correlates with cure state. The overlap may not be perfect, however, because conductivity may have a non-ideal response.

In Figure 31-6 the distortion caused by boundary layers is still present in the 1 Hz data. Using the second parameter, *Permittivity Cutoff*, can eliminate measurements affected by this phenomenon.

- **Permittivity Cutoff**
  - Maximum permittivity for acceptable loss factor data
  - Below Permittivity Cutoff, loss factor is relatively undistorted by boundary layer effect
  - Above Permittivity Cutoff, loss factor begins to artificially decrease because of boundary layer effect
  - ε″ is converted to ion viscosity only for ε″ < Permittivity Cutoff

The Cole-Cole plot of Figure 31-7 shows the distortion in loss factor caused by boundary layers, and range of loss factor that can be converted to ion viscosity with a Permittivity Cutoff of 100,000.

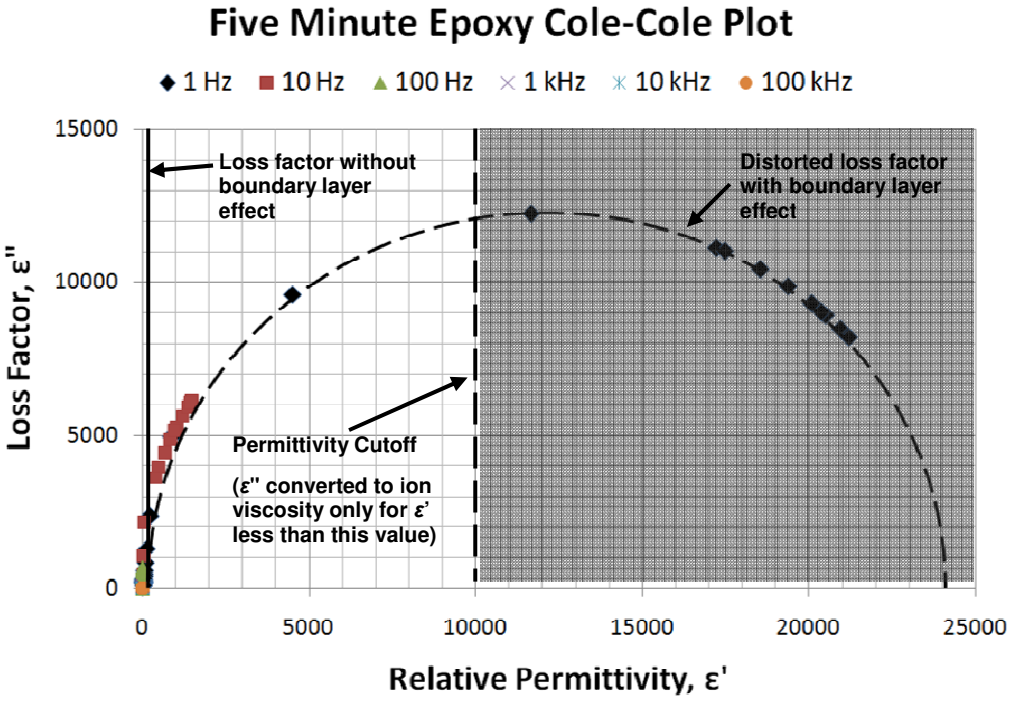

Figure 31-7
Cole-Cole plot of five-minute epoxy cure data

Figure 31-8 shows the family of ion viscosity curves after using a reasonable Loss Factor Cutoff and Permittivity Cutoff. This plot now shows the progression of frequency independent resistivity and indicates the cure state of the material.

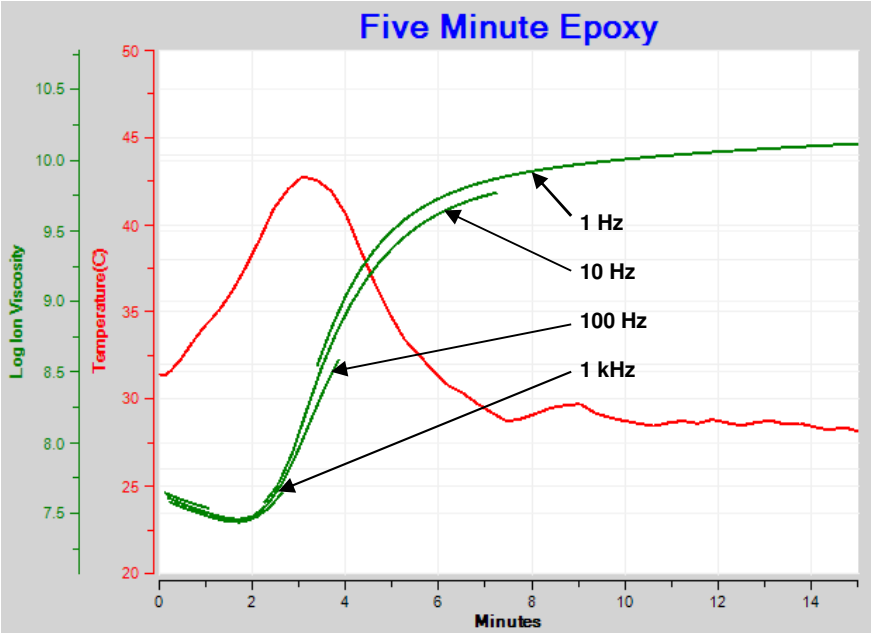

Figure 31-8
Ion viscosity with appropriate Loss Factor Cutoff and Permittivity Cutoff

To determine the time of maximum reaction rate or the time to end of cure, it is necessary to calculate the slope of log(*ion viscosity*), here simply called *slope* for brevity. Unfortunately, each of the ion viscosity segments of Figure 31-8 would produce its own segment for slope. The result would be a series of discontinuous slope curves. To avoid this problem, slope should be calculated using ion viscosity from a single low frequency, if possible, such as from the 10 Hz data of Figure 31-9. This simplification is possible because ion viscosity from a properly chosen frequency is often is very similar to the composite from multiple frequencies.

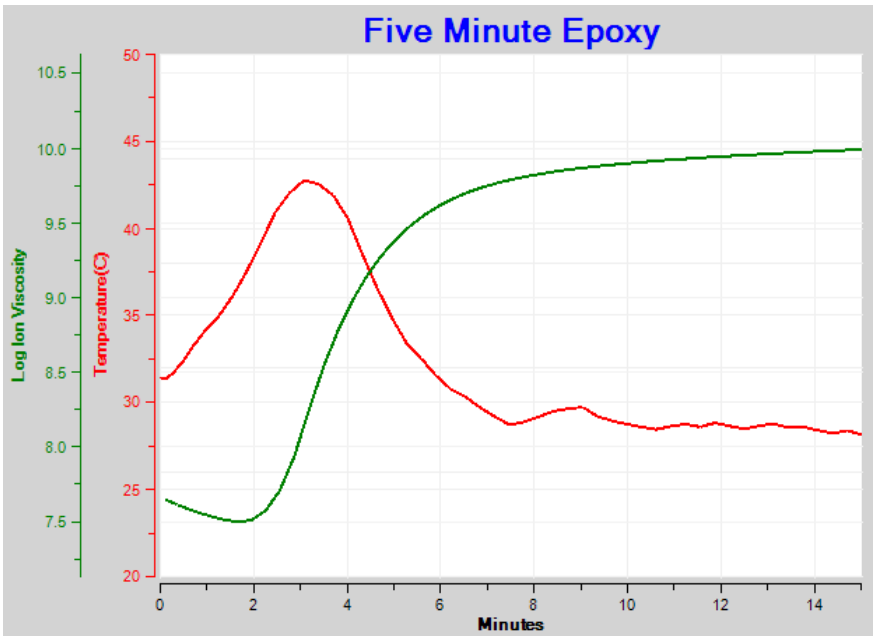

Figure 31-9
Ion viscosity for 10 Hz frequency only

Figure 31-10 shows ion viscosity from 10 Hz data as well as the resulting single curve for slope.

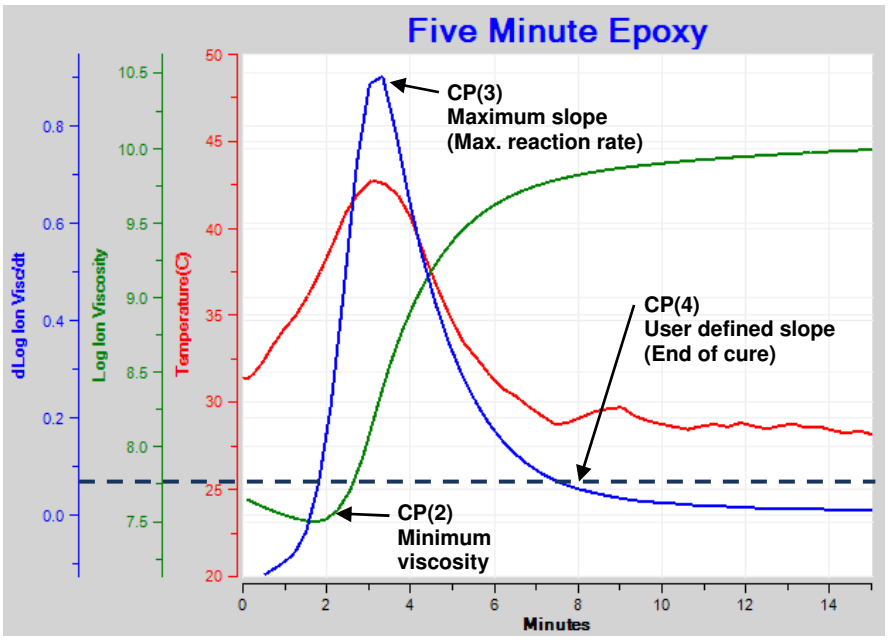

Figure 31-10
Ion viscosity and slope for 10 Hz frequency only

Now it is possible to clearly identify the following events during cure:

- Critical Point 1—CP(1)—Onset of flow
  - Identified when ion viscosity passes a user defined level
- Critical Point 2—CP(2)—Viscosity minimum
  - Identified when ion viscosity reaches a minimum value
- Critical Point 3—CP(3)—Point of maximum reaction rate
  - Identified when slope reaches a maximum value
- Critical Point 4—CP(4)—End of cure
  - Identified when slope reaches a user defined level

Electrode Polarization Correction

Electrode polarization occurs when the Material Under Test has a very high loss factor. Under this condition it is usually both highly fluid and highly conductive, and has an insulating boundary layer on the surface of the sensor electrodes. This boundary layer can distort permittivity and loss factor data as shown in the Cole-Cole plot of Figure 31-11 for the "five minute" epoxy data in this chapter.

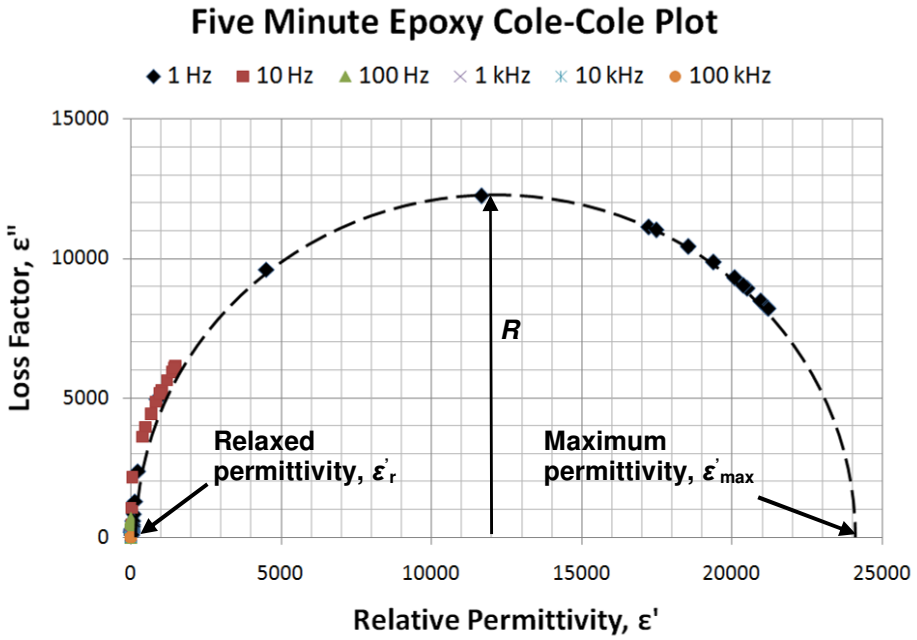

Figure 31-11
Cole-Cole plot of dielectric data distorted by electrode polarization

The arc of distorted data is a semi-circle with radius *R*. *Relaxed permittivity* ε'_r is relative permittivity toward the end of cure, or high frequency relative permittivity. *Maximum permittivity* ε'_{max} is the maximum value of relative permittivity when loss factor is zero as a result of boundary layers.

With a suitable choice of relaxed permittivity, it is possible to find an arc that fits the data and corrects the distortion caused by electrode polarization. This correction extends the measurement range for loss factor and resistivity, as shown in Figures 31-12 and 31-13.

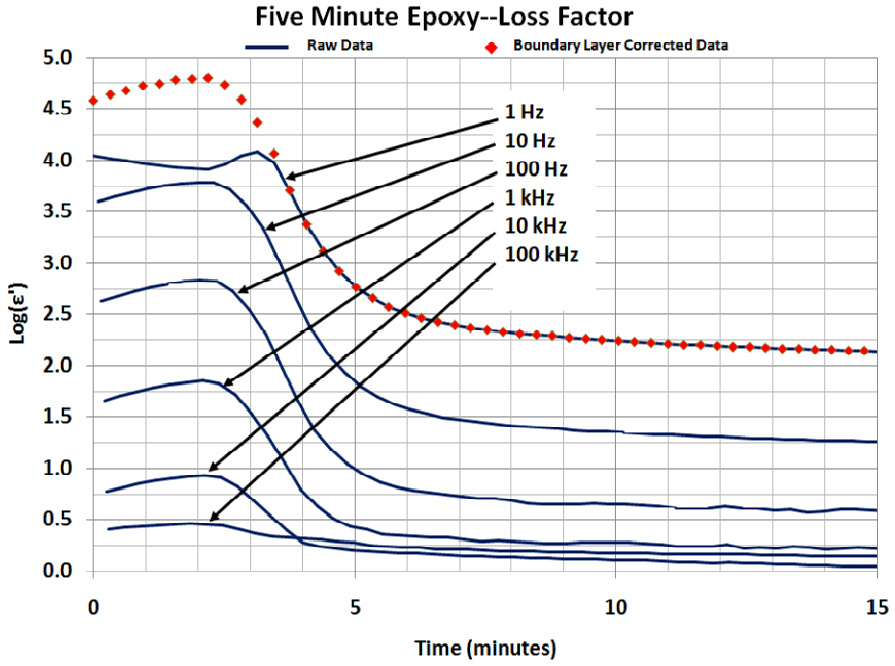

Figure 31-12
Loss factor, showing distortion from boundary layer and correction of data

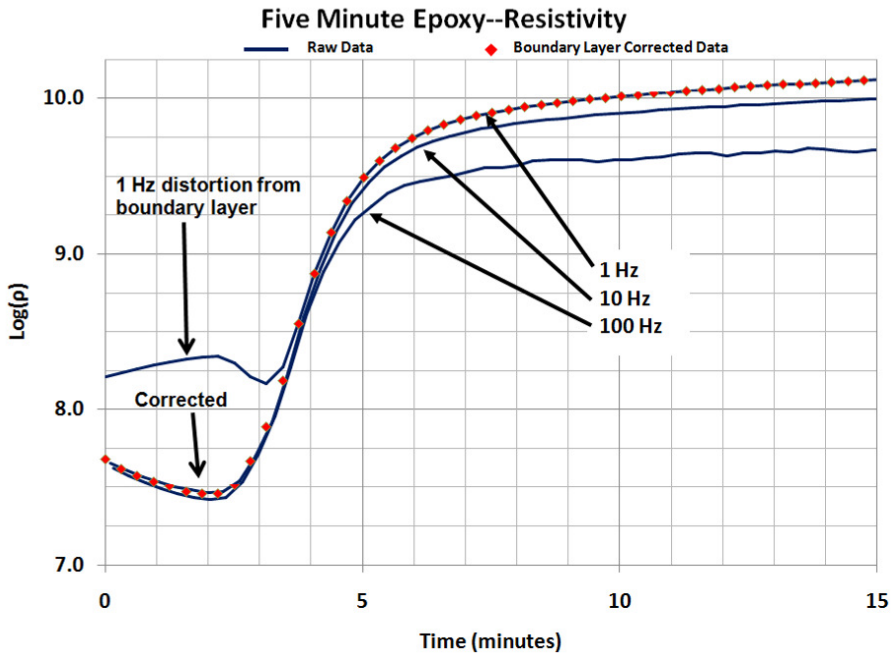

Figure 31-13
Resistivity, from loss factor data of Figure 31-12

Limitations of ion viscosity for measuring cure state

To avoid misinterpreting dielectric measurements, it is important to understand the limitations of using ion viscosity. For the "Five-Minute" epoxy data at 1 Hz, frequency independent resistivity ρ_{DC} dominates dielectric response during the entire cure. As a result, ion viscosity (ρ_{DC}) is a valid measure of cure state throughout the test, indicating viscosity before gelation and modulus after gelation.

In situations when frequency independent resistivity does not dominate the entire cure, it is necessary to know when the influence of ρ_{DC} ends and the influence of dipolar relaxation begins. For example, Figure 31-14 shows data for the cure of a vinyl ester. Loss factor curves are inversely proportional to frequency—indicating frequency independent resistivity—only for early cure. At the end of cure, loss factor for all frequencies are very similar, a response caused by dipolar relaxation.

Figure 31-15 shows ion viscosity derived from the data of figure 31-14. For the frequencies used, resistivity curves overlap only for the first 125 minutes. After this time ion viscosity—that is, frequency *independent* resistivity—no longer applies and cannot be used to determine cure state. Cures near room temperature most often display this limitation. In contrast, because conductivity increases with temperature, cures at elevated temperatures are more likely to be

dominated by frequency independent resistivity, and therefore ion viscosity, for the entire process.

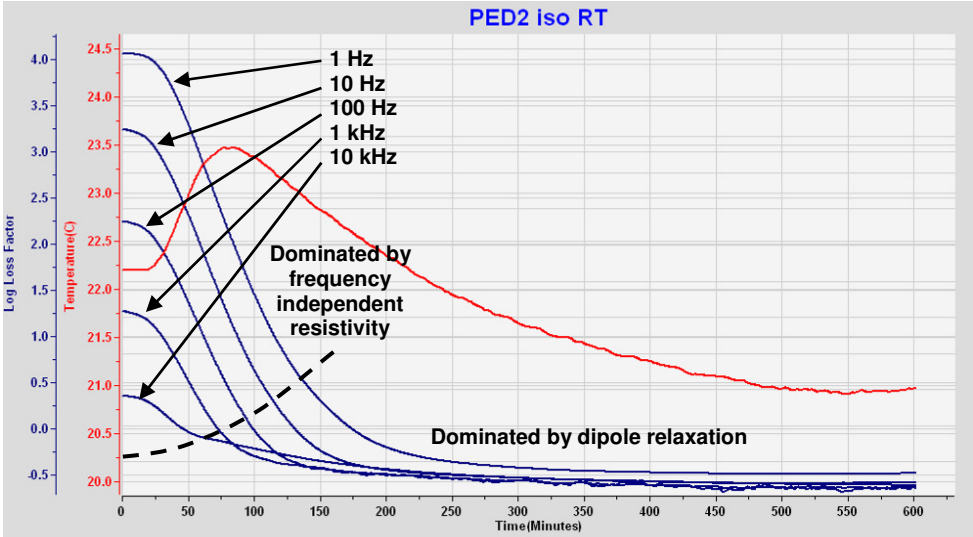

Figure 31-14
Loss factor for a vinyl ester cure

Even when dipolar relaxation influences dielectric response, it is still possible to understand the progress of cure by observing loss factor. Loss factor is more useful in this case because the contributions of conductivity and dipole rotation are simply additive, and are easier to distinguish visually.

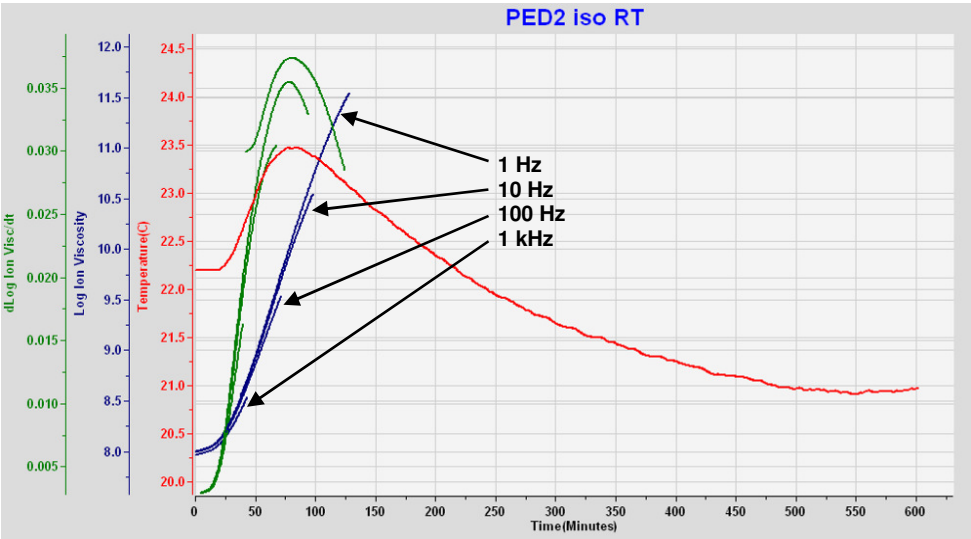

Figure 31-15
Ion viscosity and slope of ion viscosity for a vinyl ester cure

Summary of Material Properties

Many factors can cause confusing interpretation of dielectric data. Selection of appropriate ***Material Properties*** can guide data processing algorithms to remove artifacts caused by dipole relaxation or electrode polarization. The result, ideally, would be frequency independent resistivity, also known as *ion viscosity*, which correlates well with cure state. Table 31-1 summarizes the *Materials Properties* discussed in this chapter.

Table 31-1
***Material Properties* for converting loss factor to ion viscosity**

Material Property	Description
Loss Factor Cutoff	Allows conversion of data to ion viscosity for loss factors above the Loss Factor Cutoff Loss factors below Cutoff assumed to be dominated by AC conductivity
Permittivity Cutoff	Allows conversion data to ion viscosity when permittivity is below the Permittivity Cutoff Permittivities above Cutoff assumed to be distorted by electrode polarization
Relaxed Permittivity	Permittivity of material at end of cure or at high frequency Used for boundary layer correction
Maximum Permittivity	Maximum permittivity of material at zero loss factor due to electrode polarization Used for boundary layer correction May be determined mathematically from relaxed permittivity and distorted data

References

1. CureView software, manufactured by Lambient Technologies, Cambridge, MA USA. https://lambient.com

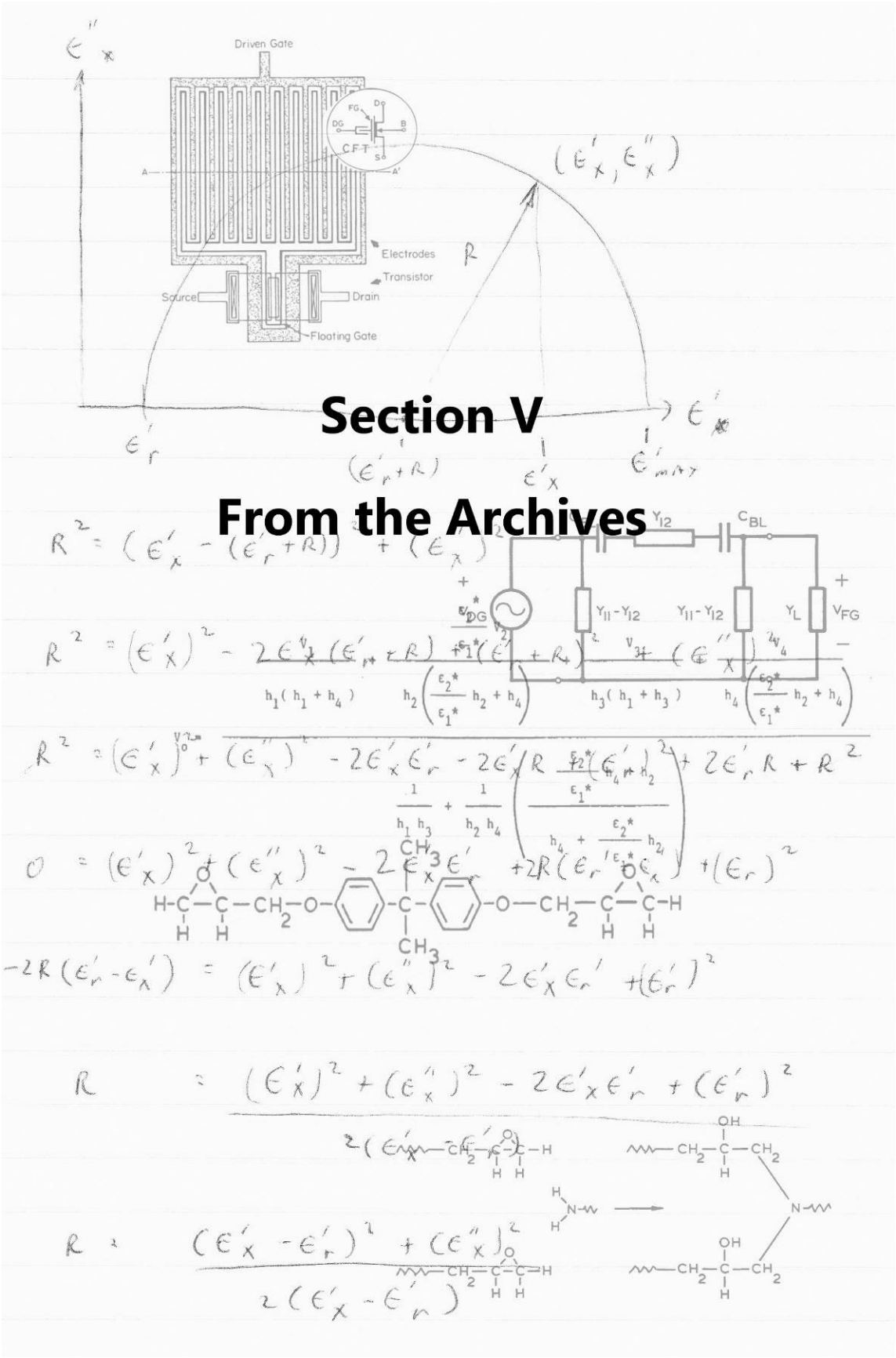

Section V

From the Archives

Spinoff

1987

NASA

Cure Monitoring

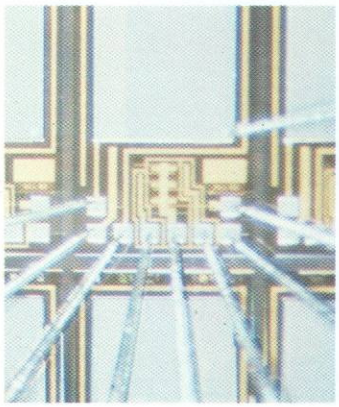

Microdielectrometry is definitely not a household word and few can define it, but it is a technology of growing importance at a time of rapidly increasing use of composite materials in high performance military and commercial products. Composites, invariably lighter and usually stronger than the metals they replace, are sheets of woven fibers impregnated with a matrix of resin or other material. A vital step in their manufacture is the curing process, which is critical to the strength, quality and consistency of the product.

That's where microdielectrometry comes in. Its principal application is monitoring the chemical changes that take place when resins, adhesives and plastics are cured or processed, for example, measuring the behavior of the resins used to bind fiber reinforced composites for aircraft, spacecraft or jet engines—in other words, providing information that enables precise control of the curing process for optimum results.

Micromet Instruments, Inc., Cambridge, Massachusetts, manufactures the Eumetric System II Microdielectrometer, key to which is a miniature electronic probe—a silicon microchip—that contains electrodes and circuitry for measuring the electrical properties of whatever material is placed in contact with the electrodes; the microchip, magnified 15 times, is shown at left. The rest of the system consists of additional sensors, electronic components, microcomputer modules and software.

In composite curing, usually carried out in autoclaves, large pressure vessels that can be heated to as much as 800 degrees Fahrenheit, the microdielectrometer is used to probe the resins as they cure in the autoclave. The sensors communicate data to the system's computer about the chemical changes occurring. At left below, Micromet's Dr. Huan Lee is preparing a test of a polymer resin, dipping a ribbon sensor in the resin; the large black box is the Eumetric System II Microdielectrometer. Above, Lee is using a microscope to position the silicon microchip on the ribbon and at center right engineers are studying the results of the test.

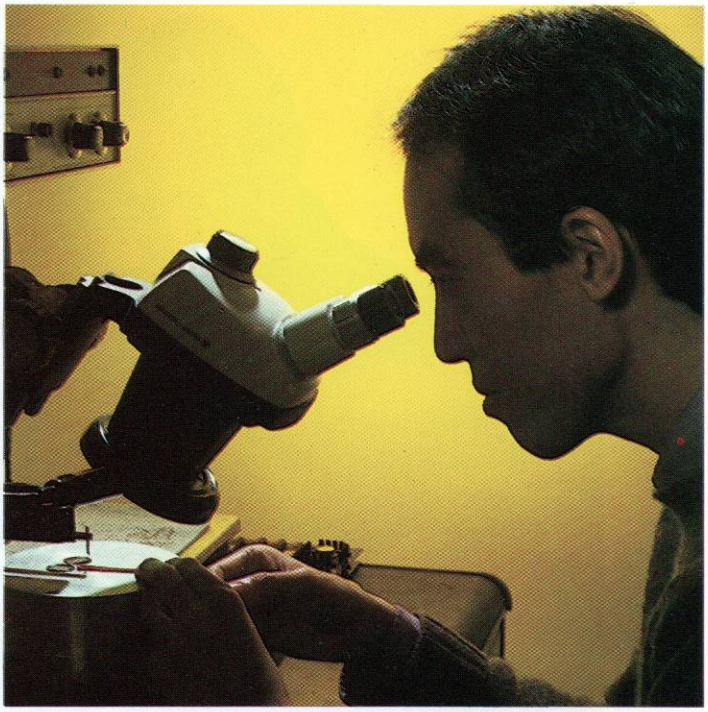

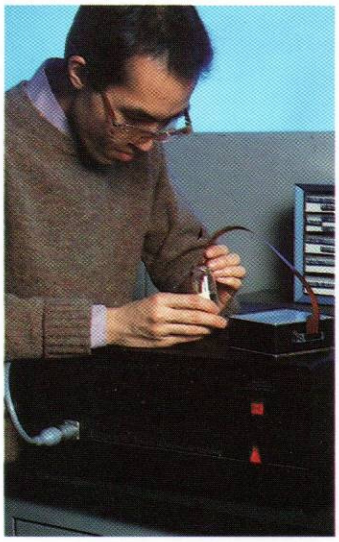

The instrument is also used in quality control laboratories to verify the properties of new batches of materials and in research laboratories to investigate the cure behavior of new materials. At far right, Dr. Brenda Holmes, research scientist at the Naval Research Laboratory in Washington, D.C., is using the microdielectrometer to study the cure characteristics of a polymer network.

The System II Microdielectrometer and the art of microdielectrometry trace their roots to NASA's Technology Utilization Program. Principal inventor of the technology is Stephen D. Senturia, a professor of electrical engineering at Massachusetts Institute of Technology (MIT). During the early 1970s, Senturia served as a consultant to a NASA technology utilization contractor seeking to develop urban applications for NASA technology, in particular a project involving development of an advanced home fire alarm. The consulting group found potential utility in research performed by Dr. Norman Byrd of McDonnell Douglas Corporation who, investigating safety devices for spacecraft, had been working on

"Cure Monitoring", *NASA Spinoff* 1987, pp. 108-109, National Aeronautics and Space Administration, Office of Commercial Programs, Technology Utilization Division, by James J. Haggerty, August 1987

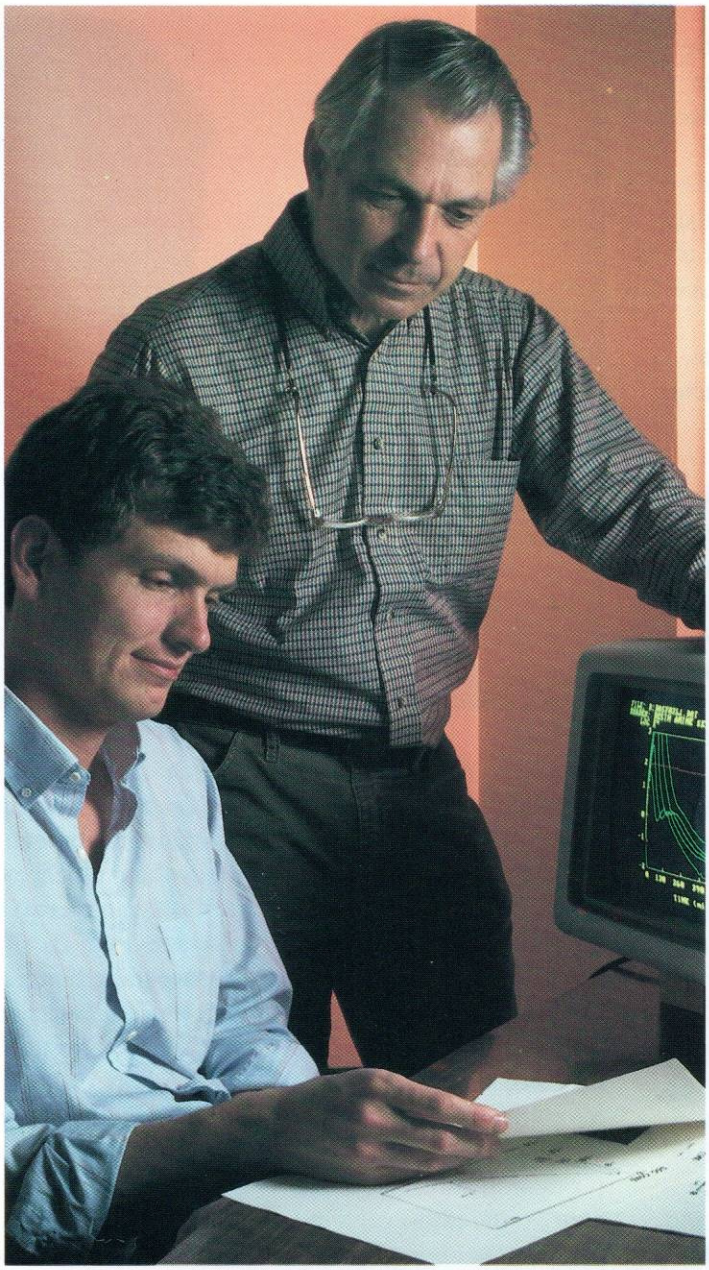

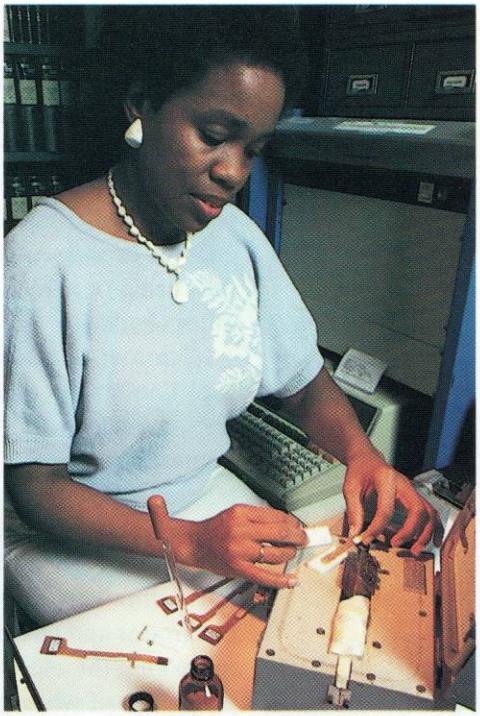

polymeric thin films that would change their electrical properties when exposed to hazardous gases.

NASA funded two contracts to explore this potential, one with McDonnell Douglas for additional polymer research and another with MIT under which Senturia was to seek new methods of measuring electrical properties with an eye toward developing low-cost components of a home fire alarm. In the course of this contract, Senturia invented the "charge-flow transistor," a microchip for measuring the electrical properties of thin polymer films. A direct ancestor of the microdielectrometer, the first successful device was built at MIT in 1976.

The NASA contract failed to produce a commercial product but Senturia continued his work under sponsorship of the Office of Naval Research and the National Science Foundation; ultimately, with the aid of others at MIT, he developed the present microdielectrometer. In 1982, Senturia and four colleagues obtained a license from MIT for the technology and founded Micromet Instruments. The technology is finding wide acceptance among government agencies, aerospace firms, chemical and electronic companies. ▲

"Cure Monitoring", *NASA Spinoff* 1987, pp. 108-109, National Aeronautics and Space Administration, Office of Commercial Programs, Technology Utilization Division, by James J. Haggerty, August 1987

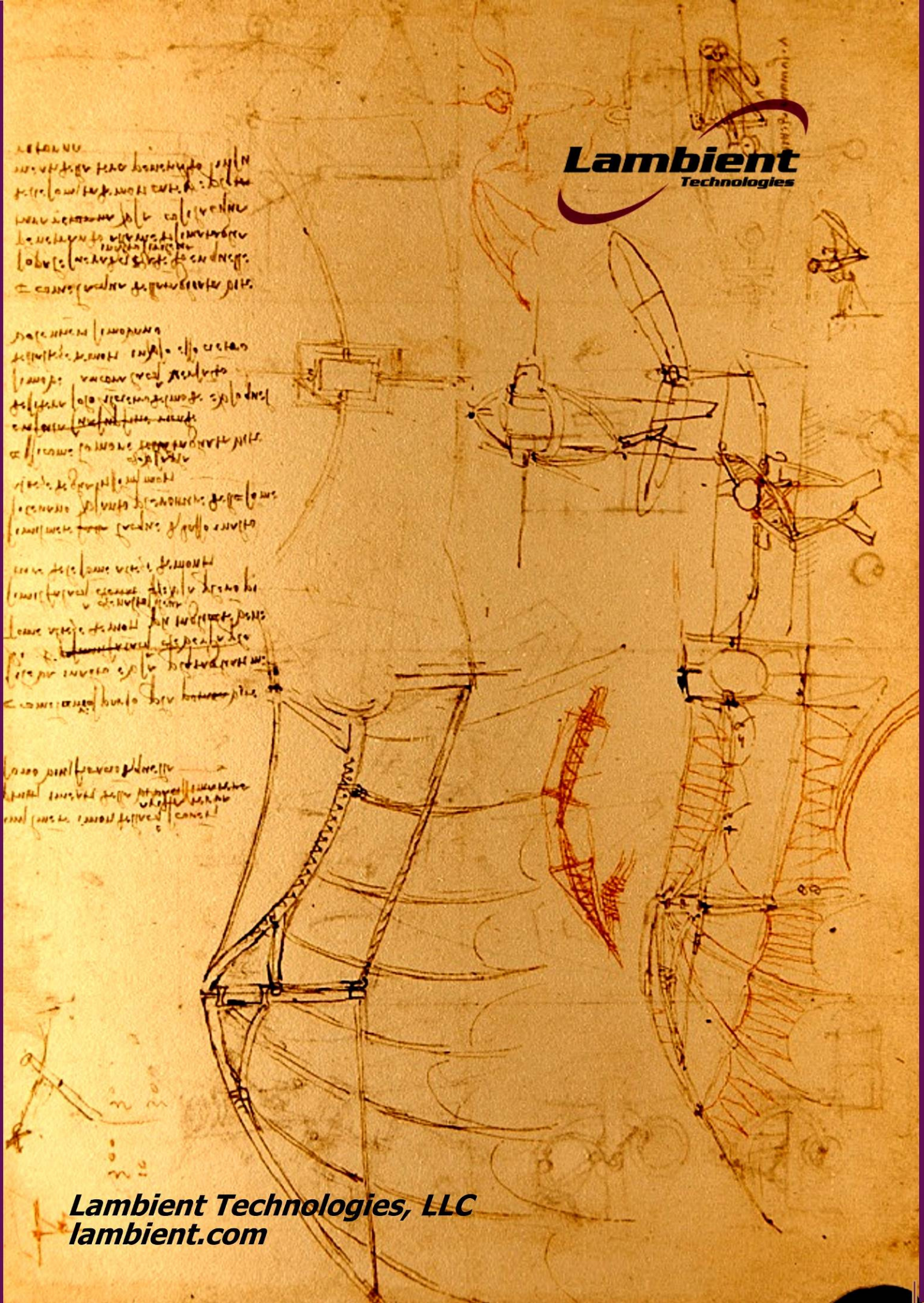

Lambient Technologies, LLC
lambient.com